RISK ASSESSMENT OF POWER SYSTEMS UNDER A CORRECTIVE CONTROL PARADIGM

A Thesis submitted to the University of Manchester for the degree of
Doctor of Philosophy
In the Faculty of Engineering and Physical Sciences

2011

Kang Ma

School of Electrical and Electronic Engineering
Electrical Energy and Power Systems Group

Contents

List of Tables

List of Figures

Abstract

Submitted by Kang Ma

for the degree of Doctor of Philosophy

and entitled Risk Assessment of Power Systems under a Corrective Control Paradigm

Date of Submission: 31st May 2011.

Given the fact that the load is continuously growing as a sign of economic development and that renewable intermittent generation is growing rapidly driven by global climate change concerns and rising fuel costs, existing power systems need to be reinforced in order to accommodate the growing load and intermittent generation. Corrective control is a promising alternative solution to preventive control which, in this context, is represented by traditional system reinforcement of building more transmission facilities.

The concept of reliability, existing reliability assessment methodologies and the latest development in this field were reviewed. The corrective control system was modelled as a common cause failure. New indices were derived and presented in the context of corrective control. They are Linear Weighed Reliability Index (LINWRI), Incremental Benefit of System Reinforcement (IBSR), Demand Response Incremental Cost Benefit (DRICB), and Voluntary Energy Curtailment Level (VECL).

Three means of corrective control considered in this research are Demand Response (DR), Flexible AC Transmission Systems (FACTS) and Energy Storage (ES). One of the corrective control applications is the Active Management (AM) on distribution systems. The model of AM control system was developed and incorporated into chronological Monte Carlo simulation (CMCS). Different AM configurations and different reliability levels of AM with the same configuration have been proposed. Their impact on the ability to accommodate wind generation and on power system reliability was investigated. Economic assessment was also performed. A 'win-win' situation was achieved when a relatively reliable AM system is configured with Wind Generation Output Control (WGOC) function and the capacity of wind generation is adequate.

DR models and the models of typical FACTS devices were reviewed and summarised. The Battery Energy Storage (BES) and Static Synchronous Compensator/BES (STATCOM/BES) models were developed based on the general structure of Energy Storage (ES) and a list of assumptions regarding their operation. Their models together with the model of the control system have been incorporated into CMCS which is applied as the reliability assessment methodology. The impact of DR, FACTS and ES on power system reliability was studied to a detailed level through test cases. The results have demonstrated the reliability improvement from corrective control compared to 'doing nothing at all' as well as the potential advantage of corrective control over traditional reinforcement in terms of cost effectiveness.

The direction for future research related to this field was identified to be the investigation in network planning as an upstream project under a corrective control paradigm, the development of a more efficient and accurate nonlinear optimisation toolbox, the upgrade of DR models and FACTS models and the incorporation of transient analysis, etc.

Declaration

No portion of the work referred to in this thesis has been submitted in support of an application for another degree or qualification of this or any other university or other institute of learning.

Copyright Statement

Dedication

To the one I love

Acknowledgement

I am wholly indebted to my supervisor, Dr. Joseph Mutale, whose continuous guidance, consideration and patience contributed to my challenging PhD studies. He has inspired me of key academic ideas, was always ready to discuss academic problems and has fully supported me in disseminating my work to the world. He has also provided me with critical financial support.

I would like to thank my ex-advisor, Prof. Daniel Kirschen, who has also given me invaluable academic advice and part-time academic jobs that helped me ride through financial difficulties.

I would further like to thank my colleagues: Ali Kazerooni, Brian Azzopardi and Eduardo Alejandro Martínez Ceseña, for fruitful research discussions.

I also thank the Engineering and Physical Science Research Council (EPSRC) for their financial support, and the Flexnet research consortium for the invaluable exchange of research ideas.

My deepest gratitude goes to my family for their unconditional support and love; keeping me always in their mind and heart.

List of Abbreviations

AAOD	Annual Average Outage Duration
AM	Active Management
ASAI	Average Service Availability Index
BES	Battery Energy Storage
CCDF	Composite Customer Damage Function
CCF	Common Cause Failure
CCS	Corrective Control System
CDCS	Charge-Discharge Control System
CMCS	Chronological Monte Carlo Simulation
DNO	Distribution Network Operator
DR	Demand Response
DRICB	Demand Response Incremental Cost Benefit
EENS	Expected Energy Not Supplied
EIC	Expected Interruption Cost
EILP	Emergency Interruptible Load Programme
ES	Energy Storage
FACTS	Flexible AC Transmission Systems
FEC	Forced Energy Curtailment
GA	Genetic Algorithm
HLI	Hierarchy Level I
HLII	Hierarchy Level II
HLIII	Hierarchy Level III

IBCC	Incremental Benefit of Corrective Control
IBP	Incentive-Based Programme
IBSR	Incremental Benefit of System Reinforcement
ICCI	Incremental Corrective Control Investment
ISRI	Incremental System Reinforcement Investment
LINWRI	Linear Weighted Reliability Index
LOEE	Loss of Energy Expectation
LOLE	Loss of Load Expectation
LOLP	Loss of Load Probability
MAIFI	Momentary Average Interruption Frequency Index
MCS	Monte Carlo Simulation
MRTS	Modified 24-Bus Reliability Test System
O&M	Operation and Maintenance
PBP	Price-Based Programme
PI	Performance Index
PTS	Power Transformation System
RBTS	6-Bus Roy Billinton Test System
RTP	Real-Time Pricing
RTS	IEEE 24-Bus Reliability Test System
RTU	Remote Telemetry Unit
SAIDI	System Average Interruption Duration Index
SAIFI	System Average Interruption Frequency Index
SCADA	Supervisory Control and Data Acquisition
SEM	State Enumeration Method

SLOM	Standard Linear Optimisation Model
SQP	Sequential Quadratic Programming
SSSC	Static Synchronous Series Compensator
STATCOM	Static Synchronous Compensator
SVC	Static Var Compensator
TCC	Thyristor-Controlled Capacitor
TCR	Thyristor-Controlled Reactor
TCSC	Thyristor Controlled Series Compensator
TOU	Time-of-Use
TRS	Traditional Reinforcement Scenario
TTF	Time to Failure
TTR	Time to Repair
TTDS	Time to Derated State
UCAP	Ultracapacitor
UPFC	Unified Power Flow Controller
VEC	Voluntary Energy Curtailment
VECL	Voluntary Energy Curtailment Level
VSI	Voltage Source Inverter
WGOC	Wind Generation Output Control

List of Mathematical Symbols

T_k	The power flow in branch k
P_g	Real power generation
Q_g	Reactive power generation
P_l	

	The real power of load
Q_l	The reactive power of load
V	Voltage magnitude
θ	Voltage angle
P_G^{Cur}	Curtailment of real power generation
P_L^{Cur}	Load curtailment
pf	Power factor
X_{SVC}	Shunt reactance of SVC
X_{TCSC}	Series reactance of TCSC
P_{ES}	Real power output of energy storage device
Q_{STATCOM}	Reactive power output of STATCOM
P_{Trans}	Transitional matrix of Markov process
λ_{FACTS}	The observed failure rate of FACTS device
λ_{Self}	The failure rate of independent failure
λ_{CCF}	The failure rate of common cause failure
λ_{Con}	The failure rate of central control unit
λ_{Comm}	The failure rate of communication system
λ_{UComm}	The failure rate of upstream communication channel
λ_{CH}	The failure rate of communication channel
β	The percentage that attributes to common cause failure
NB	Net benefit
PV	Present value

List of Publications

1) Ma, Kang; Mutale, Joseph, “Risk and reliability worth assessment of power systems under corrective control”, Proceedings of North American Power Symposium 2009, Starkville, MS, USA, 4-6 Oct 2009.

2) Ma, Kang; Mutale, Joseph, "Incorporating control system reliability in active management of distribution systems with distributed generation", Innovative Smart Grid Technologies Conference Europe (ISGT Europe), 2010 IEEE Power Energy Society , vol., no., pp.1-7, 11-13 Oct. 2010.

1 Introduction

Summary

This chapter gives an overview of the background and motivation of this research highlighting two challenges facing today's power systems namely continuous load growth and the increasing penetration of intermittent generation. The advantages and disadvantages of two fundamentally different solutions (corrective control and traditional reinforcement) that can be deployed to address the challenges are then summarised. The definition of corrective control as well as its scope in this project is clarified. The aim and the objectives of this research are then identified followed by a summary of the main contributions of this work and the thesis structure.

1.1 Background of the Change towards Flexible Networks

While current power systems in developed countries seem to function perfectly well without major disturbances or widespread public dissatisfaction, there are several factors that are driving the imperative for change to the way these power systems are presently planned and operated. The key drivers include the following:

1) liberalisation of electricity markets;
2) continuous load growth;
3) increasing penetration of intermittent renewable generation;
4) pressure to meet environmental targets; and
5) economic, political and legal barriers to reinforcement of existing or construction of new power transmission infrastructure.

These drivers can be grouped into three main areas which are elaborated further below:

1.1.1 The Liberalisation of Electricity Market

Different countries in Europe have different agendas of transformation from a vertically monopolistic electricity company to a competitive multi-layer market with numerous private firms [1]. The UK government conducted a consultation on electricity market reform earlier this year (2011) [2]. Three key objectives of such a reform is the security of supply, decarbonisation and affordability [2]. To safeguard the security of electricity supply while pushing forward the reform towards a more competitive market, the UK needs to maintain a sufficient level of power system flexibility to balance supply and demand at any moment and avoid outages [2]. By sending the right signals to investors for an appropriate level of investment in flexible plants, interconnections, energy storage and demand response etc, the electricity market serves as one of the major drivers for these elements that form a flexible network [2, 3].

1.1.2 The Pressure of Continued Load Growth and the Barriers to Traditional Reinforcement

The pressure of continuous load growth should not be underestimated. A 20% rise in demand was expected from 2007 to 2017 in North America, compared to only 10% rise in committed power supply over the same period [4]. Load growth is identified as one of the major challenges in Europe as well [5]. As part of decarbonisation agenda, it is expected that a substantial portion of energy consumption in the UK, for example heating and transport, is to be electrified in the long term [2]. As a result, the UK's electricity demand is expected to increase, or even double by 2050 [2]. The continuous growth in peak demand is gradually 'eating up' existing system margins in both generation system and transmission system and is causing the power system to be more vulnerable to failure. The risk associated with load growth must be resolved without delay. And this is one of the major drivers for system reinforcement.

From the power network point of view, there are two fundamentally different types of system reinforcement to address the issue mentioned above. One of them is traditional system reinforcement which normally entails building more transmission facilities [3].

This solution belongs to the preventive control domain which aims to provide sufficient system margin in advance. However, it is facing increasing barriers, both economic and political which can be summarised as follows:

1) The cost of investing in a new power line is prohibitive, especially in countries with a shortage of land;
2) The lead time on construction of new lines can be very long, depending on numerous factors including the length of the line;
3) There are serious environmental issues and political barriers associated with construction of new power lines. The construction of new lines is likely to involve the alteration of natural habitats of wild life, e.g., chopping down a large area of forest. This significant environmental impact is likely to result in strong political objections;
4) The legal process of acquiring the land permission for a large piece of land may be complicated and time-consuming.

A less costly and less politically controversial alternative to construction of new power lines is the implementation of corrective control as a key feature of a flexible network [3]. It represents a revolution in power system operation philosophy from preventive control to corrective control. The major advantages of corrective control are:

1) It circumvents or at least delays the prohibitive investment cost of traditional reinforcement, i.e., building new transmission facilities;
2) It requires a minimum area of land and hence causes much less environmental hassles than traditional reinforcement scenarios. In this way, it is much 'greener' than traditional reinforcement.

In short, this solution can be defined as the investment in flexibility. Therefore, corrective control is a promising solution towards a flexible network driven by continuous load growth and other factors.

1.1.3 Pressure to meet Environmental Targets and Increasing Penetration of Intermittent Renewable Generation

The increasing penetration of intermittent renewable generation is also the result of the liberalisation of electricity markets [6]. One of the key objectives of an efficient electricity market is decarbonisation, which is also a legally binding promise by the UK government. The UK government has set up ambitious low-carbon target: by 2020, the level of UK carbon emissions is expected to be 34% lower than that of 1990 [7, 8]. By 2050, this level is expected to reduce by 80%, relative to the level of 1990 [8]. This target inevitably requires a generation portfolio very different from that of today. The carbon-intensive coal generation is ageing and will be almost completely replaced by less carbon-intensive types of generation such as renewable generation and nuclear generation by 2050 [2]. At the same time, there is a need for flexible plants such as gas-fire plants, which are necessary in maintaining the security of supply.

In response to the pressure to meet environmental targets and sustainability criteria, renewable generation, which has been undergoing rapid development in Europe, is expected to constitute a substantial proportion in the UK's generation portfolio by 2050 [2]. At the same time, there is also pressure for change towards a flexible network which can cost effectively and securely accommodate increasing capacity of intermittent generation, such as wind generation and photovoltaic generation, or in short, the increasing penetration of intermittent generation [3].

Although the trend towards a less carbon-intensive generation portfolio is clear, there are also unknown factors that potentially have a significant impact on this portfolio. For example, following the recent nuclear disaster in Japan, there is a worldwide public concern of the security of nuclear generation [7]. Public concerns have turned into political pressure in countries like Japan and Germany, and their long-term strategies of nuclear development are subject to an increased level of scrutiny, if not completely halted [7]. This pressure, in the long term, may lead to less percentage of nuclear generation and more percentage of intermittent renewable generation than previously proposed in the UK. However, it is difficult to predict the quantitative impact at this stage. The uncertainly in the future generation portfolio, coupled with the increased penetration of intermittent renewable generation, reinforces the requirement for future networks to be flexible.

1.1.4 Research Gaps and Introduction of Corrective Control

With the implementation of corrective control, power systems are able to accommodate growing loads and increasing penetration of intermittent generation by utilising the system margin which should be reserved under traditional reinforcement. Rather than providing sufficient system margin in advance, corrective control aims to correct system violations in a reasonably short period of time after they occur. The prevailing 'N-1' or 'N-2' rule is challenged under corrective control. For example, the power line may be pushed to its limit under corrective control: the power transmitted is right at the threshold where the line can operate in a stable mode, whereas, under preventive control, 'N-m' rule should be maintained which requires a large reserved capacity of the line. According to GB Seven Year Statement published by National Grid, for most power lines more than half of their capacity is reserved for security, despite the fact that their thermal ratings change in different seasons [3]. The implementation of corrective control corresponds to a more sophisticated way of power system management. It is a vital question whether such increased flexibility will bring extra risk to the power system, or in other words, whether a satisfactory system reliability level is guaranteed during the transition to a more sophisticated way of management. This question had not been answered before this research took place. More specifically, the following gaps have been identified:

1) Although the classical framework of reliability assessment is well established, previous work paid little attention to the modelling of flexibility in reliability assessment. Previous publications mainly focus on generation re-dispatch, network reconfiguration and load shedding in reliability studies. Some papers investigate the Flexible AC Transmission Systems (FACTS), Demand Response (DR) and Energy Storage (ES) in contexts other than reliability assessment. The modelling of these means of corrective control in the context of reliability assessment is largely absent.

2) The well-defined, widely applied existing indices have drawbacks of being 'partial-sighted' and 'non-representative', i.e., each of them quantifies only one aspect of power system reliability and may not represent overall reliability. Furthermore, economic analysis considering risk-associated cost is necessary

under corrective control. However, indices that quantify overall system reliability as well as the economic aspect in the context of increased system flexibility are lacking.

3) For the reason of simplicity, the assumption that different components are independent of each other is prevalent in reliability studies. However, apart from independent failures, corrective control devices are also subject to control system-originated failures. Previous work did not consider the impact of control system failure on power system reliability.

4) Whether the investment in flexibility offers higher system reliability as well as better benefit/cost ratio compared with investment in transmission was a question unanswered in previous publications. This question is critical for network planners and policy-makers when deciding the network reinforcement strategy.

In response to the trend towards a flexible network, the Supergen Flexnet (the 'Flexnet') research consortium was established in 2006, funded by Engineering and Physical Science Research Council (EPSRC), UK. This four-year research consortium (from 2007 to 2011) is a £7m project with four workstreams under which there are numerous sub-projects investigating the technical issues, economic issues, public acceptance and the roadmap towards a flexible network [9]. The fundamental objective of the 'Flexnet' is to help realise a flexible network that delivers electricity to customers in a secure, environmental friendly and affordable way [9]. One of the key research issues under the 'Smart, Flexible Controls' workstream is to study the impact of increased flexibility on power system reliability. And this thesis serves as the research output of this programme which is meaningful in practice: it demonstrates to policy-makers the power system risk level of investing in more flexibility rather than more transmission facilities; it also advises them about whether such risk associated with the transition is still manageable and whether more flexibility is economically favourable over traditional reinforcement.

Corrective control brings flexibility to the system. Corrective control, in the broad scope, includes all means that aim to 'correct' the problem after it has occurred, e.g., generation re-dispatch, spinning reserve and load shedding etc [6]. Conventional generation has serious drawbacks as a candidate for corrective control: they incur an

expensive operation cost; the carbon emission is substantial; and their ramp-up time is not negligible. Renewable generation such as wind generation is not suitable for providing corrective control either, since it is far less flexible than gas-fire plants. Load shedding, which incurs a potentially huge social cost and customer dissatisfaction, is normally the least favourable corrective action. By being flexible, environmental friendly and potentially cost-effective, the Flexible AC Transmission Systems (FACTS), Demand Response (DR) and Energy Storage (ES) are three promising means of corrective control. Therefore, the term 'corrective control' refers to the above three means in this project.

FACTS have become mature with the development of power electronics technology and have been widely deployed in real applications. They are expected to provide fast and robust control to system variables such as bus voltage and branch power flow. DR relieves system stress during peak time and under emergencies by serving as an alternative to spinning reserves. Installing a stand-alone ES device at load centre or integrating ES into intermittent generations may potentially be a cost-effective alternative to the investment of a new power line.

1.2 Aim and Objectives of the Research

Reliability is one of the critical criteria against which power system performance is assessed. It has rightly drawn much attention from system planners, network operators and researchers although it is taken for granted by ordinary customers in the developed world. A reliability issue is only recognised by the general public when there is an outage which has already triggered a serious social cost and widespread customer concern, even anger. Up till now, the prevailing 'N-2' rule in the UK has maintained a relatively reliable power system [1].

It is vital that the impact of corrective control on power system reliability is thoroughly investigated before the decision to transit from preventive control to corrective control is made because:

1) The last thing decision-makers would like to see is the widespread customer dissatisfaction against 'frequent' (a subjective feeling relative to the current status) power outages and chaos under corrective control;

2) It is critical to assess whether power system reliability is still in the acceptable range if corrective control replaces preventive control of building more transmission branches to maintain the system margin.

The aim of this research is therefore to assess the impact of corrective control on power system reliability, or stated in another way, to assess the impact corrective control has on system risk.

More specifically, this research has the following objectives:

1) ***To implement Active Management model into distribution system reliability assessment***

Active Management (AM) is a promising solution in accommodating increasing penetration of intermittent renewable generation. The configuration of AM system directly affects its ability in accommodating intermittent renewable generation as well as power system reliability. Furthermore, for AM to be a sustainable solution in the long term, it is expected to provide economic benefits for both the network operator and the owner of renewable generation. These issues have to be thoroughly investigated before the decision to adopt AM is made. Although existing publications paid some attention to AM, they left a vast space for further exploration. As a comprehensive corrective control application, AM deserves substantial research effort in this project. Therefore, the first objective of this research is to implement AM model into distribution system reliability assessment methodology and to assess the issues mentioned above. The research in AM serves as a support tool for decision makers to determine whether AM is a feasible long-term solution to accommodating increasing penetration of renewable generation.

2) ***To incorporate representative DR models in reliability assessment methodology***

As an essential element in the future flexible network, DR has received much attention from researchers. Work in this area is still ongoing. Although numerous papers and reports mentioned that DR improves power system reliability, yet few have presented a comprehensive analysis of power system reliability in the context

of DR. As a means of corrective control, DR warrants the research effort in thoroughly investigating its effect on power system reliability. And it is vital to model different types of DR programmes and to incorporate their models into reliability assessment methodology. Although DR programmes differ from case to case, they can be represented by a combination of three basic models. Therefore, one of the objectives is to implement representative DR models into reliability assessment methodology and to assess the impact of different DR scenarios on system reliability. The research then validates the DR models through case study and presents a comprehensive picture on the effect DR has on system reliability.

3) ***To develop reliability models of FACTS and ES devices***

Corrective control includes the application of FACTS and ES devices. In order to assess their impact on system reliability, it is necessary to develop their reliability models. FACTS and ES devices correspond to different behaviours in reliability studies and exhibit different characteristics in power flow studies. Therefore, their effects on system reliability are different. Previous work presented the state space models of SVC and STATCOM which are subject to scrutiny and modifications. Furthermore, the reliability models of BES and STATCOM/BES are lacking. Therefore, this objective is to model FACTS devices and ES devices, and implement these models into reliability assessment methodology to assess their impact on system reliability, and perform cost-benefit analysis considering risk-associated cost. The validity of these models is demonstrated in case studies.

4) ***To incorporate control system failure in reliability assessment of power systems under corrective control***

As is mentioned above, the assumption of independence is prevalent in reliability studies. It requires justification and should not be misused. In this project, local control devices including FACTS and ES devices are not independent of each other. Rather, they are subject to common cause failure (CCF) arising from corrective control system failure. This type of failure may affect system reliability. However, previous publications left a gap on this issue. Therefore, it is an objective to model control system failure, to implement it into reliability assessment methodology and to assess its impact on system reliability. The research considers the AM control

system, FACTS control system and ES control system in three different chapters and quantifies their impact on system reliability through sensitivity analysis.

5) To develop new user friendly fit for purpose reliability indices

Having identified the drawbacks of existing reliability indices, the aim of objective is to develop a new reliability index which represents overall system reliability by taking into account various aspects, and to visualise this index in a clear, friendly way. This research has achieved this objective and has demonstrated this index in case studies. Furthermore, economic analysis considering risk-associated cost is a necessary step in the study of corrective control as a type of network reinforcement. This requires new indices that take into account the economic aspect, and it is where previous work left a gap. Therefore, another objective is to develop indices that quantify the system reliability benefits of different types of network reinforcement. This research has tested these indices in case studies and demonstrated their value as an indispensable element in a comprehensive economic assessment of corrective control.

1.3 Main Thesis Contributions

This research has made substantial contributions and innovations in the area of reliability assessment of power systems under corrective control. They are summarised briefly below:

1) A comprehensive literature survey on reliability assessment of power systems

A comprehensive literature survey on reliability assessment of power systems has been undertaken and is presented in Chapter 2. The review also appears in later chapters as well. The review covers the major existing reliability assessment methodologies, the constraint optimisation issues, and the background of AM, FACTS, DR and ES. Based on this review, the gaps have been identified, some of which have been bridged in this thesis.

2) The development of new indices

Linear Weighted Reliability Index (LINWRI) as a composite index represents the overall system reliability considering multiple aspects. Demand Response

Incremental Cost Benefit (DRICB) represents the incremental monetary benefit in system reliability when one more unit of DR (expressed in MWh/year) is implemented. Incremental Benefit of Corrective Control (IBCC) represents the incremental benefit in reliability from incremental implementation of corrective control, whereas Incremental Benefit of System Reinforcement (IBSR) quantifies the incremental reliability benefit from incremental system reinforcement; Voluntary Energy Curtailment Level (VECL) represents annual voluntary energy curtailed as a percentage of annual total energy curtailed under emergency circumstances. The validity of these indices has been demonstrated in case studies. These indices are an indispensable element in reliability assessment under corrective control.

3) The modelling of control system failures

The control system failure is modelled as a common mode failure (CCF).

All FACTS and ES devices are subject to CCF, apart from their independent failures. The CCF model is implemented into chronological Monte Carlo simulation (CMCS) as the reliability assessment methodology. By varying the failure rate of the CCF, the impact of control system failure on system reliability has been investigated.

4) The development of state space models of BES and STATCOM/BES

Based on physical configurations, full state space models as well as simplified models of BES and STATCOM/BES have been developed. Although these models depend on a list of assumptions, the procedure of deriving these models is applicable under a general circumstance. These models have been implemented into the reliability assessment methodology.

5) The incorporation of risk-associated cost into the economic assessment under AM

An existing formula that was used for calculating the net benefit for Distribution Network Operator (DNO) has been updated with risk-associated cost implemented when performing economic assessment under AM. This formula takes into account the connection and AM service charges imposed on the owner of wind generation, the risk-associated cost, and AM investment cost, thus serving as the core of a comprehensive economic analysis.

6) The modelling of post-contingency behaviours of a distribution system

The post-contingency reactions of a typical distribution system have been modelled. These include the tripping of an upstream circuit breaker, the identification and isolation of the faulted component, and the network reconfiguration process. An algorithm that performs network reconfiguration has been developed. It is highly efficient for radial network. However, as a trade-off, it does not guarantee the optimal switching scenario where the number of affected load points reaches the minimum.

1.4 Thesis Structure

The thesis structure corresponds to the objectives mentioned above. It is summarised as follows:

Chapter 1 gives a brief overview of the research background, the comparison of traditional reinforcement and corrective control scenarios and the scope of corrective control in this project. The aim and objectives of this research are then identified followed by a brief summary of the contributions and the thesis structure.

Chapter 2 gives an in-depth review of existing work in the field of power system reliability. Established reliability assessment methodologies including State Enumeration Method (SEM), Monte Carlo Simulation (MCS) and Genetic Algorithm (GA) are reviewed in this chapter with their pros and cons summarised. The concept and methodology of constraint optimisation have also been reviewed followed by a summary of several toolboxes in Matlab for solving nonlinear optimisation problems.

Chapter 3 reviews the features of Supervisory Control and Data Acquisition (SCADA) system and the configurations of corrective control system. The reliability model of corrective control system is then proposed after introducing the definition of CCF.

Chapter 4 proposes five new indices after a brief review of existing reliability indices. These new indices are LINWRI, DRICB, IBCC, IBSR and VECL. Their definitions are presented in detail in this chapter.

Chapter 5 quantifies the reliability of distribution network under AM with Distributed Generations (DG). The concept and purpose of AM as well as its control system model

are introduced. Both the wind generation and AM control system model are integrated into the reliability assessment algorithm. The impact of AM control system failure on the overall reliability is quantified in the case study. The net benefits for both the owner of the wind generation units and the DNO are calculated.

Chapter 6 introduces the background of DR. Three typical models, the load shifting model, load reduction model and emergency interruptible load model are summarised and incorporated into the reliability assessment methodology. The LINWRI results for all scenarios are calculated with detailed discussions. DRICB and VECL results are also calculated for the test case. The impact of DR on power system reliability is then concluded from the case study.

Chapter 7 introduces the reliability model of FACTS devices as a means of corrective control and performs reliability assessment of a transmission network incorporating FACTS in the context of load growth. The LINWRI results for all scenarios are visualised on a reliability bar followed by detailed discussions. IBSR results are calculated as a critical part of the economic assessment. The impact of FACTS on power system reliability is concluded from the test case.

Chapter 8 starts by summarising the potential benefits and possible applications of ES through literature survey. Different ES technologies are then compared. This chapter also reviews the general configuration of ES which consists of the central storage, power transformation system and Charge-Discharge Control System (CDCS). The assumptions and full state space models of BES and STATCOM/BES are proposed. They are then simplified and applied in the reliability assessment of the power system. The LINWRI results and IBSR results are calculated for corrective control scenarios, the traditional reinforcement scenario and the reference scenario. The impact of ES on power system reliability is concluded from the test cases.

Chapter 9 gives an overview of the project followed by a summary of contributions and achievements of this research. Future work is also suggested in this chapter.

Appendix A presents the input data for the 16-bus test case used in chapter 5. These include the data of the network and corrective control devices, the load profile, and the reliability data of the central control unit. The results of economic analysis and the reliability results of the traditional reinforcement scenario are also given in Appendix A.

Appendix B presents the input data including the composite customer damage cost for the 16-bus test case used in chapter 6.

Appendix C presents the input data for the IEEE 24-bus Reliability Test System (RTS) used in chapter 7. These include the network data, the data of FACTS devices and the input data for economic analysis.

Appendix D gives the network data, the data of FACTS devices and the central control unit, and the load profile for Roy Billinton Test System (RBTS) used in chapter 8.

Appendix E gives the network data and the data of the STATCOM/BES and the central control unit for the Modified IEEE 24-bus Reliability Test System (MRTS) studied in chapter 8.

1.5 Conclusion

This chapter has summarised five major drivers for this research and identified the gaps from previous work in this area. The broad definition of corrective control has been introduced. However, its scope in this project has been clarified as including FACTS, Demand Response and Energy Storage. A brief introduction of the 'Flexnet' research consortium to which this project belongs has been given. The objective of the 'Flexnet', as its name suggests, is to investigate research issues associated with the transition towards a flexible network which is an essential element of a future smart grid. Based on this background and the gaps, the aim and objectives have been outlined. A summary of the main contributions of this work and the thesis structure were also given.

2 Concepts of Power System Reliability and Existing Methodologies

Summary

This chapter reviews the concept of reliability, the basic assumption, different types of reliability criteria, and the division of power system reliability for a structured calculation purpose. Established reliability assessment methodologies including State Enumeration Method (SEM), Monte Carlo Simulation (MCS) and Genetic Algorithm (GA) are reviewed in this chapter with their pros and cons summarised. The concept and methodology of constraint optimisation are also reviewed followed by a summary of several toolboxes in Matlab for solving nonlinear optimisation problems.

2.1 Concept of Reliability

Reliability is 'the ability of a component or a system to fulfil its expected functions for a specific period of time under the condition which it is designed to function' [10]. When applied to power systems, reliability is the ability to serve customers with the required amount of energy of required power quality [11].

Various probability distributions can be used in modelling random behaviours in reliability evaluation. These include Poisson distribution, normal distribution, exponential distribution, Weibull distribution and uniform distribution etc. Before further discussion, it is necessary to clarify the fundamental assumption adopted throughout this project: all components in power systems are in their normal operating life when the hazard rates are assumed to be constant [12]. Regular maintenance is conducted so that the above assumption remains valid: components are replaced before they enter the wear-out period when their hazard rates grow significantly through time.

Under this assumption, the exponential distribution is applicable. The justification is presented as follows [12].

1) Exponential distribution with constant failure rate provides necessary simplification of a problem which may be highly complicated by its nature;

2) Historical reliability data may be limited, from which it is not possible to determine the distribution. Therefore, using a more complicated distribution model is not justified by the availability of data; and

3) Different types of distributions make no difference if only system probability values are considered.

A key characteristic of exponential distribution is memory-less, i.e., the probability of failure in any given time interval is only dependent on the length of that period without being affected by prior operating status [12]. In other words, its history does not influence its present and future in any way.

2.2 Adequacy and Security

Reliability assessment is divided into two categories for a structured calculation purpose: adequacy assessment and security assessment [11]. Adequacy is defined as having sufficient generation, transmission and distribution capacities to supply customers with the amount of electrical energy they require without causing any violations to system constraints. This concept is in the steady state domain. Adequacy assessment is concerned about whether an adequate state exists or not. Whether such a state is accessible in the transitions is of no concern in adequacy assessment [11].

On the other hand, the concept of security focuses on whether a power system is capable of riding through dynamic disturbances, or in other words, whether a dynamic path to the final steady state exists following a disturbance [11].

2.3 Deterministic and Probabilistic Criteria

The deterministic reliability criteria have been applied in utility companies up till now. They are straightforward and clear enough for practice in the real world. Sufficient margin in generation and transmission capacity is reserved according to deterministic

criteria. Typical deterministic criteria in generation and network capacity are given below [11].

1) Generation capacity: installed capacity equals the maximum expected load plus a percentage of the peak load as margin.

2) Network capacity: 'N-m' (normally m=1 or 2) where the system can survive with up to m lines out of service at the same time.

In the UK, 'N-2' has been adopted in the transmission system [13]: the system can survive contingencies where up to two branches fail simultaneously without any system violations.

However, deterministic criteria are unable to account for the stochastic nature of system behaviours. According to [11], deterministic criteria arbitrarily assume certain hazard events and suggest precautions against them. It does not take into account the probability of these hazards. Nor does it ensure that all hazard events that contribute much (above a certain threshold) to the true risk are considered. They are not likely to result in an optimal solution where the total cost reaches the minimum. Overinvestment or underinvestment is likely under deterministic criteria. In short, they are not consistent in terms of risk evaluation. On the other hand, probabilistic criteria take into account the stochastic nature of power systems. They not only reveal the true risk by considering the probability of hazard events, but also enable a robust economic assessment which requires the computation of mathematical expectation.

There are still barriers that prevent decision-makers from adopting probabilistic criteria in practice. One of them is the lack of a comprehensive set of data [11]. A credible probabilistic assessment requires a large volume of data from which the means and standard deviations can be calculated. Historical records may not exist, or may not be of a credible sample, or may be confidential. However, this barrier is no longer true in some utility companies where a sufficient volume of applicable data exists for probabilistic evaluation.

Another barrier is the lack of incentive to transit from deterministic to probabilistic criteria. As far as the current criteria work perfectly well with no major disturbances or public pressure, network operators are prone to be conservative to changes. There is no incentive for them to replace the familiar, straightforward, well functioning deterministic criteria with the unfamiliar, complicated, 'risky' probabilistic criteria.

However, as power systems are expected to undergo revolutionary changes with the adoption of corrective control, the importance of probabilistic reliability assessment is greater than ever. A credible reliability level in the context of corrective control can only be evaluated with probabilistic methods. Furthermore, the question how corrective control affects power system reliability can only be answered through a comprehensive, credible probabilistic-based evaluation.

2.4 Hierarchy Levels of Power Systems

Because of the formidable physical size of power systems, it is almost impossible to conduct analysis on the generation, transmission and distribution system as a whole. As a simplification which enables a structured calculation, a power system is divided into three hierarchy levels according to their functioning zones. They are the generation system (Hierarchy level I or HLI), the composite generation and transmission system (HLII), and the whole system including the generation, transmission and distribution system (HLIII) [11].

When performing reliability calculations on HLI, the ability of the generation system to supply the demand is evaluated. All generation units are modelled as a bulk supply without considering the network [11].

On HLII, the ability to generate and the ability to pass the electrical energy through the network to load points are of the same importance. The network modelling is essential in HLII [11].

A distribution system is the ‘zoom-in’ image at the load point of the transmission system. On the distribution level, the interface between the distribution and the transmission system is the bulk supply point. It is a main concern whether each load can be supplied by the bulk supply or distributed generation (DG) through the distribution network.

2.5 Reliability Indices

This section briefly summarises existing reliability indices. A detailed revision is given in Chapter 4. These indices are categorised according to the hierarchy level to which they are normally applied, as presented in Table 2.1 [11].

Table 2.1: Typical reliability indices [11].

Name of index	**Definition**	**Hierarchy level which it is normally applied in**
LOLP (loss of load probability)	The probability that the load exceeds the available generation capacity	HLI
LOLE (loss of load expectation)	The expected number of days (or hours) in a given period of time when daily (or hourly) peak load exceeds the available generation capacity	HLI
LOEE (Loss of Energy Expected)	The total energy curtailed within a given period of time	HLI
EENS (Expected Energy Not Served)	The same as above	HLII
EIC (Expected Interruption Cost)	The interruption cost resulted from load losses	HLI & HLII
SAIFI (System Average Interruption Frequency Index)	The average number of outages a customer experiences within a period of time	Distribution systems
SAIDI (System Average Interruption Duration Index)	The average outage duration a customer experiences within a period of time	Distribution systems

Each existing index has its limitations. It reveals one facade of system reliability only. The ranking of an individual reliability index does not always correspond to the ranking of overall system reliability. In response to this problem, a new index called Linear Weighed Reliability Index (LINWRI) is proposed in this project. A detailed discussion is given in Chapter 4.

A few more indices are proposed in this research. They are Demand Response Incremental Cost Benefit (DRICB), Incremental Benefit of System Reinforcement (IBSR) and Voluntary Energy Curtailment Level (VECL). The former two focus on the economic aspect. DRICB and VECL are applied in the context of demand response (DR), whereas IBSR can be used in a general context of system reinforcement. These indices are demonstrated in detail in Chapter 4.

2.6 Reliability Assessment Methodologies

Methodologies for assessing the reliability of power systems can be put into two categories, analytical methods and simulation methods [11]. Three representative methodologies reviewed in this chapter are the state enumeration method (SEM), Monte Carlo simulation (MCS), and Generic Algorithm (GA). The first one is an analytical method, and the latter two are simulation methods.

2.6.1 State Enumeration

Analytical methods create mathematical models of a system based on the mechanism of the system. A commonly used analytical method is the SEM, which enumerates possible system states, evaluates the consequence of each state and aggregates the results to form the risk profile of the system. All mutually exclusive system states should be enumerated for an accurate result. In other words, the enumeration should be exhaustive. The total number of possible states increases exponentially with the system size until it finally becomes too prohibitive to enumerate. This phenomenon is called combinatorial explosion [14]. Therefore, simplifications should be made that only a limited number of states are enumerated according to a predefined filtering rule. For

example, only the states whose probabilities are greater than a certain threshold are enumerated, or only the states up to the second order failure are considered where at most two components fail at the same time. With a carefully chosen filtering rule, SEM can be faster than its alternative simulation method. However, the drawback is that some states with low probability but severe consequences may be ignored. There is no guarantee for 100% consistency for most filtering rules. A fast pre-screening technique was developed to promote consistency by ranking the states according to risk, but it is not free from misranking problems [15]. Moreover, SEM produces mathematical expectations only. It does not produce the shape of the distribution.

The ideal criterion to filter system states is to consider only the states whose contribution to risk indices is greater than a predefined threshold. An ideal contingency selection technique ranks all system states according to their contribution to risk indices with a high level of efficiency. These two goals, accuracy and efficiency often contradict each other. Therefore, a balance is necessary. Several contingency selection approaches were developed based on conventional power flow.

One of them is the Performance Index Method (PIM) where a representative index J is selected to describe the system [16]. J can be either the branch power flow index or the bus voltage index. J is calculated under normal conditions. When contingency occurs, J is calculated again. The difference between pre-contingency J and post-contingency J, or ΔJ, is calculated for each contingency. The magnitude of ΔJ is deemed to indicate the impact of the corresponding contingency on system operation conditions. A larger ΔJ corresponds to a larger impact the contingency state has on the risk of the power system. Therefore, the contingencies are ranked according to ΔJ. The threshold is specified to filter out the contingency states which make little contribution to risk indices.

A highly efficient method called costate method was developed to calculate ΔJ [15]. The control variable u is defined as a digital indicator: if component operates in normal state, $u = 1$; otherwise $u = 0$.

The performance index J is a function of control variable u and system state x [15].

$$J = f(x,u) \qquad \textbf{(2.1)}$$

Taylor expansion is performed. The first order approximation of post-contingency J is obtained. Therefore ΔJ can be calculated as illustrated in [16]:

$$\Delta J = J_{u=0} - J_{u=1} = -\frac{dJ}{du}\Big|_{u=1} \quad \textbf{(2.2)}$$

where $\frac{dJ}{du}$ is calculated by the costate method.

However, this method is vulnerable to misranking because of the error in ΔJ caused by the linearisation. For extremely nonlinear cases, the error may be substantial enough that the ranking of ΔJ is completely distorted.

A screening method is an alternative solution which is more accurate than PIM but less efficient [17]. This method is based on approximate power flow analysis technique such as Fast Decoupled Power Flow Solution. Because of the underlying assumption of the Fast Decoupled Power Flow Solution, its application is limited to high voltage transmission systems where the ratio of resistance to reactance is low.

A hybrid method was proposed as a balance between accuracy and efficiency: first the PIM is applied to select a set of contingencies; then the screening method is used to rank the contingencies in the set [17]. It is expected that the hybrid method takes benefits from both the PIM and the screening method.

2.6.2 Monte Carlo Simulation

Simulation methods are conceptually similar to conducting experiments. When an actual system is of a complicated nature, simulation methods reveal their advantage since they circumvent the barriers faced by analytical methods. The barriers include having to understand the mechanism of the system and to establish mathematical description accordingly. A typical simulation method is MCS. Its potential merit is revealed when dealing with large systems since it does not discriminate any system state. Therefore, it is consistent in risk assessment. Unlike the analytical method, those states with extremely low probability but lead to complete system black-out also have the opportunity to show up in MCS. Furthermore, chronological MCS (CMCS) provides a more informative set of indices than analytical methods: time-related indices and the distribution of indices through years can be obtained by CMCS. However, MCS may impose greater computational burden than filtered SEM since a sufficiently large number of experiments have to be conducted before the result converges. MCS may not be able to reach the same accuracy level as the analytical method since the result varies

with each sampling. One more sampling does not guarantee a more accurate result due to the stochastic nature of this methodology.

Three types of MCS are introduced in [11]. They are state sampling, state duration (CMCS), and state transition sampling. State sampling approach samples system states by their probabilities. A system state is the combination of the state of each component. Unlike CMCS, state sampling does not consider chronological behaviour of components. Because any two samplings are independent of each other, state sampling does not store results of previous samplings so that disc space can be saved. Instead, it merely updates risk indices in this process. Therefore, it does not produce frequency or duration-related results.

To the contrary, the CMCS approach provides comprehensive results including the frequency and duration-related results but requires more disc space than state sampling. In CMCS, the chronological behaviour of each component is simulated and sampled. The system sequential behaviour is the combination of the behaviour of each component. System analysis is performed for system behaviour over the entire time sequence, and risk indices are updated in the process. The CMCS approach is explained in detail below:

Random numbers are generated to simulate the sequential behaviour of every component. Suppose that a component represented by the two-state model is residing in the up state initially. A random number U_1 is generated, and the time to failure (TTF) is expressed below [11].

$$TTF = -\frac{1}{\lambda}\ln U_1 \qquad \textbf{(2.3)}$$

When t=TTF, the component enters the down state. The second random number U_2 is generated, and the time to repair (TTR) is calculated:

$$TTR = -\frac{1}{\mu}\ln U_2 \qquad \textbf{(2.4)}$$

When t=TTF+TTR, the component returns to the up state. The third random number is generated, and the whole process repeats until a sufficiently long sequence of behaviours is simulated.

A similar technique can be applied to components with a multi-state model. A component represented by the three-state model has a normal state, a derated state and

an outage state. Suppose that its initial state is the normal state. Two random numbers, U_1 and U_2 are generated. TTF and the time to derated state (TTDS) are given below.

$$TTF = -\frac{1}{\lambda_1} \ln U_1 \quad \textbf{(2.5)}$$

$$TTDS = -\frac{1}{\lambda_2} \ln U_2 \quad \textbf{(2.6)}$$

If TTF<TTDS, the component enters the failure state when t=TTF. Otherwise the component enters the derated state when t=TTDS. Then another two random numbers are generated, and the process repeats until a sufficiently long sequence of component behaviours is simulated.

The system behaviour is obtained by convolving the behaviour of each component. At any given time, the snapshot of the system state is the aggregation of each component state. An optimisation with a customised objective function is then performed on the system state at every hour. Reliability indices are updated based on the results of the optimisation. After passing the threshold hour in the simulation, a convergence check is performed by comparing the standard deviation of a series of results with the predefined threshold. If the former is less than the latter, the results are deemed converged, and the algorithm outputs all results; otherwise, the algorithm goes back and continues the simulation until the results later converge or the algorithm reaches the maximum number of hours.

2.6.3 Genetic Algorithm

As a reliability assessment methodology, Genetic Algorithm (GA) simulates the nature of evolution where adaptive chromosomes (individuals) survive through generations [18]. Chromosomes experience crossovers and are subject to mutations. A fitness function is applied for selecting adaptive individuals. GA traces the failure states where load curtailment is most likely to occur. In this context, the term ‘adaptive’ means the

ability to lead to load curtailment which contributes to risk indices. Later generations are expected to have more chromosomes that are adaptive. This method circumvents the enumeration of prohibitive number of system states. It is applied in [18] where DC optimal power flow method calculates the load curtailment of each selected state. GA is found to be superior over MCS due to its intelligent search ability in [18].

Chromosomes bearing different genes fit the environment to different degrees. The fitter ones have greater chances to survive and crossover (or 'mate'), thus to pass on their adaptive gene series to the next generation, which is subject to random but often minor 'mistakes' in the reproduction process (this phenomenon is called 'mutation'). Mutation may either improve or degrade the fitness of a chromosome. However, 'weak' chromosomes with a small fitness value are not without a change to survive. They may have some 'fit' gene coding that is potentially beneficial to future generations. This is the reason for not completely eliminating the survival chance of the 'weak' chromosomes.

A basic GA algorithm consists of the following steps [18]:

1) Initialisation: an initial population of chromosomes are randomly generated. The status of each component is indicated by the chromosome;

2) Selection: fitness is normally defined as the product of the probability and the amount of active load curtailment. The probability and the fitness value of each chromosome are assessed. Chromosomes are randomly selected to survive based on their fitness values. The resulting population is the parent generation;

3) Crossover: chromosomes are randomly paired. They crossover with each other. The resulting population is the child generation;

4) Mutation: a number of chromosomes from the child generation are randomly chosen. A random gene of each selected chromosome is altered;

5) The parent generation and the child generation form a single population. The process then goes back to step 2 until the stopping criteria is met;

6) During the above steps, the probability and the fitness value of each chromosome ever appeared are stored in a matrix. The fitness values are summed up, and the result is the 'fitness' of the power system (The fitness result is EENS, if the fitness for individual chromosome is defined as the amount of active load curtailment).

There are several selection approaches that can be used in step 2 [19]. The roulette wheel approach is one of the stochastic selection approaches. Each time the wheel is spun, a chromosome is selected for crossover [19]. This process repeats until a sufficient number (pre-specified) of chromosomes are selected. The fitter chromosomes have a larger share of the wheel, so that the 'ball' is more likely to fall into this share. 'Weak' chromosomes still have a small positive share: there is still a chance for them to survive.

The tournament approach is an alternative stochastic selection approach: it runs several 'tournaments' among a few randomly chosen chromosomes. The fitter ones win the 'tournaments' and are selected for crossover. Weak chromosomes have a small chance to win when the tournament size is large enough [20].

Various crossover techniques exist, e.g., the one-point crossover, two-point crossover and "cut and splice" crossover [19]. A series of data between the parents is swapped to produce two new offspring. The techniques mentioned above are different ways to determine which part of data to be swapped. For example, the two-point crossover technique randomly chooses two points between which all data are swapped. This technique does not change the length (number of genes) of the chromosome. Crossover allows the fitter gene series to be passed on to the offspring. Thus, the overall fitness of the next generation improves.

There are different stopping criteria [18]. One of the simplest ways is to define the maximum number of generations: when reaching this number, the iteration automatically terminates. Another stopping criterion is explained as follows: when the change in EENS brought by an incremental generation of chromosomes is below a threshold, EENS is deemed converged and GA iteration ends. In practice, the above two criteria can be mixed: after a certain number of iterations, the EENS result is checked for convergence. If the EENS result converges, GA process then terminates.

2.7 Optimisation

2.7.1 Optimisation for State Analysis

After the system state is obtained, the state is then analysed with an optimisation algorithm.

Load flow analysis is performed on the system state, and violations are checked. If a violation occurs, an optimisation to minimise the consequence of load curtailment is often called. Load flow analysis and the optimisation can be based on either DC or AC load flow [21]. AC load flow produces more accurate results than DC does, whereas DC load flow is more efficient because it considers real power only. Normally, DC load flow analysis and DC optimisation are sufficient for system planning [11]. Because the bottleneck to achieving a high level of accuracy is load uncertainty, it is rather meaningless to run AC load flow for accuracy improvement which is largely compromised by load uncertainty. Furthermore, AC load flow is subject to non-convergence problem because of the nonlinear nature. On the other hand, DC load flow is more robust in the sense that it always yields a result with no convergence problem. However, DC load flow is incapable of dealing with FACTS devices that regulate the voltage, since the voltage is assumed to be 1.0 per unit under DC load flow. Under this circumstance, AC load flow is necessary.

A summary of the pros and cons of AC and DC load flow is given in

Table 2.2:

Table 2.2: Pros and cons of AC load flow and DC load flow.

	Pros	Cons
AC load flow	1) more accurate, if data uncertainty is not considered 2) capable of dealing with voltages and network devices that regulate voltages	1) slow; 2) may not converge.
DC load flow	1) efficient 2) no convergence problem	1) less accurate 2) not capable of dealing with voltages or devices that regulate voltages

The optimisations under DC and AC are the same in concept: to achieve the minimum amount of load curtailment or the minimum cost of load curtailment while satisfying power balance and physical limits of system components. The DC optimisation model is presented below [21].

$$\min \sum C_i \qquad \textbf{(2.7)}$$

subject to

$$\mathbf{T(S)} = \mathbf{A(S)}(\mathbf{P_g} - \mathbf{P_l} + \mathbf{C}) \qquad \textbf{(2.8)}$$

$$\sum P_{gi} + \sum C_i = \sum P_{li} \qquad \textbf{(2.9)}$$

$$P_{gi}^{\min} \le P_{gi} \le P_{gi}^{\max} \qquad \textbf{(2.10)}$$

$$0 \le C_i \le P_{li} \qquad \textbf{(2.11)}$$

$$\left|T_k(S)\right| \le T_k^{\max} \qquad \textbf{(2.12)}$$

where C_i and $\mathbf{C}$ are the load curtailment at bus i and the load curtailment vector, respectively. $\mathbf{T(S)}$, $\mathbf{A(S)}$, $\mathbf{P_g}$ and $\mathbf{P_l}$ are the real power flow vector, the relationship matrix, the real power generation vector and the load vector, respectively. P_{gi} and P_{li} are the real power generation and the load at bus i. $T_k(S)$ and $T_k^{\max}$ are the power flow and the maximum power flow in branch k. The power balance is expressed by (2.9). The component and load constraints are expressed by (2.10) – (2.12).

The AC optimisation model is expressed below with the assumption that the power factor remains constant when load curtailment is performed [21].

$$\min \sum C_i \qquad \textbf{(2.13)}$$

subject to

$$P_{gi} - P_{li} + C_i = P_i(\mathbf{V}, \boldsymbol{\theta}) \qquad \textbf{(2.14)}$$

$$Q_{gi} - Q_{li} + C_{qi} = Q_i(\mathbf{V}, \boldsymbol{\theta}) \qquad \textbf{(2.15)}$$

$$C_{qi} = \frac{C_i}{P_{li}} Q_{li} \qquad \textbf{(2.16)}$$

$$0 \le C_i \le P_{li} \qquad \textbf{(2.17)}$$

$$P_{gi}^{\min} \le P_{gi} \le P_{gi}^{\max} \qquad \textbf{(2.18)}$$

$$Q_{gi}^{\min} \le Q_{gi} \le Q_{gi}^{\max} \quad \textbf{(2.19)}$$

$$T_k(\mathbf{V},\boldsymbol{\theta}) \le T_k^{\max} \quad \textbf{(2.20)}$$

$$V_i^{\min} \le V_i \le V_i^{\max} \quad \textbf{(2.21)}$$

where C_i, P_g and T_k are the same as those defined in the DC optimisation model. Q_{gi}, Q_{li} and C_{qi} are the reactive power generation, the reactive load and the reactive load curtailment, respectively. $P_i(\mathbf{V},\boldsymbol{\theta})$ and $Q_i(\mathbf{V},\boldsymbol{\theta})$ are the real and reactive power injection at bus i, respectively. $\mathbf{V}$ and $\boldsymbol{\theta}$ are the voltage magnitude and angle vector, respectively. The power balance is expressed by (2.14) and (2.15)

2.7.2 Constraint Optimisation: Concept and Methodology

Before discussing the algorithms for solving optimisation problems, it is necessary to review the concept of constraint optimisation.

Constraint optimisation aims to achieve the best outcome (the maximisation or minimisation of the objective function) subject to a set of constraints. A maximisation problem can be converted to a minimisation problem, which is represented by the following general model consisting of *n* equality constraints and *m* inequality constraints [22]:

$$\min \quad f(\mathbf{x}) \quad \textbf{(2.22)}$$

$$\text{subject to} \quad g_i(\mathbf{x}) = c_i \qquad i = 1,...,n \quad \textbf{(2.23)}$$

$$h_j(\mathbf{x}) \le d_j \qquad j = 1,...,m \quad \textbf{(2.24)}$$

For linear optimisation, the objective function and constraints are all linear. For nonlinear optimisation, either the objective function or at least one of the constraints is nonlinear.

Typical analytical solutions to constraint optimisations are the branch and bound solution, simplex algorithm, interior point and active set, etc. There are also simulation-based solutions such as GA, simulated annealing and particle swarm.

The branch and bound solution is an enumeration approach which discards a large subset of non-optimal ('fruitless') candidate solutions by branching, bounding and

pruning [23]. This approach is only applicable when a problem has limited number of feasible solutions. For a general constrained minimisation problem, this method searches within the feasible solution set (the 'feasible set'). The 'feasible set' is continually divided into smaller subsets (the 'branching' process). The upper and lower bounds of each subset are calculated. This is a recursive process. Those subsets of which the lower bound is greater than the upper bound of another subset are 'fruitless' and are discarded (the 'pruning' process). In this way, the number of subsets that should be considered is significantly reduced. The optimal solution is found when the subset reaches a 'single' value, i.e., a set where the difference between the upper bound and the lower bound is lower than a pre-specified threshold [22].

Matlab provides a number of optimisation toolboxes which are capable of solving linear/nonlinear/integer optimisation problems. For linear optimisation, two algorithms used in Matlab are the simplex algorithm and interior point algorithm [24].

The simplex algorithm considers the standard linear optimisation model (SLOM). Non-standard linear models can be converted to SLOM by introducing slack variables and surplus variables [22]. The SLOM is presented below [22]:

$$\min \quad z=\mathbf{c}^{\mathrm{T}}\mathbf{x} \tag{2.25}$$

$$\text{subject to} \quad \mathbf{Ax}=\mathbf{b} \tag{2.26}$$

$$\mathbf{x} \geq 0 \tag{2.27}$$

$$\text{where } \mathbf{x}=(x_1, x_2, ..., x_n)^{\mathrm{T}} \tag{2.28}$$

$$\mathbf{c}=(c_1, c_2, ..., c_n)^{\mathrm{T}} \tag{2.29}$$

$$\mathbf{A}=(a_{ij})_{m\times n} \qquad (m \leq n;\ \mathbf{A} \text{ has a full row rank}) \tag{2.30}$$

$$\mathbf{b}=(b_1, b_2, ..., b_m)^{\mathrm{T}} \qquad (b_i \geq 0 \quad i=1,2,...,m) \tag{2.31}$$

$\mathbf{x}$, $\mathbf{c}$, $\mathbf{A}$ and $\mathbf{b}$ are the decision vector with decision variables, the coefficient vector, the equality constraint matrix and the right hand nonnegative vector, respectively.

The feasible solution space is determined by the equality constraint and the nonnegative inequality constraint in SLOM. If $m=n$, the feasible solution can be calculated directly from the equality constraint $\mathbf{Ax}=\mathbf{b}$. In a more general circumstance where $m<n$, a group of solutions may be found (or no feasible solution exists) by solving $\mathbf{Ax}=\mathbf{b}$ after assigning the values of $n-m$ decision variables (in all possible combinations) as zero. This group of solutions is called basic solutions. Any basic solution is a basic feasible

solution which is at least a local minimum if it is a feasible solution to the SLOM. The global optimal solution can be found by comparing the values of the objective function where each basic feasible solution is substituted for $\mathbf{x}$ in (2.25) [22].

The interior point algorithm is used in Matlab for linear optimisation of large-scale problems. As an iterative process, it approaches the optimal solution from within the feasible region. It has an advantage in speed for large-scale problems with millions of variables [22]. This project does not involve large-scale problems and does not apply the algorithm.

The active set algorithm is used in Matlab for both quadratic optimisation and linear optimisation. Define a quadratic problem as follows [22]:

$$\min \quad f(\mathbf{x}) = \frac{1}{2}\mathbf{x}^{\mathrm{T}}\mathbf{H}\mathbf{x} + \mathbf{c}^{\mathrm{T}}\mathbf{x} \tag{2.32}$$

$$\text{subject to} \quad \mathbf{A}\mathbf{x} \le b \tag{2.33}$$

The active set at x is the set of constraints that are active. Equality constraint is always active, whereas inequality constraint $g_i(x) \ge 0$ is only active at x when $g_i(x) = 0$. The active set method searches for Karush-Kuhn-Tucker (KKT) point of the quadratic problem through an iterative process. Details can be found in [22, 25]. Its basic procedure is illustrated below [22, 25].

1) First start from a feasible point;

2) In the k th iteration with solution $\mathbf{x}_k$, the iterative increment $\mathbf{d}_k$ is found by solving the equality problem defined by the corresponding active set J_k.

3) If $d_k \neq 0$, determine α_k ($0 \le \alpha_k \le 1$) and let $\mathbf{x}_{k+1} = \mathbf{x}_k + \alpha_k \mathbf{d}_k$. If $\alpha_k = 1$ and $J_{k+1} = J_k$, $\mathbf{x}_{k+1}$ is a feasible solution. Otherwise if there is $p \notin J_k$ which satisfies $\alpha_p \mathbf{x}_{k+1} = \mathbf{b}_p$, p should be added to the active set, i.e., $J_{k+1} = J_k \bigcup \{p\}$. In this case go back to step 2;

4) If $d_k = 0$, $\mathbf{x}_k$ is the KKT point of the equality problem. If all Lagrange multipliers of the equality problem are nonnegative, $\mathbf{x}_k$ is the KKT point of the quadratic problem, and the iteration terminates. Otherwise $\mathbf{x}_k$ is not the KKT point of the quadratic problem,

and the procedure goes back to step 2 after deleting the equality constraint(s) of which the Lagrange multiplier(s) is (are) negative.

Sequential quadratic programming (SQP) is an optional algorithm that Matlab provides for small/medium scale nonlinear optimisation. By approximating the Lagrange function with a quadratic function, the nonlinear problem is converted into a quadratic problem which can be solved using the active set method. The SQP consists of three steps. Details can be found in [22, 26].

1) Solve the quadratic sub-problem;

2) Calculate the step length using linear search;

3) Determine the formula used in iteration.

Some of the optimisation functions in Matlab are summarised in

Table 2.3 [22].

Table 2.3: a summary of some optimisation functions in Matlab

Function name	**Problem type**	**Annotation**
Linprog	Linear optimisation	Three options of algorithms, i.e. the simplex algorithm, active set algorithm and interior point. The first two are for small and medium scale problem. The last one is for large scale problem only.
Quadprog	Quadratic optimisation	Active set method for small and medium scale problem. Trusted region method for large scale problem.
Fmincon	Nonlinear optimisation	SQP for small or medium scale problem. Trusted region method for large scale problem.

Analytical methods are generally faster than simulation methods because the former have the ability to find the direction towards the minimum by evaluating the gradient.

The 'fmincon' function is applicable to nonlinear problems whose objective function, constraints, and first derivatives are all continuous [27]. It does not always find the global minimum because of the nonlinear nature of the problem, unless

i) the global minimum is the only minimum; and

ii) the objective function is continuous [27].

Oscillatory objective function prohibits 'fmincon' from finding the global minimum [27]. For other types of problems with more than one 'valleys' but only one 'global valley', 'fmincon' function may be trapped in the 'local valley', depending on the initial value. A closer initial value to the global minimum is likely to enhance the chance of finding the global minimum. The 'fmincon' function may sometimes output 'no feasible result', if the initial value provided by the user is far from reasonable. For example, let the bus voltage be 1.5 pu. This highly unrealistic value may result in 'fmincon' reaching the maximum number of iterations with an output of 'no feasible result'. When 'fmincon' is applied for optimisation of the power flow, a flat start, i.e., 1.0 pu bus voltage magnitude and 0^{o} voltage angle yields a minimum (at least a local minimum but global minimum is not guaranteed) in practice. For basic load flow analysis, the result from 'fmincon' is proved to be the same as that obtained by Newton-Raphson method. In this way, the 'fmincon' function is validated.

Apart from analytical methods, there are also simulation methods for optimisation problems. GA is one of them. In previous sections, GA was presented as a reliability assessment methodology. When GA is applied for optimisation, the basic procedure is similar to that mentioned before.

GA is applied to various types of problems including linear optimisation, nonlinear optimisation and mix-integer/pure integer optimisation. When solving different types of optimisation problems, a general GA function can be applied for different types of problems. Compared with using a number of toolboxes, a general GA function reduces the workload of programming.

GA does not evaluate the gradient which may be hard to calculate in nonlinear problems. On the other hand, GA has disadvantages, some of which are shared with other methodologies.

1) There is no guarantee that GA always finds the global minimum. It depends on the initial range of chromosomes [28]. If the range is far from the global minimum point, it may not be possible for GA to find the global minimum. An example showing the effect of the initial range is presented in [28] and is also presented below:

$$f(x)=\begin{cases}-\exp(-(\frac{x}{20})^2) & \text{for x} \le 20\\ -\exp(-1)+(x-20)(x-22) & \text{for x>20}\end{cases} \quad \textbf{(2.34)}$$

which has a local minimum at $x=0$ and a global minimum at $x=21$.

Given the initial range of [0, 1] which is far from $x=21$, the experiment conducted by Mathworks clearly shows that GA fails to get anywhere near $x=21$, although the mutation function allows GA to explore beyond the initial range [28].

However, if the initial range is set as [0, 15], GA successfully finds the global minimum point at $x=21$.

2) GA approaches the minimum slower than analytical methods that use analytical/numerical gradients. Tens or hundreds of iterations are required before the result converges, whereas analytical methods may converge in several iterations.

3) More iterations in GA do not guarantee a better result because of the stochastic nature of GA.

4) GA cannot simulate digital (0 or 1) variables. This results in non-convergence because there is no 'hill' to climb [28].

Matlab offers a GA toolbox which allows users to scale down the fitness function. It also allows users to specify the mutation rate and the crossover fraction. However, this toolbox is not used in this project mainly because of its slow speed. In reliability assessment where GA for optimisation runs for hundreds of thousands of times, the computational burden becomes intolerable.

The "fmincon" function is used as the optimisation tool in this project for the following reasons:

1) it deals with nonlinear optimisation which is necessary when considering network voltages;

2) it imposes less computational burden than GA; and

3) it may sometimes yield local minimum, but this is a common weak point shared by nonlinear optimisation toolboxes.

Trying with different initial values improves the chance of finding the global minimum. However, it increases the computational burden, yet the finding of global minimum is still not guaranteed. A local minimum is at least a feasible solution. A 'perfect' optimisation tool with high efficiency and the capability of always getting the global minimum is still to be developed.

2.8 Existing Literatures on Power System Reliability

This section gives a brief review of the progress in the field of power system reliability based on literature survey.

A bibliography of papers before 1999 is presented [29]. According to [29], most papers (39 out of 42 papers and 2 out of 19 papers, respectively) in the categories of 'Composite generation-transmission system reliability evaluation' and 'Transmission and distribution system reliability evaluation' are in the scope of conventional reliability assessment. They consider traditional facilities including generation, branches, protection devices, HVDC and shunt capacitors.

In this section, existing publications are categorised in a different way from that in [29]. Representative papers are summarised as follows:

Category 1: Conventional Power System Reliability Assessment

A review of a general integrated structure for assessing power system reliability is presented in [30]. However, there is no consensus on which approach is the best for each hierarchy level. This paper specifically emphasises the importance of defining the time frame which ranges from milliseconds to a number of years [30]. Static reliability assessment is concerned about a time frame from a couple of hours to years, whereas

dynamic assessment is concerned about the dynamic transition period ranging from a cycle to minutes.

The basic framework for reliability assessment is presented in Figure 2.1 [30]:

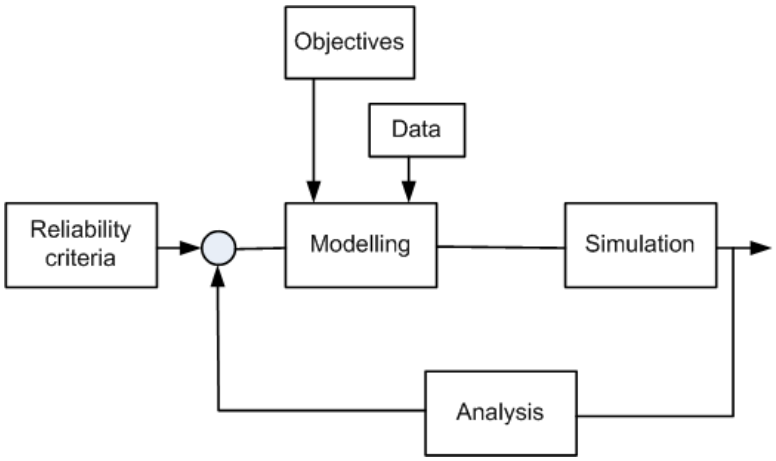

Figure 2.1: the basic framework for reliability assessment [30].

Detailed explanations of the terms in Figure 2.1 are presented below [30]:

1) Objective: this includes the hierarchy level that is of concern, the type of causes that result in failures, the consequences, and the time frame.
2) Data: they include issues such as data accuracy, data age, and the lack of a sufficiently large data sample for rare events, etc.
3) Model: this refers to state space models where crucial information needs to be captured while restraining the complexity within a manageable level.
4) Simulation: this refers to analytical approaches, MCS, or a hybrid of the two.
5) Analysis: this refers to reliability indices as simulation results.
6) Reliability criteria: include cost/benefit criteria, loss of load/energy, and legally binding criteria.

Not only the expected values of reliability indices are of concern, the probability distributions are of the same importance under the circumstance where variations of indices over a long period need to be considered. For example, delivery point indices, depending on network topology and operating philosophy are defined, and their probability distribution is obtained through CMCS [31].

Category 2: Power System Reliability incorporating Renewable Generation and Active Management

A number of papers focus on renewable generation and their impact on power system reliability.

A review is presented in [32]. This paper summarises the wind speed model (by Weibull function) and the output characteristic of wind turbines. It also reviews indices in the context of wind generation. They include Load Carrying Capacity Benefit Ratio (LCCBR), Equivalent Capacity Rate (ECR) and Wind Generation Interruption Cost Benefit (WGICB).

Compared with traditional generation, wind generation has special effects on power systems reliability [32]. They are summarised below.

1) The wake effect (the shadowing effect): wind generation units placed upstream of the wind direction affect the wind speed received by downstream wind generation units.
2) The correlation of wind speeds at different locations: this phenomenon is obvious in countries like the UK of which the geographical size is not large enough to justify uncorrelated wind speed. Therefore, wind farms across the UK are not independent of each other.
3) Effect of wind turbine parameters: parameters such as the rated power, cut-in speed and cut-out speed all affect system reliability.
4) Effect of the total wind generation capacity installed in the grid.
5) Effect of the environment: the environment will affect the reliability of wind turbines, thus affecting power system reliability.

Generation adequacy assessment with wind generation is performed in [33, 34]. The state space models of wind turbine generation are core innovations in these papers. The battery energy storage (BES) is integrated into wind generation, and generation adequacy assessment is performed in [35, 36].

The impact of wind generation on distribution network reliability is studied in [37], based on a three-state model of the wind turbine. It demonstrates that different

capacities of wind generation are needed at different locations, so that the same reliability level as that with traditional generation only can be maintained.

Reliability assessment of composite generation and transmission system with wind farms is performed in [38]. The maximum wind capacity that can be connected to the system is determined, and network reinforcement scenarios are proposed to accommodate more wind generation.

Category 3: Power System Reliability incorporating FACTS

There are relatively few publications on reliability assessment with FACTS devices. A reliability assessment methodology that incorporates FACTS devices is proposed in [39]. Unified Power Flow Controller (UPFC) is modelled by a three-state model, and the system is analysed with DC load flow.

The impact of FACTS devices on system security is summarised in [40]. The rules for the security purpose are listed as follows [40]:

1) 'N-1' criteria for FACTS devices, i.e., the loss of a single FACTS device will not lead to system collapse;
2) FACTS devices should be able to function upon credible contingencies;
3) FACTS devices should be designed in the way that there is no undesirable interaction with other devices in local vicinity.

Although the implementation of FACTS will introduce some risks, it is still better than the 'doing nothing at all' scenario which leaves the transmission system at risk in the context of load growth [40].

It is not possible to enumerate all relevant publications in this thesis. The above publications represent a clear trend: power system reliability assessment in a new context with increasing penetration of renewable generation, the implementation of FACTS, and the implementation of Energy Storage. In short, it is a trend to assess power system reliability in the context of a flexible network.

2.9 Conclusion

This chapter gave an in-depth review of existing work in the field of power system reliability. Three representative reliability assessment methodologies reviewed in this chapter are State Enumeration Method (SEM), Monte Carlo Simulation (MCS) and Genetic Algorithm (GA). Their pros and cons have been summarised.

The concept and methodology of constraint optimisation have also been reviewed. System contingency analysis under AC load flow is essentially a nonlinear optimisation problem. A summary of several toolboxes in Matlab for solving nonlinear optimisation problems was presented in this chapter.

3 Modelling of the Corrective Control System

Summary

This chapter reviews the definition of control systems and introduces the Supervisory Control and Data Acquisition (SCADA) system. Different configurations of control systems are summarised. The corrective control system is modelled by Common Cause Failure (CCF) to which all local control devices are subject.

3.1 Concepts of control systems and SCADA

A control system is defined as a device or a group of devices that monitor and command other devices. A closed loop control system where information is transmitted through a real-time network consists of four parts, categorised by their functions [41]:

1) sensors or measurement devices with the function to collect local information;

2) a central control unit, analogous to the 'brain' that analyses local information and suggests a control decision (Alternatively, the control decision can be made by man);

3) local control devices which execute the command from the central control unit; and

4) a communication system through which all information is transmitted.

In power systems, the type of control system is specifically called Supervisory Control and Data Acquisition (SCADA) system. Its definition, as is given by IEEE, emphasises remote monitoring and control [42, 43].

A SCADA system consists of the following subsystems [42]:

1) a human interface;

2) a supervisory system;

3) remote terminal units (RTU);

4) programmable logic controllers (PLC); and

5) a communication system.

A brief structure of the SCADA system is presented in Figure 3.1 [42].

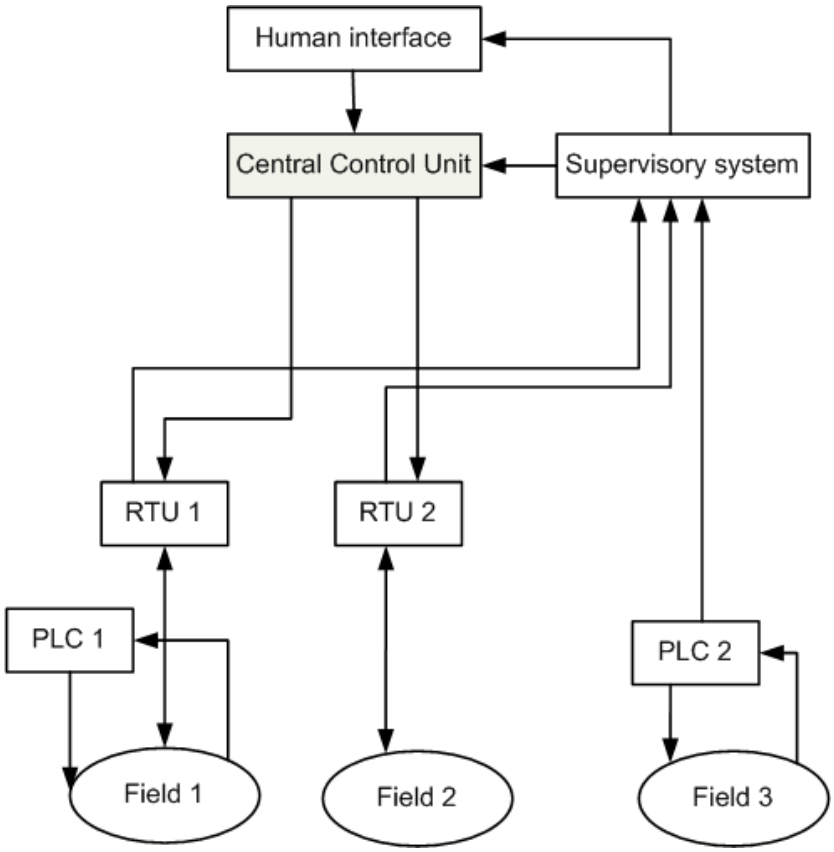

[Author's compilation]

Figure 3.1: Structure of the SCADA system [42].

In this structure, RTU serves as the 'eyes' and 'hands' of the central control unit (or the 'master station'). It converts the analogue data collected from local sensors to digital data which is then sent to the supervisory system. It also passes the command from the central control unit down to local devices. In most applications, RTU serves as the slave of the central control unit, i.e., it does not have the ability to make control decisions [42]. However, under some circumstances, optimisation functions can be implemented into RTU which will then be able to reach a control decision [42].

Not all devices are controlled by the central control unit. Some devices exercise autonomous control with a local control target. For example, a Static Var Compensator

(SVC) configured to operate independently of the central control aims to keep the local bus voltage magnitude at 1.0 pu. RTU is not necessary under this circumstance.

As a critical part of the SCADA system, the communication system is the media for all data flows. Its performance largely affects the software/hardware configuration of RTUs and the central control unit. It is a potential bottleneck in the SCADA system because of the constraint factors such as data transfer speed and noise [42]. Communication can be conducted via radio, microwave, telephone line, power line carrier system and fibre optics, etc [42].

3.2 SCADA serving as a Corrective Control System with FACTS

3.2.1 Corrective Control System Configurations

FACTS devices, implemented in power systems as a means of corrective control, serve as a part of the corrective control system (CCS). Four types of CCS configurations are introduced in this chapter.

1) One-on-one configuration [42]:

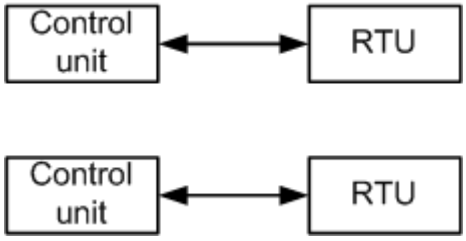

Figure 3.2: One-on-one configuration.

This is a decentralised configuration where each control unit corresponds to an RTU and achieves its own control target. However, this is not consistent with a transmission network where the central control room performs coordinated control in practice.

2) Star configuration [42]:

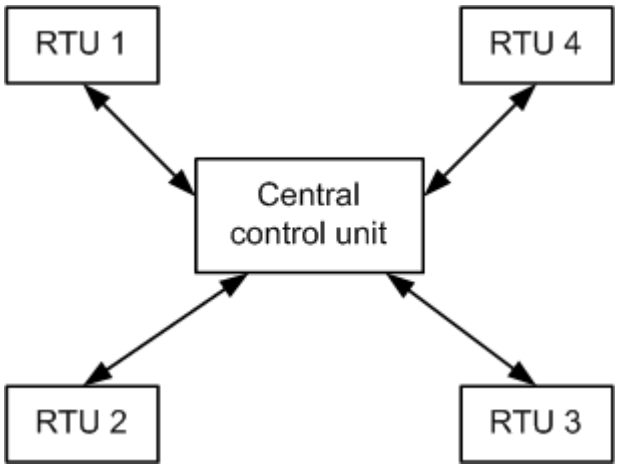

Figure 3.3: star configuration.

A central control unit controls all RTUs. Each RTU is connected to the central control unit with a dedicated communication channel. The failure of one communication channel does not affect other channels.

3) Party-line configuration [42]:

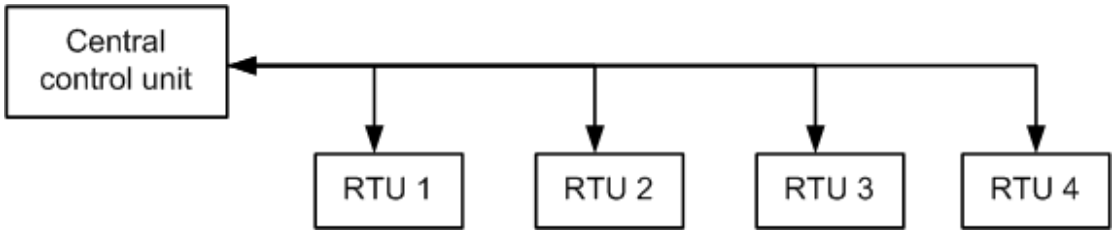

Figure 3.4: Party-line configuration.

A central control unit controls all RTUs which are connected to the central control unit with a common communication channel. Compared to 'star' configuration, this configuration may save investment cost in cables but at the price of poorer reliability. The failure of an upstream channel leaves all downstream RTUs out of control.

The communication channel may be combined with the failure of the central control unit, thus forming a single component which disables all RTUs when it fails. This simplification is applicable when the communication is conducted via radio.

4) Mixed ‘star’ and ‘party-line’ configuration [42]:

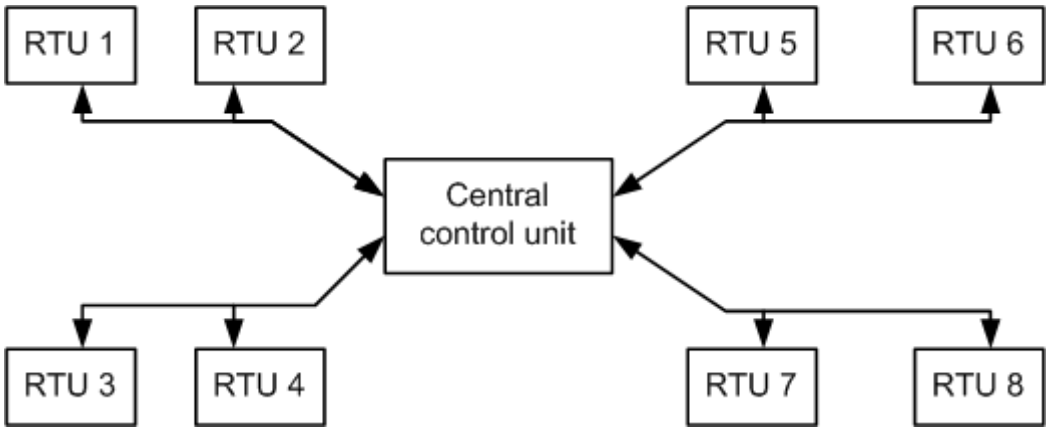

Figure 3.5: Mixed ‘star’ and ‘party-line’ configuration.

A central control unit controls all RTUs. Some of the RTUs are on the same communication channel whereas others are on different channels.

3.2.2 Reliability Model of CCS

Before introducing the CCS model, it is necessary to review the concept of dependent failure. Contrary to independent failure where probabilities can be multiplied, dependent failure is where a correlation exists among individual failures of which the probabilities cannot be multiplied. Dependent failure can be put into two categories as shown in Figure 3.6.

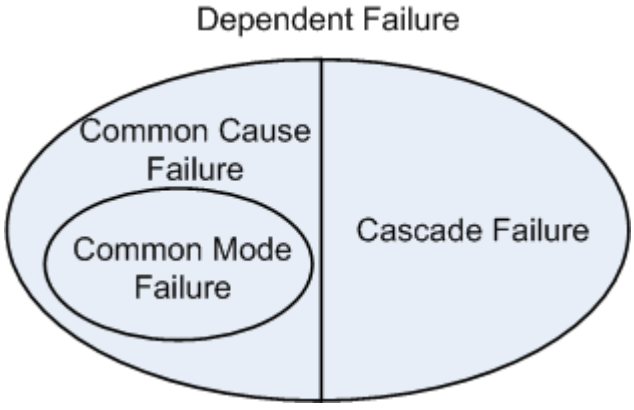

[Author’s compilation]

Figure 3.6: Gategories under dependent failure [44].

Common cause failure (CCF) is a type of dependent failure where multiple components fail due to a single common cause [44]. As a subset of CCF, Common mode failure emphasises that all components fail in the same mode.

Cascade failure is another type of dependent failure where the failure of one or some components triggers the failure of some other components. Their failure may further trigger the failure of more components. There is no common cause for cascade failure. To distinguish CCF from cascade failure, it is critical to ensure that the failures of multiple components are not consequences of each other in CCF.

The beta factor method is a straightforward approach for CCF modelling. It detaches CCF from independent failures. A β factor ($0 \le \beta \le 1$) is estimated from historical data: β (percentage) of the failure rate is attributed to CCF and $(1-\beta)$ to the independent failure [45, 46].

The multi-beta factor method is derived from the basic beta factor method. The multi0beta factor method corresponds to a triple redundant or higher system where there are combinations of failures. For example, a common cause trips only some of the components, whereas another common cause trips all. Each common cause is assigned a beta factor under this circumstance [45].

Previous literatures normally assume that all components (generation, lines and FACTS devices) of a power system are independent of each other. However, this is not true in this research, since FACTS devices are subject to CCF.

When the SCADA system is in a ‘party-line’ configuration, all FACTS devices are subject to CCF, i.e., the failure of the central control unit or the communication system. The outage of FACTS devices is the result of any one of the three types of failure, i.e., the independent failure, the central control unit failure and upstream communication channel failure.

The following assumptions have been adopted:

1) communication channels are independent of the central control unit; and

2) different communication channels are independent from each other.

Based on the configuration and the above assumptions, FACTS devices are not subject to the same CCF event as the upstream communication channel is relative to each FACTS device.

Figure 3.7 shows a party-line configuration where communication channels are numbered from 1 to 4.

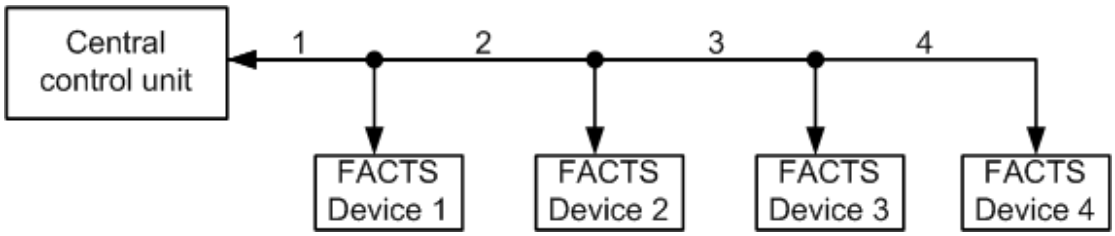

Figure 3.7: A 'party-line' example.

It is obvious from the example that the central control unit failure will disable all FACTS devices. As communication channel 1('channel 1') is the upstream channel of FACTS device 1-4 ('device 1-4'), its failure disables all FACTS devices. The failure of channel 2 only disables device 2-4 since channel 2 is the upstream channel of all FACTS devices except device 1. Similarly, the failure of channel 3 disables device 3 and 4, and the failure of channel 4 disables device 4 only. In general, the failure of a channel may not be the CCF for all FACTS devices but only some of them. In other words, FACTS devices are not completely coupled with each other.

The calculation of failure rates in a radial distribution system is demonstrated in [11]. The 'party-line' configuration is radial, and failure rates can be calculated in a similar way to that introduced in [11]. The failure rate of the end load point is simply the summation of the failure rates of all contributing failures, given that no auto-reconfiguration or protection failure is considered. However, there is a difference in the contributing failures: the assumption for the radial distribution network in [11] is that all failures trip the only circuit breaker upstream of all components, thus affecting all load points in the network. However, in this project, the above assumption is not valid, and the communication channel failure does not necessarily affect all 'terminals', i.e., FACTS devices. Take the same network topology shown in Figure 3.7 as an example. According to [11], the failure of line 4 will trip the circuit breaker on line 1, thus affecting all four 'terminals'. However, in this research, the failure of channel 4 does not affect FACTS device 1 – 3 but FACTS device 4 only.

The failure rate of a FACTS device is calculated below.

$$\lambda_{FACTS}=\lambda_{Self}+\lambda_{CCF}=\lambda_{Self}+\lambda_{Con}+\lambda_{UComm} \quad \textbf{(3.1)}$$

where λ_{Self} is the failure rate of the independent failure (self-originated) of a FACTS device. λ_{CCF}, λ_{Con} and λ_{UComm} denote the failure rate of CCF, the central control unit failure rate, and the upstream communication channel failure rate, respectively.

A fault tree is given in Figure 3.8 regarding the outage of a FACTS device.

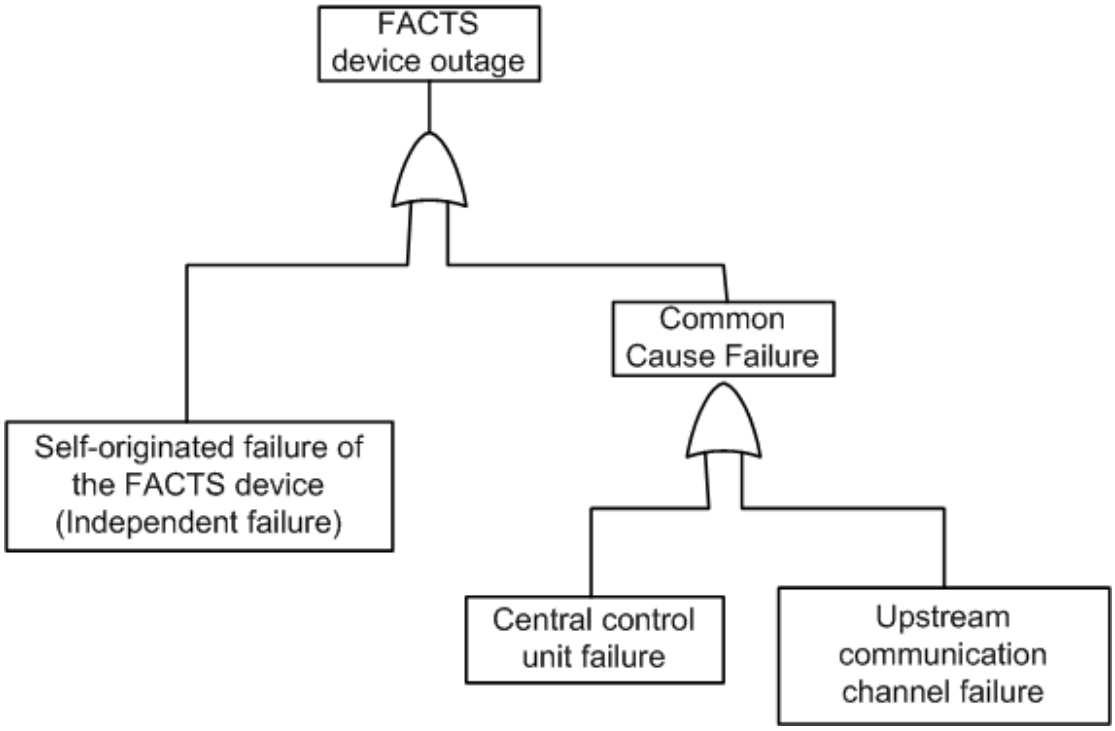

Figure 3.8: The fault tree for a 'party-line' system.

Take the same example as shown in Figure 3.7. The fault tree for the failure of FACTS device 3 is given in Figure 3.9.

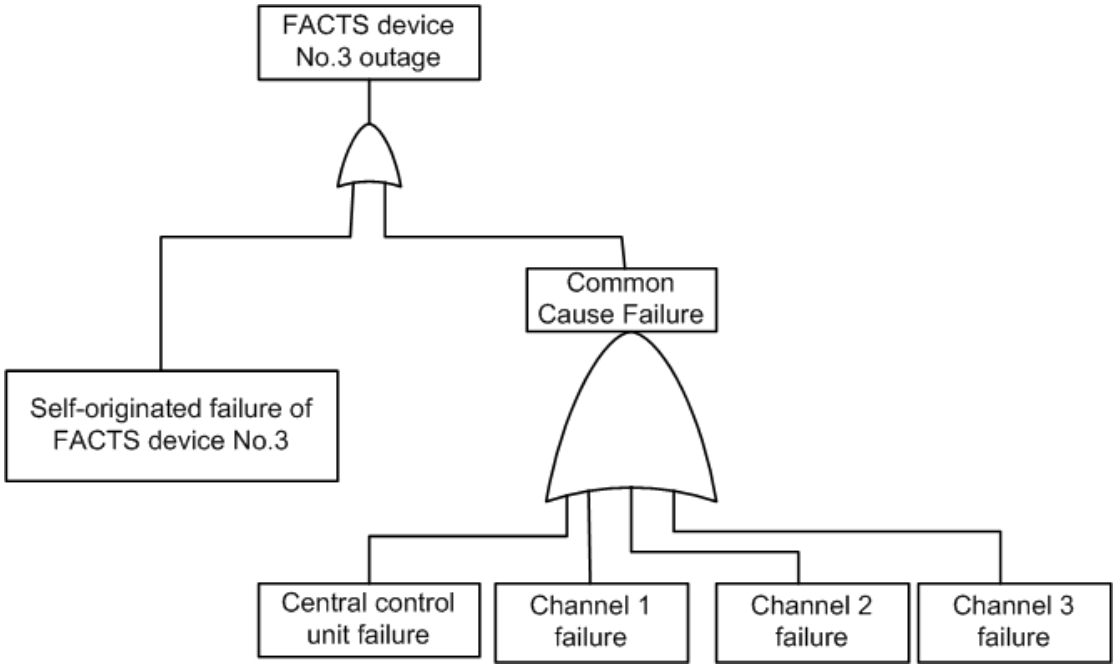

Figure 3.9: The fault tree for the failure of FACTS device No.3.

The upstream communication channel failures are different for each FACTS device. Instead of using a single beta factor, multiple beta factors are applied in this example. β_0 indicates the percentage that attributes to the central control unit failure; β_1, β_2, β_3 and β_4 correspond to the percentage that attribute to the failure of channel 1, 2, 3 and 4, respectively. The following equations hold true:

$$\begin{aligned}\lambda_{FACTS1} &= \lambda_{Con} + \lambda_{CH1} + \lambda_{Self\,1} \\ &= \beta_0\lambda_{FACTS1} + \beta_1\lambda_{FACTS1} + \lambda_{Self\,1}\end{aligned} \quad \textbf{(3.2)}$$

$$\begin{aligned}\lambda_{FACTS2} &= \lambda_{Con} + \lambda_{CH1} + \lambda_{CH2} + \lambda_{Self\,2} \\ &= \beta_0\lambda_{FACTS1} + \beta_1\lambda_{FACTS1} + \beta_2\lambda_{FACTS2} + \lambda_{Self\,2}\end{aligned} \quad \textbf{(3.3)}$$

$$\begin{aligned}\lambda_{FACTS3} &= \lambda_{Con} + \lambda_{CH1} + \lambda_{CH2} + \lambda_{CH3} + \lambda_{Self\,3} \\ &= \beta_0\lambda_{FACTS1} + \beta_1\lambda_{FACTS1} + \beta_2\lambda_{FACTS2} + \beta_3\lambda_{FACTS3} + \lambda_{Self\,3}\end{aligned} \quad \textbf{(3.4)}$$

$$\begin{aligned}\lambda_{FACTS4} &= \lambda_{Con} + \lambda_{CH1} + \lambda_{CH2} + \lambda_{CH3} + \lambda_{CH4} + \lambda_{Self\,4} \\ &= \beta_0\lambda_{FACTS1} + \beta_1\lambda_{FACTS1} + \beta_2\lambda_{FACTS2} + \beta_3\lambda_{FACTS3} + \beta_4\lambda_{FACTS4} + \lambda_{Self\,4}\end{aligned} \quad \textbf{(3.5)}$$

where subscript Con, CH and Self denote the ‘central control unit’, ‘channel’ and ‘independent (self-originated)’, respectively.

It is a different case when the communication system is combined with the failure of the central control unit. The failure of this single element disables all FACTS devices. This forms a single CCF, and a single beta factor is used to quantify this CCF.

$$\begin{aligned}\lambda_{FACTSi} &= \lambda_{Self\,i} + (\lambda_{Con} + \lambda_{Comm}) \\ &= \lambda_{Self\,i} + \beta\lambda_{FACTSi}\end{aligned} \qquad \textbf{(3.6)}$$

The corresponding fault tree is given in Figure 3.10.

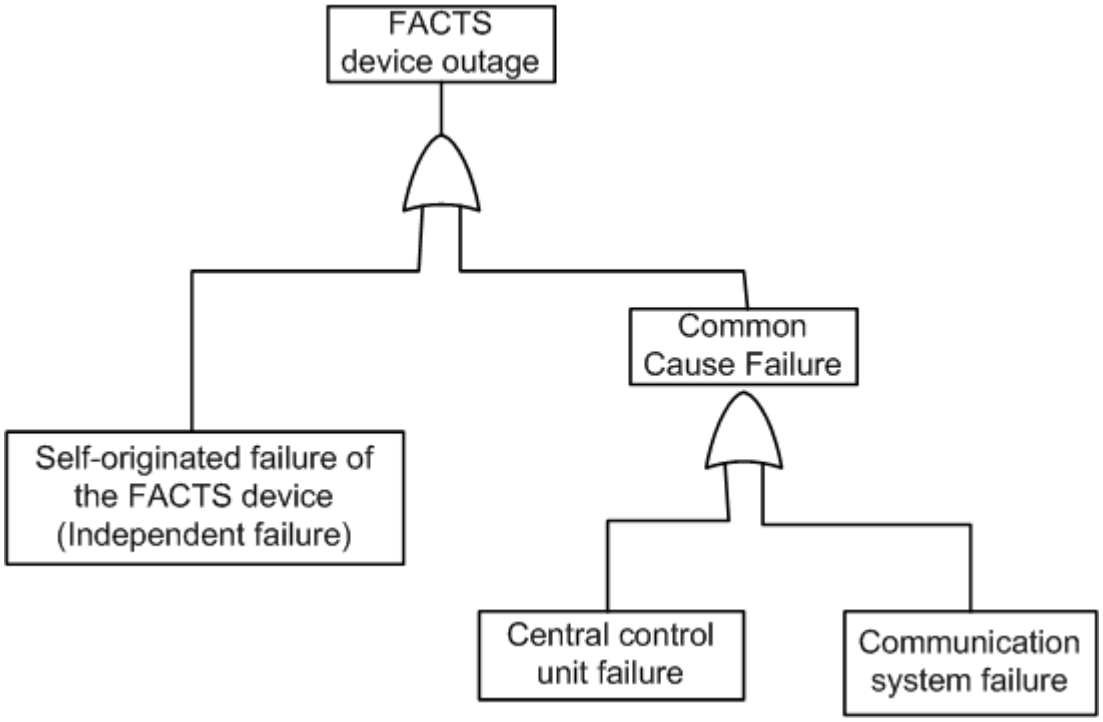

Figure 3.10: The fault tree for the simplified 'party-line' configuration.

When the control system is configured in a 'star' configuration, the difference is that the failure of a communication channel causes the outage of only one FACTS device that is connected to the channel. Under this circumstance, the CCF is the central control unit failure. Therefore, it is possible to combine the communication channel failure with the failure of the corresponding FACTS device. This forms a combined independent failure.

The failure rate of a FACTS device is calculated by

$$\lambda_{FACTS} = (\lambda_{Self} + \lambda_{Comm}) + \lambda_{CCF} \qquad \textbf{(3.7)}$$

where λ_{Comm} denotes the corresponding failure rate of the communication channel failure.

Its fault tree is presented in Figure 3.11.

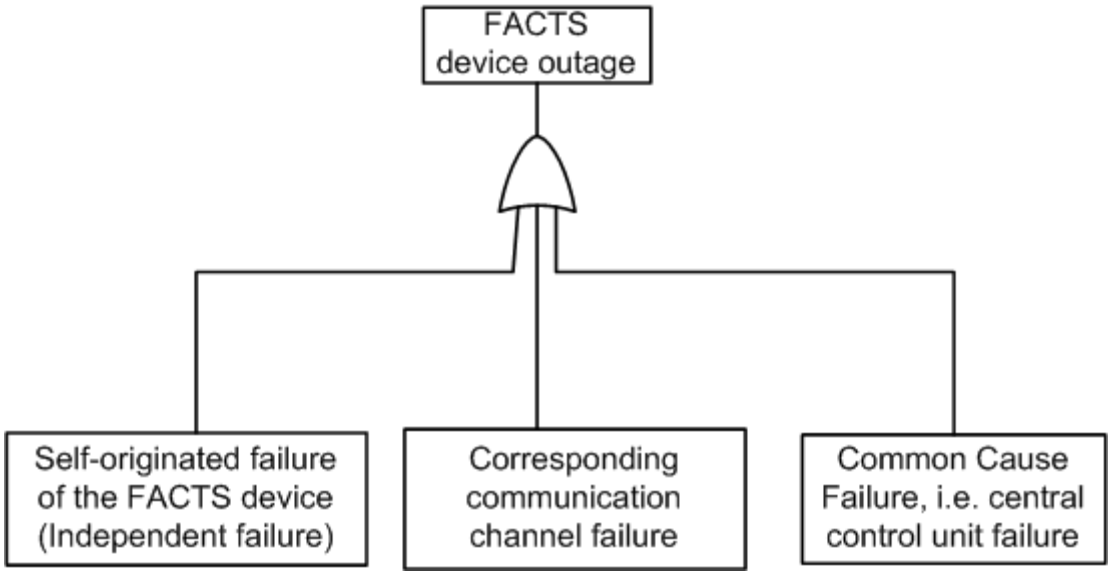

Figure 3.11: The fault tree for a 'star' configuration.

3.3 Conclusion

This chapter reviewed the features of Supervisory Control and Data Acquisition (SCADA) system and the configurations of corrective control system. Four configurations were reviewed including one-on-one configuration, 'star' configuration, 'party-line' configuration, and mixed 'star' and 'party-line' configuration. A simplified 'party-line' configuration was also presented. The definition of CCF and the beta factor method were introduced. The corrective control system was modelled as CCF.

4 New Reliability Indices under a Corrective Control Paradigm

Summary

This chapter reviews existing reliability indices through literature survey. The drawbacks of existing reliability indices and gaps are identified. In response to these drawbacks and gaps, new indices are proposed with their definitions explained in detail. They are Linear Weighed Reliability Index (LINWRI), Incremental Benefit from System Reinforcement (IBSR), Demand Response Incremental Cost Benefit (DRICB) and Voluntary Energy Curtailment Level (VECL).

4.1 Review of Existing Reliability Indices

A number of reliability indices were reviewed in Chapter 2. Different indices focus on different aspects, e.g., the amount of load/energy loss, average outage duration, the cost of outages, and the number of outages caused by voltage violations only, etc. It is necessary to know the focus and limitations of an index before applying it to real cases.

Indices in HLI can be put into two categories, i.e., loss-of-load indices and loss-of-energy indices [11]. Typical loss-of-load indices include Loss of Load Probability (LOLP) and Loss of Load Expectation (LOLE). LOLP represents the probability of the load exceeding the available generation capacity. LOLE quantifies the expected number of days (or hours) when daily (or hourly) peak load exceeds the available generation capacity in a year [47].

The calculation of LOLP requires that the probabilities of all mutually exclusive failure states in which the load is greater than available capacity be summed up. Given the table of the capacity outage probability and the load duration curve, the formula for calculating LOLE is presented below [11].

$$\text{LOLE} = \sum_{k=1}^{n} (t_k - t_{k-1}) P_k \quad \textbf{(4.1)}$$

where P_k denotes the cumulative outage probability for capacity state k. t_k is the number of time units that an outage magnitude of the k th state will result in load shedding.

Loss-of-load indices are concerned about whether load shedding occurs as well as the number of times it occurs, rather than how much the shortfall is in the available capacity. On the other hand, loss-of-energy indices are concerned about the shortfall in the available capacity. Loss of Energy Expected (LOEE) quantifies the total energy curtailed within a given period. This index is useful for energy-limited systems [11]. However, LOLP may be more of a concern than LOEE from a customer point of view [11].

Typical indices in HLII include Expected Energy Not Served (EENS) and Expected Interruption Cost (EIC). EENS is defined in a similar way to LOEE: the total energy curtailed within a period of time. EIC represents the cost of outages. It depends on the operation scenario and the cost function. A greater EENS of one system than that of another does not necessarily mean the former has poorer reliability, since EENS depends on the size (or the load level) of the system.

Typical indices in distribution systems are System Average Interruption Frequency Index (SAIFI), System Average Interruption Duration Index (SAIDI), Momentary Average Interruption Frequency Index (MAIFI), Customer Average Interruption Frequency Index (CAIFI), and the Average Service Availability Index (ASAI), etc [11].

SAIFI is the average number of outages a customer experiences within a year [11]. SAIDI is the average duration of outages a customer experiences within a year. MAIFI is defined in a similar way to SAIFI except that only momentary interruptions are counted. CAIFI is different from SAIFI in the way that only customers affected by interruptions are counted in the denominator. ASAI represents total customer hours when loads are served as a percentage of total customer hours when there is load [11].

$$\text{SAIFI} = \frac{\sum \lambda_i N_i}{\sum N_i} \quad \textbf{(4.2)}$$

$$\text{SAIDI} = \frac{\sum U_i N_i}{\sum N_i} \quad \textbf{(4.3)}$$

$$\text{MAIFI} = \frac{\sum \lambda_i^m N_i}{\sum N_i} \quad \textbf{(4.4)}$$

$$\text{CAIFI} = \frac{\sum \lambda_i N_i}{\sum N_i^A} \quad \textbf{(4.5)}$$

$$\text{ASAI} = \frac{\sum 8760 N_i - \sum U_i N_i}{\sum 8760 N_i} \quad \textbf{(4.6)}$$

where λ_i, λ_i^m, U_i, N_i and N_i^A denote the permanent failure rate of load point i, the momentary failure rate of load point i, the annual outage duration of load point i, the number of customers at load point i, and the number of customers affected by interruption at load point i, respectively.

The merit of the above indices is that they can be directly compared with each other. Take SAIFI as an example. Suppose $\text{SAIFI}_\text{A} = 0.02$ occ/year and $\text{SAIFI}_\text{B} = 0.04$ occ/year where subscript A and B denote system A and B, respectively. This clearly shows that an average customer of system B experiences twice as many times of outages as that of system A, although the two systems may have completely different topologies and network data.

However, each of the above indices reflects only one aspect of system reliability. The full spectrum of system reliability can only be revealed when different aspects are taken into account. For example, a small SAIFI value may be due to the result of a large number of customers in the system. Although the system seems reliable given SAIFI alone, this may not be true if other aspects are considered [11]. The explanation is given below.

1) There may be a small minority of customers who experience frequent outages, whereas the majority never experience any interruption at all. SAIFI fails to reveal this, whereas CAIFI can.

2) The momentary outage in the system may occur frequently – this is a problem that should not be neglected. SAIFI does not take this aspect into account.

3) The outage duration for an average customer in a year may be unacceptable, although the number of outages is small. Therefore, SAIDI is needed as a supplement to SAIFI.

Furthermore, different indices for two power systems may not show the same reliability ranking. Therefore, it is not sufficient to judge which system is more reliable merely from existing indices. Suppose $SAIFI_A > SAIFI_B$ and $SAIDI_A < SAIDI_B$, where subscript A and B denote system A and system B, respectively. It is not possible to judge merely from the two indices which system is more reliable than the other. In order to reach a conclusion it is necessary to specify how much each aspect of reliability is weighted. In other words, a clear mathematical definition of the term 'reliability' is required. Nonetheless, 'reliability' results are not directly comparable unless their mathematical definitions are the same.

4.2 New Reliability Indices

4.2.1 Linear Weighed Reliability Index

Traditional indices, e.g., SAIFI, SAIDI, MAIFI and EENS etc, have the drawback of being 'partial-sighted' and 'non-representative'. Linear Weighed Reliability Index (LINWRI) overcomes the drawbacks. Analogous to a stock market index that represents the stock market, LINWRI represents overall system reliability.

The following conditions are applied in this project.

1) LINWRI results are compared for different scenarios applied to the same system;
2) All scenarios are implemented in the same year, i.e., year 1;
3) Load is growing year by year.

Under the above assumptions, LINWRI can be interpreted as follows:

1) Given a future year, the LINWRI ranking shows which scenario results in better system reliability and the quantitative differences among the scenarios.
2) Given a LINWRI level in the future, LINWRI results show, under each scenario, how many years it takes for system reliability to degrade to that level. A larger

number of years indicates more reliability improvement a scenario brings to the system.

Although the mathematical definition of LINWRI may vary in different contexts, the fundamental idea is the same. It represents overall system reliability by calculating the weighted sum of component indices where each of them quantifies an aspect of system reliability.

$$\text{LINWRI}=1-(\rho_1 \frac{\text{INDEX}_1}{\text{INDEX}_{1\text{ref}}}+\rho_2 \frac{\text{INDEX}_2}{\text{INDEX}_{2\text{ref}}}+...+\rho_n \frac{\text{INDEX}_n}{\text{INDEX}_{n\text{ref}}}) \qquad \textbf{(4.7)}$$

where $\rho_1+\rho_2+...+\rho_n=1$. Subscript "n" and "ref" denote the nth index and the reference case, respectively.

A key assumption applies to (4.7): a greater value of a component index corresponds to poorer reliability in terms of that particular aspect. For example, the fact that $\text{INDEX}_1 > \text{INDEX}_{1\text{ref}}$ indicates that the reliability of the former scenario is poorer than that of the reference case in terms of the aspect represented by INDEX_1.

According to (4.7), the reference case has a LINWRI value equal to zero. For a given case, a positive value corresponds to an improvement in reliability from the reference case, whereas a negative value corresponds to degradation. A greater LINWRI value represents higher overall system reliability.

The reference level is normally defined as the current status without any system reinforcement. The unacceptable level of which the reliability is right at the edge of being 'unacceptable' also needs to be defined. Arbitrariness is often unavoidable in practice: the unacceptable level may be determined through experience rather than through a rigorous mathematical process. For example, the unacceptable level can be defined as the extreme point where network investment in branches and other facilities should be immediately put into practice. Once the unacceptable level is defined, LINWRI can be visualised on the reliability bar as shown in Figure 4.1.

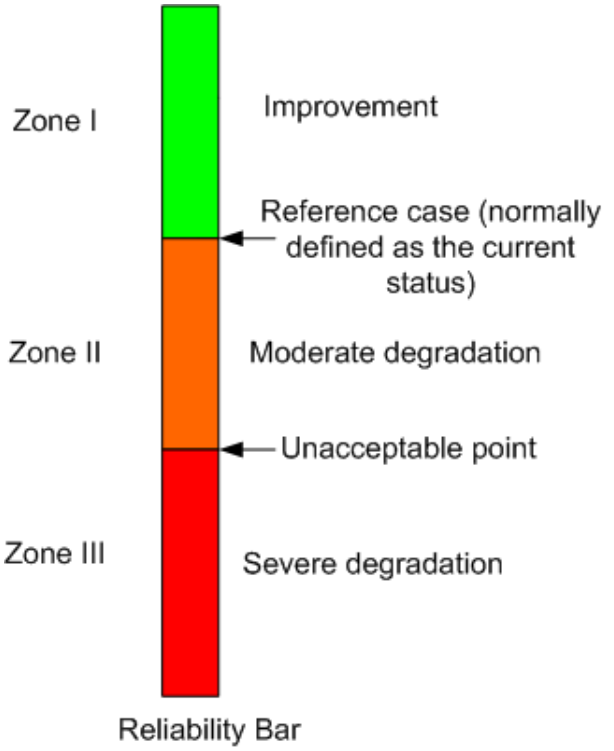

Figure 4.1: the reliability bar.

This bar, similar to the 'green-orange-red' alert system, contains three zones as shown in Figure 4.1:

Zone I: reliability improvement zone;

Zone II: moderate degradation zone;

Zone III: significant degradation zone.

The boundary of Zone I/Zone II is the reference case and the boundary of Zone II/Zone III is the unacceptable level.

4.2.2 Demand Response Incremental Cost Benefit

Demand Response Incremental Cost Benefit (DRICB) index and Incremental Benefit of Corrective Control (IBCC) index are similar since they both quantify the incremental monetary benefit in reliability brought by incremental implementation of corrective control. DRICB works in the context of demand response (DR). It is derived from EIC which quantifies the cost of outages.

$$\text{DRICB} = \frac{\text{EIC}_b - \text{EIC}_a}{\text{Incremental DR implementation}} \quad \textbf{(4.8)}$$

where subscript b and a represent 'before' (the incremental implementation of DR) and 'after' (the incremental implementation of DR), respectively. The incremental DR implementation value can be defined as the difference in annual energy consumption between the two cases being compared, if only load reduction is implemented. If only load shifting is implemented, the incremental DR implementation can be represented by the difference in the amount of annual energy shifted. If different types of DR programs are implemented at the same time, the incremental DR implementation can be expressed by the difference in the weighted sum of energy reduced and energy shifted. Although DRICB focuses on the benefit in reliability only, it is an indispensable index when assessing the overall benefits of DR.

4.2.3 Voluntary Energy Curtailment Level

Electric energy curtailed through voluntary programmes needs to be distinguished from that through force because

1) they incur completely different costs;
2) they correspond to completely different customer satisfaction levels; and
3) their contibutions to reliability indices are different.

As a result, there was a need for an index to quantify voluntary energy curtailment as a proportion of total energy curtailment. This research has bridged the gap by defining Voluntary Energy Curtailment Level (VECL) as annual voluntary energy curtailment over annual total energy curtailment in percentage under emergencies. In the context of DR, the voluntary energy curtailment is the energy curtailed through Emergency Interruptible Load Programme (EILP) in which the participation is on a voluntary basis. The mathematical expression of VECL is

$$\text{VECL} = \frac{\text{VEC}}{\text{Total Energy Curtailed}} = \frac{\text{VEC}}{\text{VEC+FEC}} \quad \textbf{(4.9)}$$

where VEC and FEC denote Voluntary Energy Curtailment and Forced Energy Curtailment, respectively. VECL quantifies the implementation level of EILP. A greater VECL value indicates a higher implementation level of EILP.

4.2.4 Incremental Benefit of Corrective Control and Incremental Benefit of System Reinforcement

Incremental Benefit of Corrective Control (IBCC) is defined as follows:

$$\text{IBCC} = \frac{\text{EIC}_\text{b}\text{-EIC}_\text{a}}{\text{ICCI}} \quad \textbf{(4.10)}$$

where subscript a and b stand for 'after' (after incremental investment in corrective control) and 'before' (before incremental investment in corrective control)", respectively. ICCI stands for 'Incremental Corrective Control Implementation' which can be expressed in either capacity (MW) or in £.

IBCC represents the reduction in risk associated cost resulting from the incremental investment in corrective control. This index is similar to DRICB in that it quantifies the benefit in reliability. It is an indispensable index when quantifying the overall benefits brought by corrective control.

The three costs, EIC_a, EIC_b and ICCI are all present values.

$$\text{EIC}_\text{b} = \sum_{t=0}^{m} \frac{\text{EIC}_\text{tb}}{(1+i)^t} \quad \textbf{(4.11)}$$

$$\text{EIC}_\text{a} = \sum_{t=0}^{m} \frac{\text{EIC}_\text{ta}}{(1+i)^t} \quad \textbf{(4.12)}$$

$$\text{ICCI} = \sum_{t=0}^{ma} \frac{\text{IC}_{at} + \text{OC}_{at}}{(1+i)^t} - \sum_{t=0}^{mb} \frac{\text{IC}_{bt} + \text{OC}_{bt}}{(1+i)^t} \quad \textbf{(4.13)}$$

where subscript 'a' and 'b' denote 'after' (after incremental investment) and 'before' (before incremental investment). m and i denote the economic life and the interest rate, respectively. EIC_t denotes the expected interruption cost in year t. IC and OC denote the investment cost and operation cost, respectively. If IBCC>0 and ICCI>0, the incremental investment has a positive effect in reducing risk (or the risk associated cost).

The concept of incremental benefit can be extended to traditional reinforcement scenarios. Incremental Benefit of System Reinforcement (IBSR) quantifies the incremental benefit in reliability brought by both corrective control scenarios and traditional reinforcement scenarios. It is calculated in a similar way to IBCC:

$$\text{IBSR} = \frac{\text{EIC}_b - \text{EIC}_a}{\text{ISRI}} \qquad \textbf{(4.14)}$$

where ISRI denotes Incremental System Reinforcement Investment which is defined in a similar way to ICCI. Other variables are defined the same as in previous formulas.

4.3 Conclusion

After presenting a brief review of existing reliability indices, this chapter proposed five new indices: LINWRI, DRICB, IBCC, IBSR and VECL. Linear Weighted Reliability Index (LINWRI) as a composite index represents the overall system reliability considering multiple aspects. Demand Response Incremental Cost Benefit (DRICB) represents the incremental monetary benefit in system reliability when one more unit of DR (expressed in MWh/year) is implemented. Incremental Benefit of Corrective Control (IBCC) represents the incremental benefit in reliability from incremental implementation of corrective control, whereas Incremental Benefit of System Reinforcement (IBSR) quantifies the incremental reliability benefit from incremental system reinforcement; Voluntary Energy Curtailment Level (VECL) represents the percentage of annual voluntary energy curtailed over annual total energy curtailed under emergency circumstances. Their mathematical definitions were introduced. These indices are applied in case studies in later chapters.

5 Reliability assessment incorporating Active Management

Summary

The commitment to fulfilling carbon emission reduction targets requires more distributed generation (DG) to be connected to a network that offers potential economic benefits to both the owners of the DG units and the network operator. However, accommodating increasing DG capacity is a challenging endeavour. In response to this challenge, existing distribution networks are expected to undergo a revolutionary change from passive to active management (AM). This chapter reviews the characteristics of AM, as well as its benefits, based on a literature survey. One of the most important features of AM is that it allows for coordinated control. An AM system consists of the central control unit and the communication system, as well as local control devices. Its model has been incorporated into reliability assessments that are based on chronological Monte Carlo simulation (CMCS).

A 16-bus network is used as the test case. Different scenarios are proposed and compared in terms of three factors: the capability to accommodate wind generation, the impact on system reliability, and economic benefits.

5.1 The benefits and challenges associated with DG

The global drive to mitigate the now widely recognised negative effects of CO_2 on the world's climate has led to the formulation of the Kyoto Protocol, which establishes CO_2 reduction targets for member nations. To fulfil its obligations under the EU Kyoto targets, the UK government has set very ambitious goals that require the installation of 8 – 10 GW of renewable generation capacity and implementation of schemes for achieving 10 GW of combined heat and power (CHP) capacity by 2010 [48]. The UK

has committed to a legally binding agreement with the EU to have 15% of its energy consumption generated from renewable sources by 2020 [49].

The importance of a more decentralised energy supply system in satisfying low carbon emission targets is illustrated in terms of the following perspectives [38]:

1) The electrical energy losses in power lines can be reduced by supplying more electricity from local sources.

2) Customer awareness can be raised, more household or community-based energy sources can be applied, and policy change can reflect carbon emissions in the energy price.

DG is one of the indispensable elements of a decentralised energy supply system. The definition of DG, however, is ambiguous [50]. It is characterised by the features outlined below, but these descriptions may be subjective and qualitative.

1) Compared with conventional generation units with capacities of tens or hundreds of megawatts, DG is small in scale, with a capacity ranging from a few kilowatts to several megawatts.
2) It is connected to medium- or low-voltage networks, i.e., distribution systems.
3) It is located near a load centre.

DG is expected to offer advantages in terms of value in the wholesale electricity market, concordance with the EU emission trading scheme, and issuance of the renewable obligation and levy exemption certificates, etc [51].

A few published works focus on the economic aspects of DG. Rodriguez advocates the consideration of externalities as part of the economic assessment during the selection of generation technologies [52]. He proposes a method for quantifying not only the economic benefit that DG provides its owner but also its effect on environments (externalities). The externalities of emission damages can be a decisive element in determining which type of generation system is the best choice.

A DG business model is proposed in [53]. It has been applied to cases in Spain, Norway, the Netherlands, and the UK. Results have shown that DG is a potentially economical approach, and is a promising means to address environmental concerns.

DG relieves system stress and reduces generation costs by decreasing output from generation systems with high marginal costs (peak generation). It also effectively minimises the dependence on central grids and reduces the costs of load curtailments [54].

The challenges associated with increasing DG should not be underestimated. The intermittent and unpredictable nature of wind generation proves to be a major challenge given that it exacerbates the worst cases: i) when load level is low and wind generation reaches its peak, the bus where wind generation units are connected may experience a serious voltage rise; ii) when wind speed falls below the cut-in speed and load reaches its peak, the system may suffer from undervoltage problems [55, 56]. Apart from this, power quality management and fault level management also pose difficulties [57]. Two fundamentally different solutions have been proposed in response to the aforementioned issues:

One is to reinforce the network by building new branches. This solution, however, comes with prohibitive costs and political barriers, i.e., the costs of land, materials, and labour, political impediments arising from environmental issues, and the legal process governing land permissions, etc. These barriers are anticipated to be even more prohibitive with the increasing scarcity of land, rising labour costs, and increasing public concern for the environment.

An alternative solution is to completely change the operational philosophy of distribution networks. This approach is expected to incur less cost and raise fewer environmental issues. Historically, as part of a centralised power system, a passively managed distribution network merely passes electricity from bulk supply points to customers. The role of the distribution system as a passive medium is expected to undergo radical changes [58]. The fundamentally upgraded distribution network is envisioned to demonstrate the following features:

1) It must coordinate different control measures (DG output control, shunt compensation, series compensation, etc.) at the system level to allow for sufficient flexibility which is essential to accommodating a large amount of DG.

2) It must provide sufficiently detailed real-time knowledge of the system through pervasive measurement devices.

3) It must transmit data among the measurement devices, control centre, and local control devices via the communication system in a reliable and efficient manner.

4) It must enable the analysis of large volumes of data and provide a control decision in real-time.

5) It is open to an accumulative upgrade process, that is, it is not merely a one-off construction.

This revolutionised philosophy for operating distribution systems is referred to as active management (AM).

5.2 Active Management

5.2.1 Overview of AM

AM is a promising solution to the challenges mentioned in the previous sections. Compared with traditional network reinforcement, which adopts the passive operational philosophy (also referred to as the 'fit-and-forget' approach), AM enables the avoidance of prohibitive investment costs as well as political barriers in building new branches and associated infrastructure.

According to [59], AM is characterised by the following features:

i) wide-area, coordinated, active control;

ii) adaptive and integrated protection/control systems;

iii) power electronic-based network management devices;

iv) real-time network simulation and performance analysis;

v) advance sensors and measurement;

vi) highly distributed and pervasive communications; and

vii) data interpretation through the use of intelligent systems.

The effect of AM on the level of DG penetration is studied in [60]. Through various sensitivity analyses, the paper concludes that the increase in network flexibility brought about by AM enables the system to accommodate more DG [60]. Different AM control strategies, including coordinated and uncoordinated voltage control, are introduced in [60]. The control variables, i.e., the tap setting of the on-load tap changer and the output of wind generation, are simultaneously considered and optimised under coordinated control [60]. Unlike uncoordinated control, the former requires highly penetrated sensors that can monitor the system to a detailed level, a fast central processing unit that can process a large volume of information, and a robust communication system.

The technical and economic effects of AM are investigated in [56] from various perspectives, i.e., the voltage profile, line losses, power generation, and net benefit. AM reduces line losses, improves voltage profile, and promotes DG penetration [56]. AM and traditional network reinforcement are not mutually exclusive. The transition from a traditional passive network to AM is not a one-off construction but rather an accumulative process with a gradual increase in network flexibility.

An AM system consists of four essential components [57]:

1) a measurement and data analysis component;

2) a decision-making module that formulates real-time decisions based on feedback from the measurement and data analysis unit;

3) a communication unit that transmits information among different components; and

4) local control devices which execute the decision formulated by the decision-making module. Examples of decisions include adjusting the set points of the transformer tap and reactive compensation devices, changing the output of DG, and performing other corrective actions if required [57].

Previous works assume that the control system for AM is 100% reliable. Given that this assumption does not hold true in practice, such an assumption may lead to overly optimistic decisions regarding the benefits of AM. This chapter presents a thorough investigation of whether AM is preferable to traditional network reinforcement schemes in terms of cost benefits. Such an examination is necessary before deciding on a final system development strategy.

5.2.2 AM Model

As previously mentioned, AM is a comprehensive control system that encompasses a decision-making unit, communication system, sensors, and local control devices. It operates under corrective control, which aims to correct system violations at the post-contingency stage; when system violations occur (such as bus overvoltage or line overflow), protection devices react to the contingency. Information on the actions of the protection devices and abnormalities in the network variables is detected by the measuring devices, and sent to the decision-making unit. On the basis of such information, corrective control decisions are generated by the decision-making unit, transmitted via the communication system, and executed by the local control devices to eliminate violations. The measured local variables are then sent back to the decision-making unit, forming a negative feedback loop.

Varied types of corrective actions are prioritised differently based on the costs they present and the time they take to respond. The following actions are listed in decreasing priority: shunt and series compensation; discharge from the energy storage (ES) device; DG output curtailment; and load curtailment. Shunt and series compensation is the fastest type of corrective action, with a response time far below 1 second for power electronic-based devices. ES devices, which support the system for a limited duration, take longer to respond. DG output curtailment exhibits a relatively short response time, but it is uneconomical because of the potentially large opportunity cost incurred from ungenerated energy. The least favourable action is to curtail load, which imposes substantial social costs and results in customer dissatisfaction.

The operational process of an AM control system is presented in Figure 5.1. It represents a compilation of the information taken from [55].

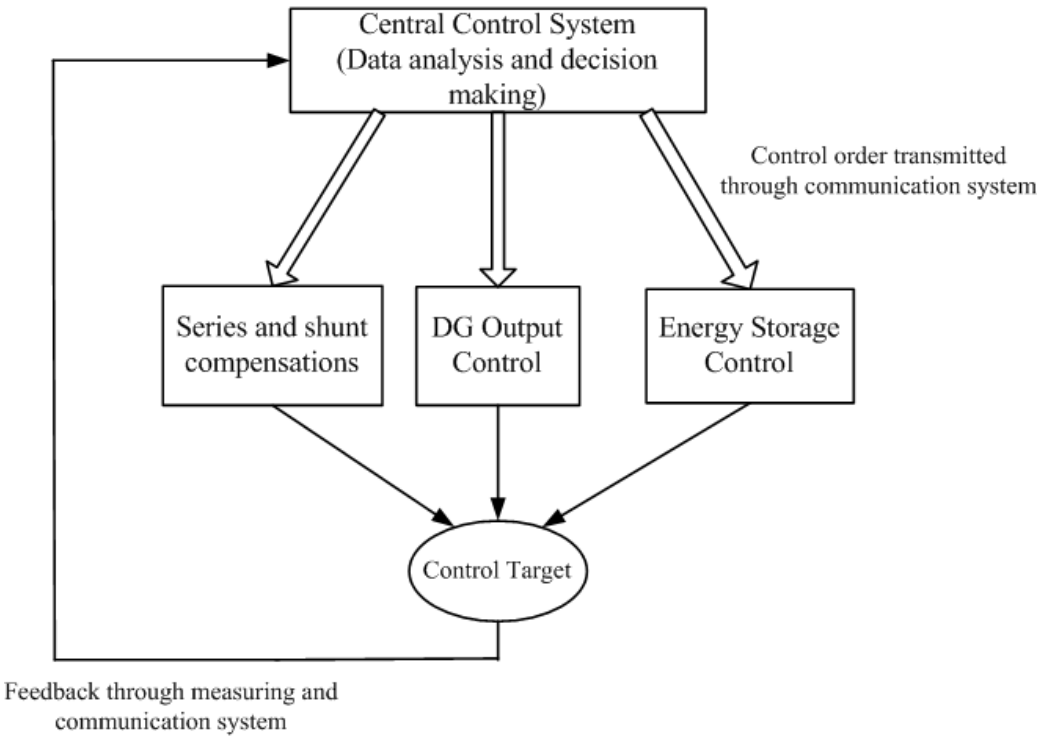

[Author's compilation]

Figure 5.1: AM control system structure [55].

A simplified 'party-line' model is adopted to simulate AM control system failure, using the following assumptions as bases:

i) The data on communication system failure are integrated with the failure of the central control unit (decision-making unit) on the assumption that communication is done via radio.

ii) The self-originated (independent) failure of any local control device does not affect the operational status of the central control unit; by way of analogy, this means that a disabled 'hand' does not affect the functionality of the 'brain'.

iii) The self-originated failure of any local control device does not affect other local control devices.

iv) All devices cease to operate when the central control unit fails.

v) The failures of other components such as branches and transformers are not considered, so that the effect of control system unreliability can be identified without it being distorted by other components.

The local control devices are not independent of each other because a malfunction in the central control disables all local control devices. The failures of local control devices are therefore classified into two types: self-originated failure (independent failure), which originates from itself, and system-originated failure, which stems from the central control. System-originated failure in the context of this study is the common cause failure (CCF). A coordinated control strategy is adopted in this project. All corrective control measures are coordinated for a global control target.

5.2.3 Optimisation Model under AM

When the central control and all local control devices are in a normal state, corrective control decisions are determined by an optimisation based on AC load flow:

$$\min \varphi_1 \sum_i P_{ESi} + \varphi_2 \sum_i P_{Gi}^{Cur} + \varphi_3 \sum_i P_{Li}^{Cur} \quad \textbf{(5.1)}$$

subject to

$$P_{Gi} - P_{Li} - P_{Gi}^{Cur} + P_{Li}^{Cur} = P_i^{inj}(V, \theta, X_{SVC}, P_{ES}) \quad \textbf{(5.2)}$$

$$Q_{Gi} - Q_{Li} + Q_{Li}^{Cur} = Q_i^{inj}(V, \theta, X_{SVC}) \quad \textbf{(5.3)}$$

$$S_{ij} < S_{ij}^{\max} \quad \textbf{(5.4)}$$

$$V_i^{\min} < V_i < V_i^{\max} \quad \textbf{(5.5)}$$

$$0 < P_{Gi}^{Cur} < P_{Gi} \quad \textbf{(5.6)}$$

$$0 < P_{Li}^{Cur} < P_{Li} \quad \textbf{(5.7)}$$

$$pf_{\min} < \frac{P_{Gi} - P_{Gi}^{Cur}}{\left|(P_{Gi} - P_{Gi}^{Cur}) + j \cdot Q_{Gi})\right|} < pf_{\max} \quad \textbf{(5.8)}$$

$$\frac{P_{Li} - P_{Li}^{Cur}}{Q_{Li} - Q_{Li}^{Cur}} = \frac{P_{Li}}{Q_{Li}} \quad \textbf{(5.9)}$$

$$X_{SVCi}^{\min} < X_{SVCi} < X_{SVCi}^{\max} \quad \textbf{(5.10)}$$

$$0 < P_{ESi} < P_{ESi}^{\max} \quad \textbf{(5.11)}$$

where

$\varphi_1, \varphi_2, \varphi_3$ Coefficient corresponding to priority level

P_{Li}, Q_{Li} Active and reactive load at bus i

P_{Gi}, Q_{Gi} Active and reactive generation at bus i

P_{Gi}^{Cur} Active generation curtailment at bus i

$P_{Li}^{Cur}, Q_{Li}^{Cur}$ Active and reactive load curtailment at bus i

P_i^{inj}, Q_i^{inj} Active and reactive power injection at bus i

$pf_{\min}, pf_{\max}$ Min and max power factor allowed

X_{SVC} Equivalent reactance of SVC

S_{ij} Load flows at branch ij

V_i, θ_i Voltage magnitude and angle at bus i

P_{ESi}, $P_{ESi}^{\max}$ Power discharged and maximum power from Energy Storage device, respectively.

SVC is installed at wind generation site in compliance with the grid code.

A large φ implies low priority assigned to a particular term. This context is represented by (5.1) in which $0 < \varphi_1 < \varphi_2 < \varphi_3$ corresponds to a decreasing order of preference, described as follows: reactive compensation over ES adjustment, DG curtailment, and load curtailment. Loads are subject to curtailment when the system exhausts all other means of control. When the central control fails, corrective control is disabled: reactive compensation and ES adjustment are bypassed in the model and DG is completely disconnected.

When the SVC or ES is down, the optimisation algorithm is altered: the corresponding element in (5.1) and corresponding constraints are excluded. When the central control is down, load curtailment becomes the only means available, and all constraints involving the SVC, ES, or wind generation output control are excluded.

5.3 Wind Generation Model

As a major type of renewable energy source in the UK, wind generation (especially offshore wind farms) has been increasing rapidly in recent years [49].

The Weibull distribution is normally used as the wind speed probability density function in generating random wind speeds [61].

The Weibull function is expressed as follows [61]:

$$f(v) = \frac{k}{c}(\frac{v}{c})^{k-1} \exp[-(\frac{v}{c})^{k}] \quad \textbf{(5.12)}$$

where

k shape parameter

c scale parameter

v wind speed

A special case of the Weibull distribution is called the Rayleigh distribution, in which parameter $k = 2$ is applied to the probability density function. This distribution is suitable for theoretical study when a credible wind speed record is unavailable [61]. In the Rayleigh distribution, the 'good' high-speed wind under which wind turbines generate the rated power occurs most frequently, followed by relatively low-speed wind and extremely high-speed wind.

The Rayleigh distribution is given by:

$$f(v) = \frac{2v}{c^2} \exp[-(\frac{v}{c})^{2}] \quad \textbf{(5.13)}$$

The Weibull function is suitable for non-sequential analysis, in which the correlation among wind speeds over time is disregarded. In other words, it does not model time-dependent wind speeds.

A method that accounts for time dependence is the Markov chain method, which generates a wind speed time series [62]. A couple of approximations are made for the Markov chain method to be valid:

1) The seasonal effect is disregarded to keep transition rates between states constant. This approach is justified if the amount of data is sufficiently large [62].
2) Wind speeds are discretised at a step of 1 m/s, which is sufficiently accurate under most circumstances [62].
3) The residence time in each state is assumed to follow an exponential distribution. When only long-term expected values are considered, using exponential distribution or other distributions makes little difference [62].

The transition rates from state i to state j is given by:

$$\lambda_{ij} = \frac{N_{ij}}{D_i} \tag{5.14}$$

where N_{ij} is the number of transitions from states i to j, and D_i is the duration of state i, normally in years. All transition rates can be calculated from a sufficiently long wind speed record using (5.14).

Given the wind speed, the function for calculating the power output of a single wind turbine is given by [21, 61]:

$$p(v) = \begin{cases} 0 & v \le v_c \\ \mathrm{K}v + \mathrm{b} & v_c \le v \le v_r \\ \mathrm{P}_{\mathrm{rated}} & v_r \le v \le v_f \\ 0 & v \ge v_f \end{cases} \tag{5.15}$$

where $p(v)$, $\mathrm{P}_{\mathrm{rated}}$, v, v_c, v_r and v_f are the power output of a wind turbine, the rated power of the turbine, wind speed, cut-in wind speed, rated wind speed and cut-out wind speed, respectively. In the function,

$$\mathrm{K} = \mathrm{P}_{\mathrm{rated}} / (v_r - v_c) \tag{5.16}$$

$$\mathrm{b} = -\mathrm{K}v_c \tag{5.17}$$

when the wind speed falls between the cut-in and the rated speeds, the power output is linearised as an approximation [21, 61].

A wind farm is a cluster of wind turbines. The disturbance caused by upstream wind turbines changes the speed at which wind is received by downstream wind turbines, thereby affecting their power output. A parameter called array efficiency is therefore

applied in quantifying the effect of wind turbine interference on wind farm output. The power output of a wind farm is given by [21, 61]

$$p_{Farm} = np_{turbine}k_e \quad \textbf{(5.18)}$$

where p_{Farm}, $p_{turbine}$, n, and k_e $(0 \le k_e \le 1)$ are the power output of a wind farm, power output of a single turbine, number of turbines, and array efficiency, respectively.

5.4 Economic Assessment

The purpose of AM is to facilitate DG penetration. The business concept applied to a distribution network operator (DNO) involves charging DG owners for AM services, enabling DG owners to increase the wind generation capacity and the electricity that can be generated [56]. A few assumptions are adopted prior to the calculation of the net benefits for a DNO [56, 63]:

1) The operation and management (O&M) charge for AM services imposed on a DG owner is proportional to the total energy generated by that DG.
2) The connection charge imposed on the DG owner is proportional to DG capacity.
3) All types of charges/costs, excluding the wind generation connection charge, wind generation investment cost, and AM investment cost, are spread over the time frame at equal intervals (a year). The amount of cash flow remains the same over the time frame.

On the basis of these assumptions, the connection charge (£) for wind generation is calculated as [56]

$$C_{\text{connection}} = CON \bullet \text{Capacity}_{\text{Wind}} \quad (£) \quad \textbf{(5.19)}$$

where $\text{Capacity}_{\text{Wind}}$ denotes the wind generation capacity. This charge is assumed to be a one-off charge imposed on the DG owner at the beginning of their investment.

The annual O&M cost for wind generation (£) is calculated as [56]

$$C_{\text{O\&MWind}} = C_{\text{fixed}} + \text{Capacity}_{\text{Wind}} \bullet C_{\text{perMW}} \quad (£/\text{year}) \qquad \textbf{(5.20)}$$

where C_{fixed} and C_{perMW} represent the fixed part of the O&M cost and the variable part per MW of wind generation capacity, respectively.

The annual charge imposed on the DG owner for AM services is [56]

$$C_{\text{O\&MAM}} = OM_{\text{AM}} \bullet W_{\text{WindGen}} \quad (£/\text{year}) \qquad \textbf{(5.21)}$$

where W_{WindGen} denotes the effective energy (in MWh) generated by a wind generation farm throughout a year.

The annual revenue for wind generation is computed as follows:

$$R_{\text{Wind}} = pW_{\text{WindGen}} \quad (£/\text{year}) \qquad \textbf{(5.22)}$$

where p is the average electricity price.

The present values of all charges/costs, except those of the connection charge $C_{\text{connection}}$, wind generation investment $PV_{\text{WindInvest}}$ and AM investment PV_{AMInvest}, are calculated using the following formula:

$$PV = \frac{C}{dis}[1 - \frac{1}{(1+dis)^n}] \quad (£) \qquad \textbf{(5.23)}$$

where C is the periodic charge/cost.

Given the lack of actual data on cash flow, the calculation of $PV_{\text{WindInvest}}$ and PV_{AMInvest} is described as follows.

The present value of wind generation investment cost is assumed to be proportional to wind capacity [64]:

$$PV_{\text{WindInvest}} = \text{Coef} \bullet \text{Capacity}_{\text{Wind}} \quad (£) \qquad \textbf{(5.24)}$$

The AM investment cost is assumed to be the same for all scenarios with AM for the following reasons:

1) Practical data on the actual cost structure of AM investment are lacking.
2) The purpose of the case study is to demonstrate the methodology, and the assumption that the AM investment cost remains the same for all scenarios does not affect the demonstration of methodology.

The original formula for calculating the net benefit for DNO has been modified to take into account risk-associated cost. The new formula is expressed as:

$$\begin{aligned} \mathrm{NB}_{\mathrm{DNO}} &= C_{Con} + \lambda C_{O\&MAM} - C_R - \lambda C_{IAM} \\ &= IC_{DG} \bullet \mathrm{con} + \lambda \mathrm{W}_{\mathrm{DG}} \bullet \mathrm{omc}_{AM} - C_R - \lambda C_{IAM} \quad (£) \end{aligned} \qquad \textbf{(5.25)}$$

where $\mathrm{NB}_{\mathrm{DNO}}$, C_{Con}, $C_{O\&MAM}$, and C_{IAM} are the net benefit for DNO, wind generation connection charge, O&M charge for AM services, and investment cost of AM, respectively. IC_{DG}, con, W_{DG}, and omc_{AM} represent the installed wind generation capacity, connection charge per unit capacity (£/kW), total effective energy generated by wind (kWh), and O&M charge for AM services per kWh of effective energy generated, respectively. λ is a binary value: λ=1 when AM is implemented; λ=0 otherwise. C_R is the risk-associated cost, i.e., the cost of load curtailment.

The net benefit for DNO is calculated by

$$\mathrm{NB}_{\mathrm{DNO}} = PV_{\mathrm{Con}} + \lambda \bullet PV_{\mathrm{AMServ}} - PV_{\mathrm{Risk}} - \lambda \bullet PV_{\mathrm{AMInvest}} \quad (£) \qquad \textbf{(5.26)}$$

PV_{Con} present value of connection charge against the wind generation owner

PV_{AMServ} present value of AM service charge against the wind generation owner

PV_{Risk} present value of risk associated cost

PV_{AMInvest} present value of AM investment cost

λ defined the same as in (5.25).

The net benefit for the owner of the wind generation is calculated using the following formula:

$$\mathrm{NB}_{\mathrm{Wind}} = PV_{\mathrm{WindRev}} - PV_{\mathrm{WindInvest}} - PV_{\mathrm{WindO\&M}} - PV_{\mathrm{Con}} - \lambda \bullet PV_{\mathrm{AMServ}} \quad (£) \qquad \textbf{(5.27)}$$

PV_{WindRev} present value of wind generation revenue

$PV_{\mathrm{WindInvest}}$ present value of wind generation investment cost

$PV_{\mathrm{WindO\&M}}$ present value of wind generation O&M cost

Other variables are defined in the same manner as in previous equations.

5.5 Case Study and Results

The case study presented in this chapter is based on the test case reported in [65], with slight modifications. In the original version, the 33 kV network is supplied by three separate 132 kV bulk supply points, whereas in the current study, the network is fed by a single 132 kV bulk supply point at bus 1.

The network topology is shown in Figure 5.2. Full sets of data that include the network data, load profile, wind profile, and reliability data are given in Appendix A.

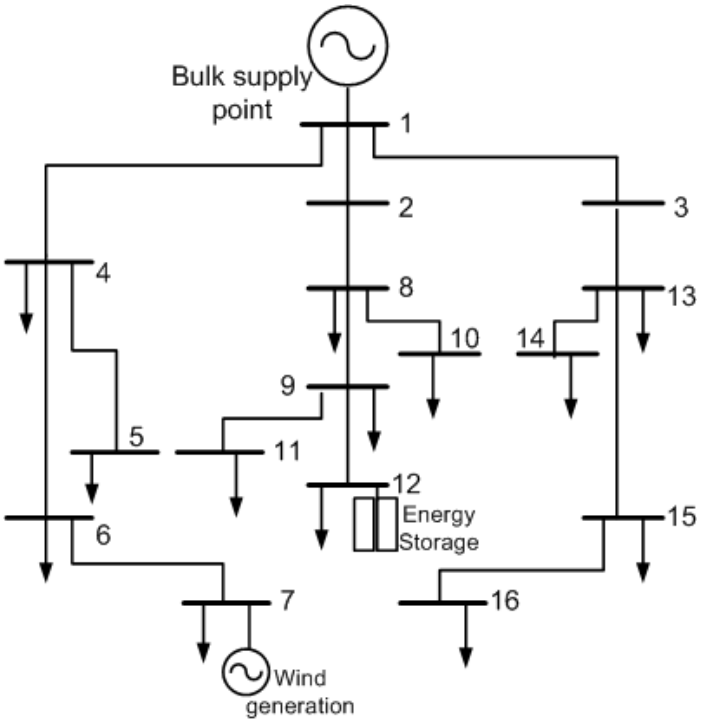

Figure 5.2: Network diagram of the 16-bus test case [65].

All loads are assumed to be fully correlated. A total of 48 discretised load levels as a combination of a typical winter and summer day are used.

The wind generation site is at bus 7. The cut-in, rated, and cut-out wind speeds for the 1 MW wind turbine are 3, 12, and 20 m/s, respectively. The hourly wind speed series is created and discretised at a step of 1 m/s. The hourly wind speed and wind generation output are plotted in Figure 5.3 and Figure 5.4, respectively.

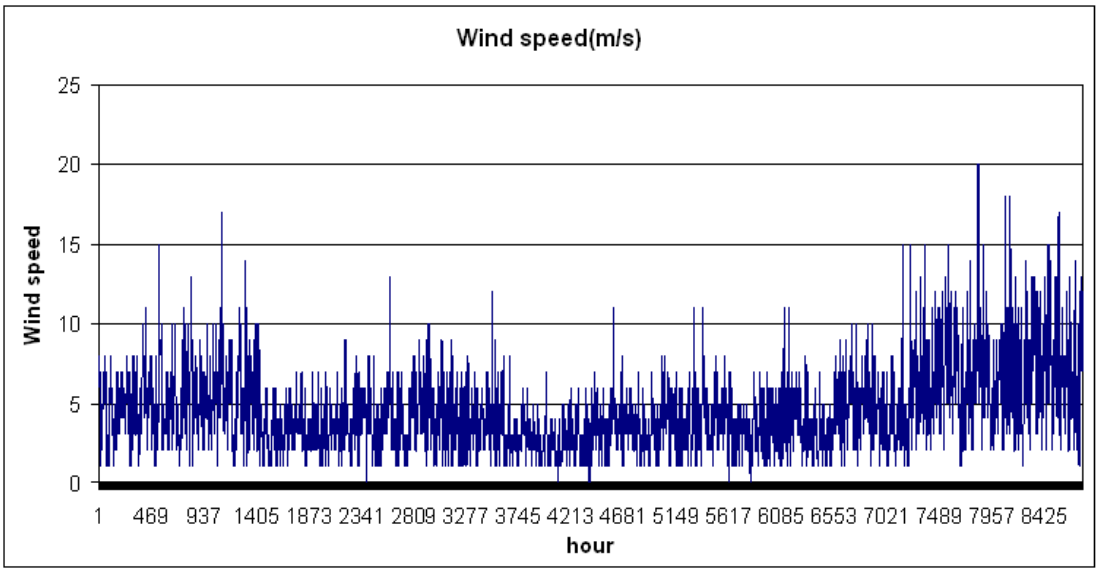

Figure 5.3: Hourly wind speed profile over a year.

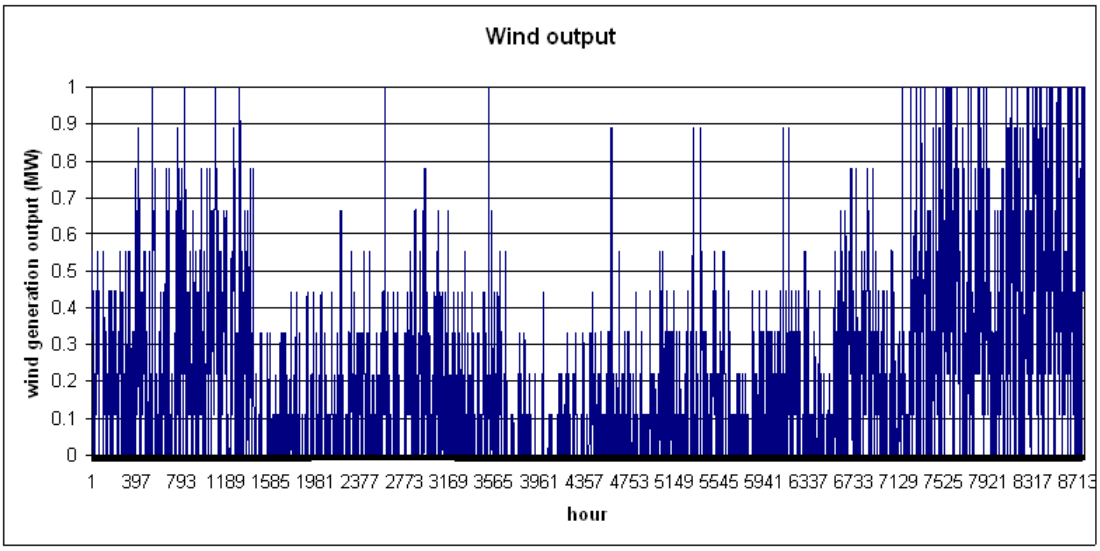

Figure 5.4: Wind generation output over a year.

The AM system in the test case consists of an SVC connected to the same bus as the wind generation, i.e., bus 7; an ES device at bus 12; and a central control unit with an optional function of wind generation output control (WGOC). The discharge and charge rates of ES are assumed to be constant at 200 and 100 kW, respectively. The maximum discharge duration is 2.5 hours. The charging and discharging efficiencies of the ES device are both 90%. The dynamic behaviours of ES are not considered.

The failures of the SVC, ES device, and central control unit are modelled. The failure rates for local control devices in Appendix A correspond to self-originated failures.

CMCS is applied in the reliability assessment.

Four scenarios are defined:

1) no AM;

2) AM with SVC and ES, but without WGOC; the AM system, including all its components, is assumed to be 100% reliable;

3) AM with SVC, ES and WGOC; the AM system, including all its components, is assumed to be 100% reliable;

4) AM with SVC, ES, and WGOC; the failure rate of the AM central control unit, SVC, and ES is 2 occurrences/year (occ/year).

The EENS for different wind capacities in the four scenarios are depicted in Figure 5.5.

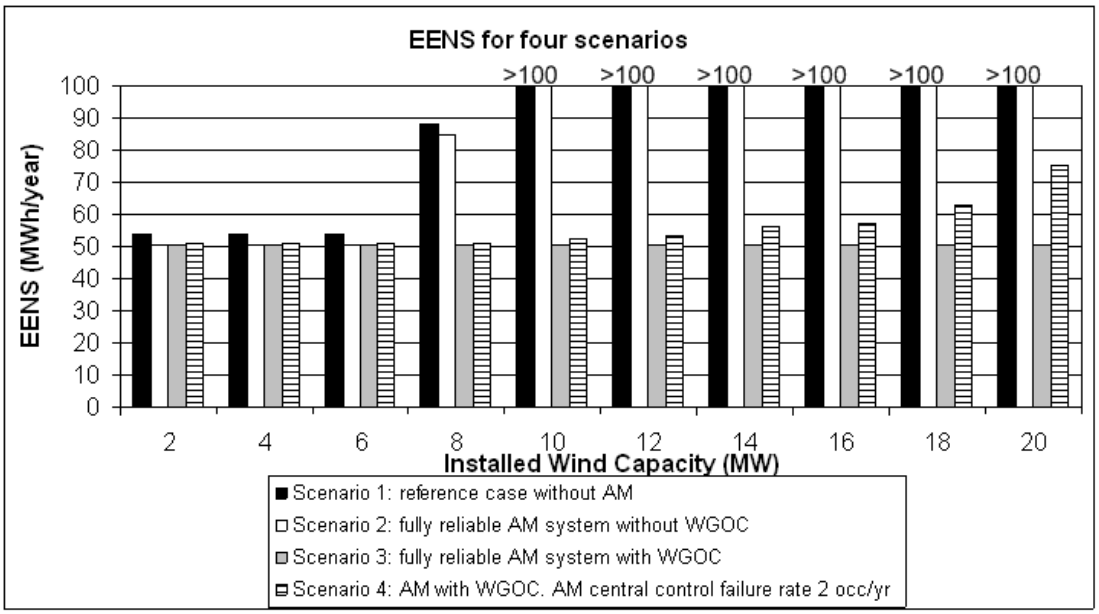

Figure 5.5: EENS results for the four scenarios.

The actual results that significantly exceed 100 MWh/year are not shown in Figure 5.5 to avoid excessively stretching the vertical scale. Instead, a '>100' annotation is placed above the corresponding bar results.

Figure 5.5 shows that the EENS results exceed 100 MWh/year for scenarios 1 and 2 when the wind generation capacity is greater or equal to 10 MW. If the unacceptable reliability level is defined as EENS=70 MWh/year, the reliability becomes unacceptable for scenarios 1 and 2 when the installed wind capacity is 8 MW or higher. In other words, the wind generation capacity that these two scenarios can accommodate is less than 8 MW. The maximum wind capacity that can be accommodated in scenario 4 is less than 20 MW, whereas scenario 3 appears to exhibit limitless capability of accommodating wind generation (EENS remains constant despite the increase in wind generation capacity). This result is attributed to the fact that in scenario 3, curtailing wind generation is always applicable because the AM system is assumed to be 100% reliable. However, this scenario and its results exist only in theory.

1) A 100% reliable AM control system is an ideal case, but non-existent in practice.

2) The cost barrier encountered by the owner of the wind generation farm is not represented in Figure 5.5, but in reality, this barrier constrains wind generation capacity. Regardless of wind generation capacity, the actual wind energy generated over a year is limited because of the necessity of wind output curtailment that arises from reliability requirements. An infinite wind generation capacity therefore corresponds to capped revenue from effective wind energy generation, infinite investment cost, and infinite connection charge proportional to wind capacity. This situation is clearly economically infeasible.

Figure 5.5 also shows that even at a small wind generation capacity (<8 MW), the EENS results remain positive for all the four scenarios. The energy curtailment in these cases stems from ‘bad’ days, during which the load is high and wind speed is low; voltage drop problems occur at buses far from the bulk supply point. The increase in wind capacity does not reduce EENS to zero because of the intermittent nature of wind generation, i.e., the wind output is zero when the wind speed is below the cut-in speed, regardless of wind generation capacity.

With the increase in wind generation capacity, however, the increase in the EENS results is contributed by a different instance of ‘bad’ days, during which the system is subject to voltage rise caused by low load and high wind generation.

Furthermore, according to Figure 5.5, the AM system failure does not have a significant effect on system reliability at low wind capacity. However, its effect grows rapidly with the increase in wind capacity. Even a low probability of failure significantly increases EENS when wind capacity is high because AM failure indicates that the DNO loses control over wind generation. The wind output is then purely determined by the capacity and wind speed at that moment. Under scenario 4, voltage rise occurs only when the failure of the AM system coincides with an 'appropriate' wind speed (falls between the cut-in and cut-out speeds) and above a 'troublesome' threshold. With the increasing capacity of wind generation, the 'troublesome'' threshold tends to decrease towards the cut-in speed, and the system experiences more days when system violations occur. An extreme theoretical circumstance is that with infinite wind generation capacity, the system experiences blackouts whenever the AM system fails and the wind speed is 'appropriate'. The 'troublesome' threshold drops to the cut-in speed under such circumstance.

The DG penetration levels for the four scenarios are shown in Figure 5.6, Figure 5.7 and Figure 5.8.

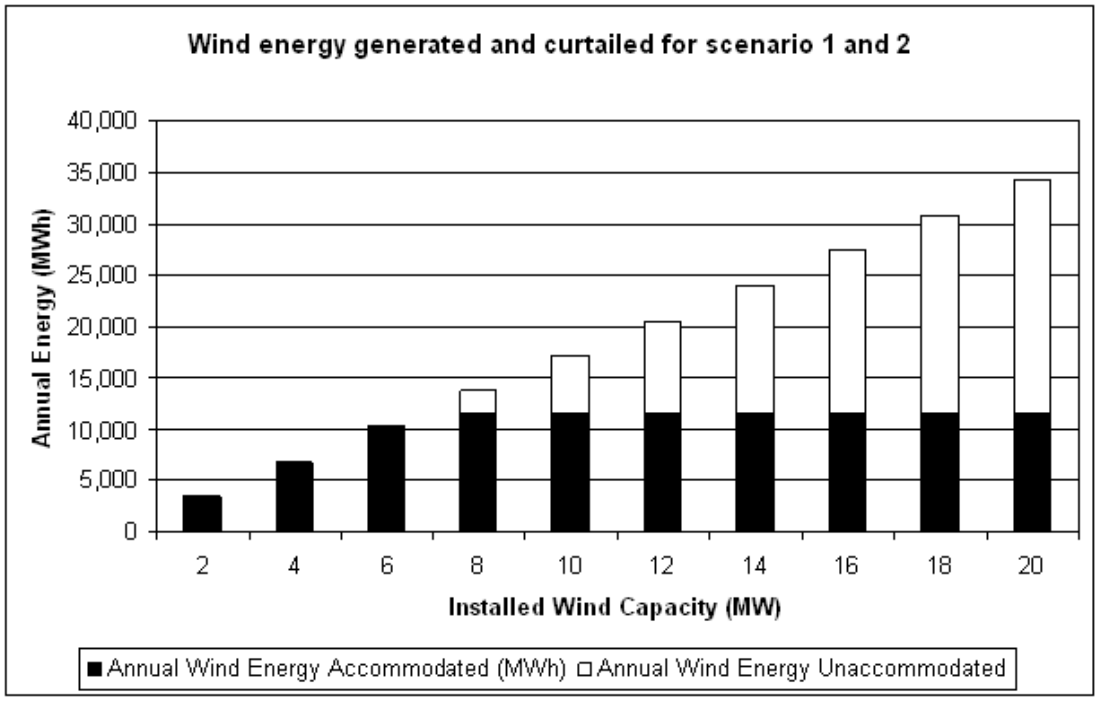

Figure 5.6: Wind energy that can be accommodated in scenarios 1 and 2.

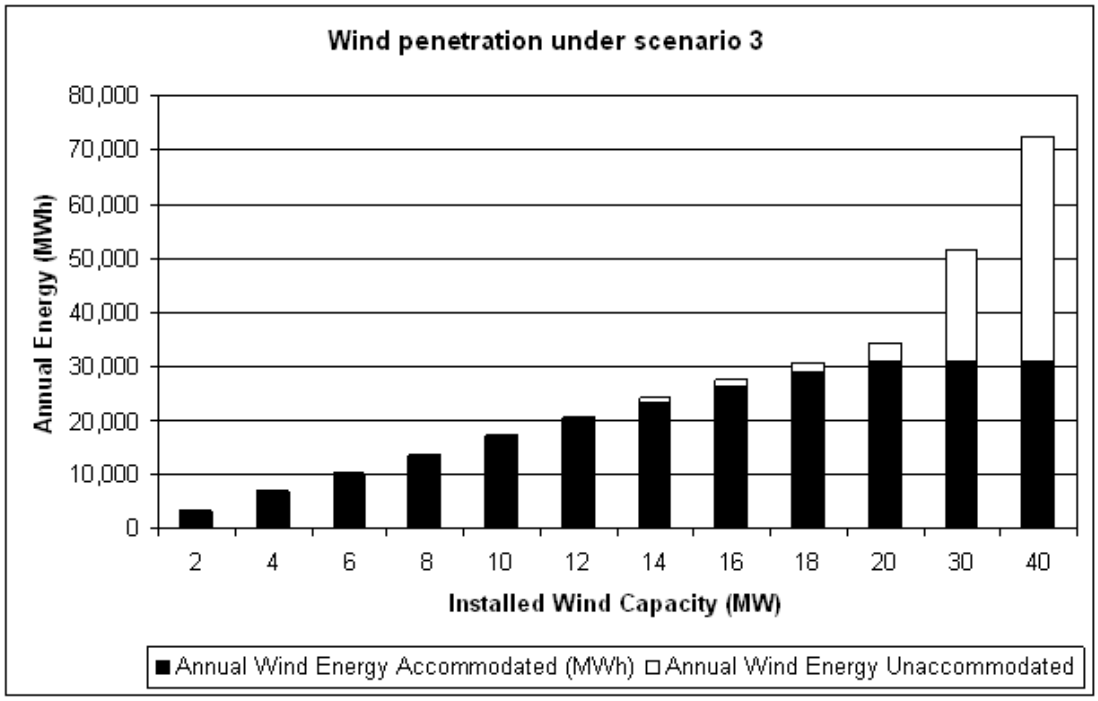

Figure 5.7: Wind energy that can be accommodated in scenario 3.

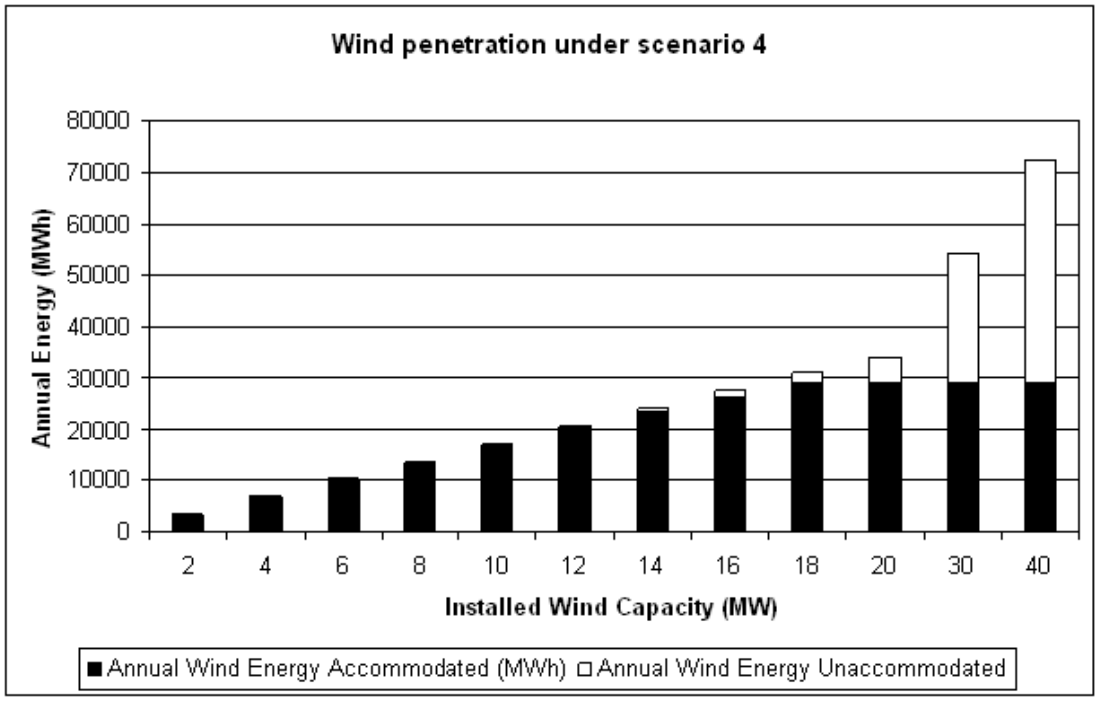

Figure 5.8: Wind energy that can be accommodated in scenario 4.

Figure 5.6 is consistent with Figure 5.5. Wind energy can be fully accommodated at a wind capacity of less than 8 MW under scenarios 1 and 2. The restricting factor is

system reliability represented by EENS in Figure 5.5. Wind energy beyond the maximum capacity causes serious problems for system reliability.

Compared with Figure 5.6, Figure 5.7 shows that more wind energy can be accommodated under scenario 3. The maximum wind energy that can be accommodated is slightly above 30,000 MWh per year at a wind generation capacity of 20 MW.

Unlike Figure 5.7, Figure 5.8 shows that the AM system failure reduces the maximum wind energy that can be accommodated. This result is consistent with that in Figure 5.5, which clearly shows that AM system failure has an obvious adverse effect on system reliability when wind capacity is high.

By implementing AM, wind penetration may be increased significantly. Furthermore, the case study has shown that the crucial factor that improves the system capability of accommodating more wind energy is the WGOC. Without the WGOC, the effectiveness of AM in terms of accommodating wind energy is largely compromised. Although the 'bad' days during which excessive wind generation is reflected do not usually occur, these days severely limit the amount of wind energy that can be accommodated. The WGOC ability helps the system survive such days by curtailing excessive wind energy generation. In this way the bottleneck is relieved and the AM capability of accommodating wind generation significantly improves.

On the basis of the data given in [64, 66, 67], the parameters for economic assessment are given below:

Connection charge rate: $CON = £50,000 / \text{MWh}$

O&M charge for AM services per MWh: $OM_{\text{AM}} = £10 / \text{MWh}$

Economic life of wind generation (years): $n = 25$

Discount rate for calculating present value: $dis = 5\%$

Electricity price: $p = 13.5$ p/kWh=£135 /MWh

In this test case, $C_{\text{fixed}} = £200,000$ and $C_{\text{perMW}} = £50,000$ /MW .

In the test case, the economic life of wind generation $n = 25$ years .

According to the data in [64], the coefficient for calculating wind generation investment cost is $\text{Coef} = £1.2\text{m}/\text{MW}$.

The present value of AM investment is assigned a constant value, expressed as $PV_{\text{AMInvest}} = £2\text{m}$.

The risk-associated cost is assumed to be proportional to EENS with a multiplier of £2,000 /MWh.

The net benefits for the owner of the wind generation unit and the DNO are expressed in Figure 5.9 and Figure 5.10, respectively.

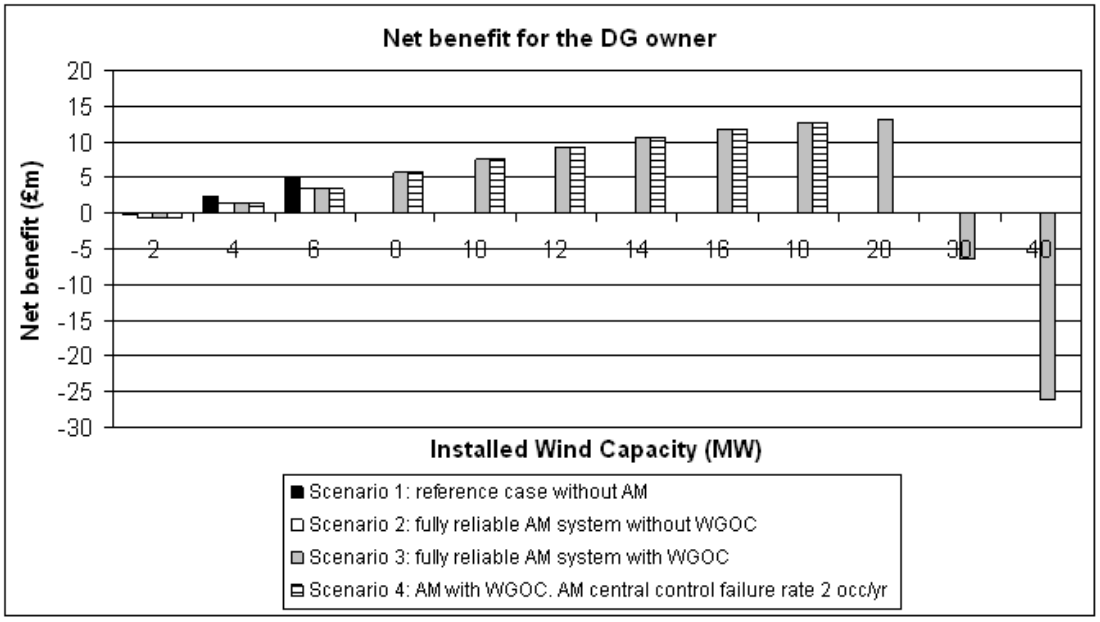

Figure 5.9: Net benefit for the DG owner.

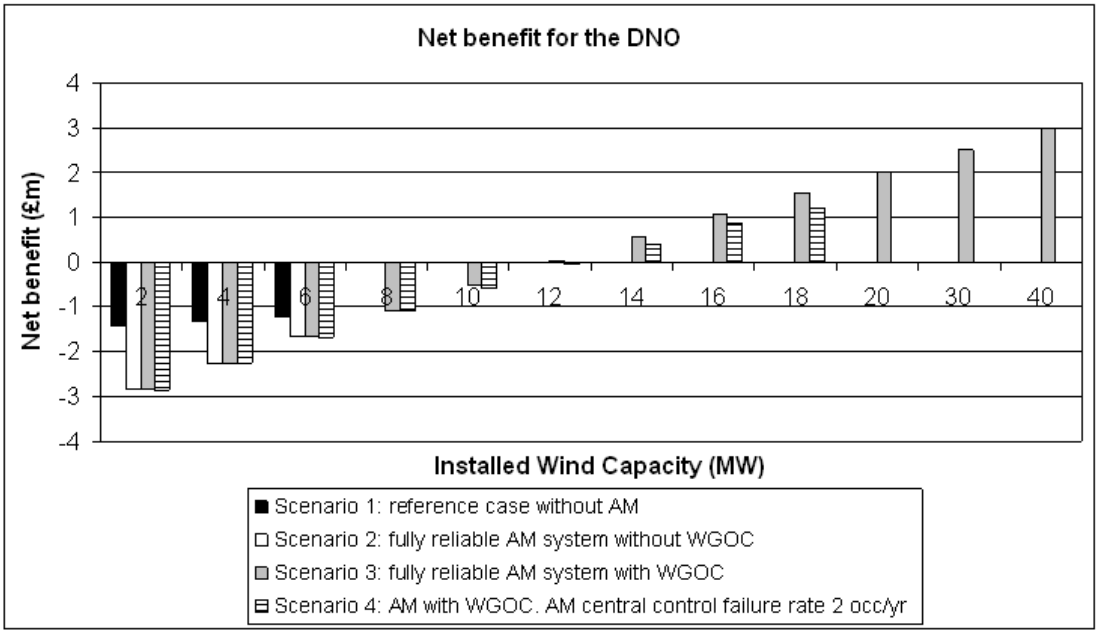

Figure 5.10: Net benefit for the DNO.

Because of reliability restrictions, it is not possible to accommodate wind generation capacity of more than 6, 6, and 18 MW for scenarios 1, 2, and 4, respectively. Scenario 1 yields a net loss for the DNO regardless of wind generation capacity, because the risk-associated cost outweighs the DG connection charge. A similar phenomenon is observed in scenario 2. The reason scenario 2 yields more loss for the DNO than does scenario 1 is because the AM investment cost outweighs the income earned from providing AM services in scenario 2. The uneconomical AM investment without the WGOC function contributes to losses for the DNO. For these two scenarios, no 'win-win' situation is observed.

The net benefit of scenario 4 for both the wind generation unit owner and the DNO seems to monotonically increase with rising wind capacity. However, this is a misconception that neglects the wind capacity limit. Because of reliability restrictions, the maximum wind capacity for scenario 4 is 18 MW. That the net benefit does not show a 'marginal benefit decrease' trend within the limited range is a reasonable result. This confirms that for scenario 4, the bottleneck in increasing wind generation capacity is system reliability. In other words, the realisation of the theoretical optimal point of maximum net benefit is impeded by the reliability constraint.

Scenario 3 is an ideal scenario that exists only in theory. For this scenario, system reliability is not a barrier to connected wind capacity. However, the maximum wind capacity is limited by economic barriers. The net benefit for the owner of the wind generation unit decreases with an increase in wind capacity of more than 20 MW. An incredibly high wind generation capacity yields a significant connection charge, as well as DG investment and O&M costs for the DG owner, whereas the revenue from selling electricity is capped because excessive wind energy is curtailed by the AM system. For these reasons, the net benefit for wind generation inevitably decreases.

A 'win-win' situation is achieved in scenarios 3 and 4 at wind capacities of 16 to 18 MW. This occurs when both the DNO and the wind farm owner earn a profit.

5.5.1 Traditional Reinforcement Scheme (TRS)

A TRS is proposed as an alternative solution to AM. Reinforcing the network with new branches is expected to alleviate constraints. Determining the best reinforcement plan is a network planning problem, whose methodology is beyond the scope of this project. For the test case in this chapter, identifying the best location for reinforcement by enumerating all possible plans and comparing them with one another is practical. The best 'one duplicated line' plan adds a duplicated line between buses 9 and 12.

The present value of the TRS investment is £500,000, and the EENS and net benefit of the DNO under the TRS are provided in Appendix A.

The maximum wind generation capacity is 6 MW. In the test case, although the TRS reduces EENS by around 8% to 15% (promoting reliability) compared with the 'doing nothing at all' base case, it neither increases the maximum wind generation capacity nor produces a positive net benefit for the DNO. Therefore, adopting the TRS to facilitate the penetration of wind generation is not a favourable approach for this test case.

5.6 Conclusion

In this chapter, the structure and reliability of the AM system has been modelled. Its effect on wind generation penetration and system reliability, as well as on the net benefit for the owner of the wind generation unit and the DNO has been investigated.

The case study confirms that the system can accommodate more wind power through the implementation of AM. Such an increase is significant when AM includes the WGOC function. Without this function, the ability of AM to accommodate wind generation is largely compromised. The reliability of AM does not have a noticeable effect on system reliability when the wind capacity is low. However, this effect grows with the increase in wind capacity. Therefore, ensuring reliable AM at a high wind capacity is critical.

The following conclusions can also be drawn from the case study:

1) Maintaining a certain level of wind penetration is necessary for DNO to earn a profit. When the wind generation capacity is within an appropriate range, a win-win situation is possible for a properly planned system where wind generation units are located at places with abundant wind resource. For such a system, the profit for DNO comes from charging connection fee from wind generation

owners and AM service fee less the investment and O&M costs; the profit for wind generation owner comes from the revenue of selling electricity less connection fee, AM service charge, investment cost and O&M cost. However, there is no win-win when the wind generation capacity is too low, because the DNO fails to recover its investment and O&M costs. On the other hand, the maximum wind generation capacity is limited by reliability constraints.

2) The theoretical economic optimal point may not be achievable because of the bottleneck, i.e., system reliability. Within zero to maximum wind capacity determined by the reliability restriction, the net benefit does not necessarily show a 'marginal benefit decrease' trend.

For the test case, although the TRS improves system reliability, it is not a favourable solution because it neither promotes wind penetration nor produces a profit for the DNO.

6 The Impact of Demand Response on Power System Reliability

Summary

Demand response (DR) is one of the key means of corrective control. This chapter quantifies the reliability improvement brought by DR. First, the background of DR is introduced. The definition of DR, the benefits of DR and the classification of different types of DR programmes are reviewed from existing publications. The gap is then identified based on the review, and it is followed by a summary of the major research work. The following section introduces the methodology. Three typical DR models are summarised. The system reliability assessment algorithm capable of simulating post-contingency system behaviours in a distribution network is proposed. The programme identifies islanding parts and performs network re-configuration at the post-contingency stage. A 16-bus distribution network is used as the test case. The conclusion is drawn from the test case regarding the key research question: DR slows down the degradation of system reliability in the context of continued load growth. The marginal benefit in reliability inevitably decreases with the incremental implementation of DR.

6.1 The Background of Demand Response

Measures must be taken as the grid is getting more and more stressed with the growing load. Compared with traditional network reinforcement, DR is a solution which incurs less cost and is more environmental friendly than the former. For most power systems, the vulnerable period when extreme load spikes occur lasts for only a couple of hours in a year. This is the moment when power systems are most vulnerable. It may be

uneconomical to accommodate the growing spikes by installing peak generation units which remain idling for most time in a year. Alternatively, DR, which can be used as a form of spinning reserve, is a cheap resource in tackling the growing peak load.

As an ongoing and fast developing application, DR brings significant potential benefits to various parties [68-70] In the broad scope, all intentional modifications of electricity consumption pattern can be classified as DR. DR brings potential benefits to various parties by directing customer 'behaviour' through incentive signals. These benefits include

1) save electricity bills for customers;

2) reduce wholesale market prices since the cost of DR is expected to be lower than the costly peak generation units;

3) reduce or delay the investment of peak facilities;

4) improve system reliability by relieving system stress under peak demand;

5) provide environmental benefits including saved lands, saved natural resources and reduced emission; and

6) facilitate intermittent renewable generation [68].

DR can be classified into two broad categories, the price-based programs (PBP) and the incentive-based programs (IBP) [68, 71]. In some IBPs, participants are given incentives according to contracts to change their electricity consumption pattern: compensations are paid if participants fulfil the contract and penalties may be imposed if not. Typically, participants have to reduce their loads when requested by the network operator for either reliability purpose or to avoid high electricity price. In direct load control programmes, utilities have the power to shut down loads remotely upon giving a short notice to the customer [68]. As another form of IBP, demand bidding programme allows participants (large customers in practice) to 'buy back' electricity from the wholesale market. Under such programme, each participant bids for load reduction offers. If a bid is lower than the market clearing price, the participant has to curtail the specified amount of load or a penalty will be imposed [68].

Compared with IBP, PBP encourages participation in DR by sending price signals to participants. Instead of facing a flat price which leads to inefficiency, customers are subject to varying price depending on the time when they consume, or directly on the

market bidding, with the help of advanced metering [5]. Typical PBPs are Time-of-Use (TOU) Tariffs, Critical Peak Pricing and Real-time Pricing (RTP) programs. The ultimate objective of PBP is to smooth the load curve by charging a high price at peak hours and a low price at off-peak hours. Over the past 20 years, EU member states have adopted various kinds of PBP, most of which are based on discrete timing and pricing for interruption [5].

In the UK, three of the ongoing DR applications are pre-agreed load shedding, real-time pricing and direct emergency load control. They are mainly for large industrial customers [5, 72]. At the other end of the scale, 'Economy 7' has been implemented on a voluntary basis for residential customers in the UK. 'Economy 7' programme offers two prices to customers: the normal price (at daytime) and the off-peak price (which lasts for 7 hours at night) [73]. In this way, customers are encouraged to shift their demand from peak time to off-peak time.

The implementation of DR incurs different kinds of costs to various parties. The costs can be classified as initial costs and running costs [5]. For participants, the initial costs resulting from the installation of smart meter and on-site generation units, etc [5]. The running costs include the fuel cost of on-site generation units and some indirect cost of inconvenience and plan rescheduling etc [5].

For utilities, the investment cost of smart metering and communication devices, the marketing cost and the cost of customer education should all be taken into account [5].

A brief summary of existing publications involving DR is given below:

European policies on DR are summarised in [5]. Under the most moderate scenario, EU-wide benefits of DR will include 100 TWh of annual energy saving, an annual reduction of 30 million tons of CO2, and tens of billions of Euros saved from avoided/delayed network investment and customer bills by 2020. The main obstacles are identified as the inelasticity of demand and asymmetries in information.

Interruptible loads and capacity market programmes are modelled in [74]. Customers participating in the interruptible load programme agree either to curtail a certain amount of electric load, or to keep their load below a pre-specified level upon a short notice of less than an hour. In return, they receive payments from the network operator. The maximum number of times and hours that the programme can be triggered in a year is specified by the contract.

A survey of DR programmes in various electricity markets is presented in [75]. DR programmes are put into two categories, 'reliability-based' programmes which are triggered in response to system contingencies and 'market-based' programmes which are responsive to market prices. As one of the 'market-based' programmes, the Economic Load Response Programme produces two options: a day-ahead option and a real-time option. In the day-ahead option, participants submit their bids in the day-ahead market for load reductions and are paid at the day-ahead hourly electricity price if their bids are accepted. A penalty is imposed for failing to deliver accepted bids. The real time option allows participants to submit load reduction bids in the intraday market with one hour notice to the Pennsylvania – New Jersey – Maryland (PJM) system operator. Participants are paid at the real-time price for accepted bids. Contrary to the day-ahead option, no penalty is charged if participants fail to deliver [75].

The utilisation of DR resources in Great Britain on the transmission level is summarised in [76]. National Grid has been utilising DR in the form of balancing services, e.g., fast reserve, firm frequency response, frequency control by demand management of large industrial customers and standing reserve [76]. Furthermore, National Grid has the power to request a DNO for demand response.

Some work has been undertaken regarding reliability issues in the context of DR. As a resource that substitutes for spinning reserves, emergency DR programme has been implemented into the reliability study, where only generation failure is considered [77]. The results indicate that DR has a positive impact on system reliability.

A brief explanation is given in [76] where DR serves reliability purposes for power systems. DR serves contracted resources for real-time load balancing activated by network frequency or a disturbance of a system. However, as a brief review, this article does not present any detailed models, methodologies or case studies.

DR is a suitable partner of renewable generation as well: with the increasing penetration of intermittent generation, DR can help maintain satisfactory system reliability by providing flexibility to the system [4].

According to [78], retail loads serving reliability purposes can participate in the day-ahead market or intraday market. The reliability of bulk systems can be improved by including retail loads into the market [78]. However, this article presents qualitative conclusions only without presenting methodology or case study.

Reference [79] demonstrates that by serving as a form of spinning reserve, aggregated demand side resources are able to improve power system reliability. This report focuses mainly on the technical feasibility and operational details of demand side resources rather than on the reliability assessment of power systems.

Two more articles give brief, qualitative introductions on the impact of DR on system reliability [80, 81]. Their main ideas largely overlap those reviewed above.

A couple of more papers on reliability assessment of distribution system are summarised as follows:

The failure mode and effect analysis (FMEA) is applied in [82] for reliability assessment on a radial distribution network. However, this method does not account for chronological loads, which are essential when modelling DR. The Monte Carlo simulation (MCS) approach applied to the reliability assessment of distribution systems is reviewed in [83]. An enhanced sampling method, which increases the speed of MCS, is applied in this paper [83]. In another paper, a CMCS approach is proposed for evaluating the probability distributions of reliability indices [84]. However, neither of them involves DR or system auto-reconfiguration at the post-contingency stage.

Fuzzy multi-objective approach is applied for auto-reconfiguration of distribution systems in [85]. Although this method yields highly optimal results, it is not suitable for application in this research because of its low efficiency. High efficiency is a critical requirement when the system reconfiguration algorithm has to be called for tens of thousands of times in CMCS.

Although numerous papers and reports mentioned that DR improves power system reliability, yet few have presented a comprehensive analysis of power system reliability in the context of DR. Below is a brief summary of the work that has been done and the gaps that this project has bridged.

1) Three representative models of DR for application in the reliability assessment are summarised. They are the load shifting model, the load reduction model and the emergency interruptible load model. These three models represent a wide range of existing DR programmes.

2) A composite reliability index and two new indices are applied in this chapter. LINWRI quantifies the overall system reliability considering multiple aspects. DRICB quantifies the incremental benefit in reliability brought by DR. It is particularly useful

to Distribution Network Operator (DNO) in assessing the benefits of DR. VECL distinguishes the voluntary load curtailment from the forced load curtailment by quantifying the implementation level of Emergency Interruptible Load Program (EILP).

3) A flexible algorithm capable of simulating actual system behaviour in a distribution network at the post-contingency stage is proposed. The algorithm performs network re-configuration and identifies islanding parts at the post-contingency stage, based on AC power flow.

6.2 DR Models

Three typical DR models, i.e., the load shifting model, the load reduction model and the emergency interruptible load model are introduced below.

The load shifting model curtails the electricity demand during the peak hour and replaces it in the off-peak hour. When the electricity price exceeds a price threshold, the load is curtailed by a certain percentage. When the electricity price falls below the price threshold, customers start to make up their electricity demand over the next few hours. This is modelled by a percentage increase from the original load spread over the off-peak period. The annual energy consumption under DR can be set either greater than that without DR, which means that the electricity demand increases considerably after being shaved at the peak hour, or less than the latter representing a moderate or slight increase in electricity demand after DR, or equal to the latter. This model simulates the load feature under the PBP where customers adjust their behaviour according to price signals. For example, households may postpone their use of washing machines from peak to off-peak hours. The model is flexible in that the signal to which customers respond is adjustable. It can be real-time prices or discrete prices.

Unlike the load shifting model, the overall load reduction model reduces the electricity demand at peak hours without making it up later. This model also simulates the response of some types of demand under the PBP. Lighting is a typical example: it automatically dims following the corresponding price signal sent in by the smart meter or a decrease in frequency, and will not be brighter than normal at a later off-peak hour since it is not necessary [86].

Emergency interruptible load programme (EILP) corresponds to a typical IBP where participants are likely to be large industrial customers. The contract can be as follows: the customer agrees to curtail its load or start its own on-site generation upon request from the DNO in hours of emergency when the system is highly stressed or the electricity price experiences spikes [87, 88]. In return, the customer gets compensation from the DNO. Such curtailment serves the function of spinning reserves [75, 89]. A typical example is an "Emergency Load Response Program" which stipulates a two-hour notification period prior to curtailment, a total duration of curtailment of up to six hours (historical average of fewer than four hours), and events occurring no more than ten times a year [88]. In the UK, the response time could be down to minutes [76].

In practice, different types of customers participate in different DR programmes with varying extents. Therefore, different DR models can be implemented in the simulation at the same time, and the overall effect on system reliability can be identified. The DR models are flexible in the sense that, with slight alterations, they are able to respond to different 'signals' such as the real-time price signal, discrete price signal, as well as various incentive contracts.

6.3 Reliability Assessment of Distribution Systems

An efficient algorithm has been developed which models the behaviour of distribution systems at the post-contingency stage. A recursive search is conducted from the faulted component (either a branch or a bus). The purpose is to locate the nearest normally open switch which, if closed, will resume at least one affected load bus. Then the faulted component is isolated, and the normally open switch is closed.

Although the algorithm is highly efficient and straightforward in a radial network, it has sacrificed optimality as a trade-off: the reconfiguration scenario generated by this algorithm may not be optimal in resuming the maximum number of load buses.

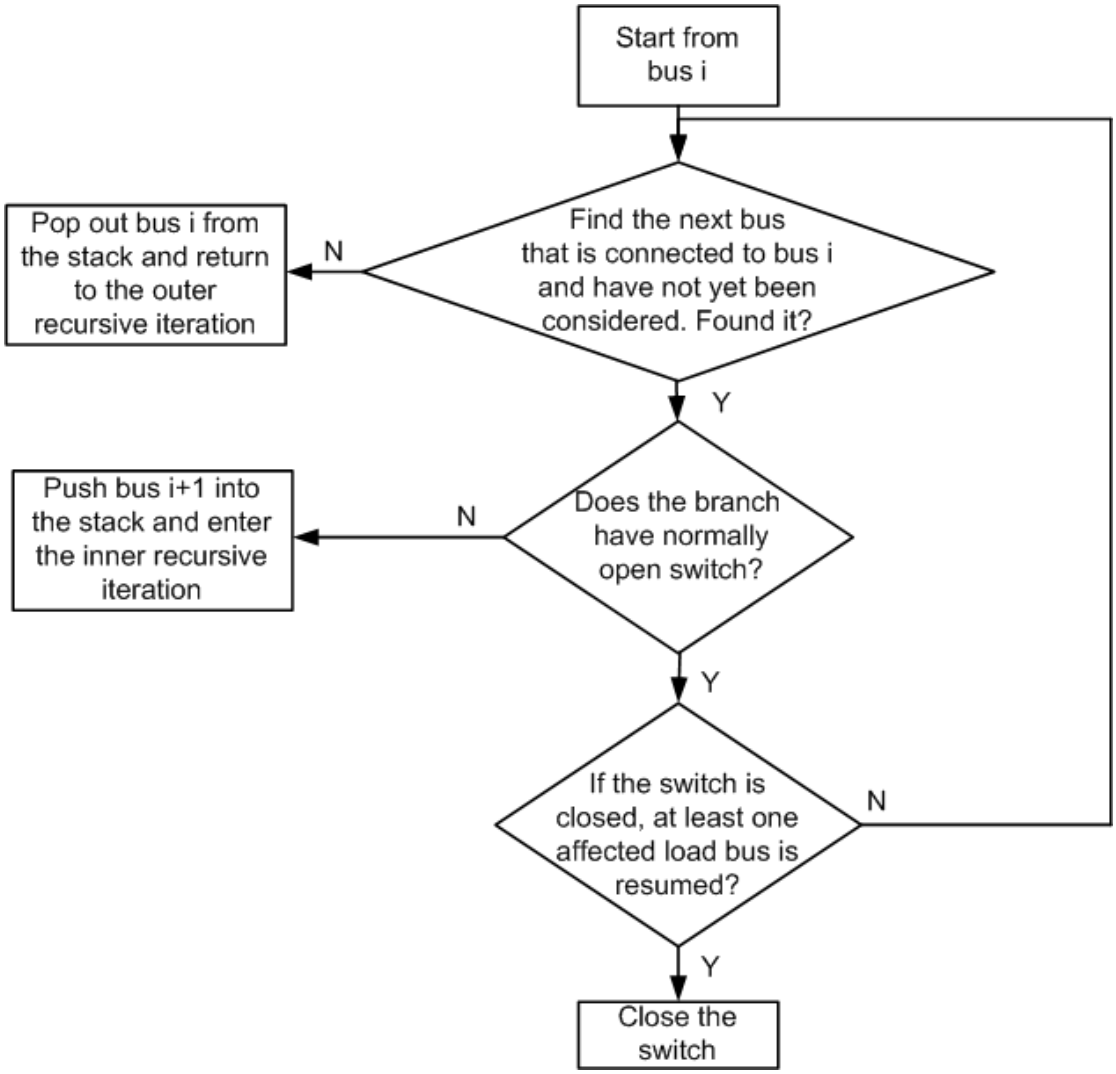

Figure 6.1: Recursive algorithm to determine network re-configuration actions.

Before performing the reliability assessment of distribution systems, it is essential to have a profound understanding and a reasonable model of the post-contingency reactions of distribution systems, such as self-clearing of faults, minimising the impact of protection system operations and fast restoration of loads by reconfigurations. The post-contingency reactions in distribution systems are illustrated as follows, in a chronological order:

1) A fault occurs in the network. With a properly coordinated protection system, the nearest upstream circuit breaker with reclosing relay trips.

2) The opened circuit breaker makes several attempts to re-close. If the fault is temporary or transient, the circuit breaker successfully closes, and all downstream load points suffer only momentary outage.

3) If the fault persists, the circuit breaker will “lock out” after several unsuccessful attempts to re-close. The operator receives warning and sends out crews to identify the fault location.

4) After the identification of the fault location, the faulted component is sectionalised by either manual or automatic switching. It then awaits further repair. The aforementioned recursive search is then conducted to resume some or all of the affected loads by closing the normally open switch. This step is called network reconfiguration.

5) The system is analysed for any voltage or power flow violations. In case of any violation, load curtailment is called to correct the problem.

6) After the completion of the repair job, the network configuration is switched back to its original status.

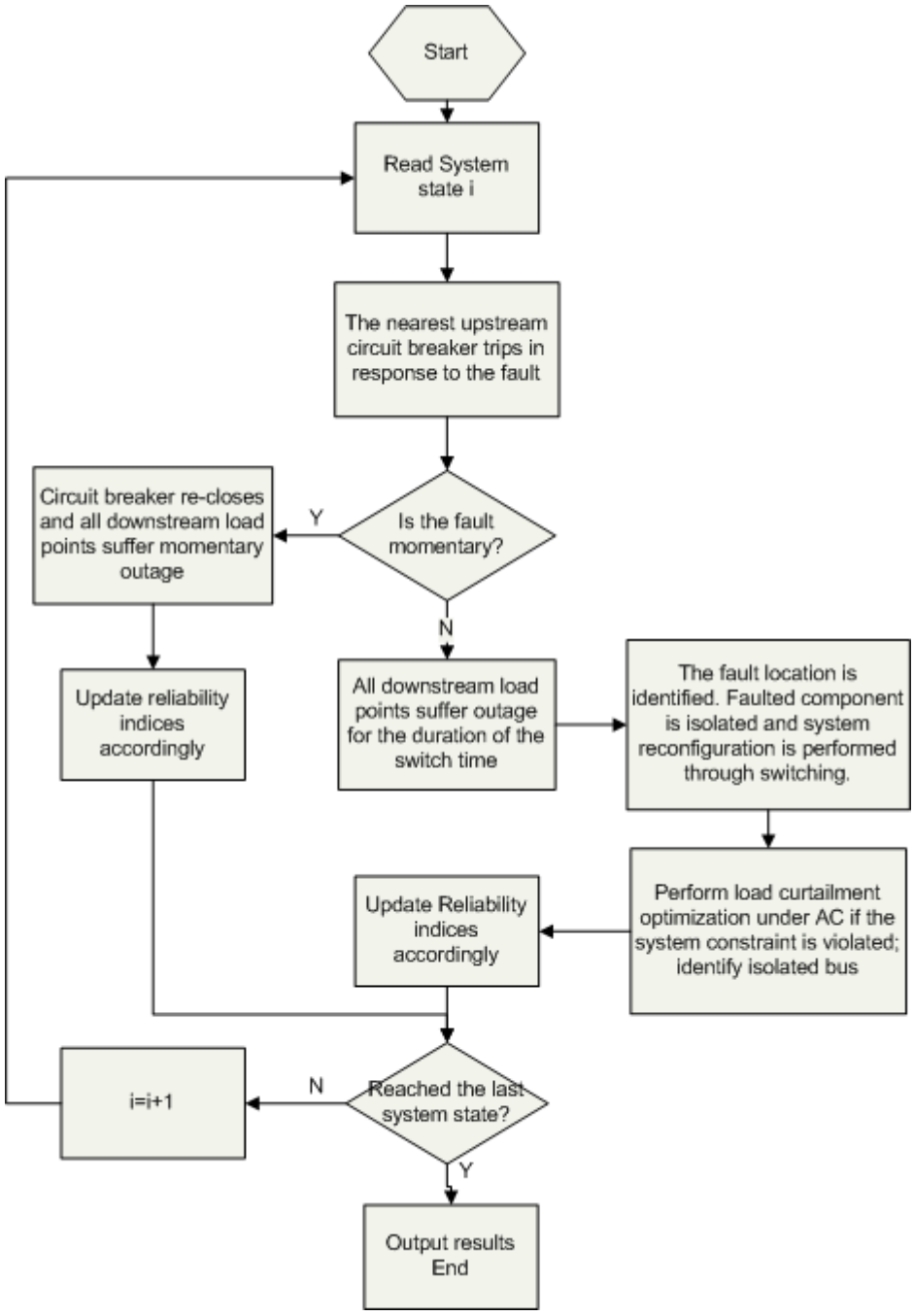

Figure 6.2: CMCS algorithm.

The above procedure is implemented into CMCS where both momentary outage and sustained outage are taken into account. When a fault occurs in the system, the optimisation algorithm with the objective to minimise the total cost of load curtailment is called. Load curtailment triggered by EILP (or 'voluntary curtailment') is treated in a different way from the forced load curtailment (or 'forced curtailment'): the forced curtailment is converted into risk-associated cost using composite customer damage

function (CCDF), whereas voluntary curtailment incurs a cost to DNO dictated by the contract.

For a distribution system where branch resistance is comparable to its reactance, the assumption on which the DC load flow is based is not valid. Therefore, AC optimisation is applied in this chapter.

The AC optimisation model is presented below.

$$\min \sum \mathrm{f}(\mathbf{P}_{\mathrm{fCur}}) + \mathrm{g}(\mathbf{P}_{\mathrm{vCur}}) \quad \textbf{(6.1)}$$

subject to

$$P_{gi} - P_{li} + P_{\mathrm{fCur}i} + P_{\mathrm{vCur}i} = P_i(\mathbf{V}, \boldsymbol{\theta}) \quad \textbf{(6.2)}$$

$$Q_{gi} - Q_{li} + Q_{\mathrm{fCur}i} + Q_{\mathrm{vCur}i} = Q_i(\mathbf{V}, \boldsymbol{\theta}) \quad \textbf{(6.3)}$$

$$Q_{\mathrm{fCur}i} = \frac{P_{\mathrm{fCur}i}}{P_{li}} Q_{li} \quad \textbf{(6.4)}$$

$$Q_{\mathrm{vCur}i} = \frac{P_{\mathrm{vCur}i}}{P_{li}} Q_{li} \quad \textbf{(6.5)}$$

$$0 \le P_{\mathrm{fCur}i} \le P_{li} \quad \textbf{(6.6)}$$

$$0 \le P_{\mathrm{vCur}i} \le P_{\mathrm{vCur}i}^{\max} \quad \textbf{(6.7)}$$

$$P_{gi}^{\min} \le P_{gi} \le P_{gi}^{\max} \quad \textbf{(6.8)}$$

$$Q_{gi}^{\min} \le Q_{gi} \le Q_{gi}^{\max} \quad \textbf{(6.9)}$$

$$T_k(\mathbf{V}, \boldsymbol{\theta}) \le T_k^{\max} \quad \textbf{(6.10)}$$

$$V_i^{\min} \le V_i \le V_i^{\max} \quad \textbf{(6.11)}$$

where

Function f(x)	composite customer damage function
Function g(x)	cost function of EILP
$\mathbf{P}_{\mathrm{fCur}}$	real power forced curtailment vector
$P_{\mathrm{fCur}i}$	real power forced curtailment at bus i
$P_{\mathrm{vCur}i}^{\max}$	maximum real power voluntary curtailment at bus i
$\mathbf{P}_{\mathrm{vCur}}$	real power voluntary curtailment vector

$Q_{\text{fCur}i}$	reactive power forced curtailment at bus i
$P_{\text{vCur}i}$	real power voluntary curtailment at bus i
$Q_{\text{vCur}i}$	reactive power voluntary curtailment at bus i
T_k	branch power flow

6.4 Case Study

The test case is the 16-bus distribution system at 33kV level. The network diagram shown in Figure 6.3 is similar to that used in Chapter 5 with the following difference: three normally open switches are added to this version.

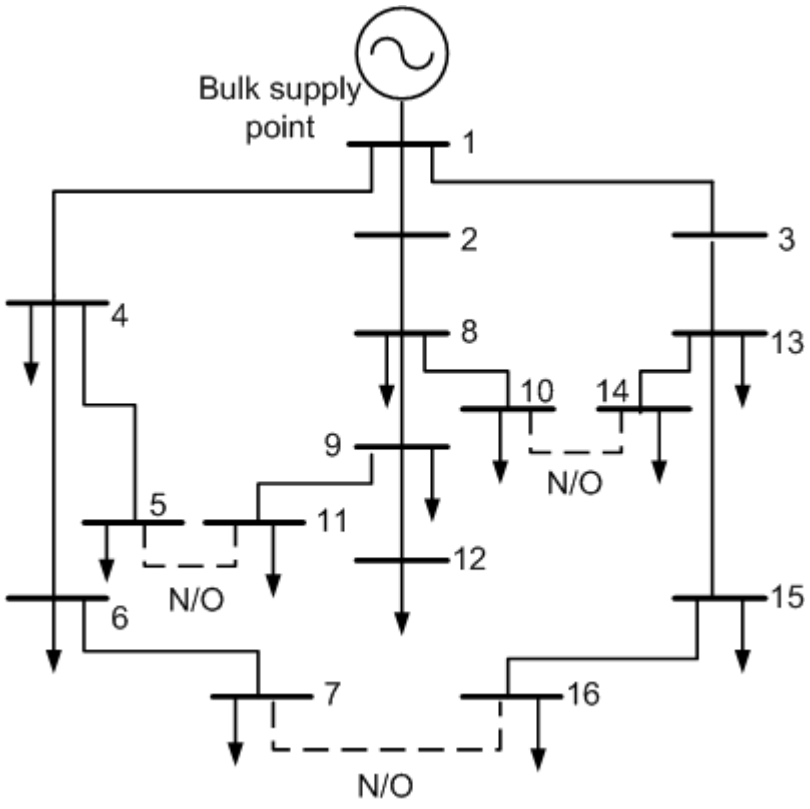

Figure 6.3: Network diagram of the 16-bus test case.

All network data are given in Appendix B.

The three types of customer considered in the study are domestic customers, commercial customers and industrial customers. Hourly load profile throughout a year is used [90].

Both branch failure and bus failure are considered. Branches and buses are subject to two types of outages, i.e., the momentary outage and the sustained outage. Each bus is fitted with a circuit breaker and a reclosing relay ('recloser'). The protection system is coordinated that the first-responsive circuit breaker is the one on the nearest bus upstream of the fault location.

The load is growing at an annual rate of 2.5%, and there is no load shedding if no fault occurs in the system.

The optimization algorithm aims to minimise the cost of load shedding. This cost is calculated as a function of the amount of load curtailed and the duration. The Composite Customer Damage Function (CCDF) is given in Appendix B.

Five scenarios are defined. They are

1) the reference scenario with no demand response;
2) load shifting only, maintaining the total energy consumption over a year to be the same as that of the reference case;
3) load reduction only;
4) joint implementation of load shifting and load reduction; and
5) EILP (for industrial customers only).

For scenario 2, 3 and 4 in year 1, the load threshold above which DR is triggered is set as 87% of the peak load, or 25MW. Such threshold increases at the same rate with the annual load growth rate which is 2.5%. When the total load in the system exceeds the threshold, loads at all buses are cut by 10% through DR (load shifting and load reduction only). For scenario 2, loads at subsequent off-peak hours increase (by no more than 5% at each bus each hour) while maintaining the total energy consumption in a year to be the same as that of the reference scenario. However, the 'bouncing' of the load in off-peak hours immediately after load shifting may cause 'the second peak'. No action is taken against "the second peak" in Scenario 2. In contrary, Scenario 4 has implemented both load shifting and load reduction. This eliminates 'the second peak'.

SAIFI, SAIDI, MAIFI and LINWRI results are shown in Figure 6.4 – Figure 6.7, respectively. Each scenario is simulated for up to 10 years.

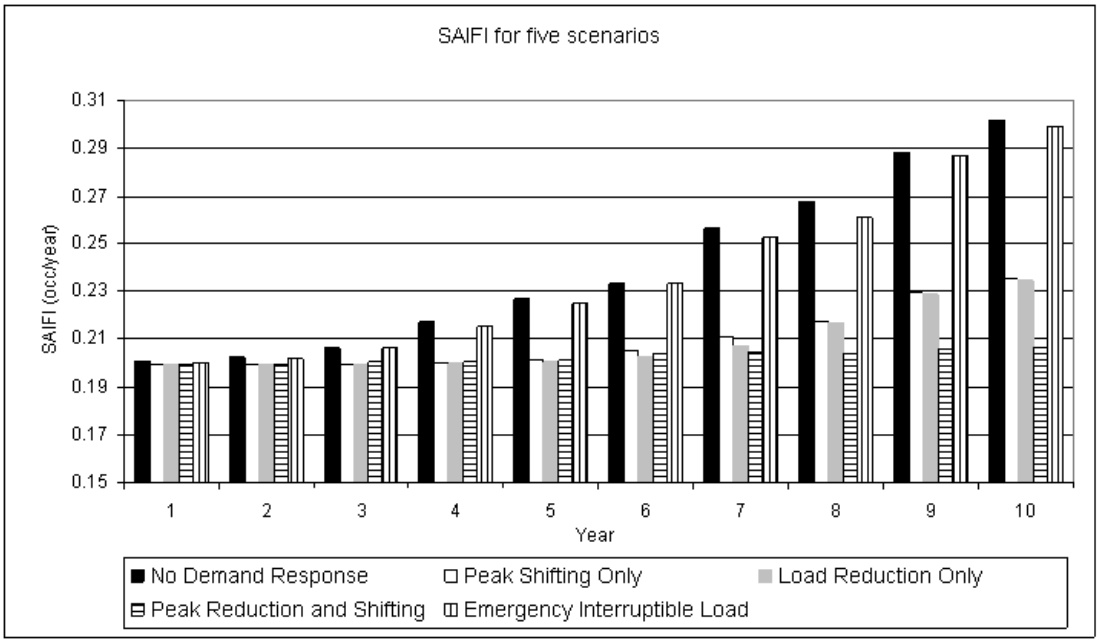

Figure 6.4: SAIFI results for the five scenarios.

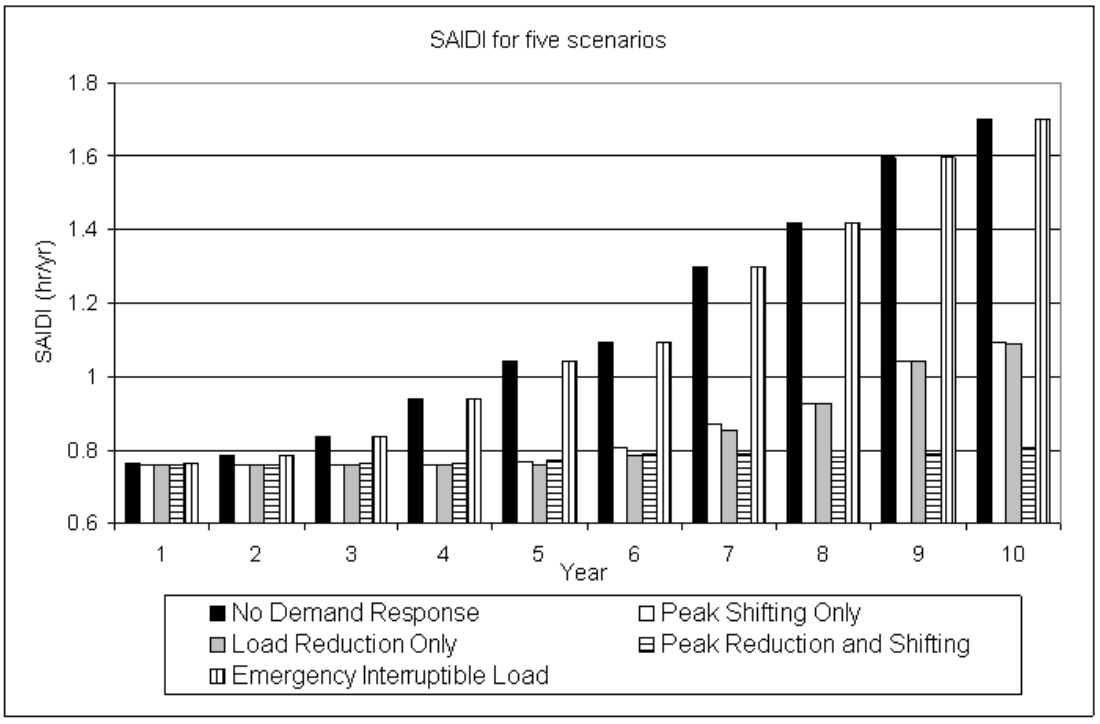

Figure 6.5: SAIDI results for the five scenarios.

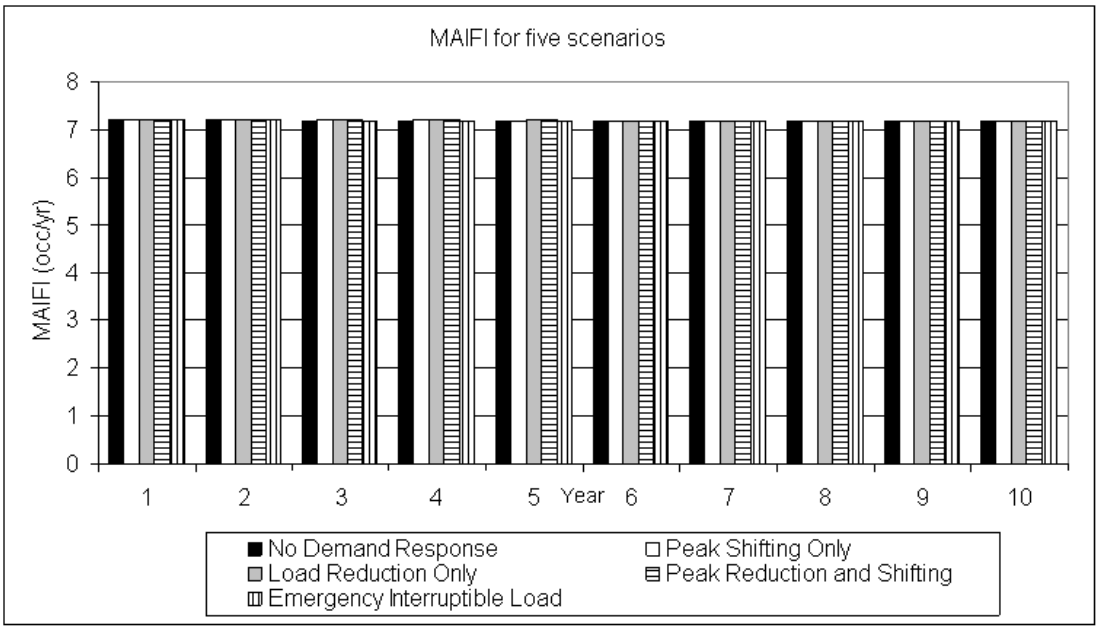

Figure 6.6: MAIFI results for the five scenarios.

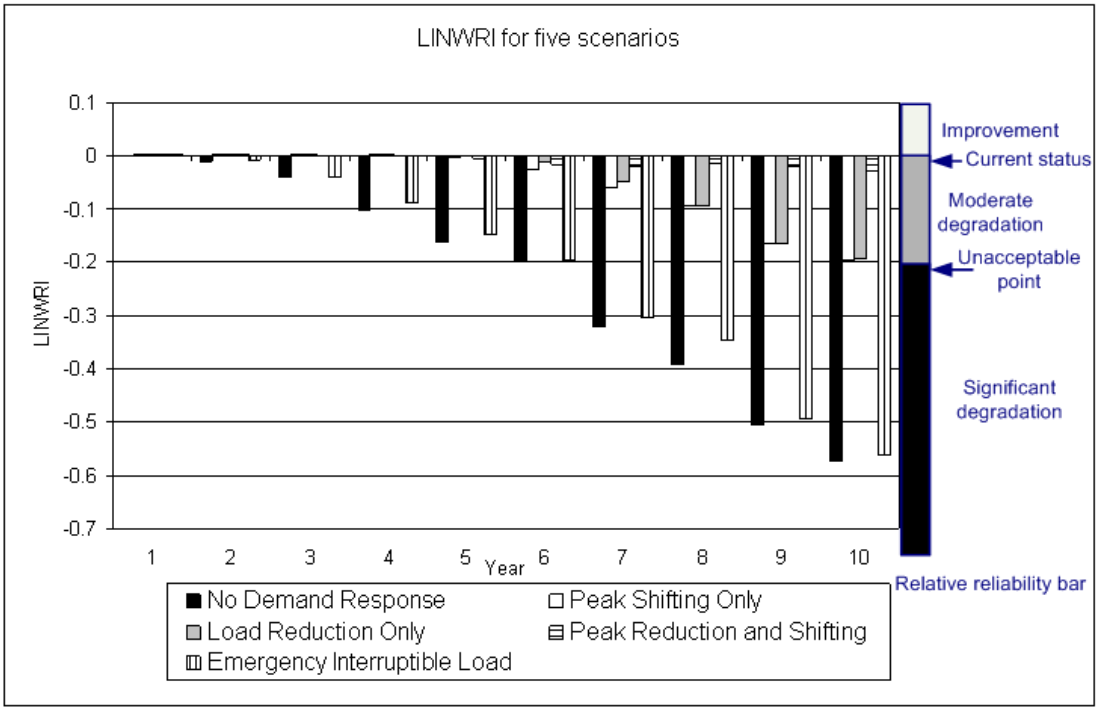

Figure 6.7: LINWRI results for the five scenarios.

SAIFI, SAIDI and MAIFI are assumed equally important in forming the overall reliability picture. Therefore, the weighting factors are equal to each other and should sum up to 1.

$$\text{LINWRI} = \rho_1 \frac{\text{SAIFI}}{\text{SAIFI}_{\text{ref}}} + \rho_2 \frac{\text{SAIDI}}{\text{SAIDI}_{\text{ref}}} + \rho_3 \frac{\text{MAIFI}}{\text{MAIFI}_{\text{ref}}} \quad \textbf{(6.12)}$$

where $\rho_1 = \rho_2 = \rho_3 = 0.3333$

Scenario 1 in year one is set as the reference case of which LINWRI is 0. As is mentioned in previous chapters, the unacceptable point is often determined through practical experience rather than through a rigorous mathematical process. In this case, it is defined as the point where $\text{LINWRI} = -0.2$, i.e., the reliability level of the reference scenario at year six. This point is deemed as the extreme point where network investment in branches and related facilities should be put into practice immediately.

The figures show that given the same year, the reference scenario (scenario 1) and the EILP scenario (scenario 5) yield approximately the same reliability results. Their SAIFI and SAIDI are higher (LINWRI are lower) than the corresponding indices of other scenarios, showing a poorer overall reliability level than other scenarios. According to LINWRI results, the scenario with the highest reliability level is the 'load shifting and reduction' scenario (scenario 4). DR clearly slows down the reliability degradation in the context of load growth: although system reliability still degrades with the load growth, the slope of such degradation is reduced by DR.

Unlike SAIFI, SAIDI or MAIFI, the absolute LINWRI value of a single case is not as meaningful as its relative value. The extensive meaning of LINWRI is only revealed when LINWRI results of different scenarios are compared with each other. One of the purposes of coining this new index is to derive the reliability ranking of different scenarios considering multiple aspects. Another purpose is to indicate clearly to which reliability zone each scenario belongs. Take the LINWRI results in year 8 as an example (see Figure 6.7): LINWRI results clearly indicate the reliability ranking in increasing order: the reference scenario < the 'emergency interruptible load' scenario < the 'peak shifting only' scenario, the 'load reduction only' scenario < the 'peak reduction and shifting' scenario. The reference scenario and the 'emergency interruptible load' scenario are in the 'significant degradation' zone, whereas the other three belong to the 'moderate degradation' zone.

Figure 6.6 shows that all cases yield almost the same MAIFI results regardless of the year. This phenomenon is reasonable: a momentary outage occurs under either of the two circumstances:

1) a momentary fault; or
2) a permanent fault followed by the tripping of the circuit breaker and the network reconfiguration process.

Under the first circumstance, all load points downstream of the nearest tripped circuit breaker (with recloser) suffers from momentary outage. The reason why they do not suffer from permanent outage is that the automatic re-closing operation will resume the power supply, given the momentary nature of the fault. Under this circumstance, whether a bus experiences a momentary outage following a fault depends on the network topology only.

Under the second circumstance, all load points that is not at a faulted bus and are reachable through alternative routes (this requires a 'connectivity' study) to the power supply bus are likely to suffer from momentary outage, provided that no system violation (power flow study is involved) occurs which may cause further load shedding. However, the probability of voltage/branch flow violation is low.

In reality as well as in the test system, momentary faults occur to network components much (in this case approximately 10 times) more frequently than do permanent faults in distribution systems. Therefore, MAIFI is mainly contributed by the first circumstance which is purely a 'connectivity' problem depending on the network topology. All scenarios have the same network topology which does not change over time. Therefore, DR programmes and the load level have little impact on MAIFI results.

Expected years of network investment deferral can be directly calculated from Figure 6.7. Take scenario 1 and scenario 3 as examples: LINWRI result of the former scenario reaches the 'unacceptable level' in year 6, whereas LINWRI of the latter degrades to the same level in year 10. Therefore, the network investment is deferred by 4 years under scenario 3. Similarly, network investments are deferred by 4 years and more than 4 years under scenario 2 and 4, respectively.

6.4.1 The Effect of Different DR Implementation Levels

Under Scenario 3 ('load reduction only'), the effect of DR implementation level on power system reliability is studied for up to 10 years. Load is reduced when it is above the pre-specified threshold as is mentioned in the previous section. The amount of load reduction, as a percentage of the peak load (or the peak load reduction rate), represents the level of DR implementation level. The sensitivity analysis is performed by varying the percentage mentioned above. SAIFI, SAIDI, MAIFI and LINWRI results are expressed in Figure 6.8 – Figure 6.11, respectively.

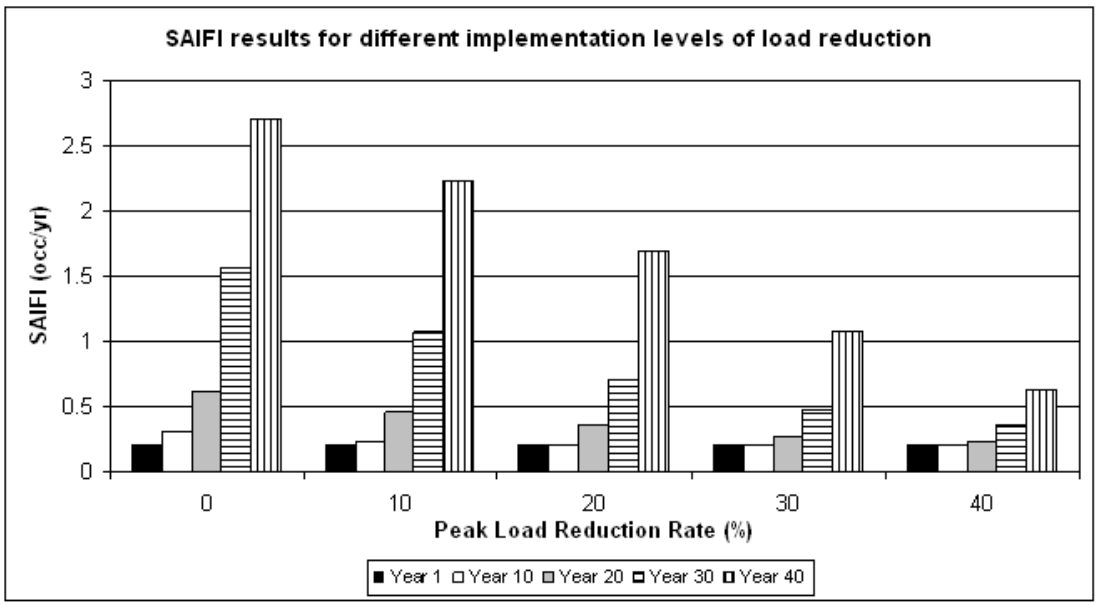

Figure 6.8: SAIFI results for different DR implementation levels of load reduction.

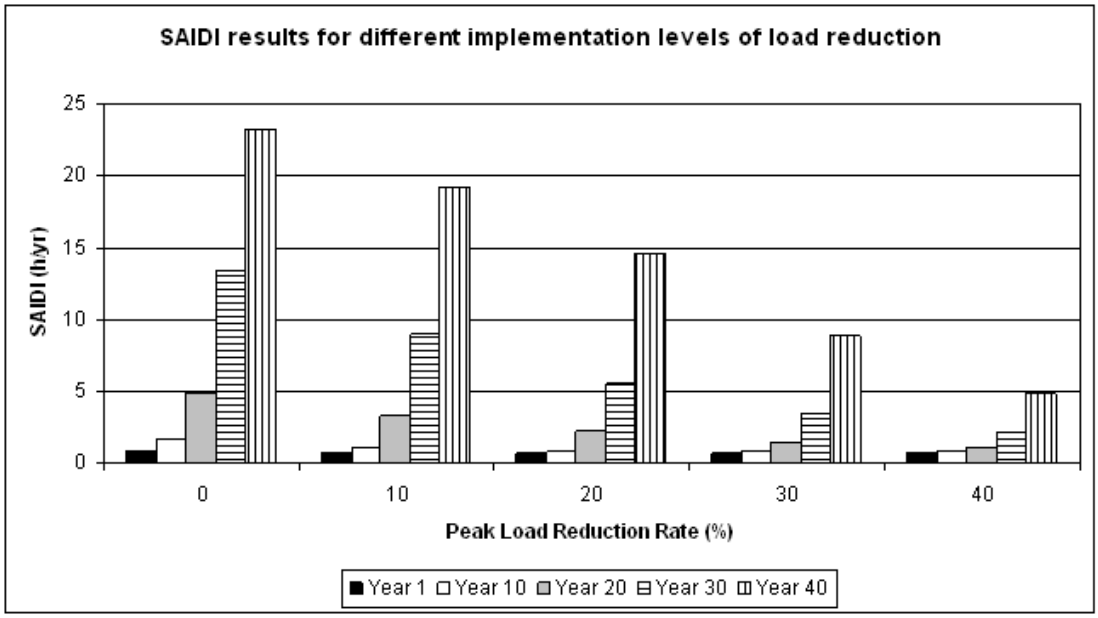

Figure 6.9: SAIDI results for different DR implementation levels of load reduction.

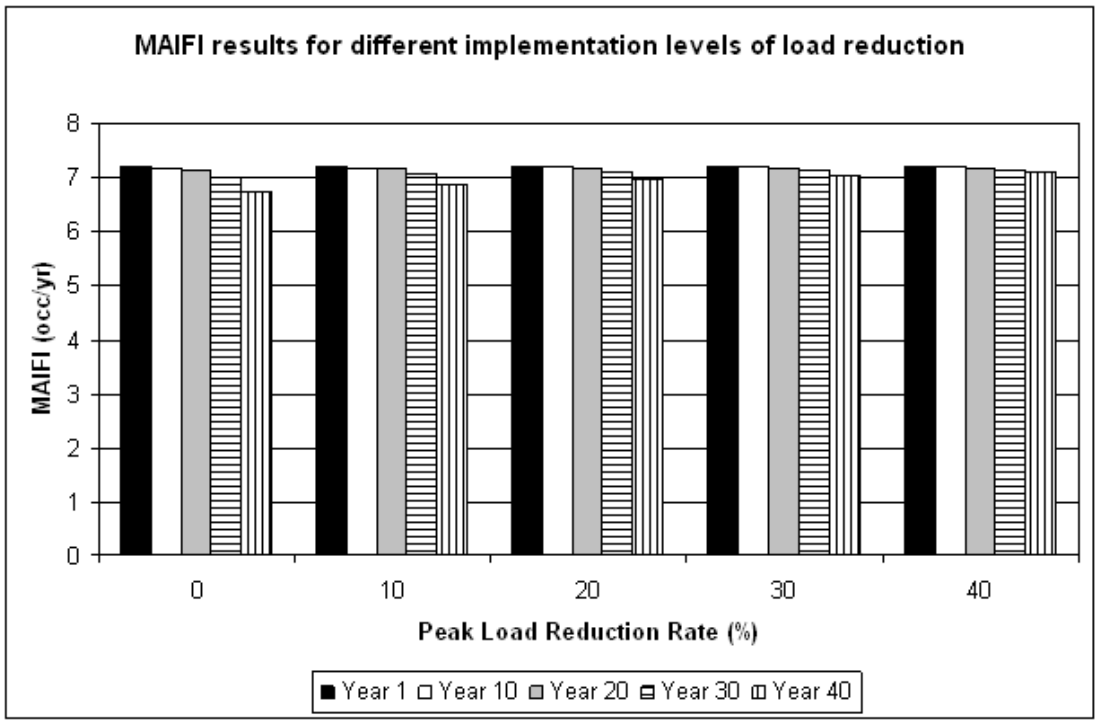

Figure 6.10: MAIFI results for different DR implementation levels of load reduction.

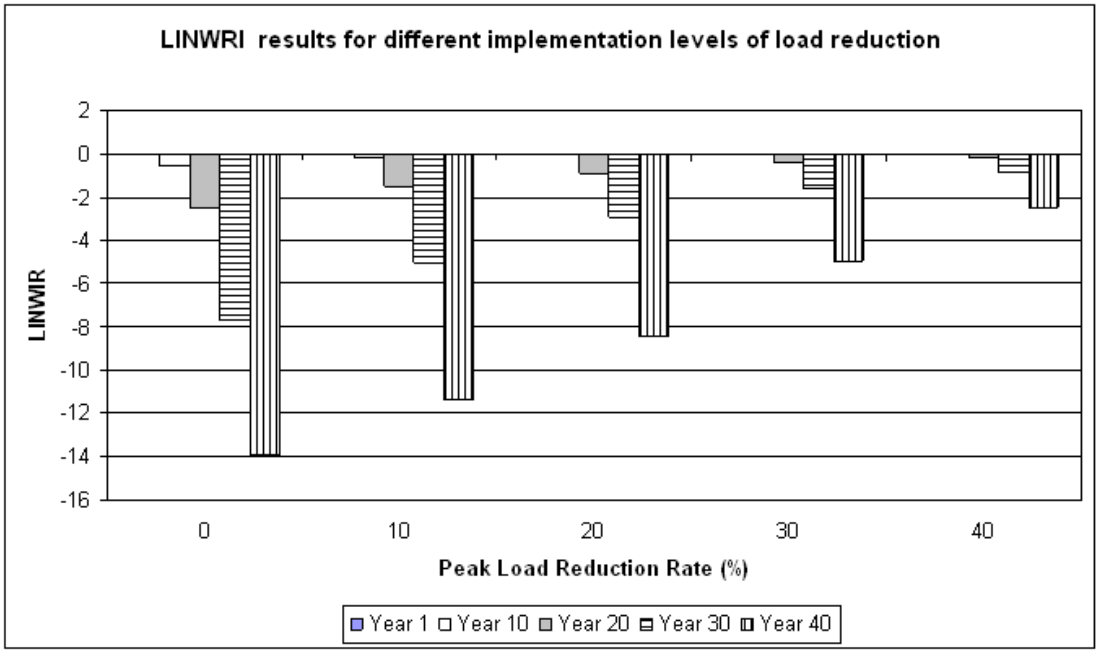

Figure 6.11: LINWRI results for different DR implementation levels of load reduction.

The reference case is the reference scenario in year one. SAIFI results remain almost the same in year one regardless of the peak load reduction rates. The same applies to other indices in year one. This phenomenon is justified by the load reduction model: loads are reduced when they are above the pre-specified threshold. Loads in year one are below the threshold for most of the time. Therefore, the increasing DR implementation has negligible effect on the reliability indices in year one. The DRICB index has also been calculated, and results are shown in Table 6.1 and Figure 6.12.

Table 6.1: DRICB results for different years and different implementation levels of DR

Peak Load Reduction Rate (%)	**DRICB (£/MWh)**			
	Year 1	**Year 10**	**Year 20**	**Year 30**
0	0.13	4.34	5.99	7.92
10	0.19	4.53	5.87	10.00
20	0	1.51	6.70	7.51
30	0	0.30	5.65	6.95

40	0	0	2.40	6.68
50	0	0	1.12	5.24
60	0	0	0	3.18

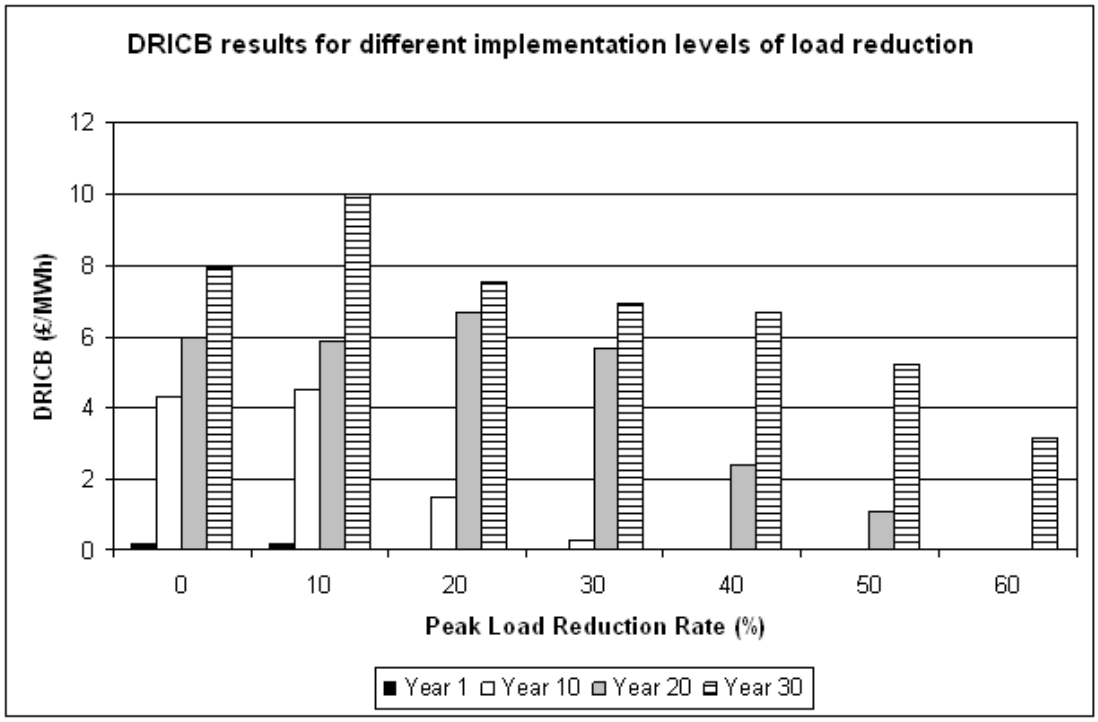

Figure 6.12: DRICB results for different DR implementation level under scenario 3.

DRICB indicates the incremental benefit in reliability (in £) of incremental reduction in annual energy consumption.

Figure 6.12 shows that the DRICB is close to zero under the load in year one. This result corresponds to that in Figure 6.11. This is because the system is already highly reliable in year one due to the light load, and further DR implementation has almost no impact on system reliability.

DRICB does not monotonically decrease with the increase in the peak load reduction rate from the starting point where the peak load reduction rate is zero. However, it inevitably decreases after a certain point. For example, DRICB in year 30 decreases after the point where Peak Load Reduction Rate=10%. Although the turning point may be different, similar trends apply to DRICB results in other years. This phenomenon

confirms that: when DR implementation level is low, incremental implementation of DR may significantly improve system reliability. However, when DR implementation reaches a certain level, incremental benefit finally decreases.

DRICB is not an all-inclusive index. Rather, it quantifies one of the key benefits of DR, i.e., the benefit in power system reliability. For a comprehensive analysis of DR benefits, it is necessary to take into account other types of benefits such as the reduction in generation costs, delayed network investments and environmental benefits, etc., which are not in the scope of this research.

6.4.2 The Effect of Emergency Interruptible Load Programme

When an outage becomes imminent as the result of a fault under scenario 5, EILP is triggered to alleviate the consequence. Only industrial loads participate in EILP.

Industrial loads can be classified as large industrial loads (maximum load in a year greater or equal to 10 kW) and small industrial loads (maximum load in a year lower than 10 kW). The threshold of 10 kW does not change over years. For a large industrial load, EILP only curtails up to a percentage of the load under emergencies. Denote this percentage as p. For a small industrial load, EILP curtails the load completely. Scenario 5 is investigated in this section with different levels of p: 1) p=10%; 2) p=20%; 3) p=30%.

The VECL and expected interruption cost (EIC) indices for the three scenarios are expressed in Figure 6.13 and Figure 6.14, respectively.

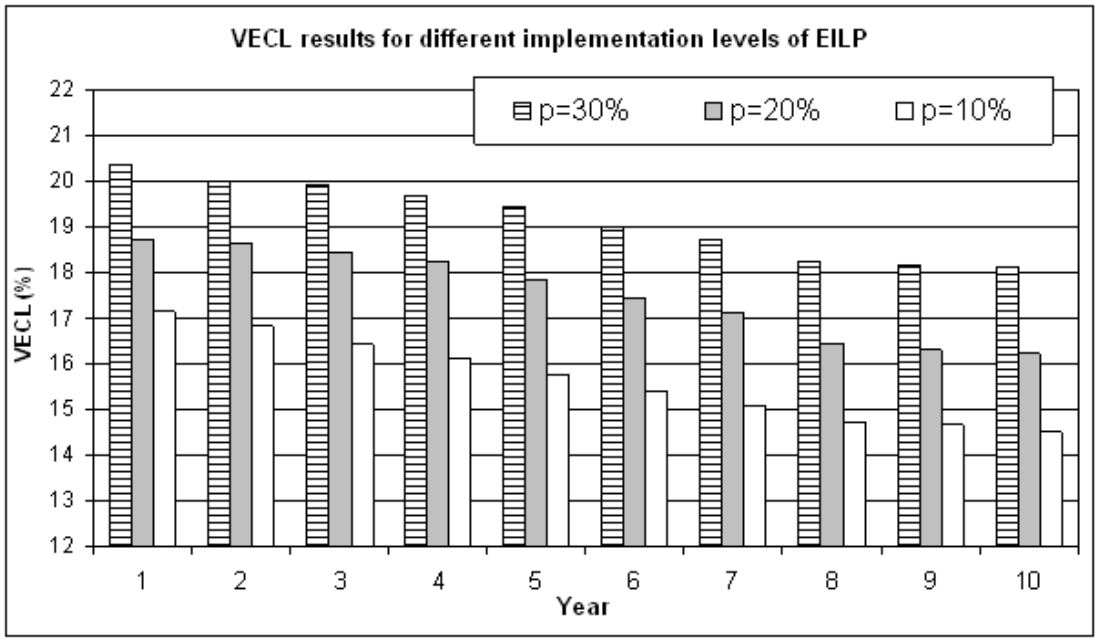

Figure 6.13: VECL for different implementation levels of EILP.

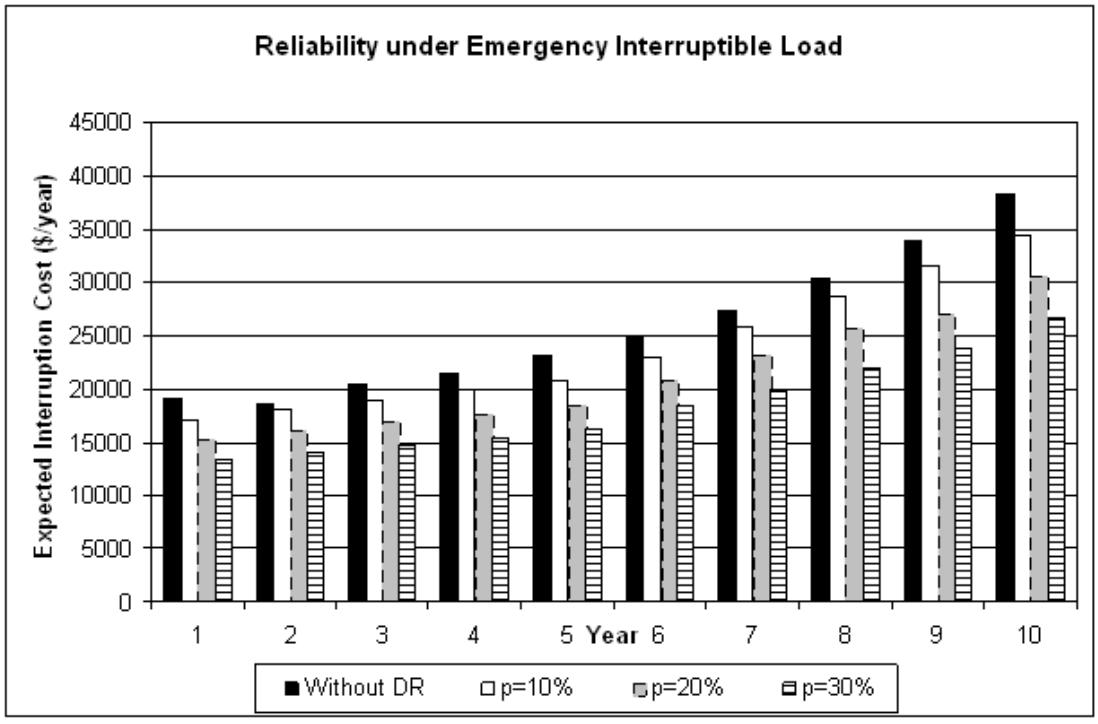

Figure 6.14: EIC for different implementation levels of EILP.

A higher p value corresponds to a higher VECL result, which represents the implementation level of EILP. Figure 6.13 has shown that VECL slowly decreases over time. This is justified by the model: the model stipulates that EILP curtails small industrial loads completely. When the load level is low (in early years), small industrial

loads curtailed completely through EILP appear more often than they do when the load level is high. This results in a higher voluntary energy curtailment percentage in early years than that in a later year. Such percentage finally reaches a stable value when the load growth eliminates all small industrial loads (< 10 kW). Take the 'p=10%' case as an example: VECL results show that, in year one, more than 17% of the annual total energy curtailment is curtailed on a voluntary basis through EILP. This percentage gradually decreases through time until finally reaches a stable value of around 14.5%.

In any given year, a higher VECL value (or the implementation level of EILP) results in a lower EIC result and higher system reliability. However, other reliability indices such as SAIFI and SAIDI have small changes of no more than 5%. This is because SAIFI and SAIDI do not distinguish whether it is a partial load shedding or a complete load shedding as long as the system suffers load shedding, whereas EIC is directly affected by the amount of load curtailment. In other words, different amount of load shedding (as long as it is above zero) contributes the same to SAIFI and SAID but differently to EIC. EILP reduces the amount the load shedding once the system suffers contingency, but is unlikely to eliminate the load shedding completely. Therefore, EILP has a considerable impact on EIC but rather little on SAIFI and SAIDI.

6.4.3 The Effect of Weighting Factors on LINWRI

LINWRI is the weighted sum of indices considering different aspects of power system reliability. A greater weighting factor of an aspect represents a greater concern of that aspect. The LINWRI results for different scenarios are comparable only if the mathematical definitions of LINWRI are the same. In the previous study, the three component indices are treated equally, i.e., $\rho_1 = \rho_2 = \rho_3 = 0.3333$. It is no longer the case in this section. This section investigates how changes in weighting factors affect LINWRI results. The study considers all scenarios in year 10 (similar effect can be observed for other years, but it is more obvious under a higher load level). To reduce the number of independent variables, LINWRI is defined as

$$\text{LINWRI} = \rho_1 \frac{\text{SAIFI}}{\text{SAIFI}_{\text{ref}}} + \rho_2 \frac{\text{SAIDI}}{\text{SAIDI}_{\text{ref}}} + \rho_3 \frac{\text{MAIFI}}{\text{MAIFI}_{\text{ref}}}$$

where $\rho_1 = \rho_3 = \frac{1-\rho_2}{2}$

Therefore, ρ_2 is the only independent variable, whereas ρ_1 and ρ_3 are dependent on ρ_2.

The combinations of weighting factors used for sensitivity analysis are presented in Table 6.2.

Table 6.2: The combinations of weighting factors.

Combination No.	ρ_1	ρ_2	ρ_3
1	0.5	0	0.5
2	0.45	0.1	0.45
3	0.4	0.2	0.4
4	0.3333	0.3333	0.3333
5	0.3	0.4	0.3
6	0.25	0.5	0.25
7	0.2	0.6	0.2
8	0.15	0.7	0.15
9	0.1	0.8	0.1

The sensitivity analysis is performed by varying ρ_2.

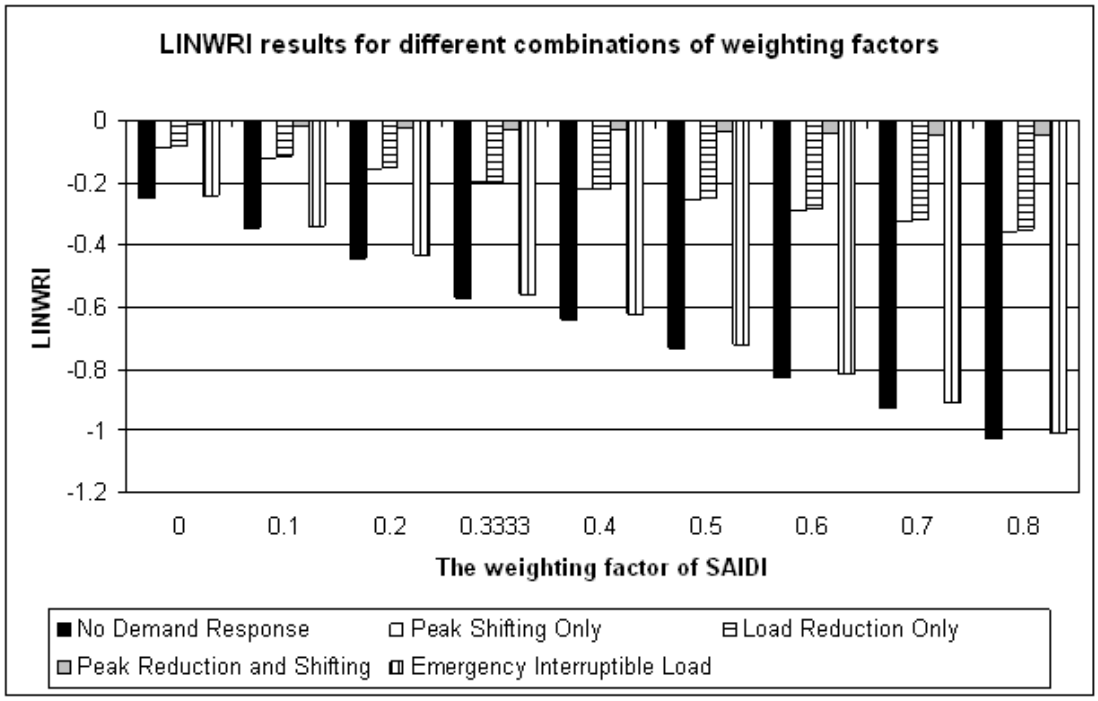

Figure 6.15: LINWRI results under different combinations of weighting factors for the five scenarios.

The above results prove that LINWRI is sensitive to ρ_2: the differences in LINWRI results among different scenarios increase with the increase of ρ_2. In other words, LINWRI is more 'polarised' when ρ_2 is greater. The reason for this phenomenon is: SAIDI is the most 'polarised' component index (or 'aspect') among different scenarios in year 10, followed by SAIFI. MAIFI results are almost the same for all scenarios. SAIDI result for the 'load shifting and reduction' scenario (scenario 4) in year 10 is 57.43% lower than that for the reference scenario. A 'polarised' aspect assigned a greater weighting factor results in a 'polarised' LINWRI value.

For any given ρ_2, the LINWRI ranking for the five scenarios does not change. This is because

1) The SAIFI ranking for all scenarios is the same as the SAIDI ranking; and
2) MAIFI remains almost constant regardless of the scenario.

Theoretically, LINWRI ranking might be different for different values of ρ_2 if SAIFI and SAIDI rankings were not the same. For example, scenario A is 'better' than

scenario B in an aspect weighted by ρ_1, whereas the former is 'worse' than the latter in another aspect weighted by ρ_2. As an overall view, whether scenario A is 'better' than B depends on whether the 'better' aspect is weighted more than the 'worse' aspect. However, this phenomenon does not exist in the test case.

In general, the choice of weighting factors has a key impact on LINWRI. When all component indices of LINWRI have the same ranking for different scenarios, the choice of weighting factors does not affect the ranking, but only affects the relative value. Under this circumstance, a polarised component index assigned a greater weighting factor results in LINWRI being polarised. When component indices have different rankings, the choice of weighting factors determines the LINWRI ranking. A component index which is weighted more than others tends to affect the LINWRI ranking more than others.

6.5 Conclusions

Demand response has been implemented in the reliability assessment of distribution systems. Three basic DR models and three new reliability indices have been implemented into the reliability assessment algorithm.

The test case has been analysed in the context of load growth, and results show that DR slows down the degradation of system reliability. However, not all indices degrade over years. MAIFI depends on the network topology, and is rather insensitive to load growth.

The sensitivity analysis shows that, with increasing implementation level of DR, power system reliability is improving. However, the marginal benefit in reliability is decreasing as is clearly indicated by DRICB results.

The case study shows that EILP contributes to system reliability by reducing EIC. However, it does not have a significant impact on SAIFI, SAIDI and LINWRI indices.

The validity of VECL has also been demonstrated under EILP. A high VECL value corresponds to a high implementation level of EILP.

Sensitivity analysis on the effect of the weighting factors proves that a ‘polarised’ component index assigned a large weighting factor results in LINWRI being ‘polarised’. It is therefore necessary to decide the weighting factors with caution.

7 Reliability with FACTS and control system

Summary

As stated in previous chapters, corrective control is a solution of great potential for overcoming the economic and political barriers encountered in conventional network reinforcement, as well as an enabling technology for accommodating increasing penetration of intermittent generation. Flexible AC Transmission Systems (FACTS) are a key aspect in the field of corrective control. This chapter investigates the following issues in the context of FACTS: 1) how the implementation of FACTS affects power system reliability; 2) how the reliability of the FACTS control system influences power system reliability; 3) whether the implementation of FACTS is preferable over traditional reinforcement in terms of cost benefit.

First, FACTS technology and its wide-area control are reviewed using existing publications as bases. The state space models of typical FACTS devices and the control system model are presented in succeeding sections. These models are then incorporated into CMCS, applied as the reliability assessment method.

The Roy Billinton Test System (RBTS) and the IEEE Reliability Test System (RTS) are selected as test systems. Scenarios with FACTS devices and traditional reinforcement scenarios are proposed and investigated in relation to the above-mentioned research issues.

7.1 Introduction to FACTS

According to the definition given by IEEE, FACTS is ‘a power electronic-based system and other static equipment that provide control of one or more AC transmission system parameters to enhance controllability and increase power transfer capability’ [91].

FACTS matured with the development of power electronics technologies such as thyristor valves, converters, and inverters. The latest application of insulated gate bipolar transistors in voltage converters provides high controllability to voltage with low harmonics [92].

The basic applications of FACTS include power flow control, voltage control, system stability improvement, etc [93]. Through mechanically switched/power electronic controlled shunt/series compensation, FACTS devices provide fast control with a response time down to the level of milliseconds. Typical FACTS devices include the SVC, static synchronous compensator (STATCOM), thyristor controlled series compensator (TCSC), static synchronous series compensator (SSSC), and unified power flow controller (UPFC) [92].

FACTS can be classified into two categories: shunt compensation and series compensation. Typical shunt compensation devices include the SVC and STATCOM. An SVC regulates voltage and stabilises a system by providing reactive compensation. It is a dynamic reactive current source with a sub-cycle reaction time [91]. Typical examples of SVC applications are presented as follows.

An SVC is installed in a 115 kV transmission system in Lower Southeastern Massachusetts to provide fast-responsive voltage support to the system in case two major generation sites simultaneously fail [94]. Under normal circumstances, the SVC remains on standby. Under emergency circumstances, it can provide reactive support at a rating of 115 kV, 0 – 225 Mvar capacitive output for 2 seconds, and 0 – 112.5 Mvar capacitive output for longer durations. The voltage is automatically monitored and the reaction of the SVC is also automatic when the voltage falls below a pre-specified level. The settings can be configured either by the local SVC control room or central network control room via SCADA [94]. This real-world example fully justifies SVC application in providing emergency reactive compensation for the purpose of reliability.

An SVC can be mobile (or relocatable), but with a compromised degree of compensation. In another application by ABB [95], an SVC is configured to improve the

stability and transfer capability of the National Grid 400/275 kV transmission network in the UK. It can be controlled either by the local control room or remote control centre.

Similar to an SVC, a STATCOM can provide instantaneous reactive support to the grid and is equivalent to a synchronous voltage source. By improving voltage stability through a STATCOM, transfer capacity can be significantly increased and power quality can be improved [96]. A STATCOM is applied as a replacement for conventional generation in Austin, Texas where the retirement of an old conventional generation unit necessitated a robust dynamic reactive compensation device [97]. In this application, the purpose of installing a STATCOM is to address voltage sags [97].

The investment cost per kvar of an SVC device itself is lower than that of a STATCOM. According to [98], an SVC costs US$ 40/kvar and a STATCOM costs US$50/kvar. However, SVC has its own disadvantages:

1) It is not as robust as a STATCOM because its control capability falls only within a limited voltage range. Beyond the range, its performance becomes largely compromised or the device becomes non-functional. The performance of a STATCOM, on the other hand, is not impaired by low voltage [93].

2) For comparable voltage and compensation levels, an SVC may be physically larger than a STATCOM (because of the limited information available, this description may not be universal).

An SVC (40 Mvar inductive to 70 Mvar capacitive) connected to a 115 kV network has a layout of 1505 m^2 (43 m $\times$ 35 m) [99], whereas a STATCOM (80 Mvar inductive to 110 Mvar capacitive) connected to a 138 kV network occupies an area of 375 m^2 (25 m $\times$ 15 m), approximately 75% less than that occupied by the former [97]. In countries where obtaining land permission is costly, the larger physical area that an SVC occupies and possibly significantly higher land costs incurred from it require consideration in economic assessment.

Typical series compensation devices include fixed series compensation, TCSC, and SSSC [100]. The first device is potentially a cost-effective way to improve the transfer capacity and stability of a long bulk transmission corridor.

An example of actual application is the installation of a series capacitor in the 230 kV transmission network of Hydro-Quebec by ABB [101]. By enhancing stability, this

series capacitor increases the transmission capacity of a critical corridor that carries hydro power from several hydro plants to the load centre. It has cost advantages over the traditional reinforcement scenario of building a new parallel 230 kV power line. The series capacitor can be controlled either by the local control room or central control room via the remote terminal unit (RTU), which is part of the SCADA system [101].

TCSC provides increased controllability compared with fixed series compensation. It can rapidly change the inserted reactance and provide effective damping on inter-area electromechanical oscillations [102]. However, because of the high capital cost of TCSC, combining TCSC with fixed series compensation for transient stability enhancement is often a more cost effective option.

One of the most important applications of TCSC for reliability is post-contingency loadability control [19]. The degree of TCSC compensation can rapidly increase to help the system survive a contingency, but remains at a low compensation level or is dormant under normal circumstances.

A theoretical SSSC model is proposed in [103]. It injects a voltage source in series to the power line. The injected voltage stays in quadrature with line current given that SSSC has no active power source. SSSC can either be capacitive or inductive depending on the magnitude of the injected voltage. Its diagram is shown in Figure 7.1.

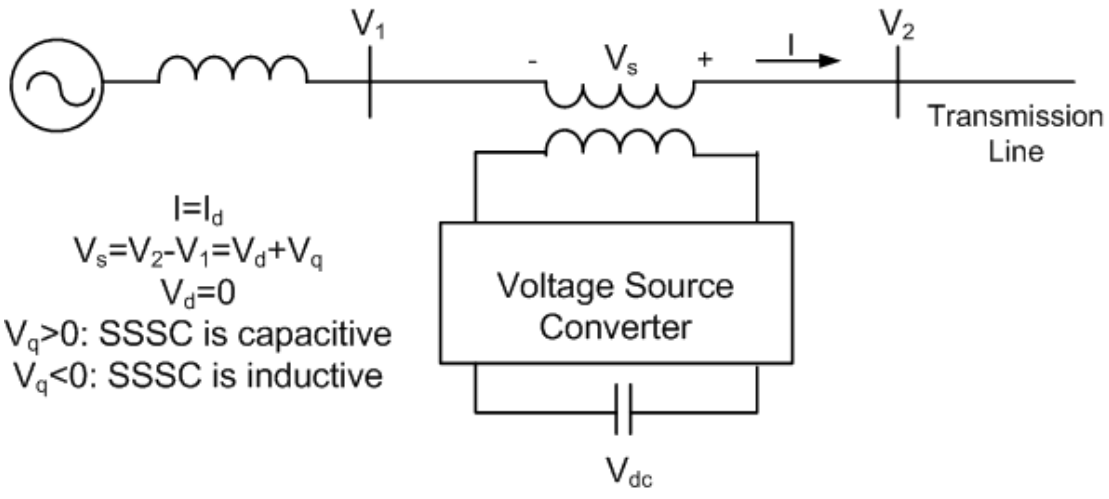

Figure 7.1: the single line diagram of SSSC [103].

Under a proper control mode, SSSC can be superior over impedance-based series compensation [103]. Two control schemes are proposed in [103]. One is the Reactance

Emulation Scheme in which SSSC serves as an additional series reactor or a series capacitor that regulates the power flow through the line. The other scheme is the Quadrature Voltage Control Scheme in which SSSC serves as a quadrature voltage source for the direct purpose of tackling voltage drop. However, SSSC is a fairly new technology and has not yet been widely applied in industry. The reliability of its technical performance in actual applications and its economic viability remain uncertain.

Previously mentioned FACTS devices provide either shunt or series compensation, whereas UPFC provides both. It can provide full dynamic control over voltage and line impedance [104]. UPFC is essentially a combination of SSSC and STATCOM with independent control over different types of parameters [105]. It is a theoretical FACTS device that has not been applied in industry thus far.

Apart from the applications of FACTS devices mentioned above, more applications are summarised from published papers:

1) the application of an SVC for local and remote disturbances in San Francisco Bay area transmission system [106];

2) the application of an SVC to increase transmission capacity and enhance voltage stability [107];

3) joint application of SVC and STATCOM as a dynamic VAR Compensator for supporting voltage and improving system stability [108];

4) substitution of an SVC for synchronous condensers at Pacific Gas & Electric Company (PG&E, San Francisco) because of the cost advantage offered by the former [109];

5) the application of FACTS devices (shunt compensators) on a 500 kV transmission system in Vietnam. A continuation load flow method has been proposed to determine the best location and type of FACTS devices [2];

6) the application of FACTS devices for generation cost reduction [110]. An economic viability study is performed on whether the savings in generation costs outweigh the costs of FACTS devices after the allocation of FACTS using a genetic algorithm [110]; and

7) the application of distributed FACTS (D-FACTS) devices as a substitute for ordinary FACTS devices. D-FACTS is expected to be less expensive, mobile, and flexible in

terms of degree of compensation [111]. It is a novel idea but still remains at the theoretical level.

A number of papers focus on the allocation of FACTS devices.

A genetic algorithm is applied in identifying the location, operating point, and number of FACTS devices simultaneously in [112]. The optimal location and settings of shunt compensators (FACTS devices) for large power systems with wind farms are determined through sensitivity analysis and optimal power flow, respectively [113].

7.2 Wide-area Control of FACTS

The full potential of FACTS can only be exploited through coordinated control. Coordination can either be system wide or regional, depending on system size. The ideal scenario is to coordinate FACTS devices on a system-wide level, in which the set point of each device is optimised for a global target. Given prohibitive system size, however, the system-wide coordination of FACTS may be impractical [114]. Instead, it is suggested that the control area be limited to where the FACTS devices have considerable effect on the control objective. The effect of FACTS devices is investigated through sensitivity analysis in [115]. Different FACTS devices correspond to varied control areas, where each area has its own control objective. These areas may overlap and the control objectives may be contradictory. This requires a multi-area control algorithm for coordinating the FACTS devices with overlapping areas of influence and different control objectives [115].

An approach for decentralised control of a power flow controller (PFC) based on a multi-agent system is proposed in [116]. The controlling agents installed at each PFC evaluates system state based on the information received from local measurement devices, and generates local control scenarios using a weighing function to avoid conflicting effects on the system level.

The importance of coordinated FACTS control in avoiding negative mutual influences in the network is emphasised in [114]. The paper proposes a supervisory controller based on optimal power flow with different control objectives. These objectives include minimising transmission losses, keeping load below a threshold, maintaining voltage within a safe limit, etc. By comparing the scenario with FACTS under coordinated

control and the base scenario without FACTS, the paper demonstrates the advantages of the former in resolving congestion, improving voltage profile, and reducing line losses.

The wide area control of a dynamic power flow controller (DPFC) is proposed in [117]; comparing it with the uncoordinated control of phase shifting transformers demonstrates the advantages of the former. The DPFC is able to address emergency situations because of its fast responsiveness; it responds automatically to sudden changes in power systems and therefore increases the transfer capacity of branches.

For small test systems such as the RBTS and RTS, dividing the system into different control zones to reduce the computational time required is unnecessary. The system-wide coordination of FACTS devices is therefore performed by calling a single optimisation algorithm to minimise total cost of load curtailment under contingencies.

7.3 Methodology

Three types of FACTS devices are modelled in this chapter: SVC, TCSC, and STATCOM. Their state space models are presented in this chapter. The FACTS devices are controlled by the central control room and are therefore subject to CCF, i.e., the failure of the central control unit. The state space models of FACTS devices and the central control unit are incorporated into CMCS, which is the reliability assessment approach. The CMCS algorithm and the optimisation algorithm are also presented in this chapter.

7.3.1 Modelling of SVC

The single line diagram of an SVC in Figure 7.2 shows a thyristor-controlled capacitor (TCC), thyristor-controlled reactor (TCR), and fixed capacitor as a harmonic filter [61].

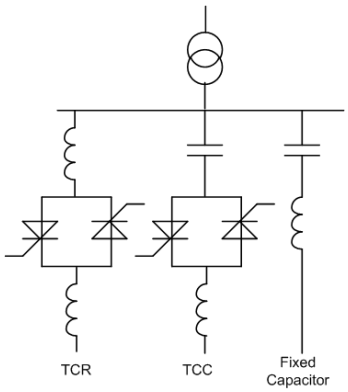

Figure 7.2: the single line diagram of SVC [61].

The following assumptions are adopted when creating the state space model of the SVC [88, 118]:

1) If any branch of TCC or TCR fails, the failed branch is bypassed, whereas other branches continue to operate normally.

2) If all TCC and TCR branches are down, SVC is bypassed.

For a typical SVC (Figure 7.3), the four-state model is presented in [88].

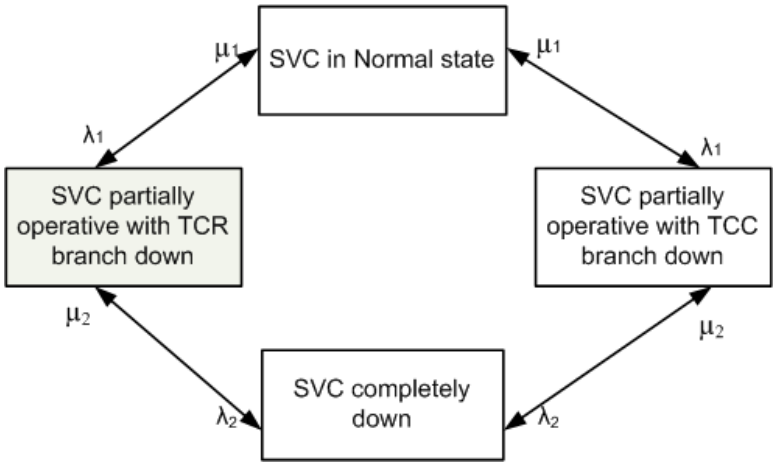

Figure 7.3: original four-state model of SVC [88].

The above-mentioned model is slightly altered in this project based on the assumption that the failure of the RTU results in the outage of the SVC. This corresponds to a direct transition route between the 'SVC normal' state and 'SVC completely down' state. The altered state space model is shown in Figure 7.4.

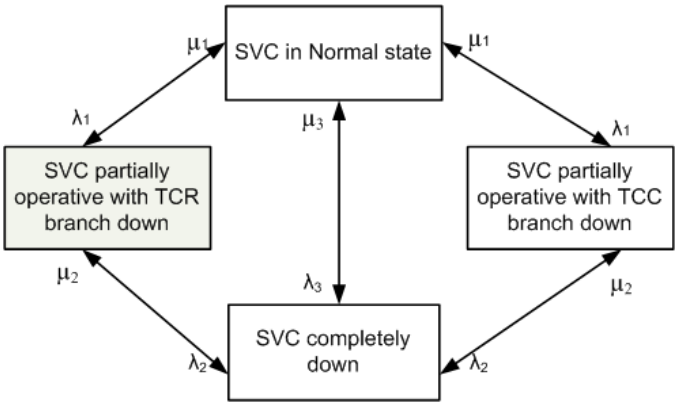

Figure 7.4: the altered four-state model of SVC.

In this project, an approximation is made, that is, the active power loss is disregarded. The SVC can continuously and rapidly absorb or generate reactive power within the range determined by the number and individual parameters of the TCC and TCR [93]. In power flow analysis, an SVC can be seen as an adjustable reactance, whose equivalent circuit is shown in Figure 7.5 [93].

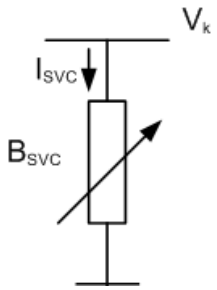

Figure 7.5: the SVC model in power flow study [93].

The current drawn from the bus is therefore [93]

$$I_{\text{SVC}} = \text{j}B_{\text{SVC}}V_k \qquad \textbf{(7.1)}$$

The reactive power injected at bus k is [93]

$$Q_k = -V_k^2 B_{\text{SVC}} \qquad \textbf{(7.2)}$$

The capacitive status of the SVC corresponds to a positive injection of reactive power into the bus, whereas an inductive one corresponds to a withdrawal of reactive power from the bus. In the iterative process, power injection into an SVC bus is iteratively corrected using (7.2).

An alternative SVC model in power flow studies is the firing angle model, where firing angle α of the TCR is regarded as a state variable. The reactive power injected into the bus in the firing angle model is given by [93]

$$Q_k = \frac{-V_k^2}{X_C X_L}\{X_L - \frac{X_C}{\pi}[2(\pi\text{-}\alpha) + \sin(2\alpha)]\} \qquad \textbf{(7.3)}$$

In this model, power injection into an SVC bus is iteratively updated using (7.3).

The firing angle model focuses more on the detailed mechanism of an SVC, whereas the adjustable reactance model regards the SVC as a black box. The adjustable reactance model is adopted because the internal mechanism is of no concern to this research.

7.3.2 Modelling of STATCOM

STATCOM provides reactive compensation independently from the bus voltage within its range [93].

A typical STATCOM is designed with redundancy in a conservative manner. The 50 MVA STATCOM prototype is adopted in this project [119]. The core of the STATCOM, i.e., the main circuit, is configured in a cascading multilevel structure, which is modelled by a series system in reliability studies. To compensate for the weakness in this series system, a redundant design is adopted in which each phase consists of 10 identical voltage source inverters (VSI); A phase is operational when no less than 8 VSI are working normally. However, the failure of any phase results in the outage of the entire STATCOM. The structure of the STATCOM three-phase main circuit is depicted in Figure 7.6.

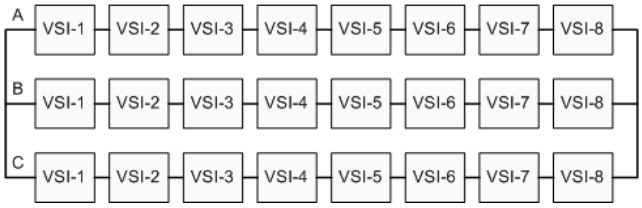

Figure 7.6: the structure of STATCOM three-phase main circuit [119].

The probability of each phase in normal condition is equal to the probability that the number of working components is greater than or equal to n (n=8 in this scenario). It

corresponds to an 8-out-of-10: G model. The mean time between failures (MTBF) and reliability (R) for each phase are therefore [119]

$$\text{MTBF}=\frac{1}{\lambda}\sum_{i=k}^{n}\frac{1}{i} \quad \textbf{(7.4)}$$

$$R(k,n)=\sum_{i=k}^{n}\binom{n}{i}p^{i}q^{n-i} \quad \textbf{(7.5)}$$

The probability that at least m components are up at time t is therefore [119]:

$$P=\sum_{r=m}^{n}[\sum_{(i_1,\ldots,i_r)\subseteq I}(\prod_{j=1}^{r}\frac{\mu_{i_j}}{\lambda_{i_j}+\mu_{i_j}}\prod_{j=r+1}^{n}\frac{\lambda_{i_j}}{\lambda_{i_j}+\mu_{i_j}})] \quad \textbf{(7.6)}$$

where $m=8$ and $n=10$ for the 8-out-of-10: G model.

The failure of any phase results in the failure of the STATCOM main circuit that consists of three phases. Assuming that the phases are independent of each other [119], the series reliability model is applicable:

$$\text{MTBF}_S=\text{MTBF}/3 \quad \textbf{(7.7)}$$

where subscript s denotes the system, i.e., the main circuit of the STATCOM.

The probability that the STATCOM main circuit is up is therefore

$$P_S=P^3 \quad \textbf{(7.8)}$$

where subscript s denotes the system, i.e., the main circuit of the STATCOM.

In CMCS, each of the 30 identical VSI (numbered 1 to 30) is simulated based on the basic two-state model comprising an ‘up’ and ‘down’ state. Phase A consists of VSI Nos. 1 to 10; phase B consists of VSI Nos. 11 to 20; and phase C consists of VSI Nos. 21 to 30. A phase is down if the failures of more than two (>2) VSI coincide. The outage of any phase results in the outage of the STATCOM.

The m-out-of-n: G model is applicable when knowledge regarding the failure rate of each individual VSI and level of redundancy is available. However, the failure rate of an individual VSI may be unavailable. This project uses a hypothetical VSI failure rate and simulates the failure of each VSI.

A circuit equivalent to the STATCOM is shown in Figure 7.7 [120]. The core is the equivalent voltage source.

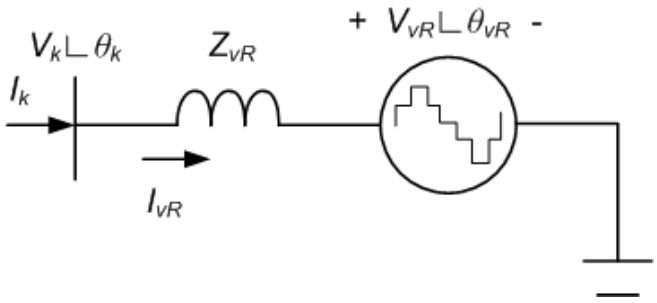

Figure 7.7: Equivalent circuit of STATCOM.

The formulae for calculating active and reactive power are given by [120]:

$$P_k = V_k^2 G_{vR} + V_k V_{vR}[G_{vR}\cos(\theta_k - \theta_{vR}) + B_{vR}\sin(\theta_k - \theta_{vR})] \quad \textbf{(7.9)}$$

$$Q_k = -V_k^2 B_{vR} + V_k V_{vR}[G_{vR}\sin(\theta_k - \theta_{vR}) - B_{vR}\cos(\theta_k - \theta_{vR})] \quad \textbf{(7.10)}$$

A STATCOM without a DC source can be simplified as a reactive power source because in steady-state operations, the active power exchange between the STATCOM and the network is negligible [121, 122]. In this case, the STATCOM is modelled by a reactive power source independent of the bus voltage.

7.3.3 Modelling of TCSC

TCSC has been applied to regulating branch flows, limiting short-circuit currents, mitigating sub-synchronous resonance, improving transient stability, etc [90]. TCSC can continuously change line impedance within a time frame down to milliseconds. Its single line diagram is shown in Figure 7.8 [123].

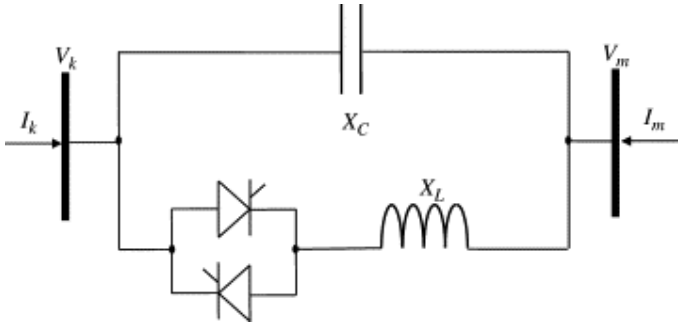

Figure 7.8: Single line diagram of TCSC [123].

Two reliability models are presented for TCSC. One has three possible states: the normal state in which TCSC has full functionality; the bypassed state in which TCSC fails and is subsequently isolated from the line without affecting the operation of the line; and the emergency state in which TCSC fails followed by the malfunction of the bypass breaker, thereby causing the protection relay to trip the line [118].

The other model is a simplified two-state model, which assumes that TCSC is always isolated from the line when TCSC fails. The difference of this model from the three-state representation is that the emergency state is disregarded. In this project, we adopt the latter given that practical data are unavailable.

In power flow studies, TCSC is modelled as a variable series reactance to control branch power flow to a specific value [93]. This model is shown in Figure 7.9 [93].

Figure 7.9: the variable series reactance model of TCSC.

The equations of active and reactive powers injected at bus k are given below [93]:

$$P_k = V_k V_m B_{km} \sin(\theta_k - \theta_m) \quad \textbf{(7.11)}$$

$$Q_k = -V_k^2 B_{kk} - V_k V_m B_{km} \cos(\theta_k - \theta_m) \quad \textbf{(7.12)}$$

where

$$B_{kk} = B_{mm} = -\frac{1}{X_{\text{TCSC}}} \quad \textbf{(7.13)}$$

$$B_{km} = B_{mk} = \frac{1}{X_{\text{TCSC}}} \quad \textbf{(7.14)}$$

7.3.4 Modelling of the Central Control Unit

FACTS devices are subject to CCF, which is either the central control unit failure only or a combination of central control unit failure and communication system failure, depending on the control system configuration.

The three types of configurations introduced in Chapter 3 are the 'party line' configuration, 'star' configuration, and 'mixed party line and star' configuration. A simplified 'party line' configuration is employed as the control system model in this chapter for the following reasons:

1) Using a configuration model beyond that justifiable by practical data is an unreasonable approach. In other words, the level of model complexity should correspond to data availability.

2) For a modern control system that uses radio or other types of wireless communication, the reliability of communication depends on the reliability of the radio terminals at both the central control room and local devices. The reliability of a central radio terminal can be integrated with that of a central control unit, whereas the reliability of the local radio terminal (or RTU) can be combined with that of the local devices. In this case, the communication system is 'absorbed'.

The failure rates of FACTS devices obtained from historical records are divided into the failure rate of the independent failure and that of the CCF using the beta factor method.

Take the SVC as an example. λ_1, λ_2, and λ_3 are denoted as the observed failure rates (Figure 7.4). These failures include independent failures and CCF.

λ_{1i}, λ_{2i}, and λ_{3i} are the failure rates of the independent failures; λ_C is the failure rate of CCF. The following relationships can be derived:

$$\lambda_{1i} = \lambda_1 \quad \textbf{(7.15)}$$

$$\lambda_{2i} = \lambda_2(1-\beta_1) \quad \textbf{(7.16)}$$

$$\lambda_{3i} = \lambda_3(1-\beta_2) \quad \textbf{(7.17)}$$

$$\lambda_C = 2\lambda_2\beta_1 + \lambda_3\beta_2 \quad \textbf{(7.18)}$$

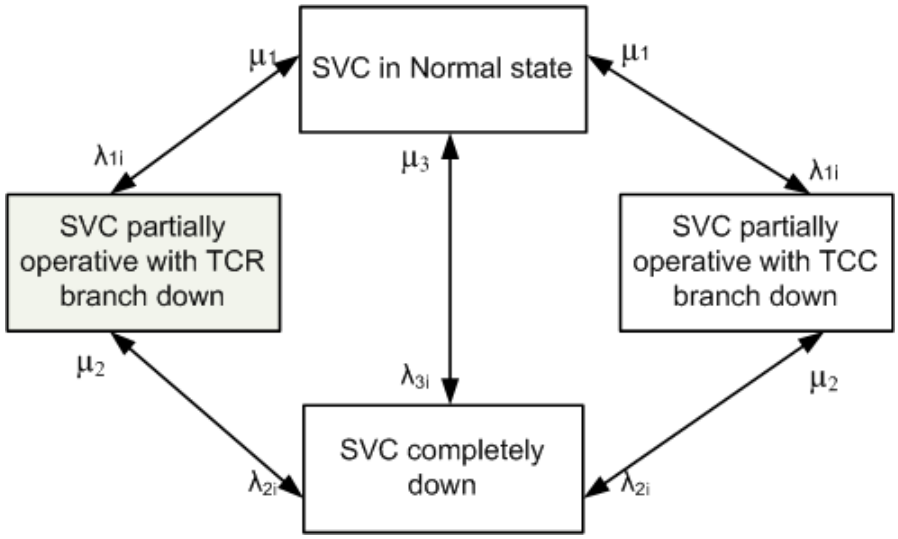

Figure 7.10: State space model of SVC considering independent failures only.

The state space model of the central control unit is shown in Figure 7.11.

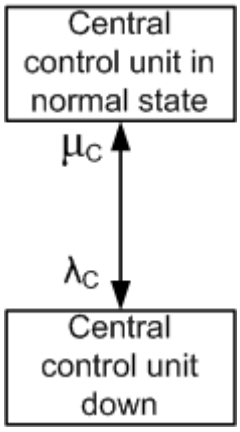

Figure 7.11: State space model of CCF.

7.3.5 Chronological Monte Carlo Simulation

CMCS is adopted as the reliability assessment method. The flowchart of CMCS is shown in Figure 7.12.

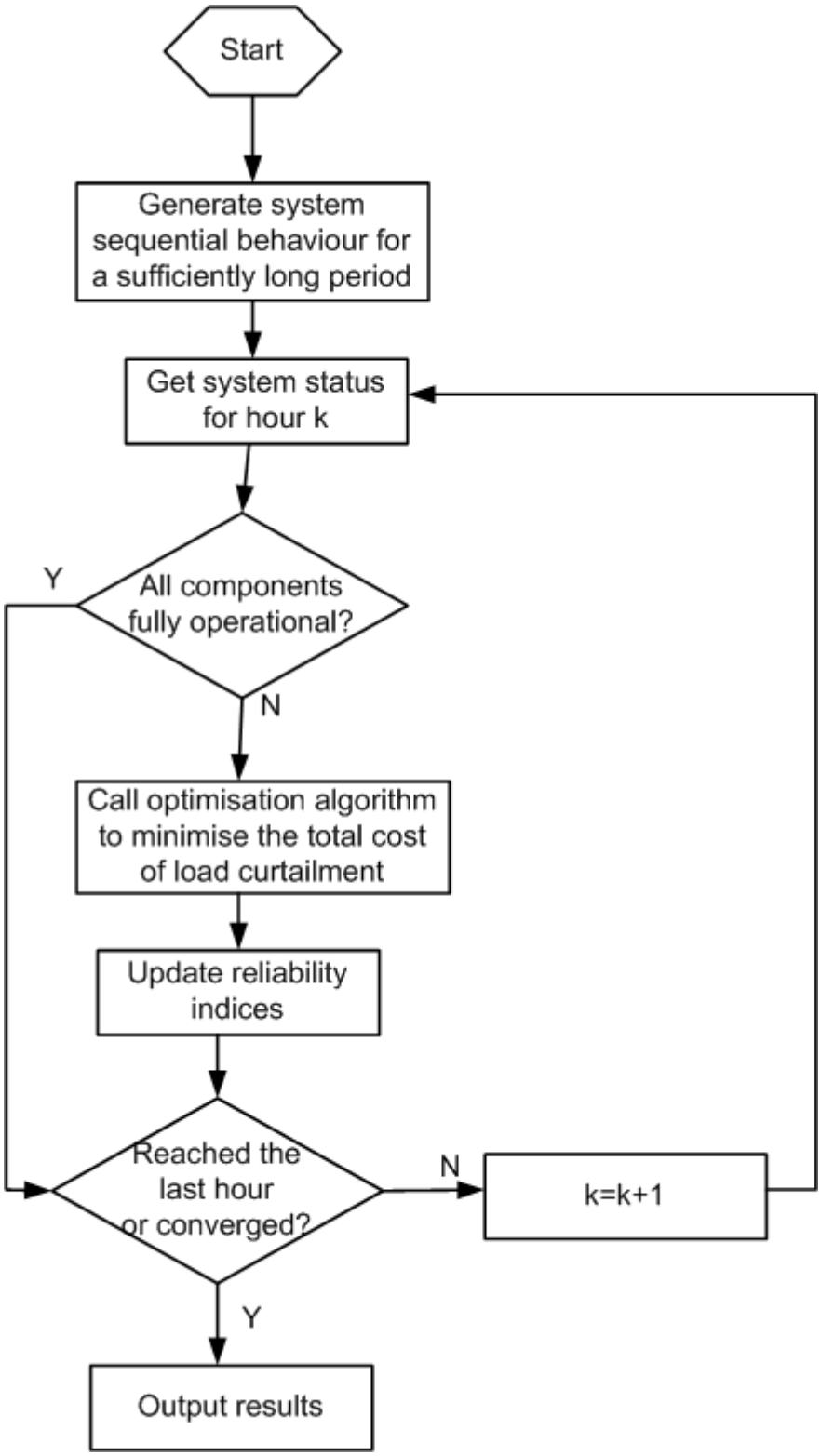

Figure 7.12: CMCS algorithm.

The optimisation algorithm for minimising total cost of load curtailment is given below:

$$\min \mathrm{CCDF}(P_L^{Cur}) \qquad \textbf{(7.19)}$$

subject to

$$P_{Gi} - P_{Li} + P_{Li}^{Cur} = P_i^{inj}(V, \theta, X_{\text{SVC}}, X_{\text{TCSC}}) \quad \textbf{(7.20)}$$

$$Q_{Gi} - Q_{Li} + Q_{Li}^{Cur} + Q_{\text{STATCOM}i} = Q_i^{inj}(V, \theta, X_{\text{SVC}}, X_{\text{TCSC}}) \quad \textbf{(7.21)}$$

$$S_{ij} < S_{ij}^{\max} \quad \textbf{(7.22)}$$

$$V_i^{\min} < V_i < V_i^{\max} \quad \textbf{(7.23)}$$

$$0 < P_{Li}^{Cur} < P_{Li} \quad \textbf{(7.24)}$$

$$\frac{P_{Li} - P_{Li}^{Cur}}{Q_{Li} - Q_{Li}^{Cur}} = \frac{P_{Li}}{Q_{Li}} \quad \textbf{(7.25)}$$

$$X_{\text{SVC}}^{\min} < X_{\text{SVC}} < X_{\text{SVC}}^{\max} \quad \textbf{(7.26)}$$

$$Q_{\text{STATCOM}i}^{\min} \le Q_{\text{STATCOM}i} \le Q_{\text{STATCOM}i}^{\max} \quad \textbf{(7.27)}$$

$$X_{\text{TCSC}}^{\min} \le X_{\text{TCSC}} \le X_{\text{TCSC}}^{\max} \quad \textbf{(7.28)}$$

where

P_{Li}, Q_{Li} Active and reactive load at bus i;

P_{Gi}, Q_{Gi} Active and reactive generation at bus i;

$P_{Li}^{Cur}, Q_{Li}^{Cur}$ Active and reactive load curtailment at bus i;

P_i^{inj}, Q_i^{inj} Active and reactive power injection at bus i;

$X_{\text{SVC}}, X_{\text{SVC}}^{\min}, X_{\text{SVC}}^{\max}$ Equivalent reactance of SVC and its lower and upper limit;

S_{ij} Load flows at branch ij;

V_i, θ_i Voltage magnitude and angle at bus i;

$Q_{\text{STATCOM}}, Q_{\text{STATCOM}}^{\min}, Q_{\text{STATCOM}}^{\max}$ Reactive power output, the lower limit of the reactive power output and the upper limit of the reactive power output of STATCOM, respectively; and

$X_{\text{TCSC}}, X_{\text{TCSC}}^{\min}, X_{\text{TCSC}}^{\max}$ Equivalent reactance, the lower limit of the equivalent reactance and the upper limit of the equivalent reactance of TCSC.

7.4 Case Study

Before the test case is presented, providing the definitions of the terms used in the context of this project is necessary.

1) The control system (or the FACTS control system): the system that consists of a central control unit and communication channels. This system is used to control the FACTS devices.

2) The reference scenario: the scenario with no system reinforcement of any kind, i.e., the 'doing nothing at all' scenario.

3) The reference case: the reference scenario in year 1.

4) System reinforcement: the installation of either FACTS devices or new power lines/transformers.

5) Traditional reinforcement scenario: the installation of new power lines.

RTS is applied as the test case [124]. All relevant data are given in Appendix C. Annualised loads have been used in the simulation, which is sufficient when different scenarios are compared in terms of their reliability and cost benefits [11]. In the present study, the simplified 'party-line' structure is adopted as the FACTS control system structure based on the assumption that all communications are conducted via radio. The central control unit failure is therefore the CCF of all the FACTS devices. The behaviours of the FACTS device, central control unit, and transmission branches are simulated. The failure of the generation units is not considered in the case study because

1) the focus is on network reliability, that is, the reliability of passing the electrical energy from generation units to load buses; and
2) power lines are generally more reliable than generation units. Considering the generation unit failure is likely to mask network reliability, which is the primary concern of this study.

A key assumption regarding the scenarios with FACTS devices is that these devices react under contingency only. They remain on standby when the power system is

working under normal conditions. In other words, FACTS devices serve only a reliability purpose by providing corrective control under contingencies.

A simplified system planning is conducted to determine the reinforcement scenarios: candidate scenarios include all scenarios that have an SVC at a PQ bus. Preliminary reliability assessment up to the first order is performed where only one element fails at a time. The scenario with the lowest EENS is found, i.e. SVC installed at bus 3. Given the fixed SVC location, all scenarios with one TCSC is studied through first-order reliability assessment, and the one with the lowest EENS is found to be a TCSC between bus 3 and bus 24. The same planning methodology has found that a duplicated element between bus 3 and bus 24 provides the most reliability benefit.

Therefore, six scenarios are defined as follows:

1) the reference scenario;

2) SVC at bus 3;

3) TCSC connecting between bus 3 and bus 24 to the low voltage terminals of the transformer;

4) STATCOM at bus 3;

5) SVC at bus 3 and TCSC connecting between bus 3 and bus 24 to the low voltage terminals of the transformer; and

6) a duplicated element between bus 3 and bus 24.

The annual load growth rate is 2.5% and the simulation covers years 1 to 6.

The EENS results are shown in Figure 7.13:

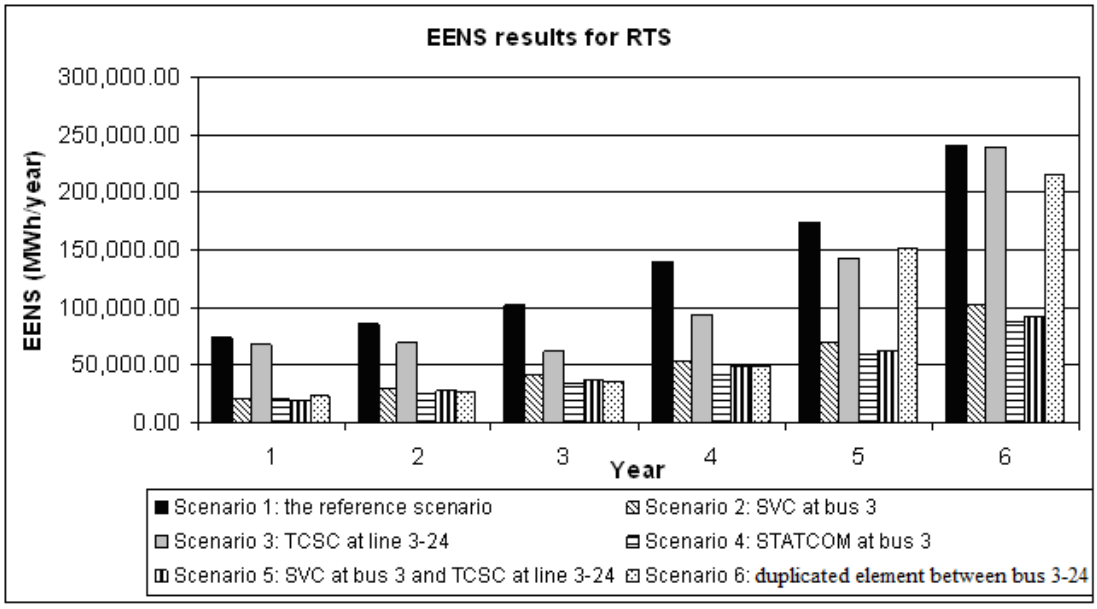

Figure 7.13: EENS results for RTS.

In this case, LINWRI is defined in as having only one component index, i.e., EENS:

$$\text{LINWRI}=\frac{\text{EENS}}{\text{EENS}_{\text{ref}}} \qquad \textbf{(7.29)}$$

The reference case is scenario 1 in year 1.

The LINWRI results are shown in Figure 7.14.

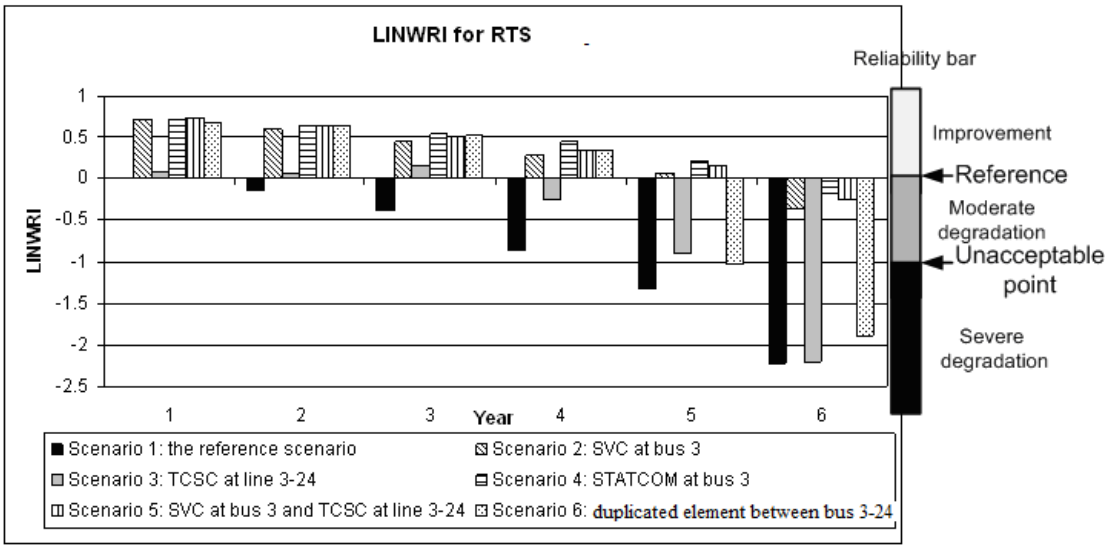

Figure 7.14: LINWRI results for RTS.

In any given year, power system reliability is at its worst under the reference scenario (i.e., scenario 1). Both corrective control represented by scenarios 2–5 and traditional reinforcement represented by scenario 6 can slow down the deterioration of system reliability in the context of load growth compared with the reference scenario. In any given year, scenario 3 (i.e., TCSC installed between bus 3 and bus 24) provides the least reliability improvement compared with scenarios 2, 4, and 5. In most years, the traditional reinforcement plan represented by scenario 6 provides higher reliability improvement than does scenario 3. Scenarios 2, 4, and 5 provide almost the same level of reliability improvement to the system.

No consistent ranking is observed in the six scenarios for all years. For example, the LINWRI ranking for years 1 and 6 follows the order

$$\mathrm{LINWRI}_{1,1} < \mathrm{LINWRI}_{3,1} < \mathrm{LINWRI}_{6,1} < \mathrm{LINWRI}_{4,1} \approx \mathrm{LINWRI}_{5,1} \approx \mathrm{LINWRI}_{2,1}$$

$$\mathrm{LINWRI}_{1,6} \approx \mathrm{LINWRI}_{3,6} < \mathrm{LINWRI}_{6,6} < \mathrm{LINWRI}_{2,6} < \mathrm{LINWRI}_{5,6} < \mathrm{LINWRI}_{4,6}$$

where subscript x, y in $\mathrm{LINWRI}_{x,y}$ denotes scenario x in year y (e.g., $\mathrm{LINWRI}_{4,1}$ is LINWRI result for scenario 4 in year 1). A scenario that provides the highest reliability improvement to the system in a certain year may not do so in another year.

The investment for each reinforcement scenario, except scenario 1, is assumed to be paid off in five equal yearly installments at the end of each year. The investment cost is converted to a present value by

$$IC = In\frac{1-(1+i)^{-n}}{i} \quad (£) \tag{7.30}$$

IC investment cost

In installment

i discount rate

n number of payments

Given that all scenarios have the same generation dispatch throughout the simulation period, the generation operational costs are the same and therefore disregarded when performing economic comparisons. The O&M cost refers to the extra O&M cost resulting from system reinforcement. For a scenario with FACTS devices, the O&M cost refers to the cost resulting from the O&M of corrective control devices. For the scenario

with a duplicated element, the O&M cost refers to that of the extra element. Therefore, the O&M cost for scenario 1 is 0. Similarly, the present value of O&M cost is given by

$$OC = O_{annual} \frac{1-(1+i)^{-m}}{i} \quad (£) \qquad \textbf{(7.31)}$$

OC present value of O&M cost

O_{annual} annual O&M cost

m economic life

The present value of the risk-associated cost is given by

$$R = R_{annual} \frac{1-(1+i)^{-m}}{i} \quad (£) \qquad \textbf{(7.32)}$$

R present value of risk-associated cost

R_{annual} annual risk-associated cost

m time span considered

The annual risk-associated cost is calculated from load curtailment using the customer damage function (CDF). In this test case, the CDF is assigned a constant value, CDF=£100 /MWh. Therefore, $R_{annual} = \text{EENS} \times \text{CDF}$.

The discount rate is assumed to be 5% and the economic life for each FACTS device and the extra line is 25 years. Economic analysis is then performed.

The cost structure is depicted in Figure 7.15:

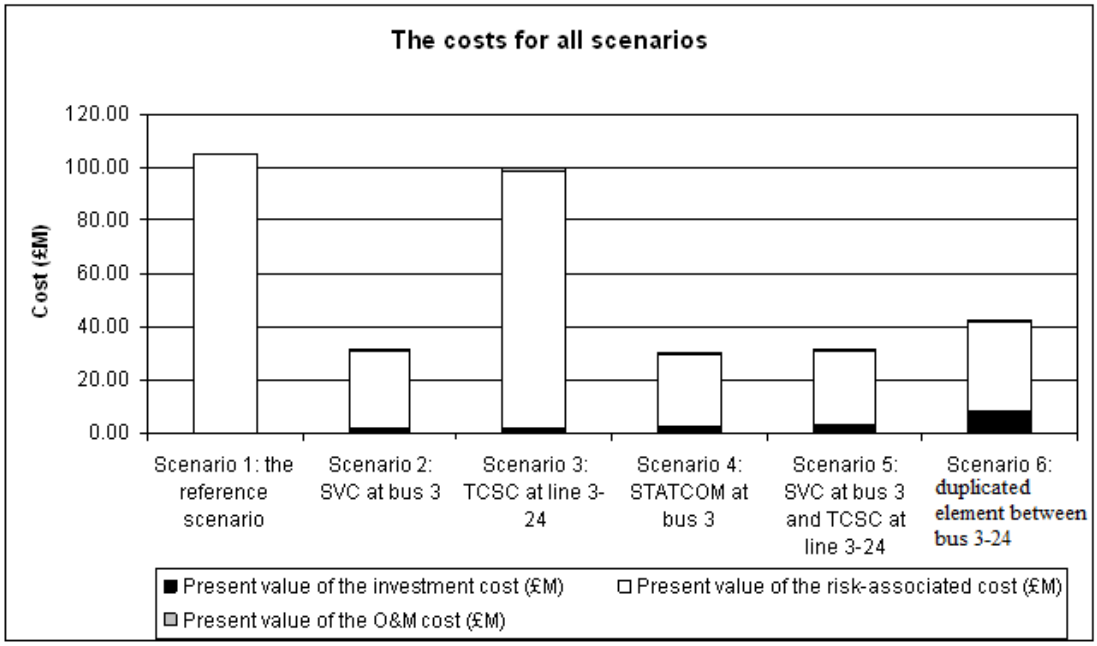

Figure 7.15: the costs for all scenarios.

The O&M costs are given in Table 7.1.

Table 7.1: O&M costs for RTS

Scenario No.	**O&M cost per year (£)**	**Present value of the O&M cost (£)**
2	50,000.00	704,697.23
3	50,000.00	704,697.23
4	50,000.00	704,697.23
5	75,000.00	1,057,045.84
6	50,000.00	704,697.23

The investment costs are provided in

Table 7.2:

Table 7.2: Investment costs for RTS

Scenario No.	**Investment cost per year**	**Present value of the**

	(£)	investment cost (£)
2	400,000.00	1,731,790.67
3	500,000.00	2,164,738.34
4	600,000.00	2,597,686.00
5	800,000.00	3,463,581.34
6	2,000,000.00	8,658,953.34

The risk-associated costs for RTS are shown in Table 7.3:

Table 7.3: Risk-associated costs for RTS

Scenario No.	Risk-associated cost per year (£)	Present value of the risk-associated cost (£)
1	7,450,862.50	105,012,043.04
2	2,057,961.79	29,004,798.40
3	6,877,945.32	96,937,379.93
4	1,892,526.26	26,673,156.53
5	1,928,533.11	27,180,638.61
6	2,361,502.82	33,282,889.56

As in the previous test case, the O&M and investment costs for scenario 1 is zero. By investing in a corrective control system or an additional branch, the risk-associated cost tends to drop with the increase in investment and O&M costs. The IBSR indicates whether the system reliability improvement outweighs the increase in investment and O&M costs. It is calculated on a present value basis.

As is introduced in Chapter 4,

$$\mathrm{IBSR} = \frac{\mathrm{EIC_b}\text{-}\mathrm{EIC_a}}{\mathrm{ISRI}} \qquad \textbf{(7.33)}$$

$$\mathrm{ISRI} = \sum_{t=0}^{ma} \frac{\mathrm{IC}_{at} + \mathrm{OC}_{at}}{(1+i)^t} - \sum_{t=0}^{mb} \frac{\mathrm{IC}_{bt} + \mathrm{OC}_{bt}}{(1+i)^t} \quad (£) \qquad \textbf{(7.34)}$$

The IBSR result is shown in Figure 7.16.

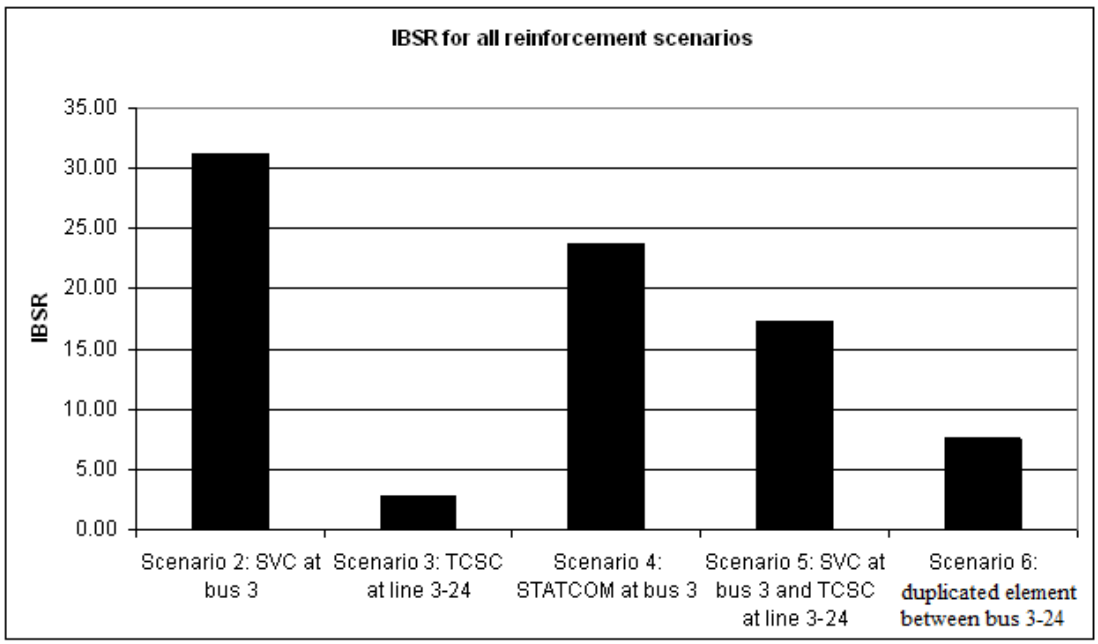

Figure 7.16: IBSR results for RTS.

The calculation of the IBSR requires a 'departure status', i.e., the pre-reinforced system status. In Figure 7.16, the 'departure status' on which the incremental reinforcement is built is the reference scenario; that is, all the reinforcement scenarios (scenarios 2 – 6) are considered 'incremental' to the reference scenario. Under this circumstance, each reinforcement scenario is regarded as a one-off construction in which the IBSR is calculated based on the cost data of the reference (pre-reinforcement status) and reinforcement scenarios. However, a reinforcement scenario may well be achieved through multiple stages in which every step is an individual project. In other words, the reinforcement scenario is the result of an accumulative process. Therefore, the IBSR for each individual project can be calculated.

Scenario 5 is investigated under these two circumstances. Figure 7.17 shows the difference between the above-mentioned circumstances.

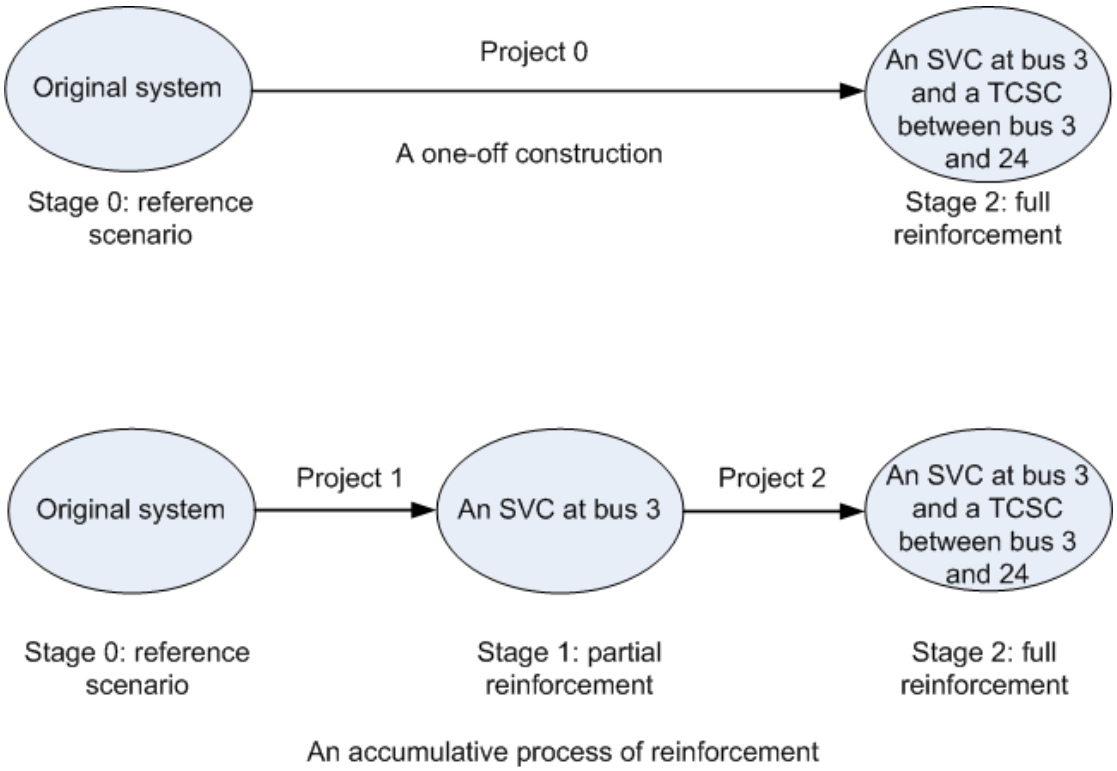

Figure 7.17: one-off reinforcement and accumulative reinforcement.

For a 'one-off construction',

$$\mathrm{IBSR}_0 = \frac{\mathrm{EIC}_0 - \mathrm{EIC}_2}{\mathrm{ISRI}} \tag{7.35}$$

$$\begin{aligned}\mathrm{ISRI} &= \sum_{t=0}^{m_2} \frac{\mathrm{IC}_{2t} + \mathrm{OC}_{2t}}{(1+i)^t} - \sum_{t=0}^{m_0} \frac{\mathrm{IC}_{0t} + \mathrm{OC}_{0t}}{(1+i)^t} \\ &= \sum_{t=0}^{m_2} \frac{\mathrm{IC}_{2t} + \mathrm{OC}_{2t}}{(1+i)^t} \quad (£)\end{aligned} \tag{7.36}$$

where the subscripts of IC, OC, and EIC denote the stage numbers (Figure 7.17).

IBSR_0 is the IBSR for project 0.

The IBSR result is shown in Figure 7.16. $\mathrm{IBSR}_0 = 17.22$.

This result has clear physical meaning. Of each £ of the reinforcement scenario incremental cost (comprising investment and O&M costs), the reliability benefit is £17.22. The incremental benefit in terms of system reliability clearly outweighs the incremental cost by a considerable margin.

For 'an accumulative process of reinforcement', the IBSR for each project is calculated as follows:

$$\mathrm{IBSR}_1 = \frac{\mathrm{EIC}_0 - \mathrm{EIC}_1}{\mathrm{ISRI}_1} \quad \textbf{(7.37)}$$

$$\mathrm{ISRI}_1 = \sum_{t=0}^{m_1} \frac{\mathrm{IC}_{1t} + \mathrm{OC}_{1t}}{(1+i)^t} \quad (£) \quad \textbf{(7.38)}$$

$$\mathrm{IBSR}_2 = \frac{\mathrm{EIC}_1 - \mathrm{EIC}_2}{\mathrm{ICCI}_2} \quad \textbf{(7.39)}$$

$$\mathrm{ISRI}_2 = \sum_{t=0}^{m_2} \frac{\mathrm{IC}_{2t} + \mathrm{OC}_{2t}}{(1+i)^t} - \sum_{t=0}^{m_1} \frac{\mathrm{IC}_{1t} + \mathrm{OC}_{1t}}{(1+i)^t} \quad (£) \quad \textbf{(7.40)}$$

where the subscripts of IBSR and ISRI denote the project numbers (Figure 7.17).

The results are given below.

$\mathrm{IBSR}_1 = 31.20$ and $\mathrm{IBSR}_2 = 0.875$.

Project 1 provides a reliability benefit that significantly outweighs the incremental investment and O&M cost, whereas project 2 fails to deliver a reliability benefit that outweighs the latter. The IBSR ranking therefore follows the order $\mathrm{IBSR}_1 > \mathrm{IBSR}_0 > \mathrm{IBSR}_2$. This result is consistent with that shown in Figure 7.14. System reliability at stage 2 (under scenario 5) is only slightly higher than that at stage 1. The slight improvement in reliability fails to justify the investment in project 2.

IBSR_1 is greater than IBSR_0 because

1) the negligible difference in reliability between states 2 and 1; and
2) the significantly lower investment and operation cost presented by project 1.

If no benefit or cost other than the reliability benefit, investment cost, and O&M cost is considered, project 2 is economically infeasible. However, the conclusion may differ if possible benefits in other aspects are taken into account (e.g., the benefit in reduction of line losses and externalities, etc.).

The two-step reinforcement can also be to first install a TCSC between bus 3 and bus 24, and then install an SVC at bus 3, where the former provides negligible reliability benefit and the latter provides significant reliability improvement. The calculation is not repeated in this research because the same explanation as above applies with the only difference that IBSR_1 and IBSR_2 are swapped in the ranking.

This test case shows that the implementation of FACTS devices slows down the deterioration of system reliability in the context of load growth. Such an effect is quantified and compared for different scenarios. In this particular case, the implementation of FACTS devices improves system reliability more than does the traditional reinforcement scenario of installing a duplicated element.

The failure of the central control unit as CCF results in the outage of all FACTS devices. The effect of CCF on system reliability is investigated through sensitivity analysis. Scenario 5 is the scenario in which more than one FACTS device is deployed in the system and is therefore selected for the analysis. The EENS and LINWRI results are studied under different failure rates of CCF λ_{CCF}. The results are shown in Figure 7.18 and Figure 7.19.

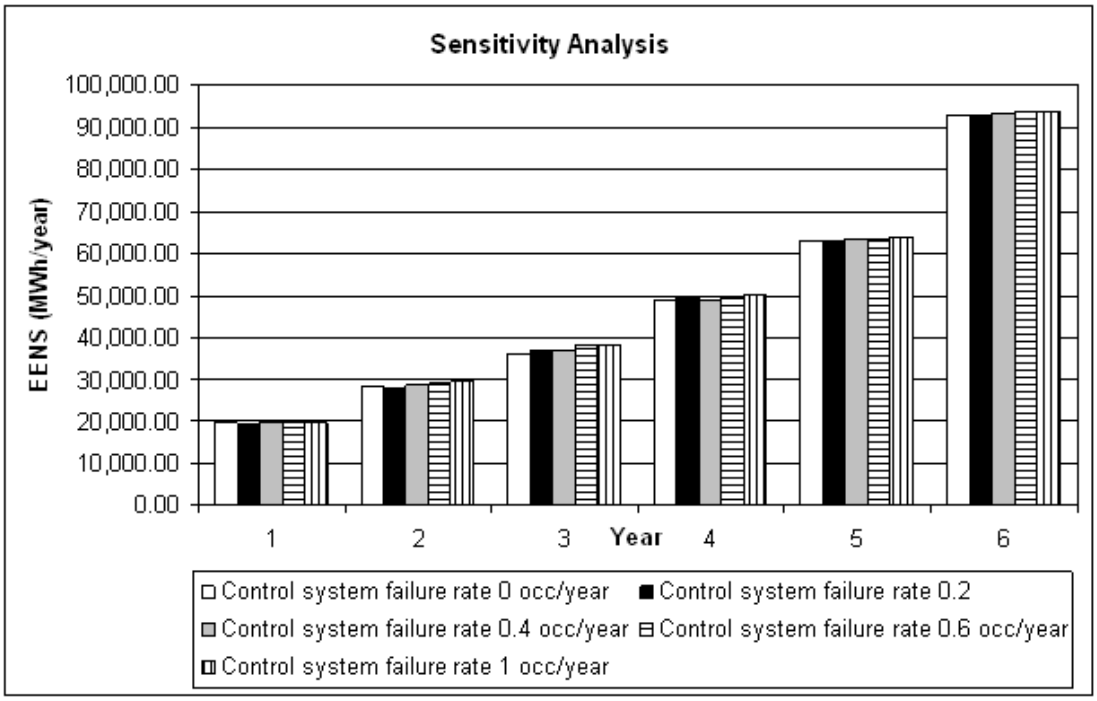

Figure 7.18: Effect of the control system failure rate on EENS results.

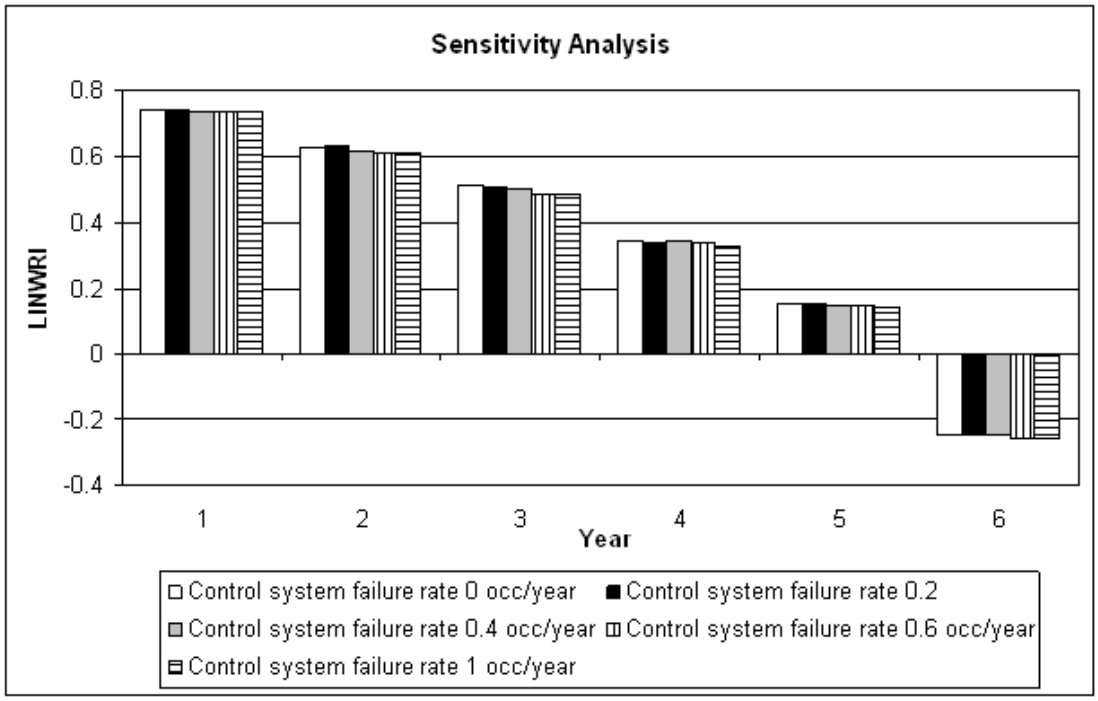

Figure 7.19: Effect of the control system failure rate on LINWRI results.

λ_{CCF} ranges from 0 to 1 occ/year. When $\lambda_{CCF} \leq 1$ occ/year (the failure rate of 1 occ/year is greater than that of a branch or a FACTS device), it has a negligible effect on the EENS and LINWRI results. Take the LINWRI results as an example. The difference in LINWRI results for any two different values of λ_{CCF} ($\lambda_{CCF} \leq 1$ occ/year) is no more than 5%. This phenomenon is attributed to two factors:

1) The failure of FACTS devices does not lead to load curtailment. However, the failure of branches alone or the coinciding failure of branches and FACTS devices may lead to load curtailment.

2) The average duration of CCF in a year is no more than 30 hours ($1 \text{ occ/year} \times 30 \text{ h/occ}$) or 0.34% of a year (8760 h). The short annual average duration makes coincidence with the failure of a branch highly unlikely. Therefore, the conclusion is that a reasonably reliable FACTS central control unit with a failure rate of the same order as that of a branch has negligible effect on system reliability.

7.5 Conclusion

The following conclusions are drawn from the study on RTS:

1) Although the corrective control and traditional reinforcement scenarios slow down the deterioration of reliability over years of load growth, this reduction does not necessarily translate to a consistent ranking of all the scenarios in terms of reliability in all the years. Load level has an effect on the ranking.

2) For RTS, traditional reinforcement does not provide higher reliability improvement than most corrective control scenarios. However, this conclusion is not general but depends on individual network.

3) The traditional reinforcement scenario has a lower IBSR value than most corrective control scenarios. This means that most corrective control scenarios are economically preferable over traditional reinforcement scenarios.

4) The IBSR indicates whether a candidate scenario is worth investing in under the condition that no benefit or cost other than reliability benefit, investment cost, and O&M cost is considered. However, if other benefits such as the reduction in line losses are taken into account, along with the benefit in reliability, the IBSR no longer serves as an indicator but remains an indispensable index that quantifies the reliability benefit.

5) The IBSR value depends on the ‘departure status’, i.e., the pre-reinforced status. A system reinforcement process can either be a lump project (one-off construction) or several small projects (accumulative construction). The IBSR results for each small project and those for the lump project are calculated; they indicate whether the incremental reliability benefit outweighs the incremental costs (whether IBSR>1). Given that a lump project consists of project A and project B in chronological order, and that project A has a higher IBSR value than the lump project, this means project B has the lowest IBSR value, or is the least cost-effective among the three.

6) A sensitivity analysis is performed by varying the failure rate of the FACTS control system. The maximum failure rate is approximately twice or three times the failure rate of a branch. Within this range, the FACTS control system has a negligible effect on system reliability.

8 Energy Storage Systems and Reliability

Summary

This chapter focuses on the reliability assessment of power systems that incorporate ES. The motivation for implementing ES into power systems and relevant technologies are reviewed. The battery energy storage (BES) is modelled, and their effects on system reliability are studied through a test case.

8.1 Background

A traditional idea is that electricity cannot be stored in large quantities; therefore, generation and load are balanced at any moment. However, this concept is being challenged by the improvements in ES technology, as well as by the growing application of ES.

The purposes of implementing ES differ from case to case. In general, they are summarised as follows:

1) ES replaces some of the costly peak generation units for tackling peak demand, e.g., peak shifting [125].

2) Generally, ES has a higher ramp rate than do conventional generation units. Therefore, it can serve as a substitute for spinning reserves [126, 127].

3) ES can be installed at the weak point of a power system to help the system ride through a fault of a relatively short duration [126].

4) ES can be applied to improve power quality and system stability [126, 127].

5) Installing an ES device at a load centre may serve as a cost-effective alternative to investing in a new power line [126].

6) With the increasing penetration of intermittent generation, there is a need for ES to smooth the output of these generation units for economic and reliability reasons [128]. ES may be required in a wind farm for compliance with the grid code of providing emergency support (e.g., to absorb excess wind energy when needed). ES can also improve the 'dispatchability' (the storage lending itself to dispatch, as in conventional generation) of intermittent generation.

8.2 ES Applications

A few published articles focus on the integration of ES into intermittent generation.

Different control strategies are proposed for the application of ES in a wind farm [36]. These strategies dictate the condition at which ES charges/discharges. The strategy is that ES stores energy when excess wind supply is generated and discharges energy when wind generation is low. The reliability assessment of the generation system shows that system reliability improves after the implementation of ES in the wind farm.

In previous studies, ES is integrated into wind generation and photovoltaic generation to smooth the fluctuating output [129, 130]. The contribution of these types of generation (with ES) to generation adequacy is highly dependent on their location. The contribution can be significant when the site is rich in wind resources and solar radiation. To maintain the same reliability level, a larger capacity of intermittent generation is needed than that required in conventional generation to compensate for the uncertainty of the former [129]. However, neither paper considers the network.

The effect of ES on the reliability of a composite system (HLII) with wind generation is studied in [19]. The rated capacity of ES has a significant effect on system reliability [19]. The limitation, however, is that the reliability of the ES device and its control system is not considered.

Hydrogen energy storage can be used to smooth the output of a wind power system [131]. A wide-area energy management system with large-scale ES is used to smooth the output of intermittent generation, whose penetration rapidly increases [132]. Several options of utility-scale ES technologies are investigated based on a number of criteria

such as the ability to frequently change output, range of output, ramp rate, duration under rated power output, cost, and technology maturity, etc [132].

A number of ES technologies and configurations have been studied for a wind farm in [133]. The objective is to reduce the fluctuations in wind generation output. A flywheel, BES, and superconducting magnetic energy storage (SMES) are selected. The study asserts that both configurations—the aggregated and distributed configurations—effectively suppress wind output fluctuations [133].

A combination of wind, fuel cell (FC), and UCAP systems for sustained power generation at varying wind speeds is introduced in [134], in which the dynamic model of the hybrid power is proposed. The FC supplies the required load when wind generation is insufficient, while UCAP further supplies power for a short period when FC reaches its rated power. The configuration demonstrates a stable output under highly fluctuating wind speed and load. This feature makes this type of generation a promising candidate for power supply at non-interconnected remote areas.

A combination of wind turbine, battery, and UCAP is used to produce predictable power output for a given time interval in [135]. The battery can serve as backup to the generation during temporary wind deficiencies for an interval of up to 10 minutes, while UCAP manages transient peak power to protect the battery.

Apart from being applied in intermittent generation, ES can also be integrated into FACTS devices for more robust and flexible control than FACTS alone. Battery storage (BS) is integrated into a STATCOM to improve dynamic stability and to increase transmission capability [136]. The independent control of active and reactive powers renders a STATCOM/BES improved capability to damp oscillations as well as perform dynamic power flow control [76, 136, 137]. An integrated design of UCAP with a voltage source converter is proposed in [138]. Its function includes power quality enhancement, voltage and frequency stabilisation, and power transfer capacity enhancement. Similarly, a combined STATCOM and super capacitor energy storage system (SCESS) for application in wind farms is proposed in [102]. The purpose is to stabilise wind generation output. The control function for a STATCOM/SCESS is decoupled into reactive and active power control. Results show that the combined device can stabilise both the wind output and grid voltage.

8.3 ES technologies

This section reviews various ES technologies including BES, pumped hydro storage, compressed air energy storage (CAES), flywheel storage, SMES, and supercapacitor energy storage [139].

The following criteria are used in classifying ES technologies [140]:

1) physically fixed or mobile type of application;
2) discharge duration: short-term storage (<1 min), medium-term storage (from a few minutes to a couple of hours), and long-term storage (from hours to months); and
3) maximum discharge power.

In this project, ES technologies are assigned into different categories according to their discharge durations. The main characteristics of each type of ES are its storage capacity, power output, discharge duration, number of cycles, efficiency, self-discharge, and technological maturity, etc [140].

A typical BES includes lead acid, lithium, nickel cadmium, sodium-sulphur, vanadium redox, and zinc bromine batteries. Their performance levels are summarised in Table 8.1 [48, 94].

Table 8.1: Summary of various types of BES

	Lead acid	Sodium-sulphur	Lithium	Zinc bromine
Maximum power	Multiple tens of MW	MW level	Tens of kW	Hundreds of kW
Energy density (Wh/kg)	35 to 50	150 to 240	150 to 200	34–54
Power density (W/kg)	75 to 300	90 to 230	200 to 315	20 to 60
Cycle life	500 to 1,500	2,500	1,000 to 10,000+	>2000
Charge/discharge Energy Efficiency	80%	≤ 90%	95%	70%
Storage duration	Medium term: hour level	Medium term: a few hours	Medium term: a few hours	Medium term: a couple of hours
Annotations	1) Lead is not environment friendly 2) Limited cycle life 3) Widely applied in utilities	Operate at a temperature of 300 to 350 °C	1) Limited maximum power 2) Immature for utility application.	In the first stage of commercialisation.

Vanadium redox is a promising type of BES for application in the grid because

1) compared with the poisonous lead acid battery, it is environment friendly [95];

2) it produces a MW-level power that is sufficient for grid application; and

3) it has a longer life cycle and higher efficiency than does the lead acid battery.

However, as a relatively new technology compared with the widely commercialised lead acid battery, whether vanadium redox is technically mature enough for large-scale industrial application and whether it is economically viable remain concerns for this technology.

Apart from BES, pumped hydro storage is another traditional type of ES normally used for load balancing. It pumps the water to a higher reservoir during off-peak periods and later releases it through generation turbines during peak periods. The maximum power it produces (at least hundreds of MW) and the maximum energy it stores are considerably greater than those of most types of ES [96]. However, it requires 1) a geographically suitable site characterised by water-rich resources and levelled terrain; and 2) an investment of up to billions of US dollars, including the costs of land, tunnels, generation facilities, and labour [96].

Compressed Air Energy Storage (CAES) is another form of ES. It compresses air at high pressure in an airtight underground cavern or aquifer during off-peak hours and de-pressurises the air, which is then heated and slowly released through a generation turbine to generate electricity when required [48]. CAES has the following advantages [97]:

1) It can supply a substantial amount of power of up to hundreds of MW.

2) The start-up time is around 10 minutes, faster than a conventional peak plant with a combustion turbine.

However, the feasibility of CAES depends on geographical conditions. A large underground cavern is required, which limits CAES application.

A flywheel converts electrical energy to kinetic energy when charged, and vice versa when discharged. It is used as short-term storage with a significantly larger number of life cycles compared with a BES. This project does not include flywheel storage because the analysis is conducted on the steady-state model of power systems requiring at least medium-term storage with a discharge duration of up to several hours.

SMES stores magnetic energy through superconducting coils under very low temperature maintained by liquid helium [139]. It exhibits a high efficiency of up to 90% and provides fast response down to microseconds. However, because of the technical barrier to SMES (i.e., the cooling requirement), this technology is still in the laboratory testing stage. One of the ongoing research directions is to identify a material that becomes superconductive at a relatively 'high' temperature (up to a hundred Kelvin) [139].

Another type of ES is the supercapacitor also called UCAP or electric double layer capacitor. Its capacitance is much greater than that of traditional capacitors (reaching up to 400 F for a standard UCAP) [58, 59]. The pros and cons of UCAP are summarised in Table 8.2.

Table 8.2: Summary of the pros and cons of UCAP.

Advantages	**Disadvantages**
1) A large number of life circles, up to millions of times 2) Fast charge and discharge, completed in seconds 3) High efficiency 4) Environment friendly 5) High power density, approximately $4,000$ W/kg	1) Low energy density, <15 Wh/kg 2) Subject to self-discharge

Given its low energy density and high-power density feature, UCAP is applied as a short-term power booster.

A summary of different types of ES technologies is provided in Table 8.3.

Table 8.3: Summary of different types of ES technologies

Storage Technology	Battery	Pumped hydro	Fly wheel
Maximum energy stored	< 200 MWh	< 24000 MWh	< 100 kWh
Power output level	< 30 MW	< 2000 MW	< 100 kW
Discharge duration at maximum power	1 – 8 hours	12 hours	Minutes to 1 hour
Response time	30 ms	30 ms	5 ms
AC to AC efficiency	60%–80 %	70%–80 %	80%– 85 %
Economic life	2–10 yrs	40 yrs	20 yrs
Technological maturity	In industrial application	In industrial application	Envisioned for industrial application

Storage Technology	CAES	SMES	UCAP
Maximum energy stored	400 – 7200 MWh	0.6 kWh	N/A
Power output level	100–300 MW	200 kW	N/A
Discharge duration at maximum power	4–24 hours	Several seconds	Several seconds
Response time	3–15 mins	5 ms	5 ms
AC to AC efficiency	85%	90%	90%
Economic life	30 yrs	40 yrs	40 yrs
Technological maturity	In industrial application	In laboratory state	Envisioned for industrial application

* N/A - No currently available data.

Extended from the original version in [126].

8.4 Configuration of an ES device

A typical ES device comprises three parts: the central storage, power transformation system (PTS), and charge-discharge control system (CDCS) [125].

The central storage is the storage vessel (e.g., the battery bank, a reservoir, etc.).

The PTS serves as the power interface between the central storage and power system. It performs AC/DC conversion and voltage magnitude transformation.

The CDCS performs necessary control functions for ES.

A general structure for ES is shown in Figure 8.1 [125].

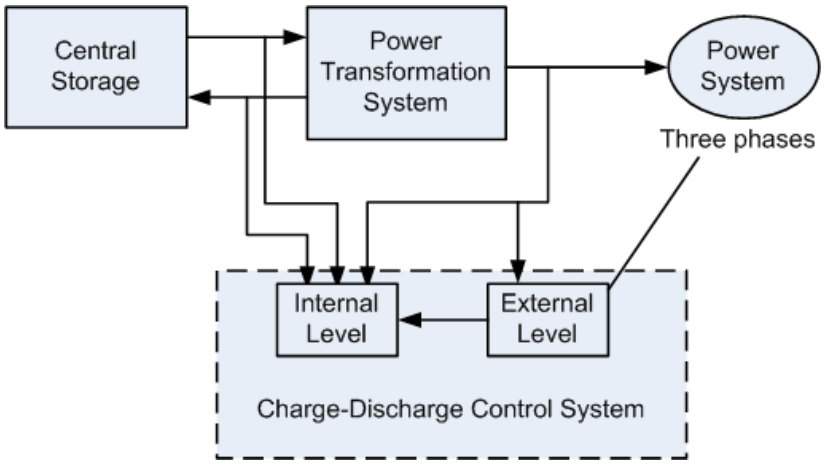

Figure 8.1: General structure of ES.

From a comprehensive literature survey, the author finds that relatively few studies have been devoted to power system reliability (considering the network) in which ES devices are incorporated into the system. In this chapter, the state space models of a BES and that of a BES integrated with a STATCOM are developed and applied to the reliability assessment process, along with the control system failure. The new reliability indices proposed in

previous chapters are applied to express the reliability and incremental benefit of system reinforcement.

This chapter looks into the following questions:

1) *How much reliability improvement ES devices bring to the power system?*

2) *Is the implementation of ES economically preferable over the traditional reinforcement scenario?*

8.5 Physical and State Space Models of BES

The state space model for the BES is derived. A BES consists of multiple banks, and it can operate at a derated state (partial failure state). However, the failures of all the banks, or the failure of either the power interface (PI) or the CDCS causes BES failure. Therefore, a combined parallel-series block diagram is applied to the BES, as shown in Figure 8.2.

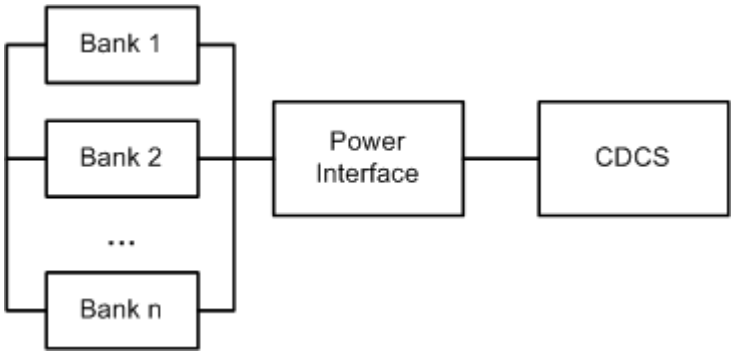

Figure 8.2: Block diagram of BES.

For a multi-bank BES, the BES can reside in any one of these states: the normal state, derated states, and outage state. In this paper, it is assumed that only one derated state exists for BES, which has only two banks. The number of derated states does not affect the fundamental idea of the state space model.

The full state space model of BES is derived based on the following assumptions:

1) All repair jobs restore the full functionality of the BES. There is no 'partial repair', in which some of its components remain inoperative.

2) When both banks are down, the BES is disconnected and no further outage develops.

3) When the PI or CDCS is down, the BES is disconnected and no further outage develops.

The full state space model is shown in Figure 8.3.

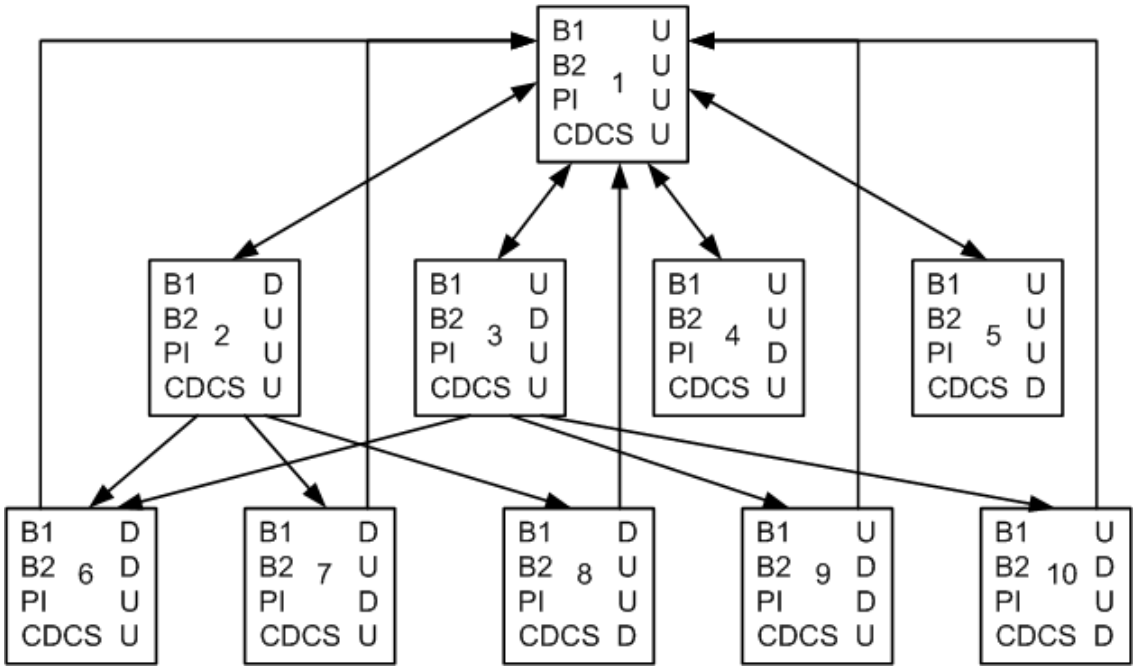

Figure 8.3: Full state space model of a BES with two banks.

The abbreviations in Figure 8.3 are explained as follows:

B1: Bank 1;

B2: Bank 2;

U: Up;

D: Down.

BES can be integrated with a STATCOM. The combined STATCOM/BES can independently output real and reactive power [136]. Furthermore, the combination improves oscillation damping. Its block diagram is shown in Figure 8.4 [141].

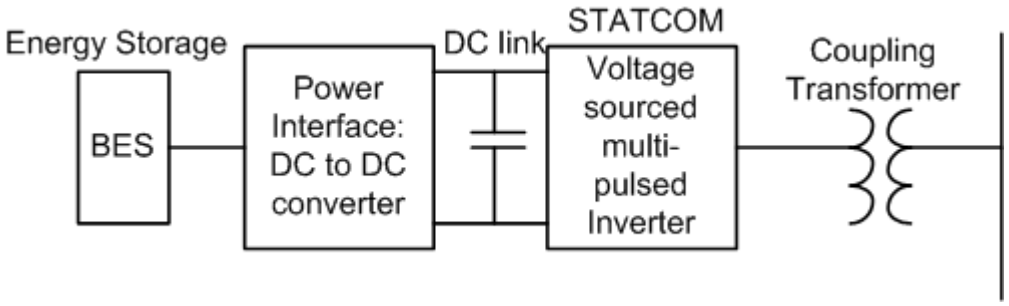

Figure 8.4: Block diagram of STATCOM/BES [141].

A STATCOM/BES consists of a self-contained BES, PI between STATCOM and BES (a DC–DC converter), STATCOM (VSI), and coupling transformer [141]. The failure of either the PI or BES results in the BES being disconnected and the device running as a pure STATCOM. The failure of the STATCOM induces the failure of the entire STATCOM/BES. The state space of the STATCOM/BES is shown in Figure 8.5 (all the abbreviations are the same as those in Figure 8.3). Such a state space model inherits all the assumptions on which the BES model is based. The full list of assumptions is given below.

1) All repair jobs restore the full functionality of the STATCOM/BES. In other words, there is no 'partial repair', in which some of the components remain inoperative.
2) The outage of both of the banks, CDCS, or the PI causes the BES to be disconnected. Under this circumstance, the device runs as a pure STATCOM.
3) When the STATCOM is down, the STATCOM/BES becomes inoperative and no further component outage occurs.

The full state space model of the STATCOM/BES is depicted in Figure 8.5.

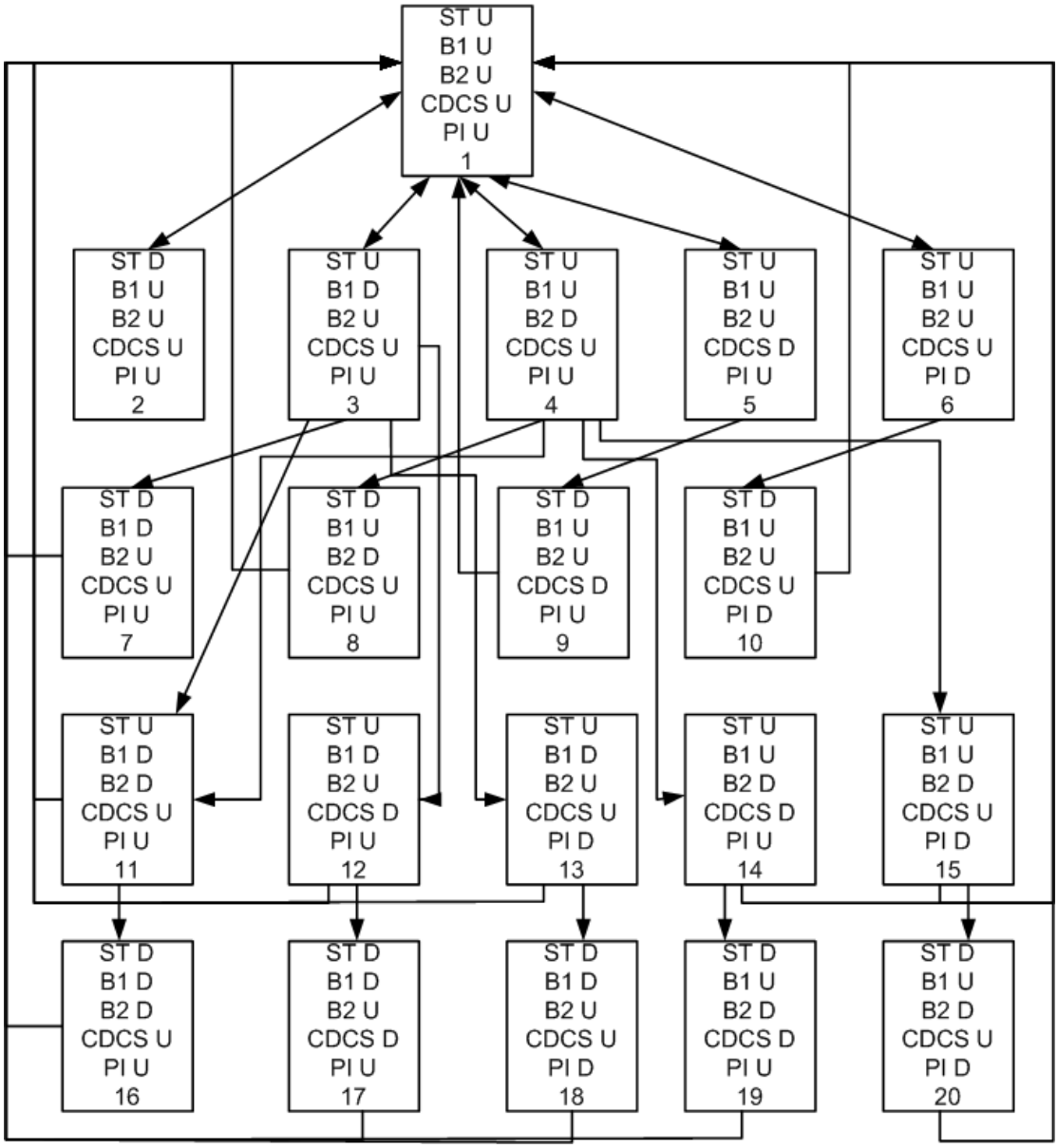

Figure 8.5: State space model of STATCOM/BES.

The above-mentioned state space model can be further simplified into four states:

1) The BES and STATCOM are both working normally, corresponding to state 1 in Figure 8.5.

2) The BES is in the derated state and STATCOM is in the normal state, corresponding to states 3 and 4 in Figure 8.5.

3) The BES is completely down and the STATCOM is in the normal state, corresponding to states 5, 6, 11–15 in Figure 8.5.

4) The STATCOM is down resulting in the outage of the STATCOM/BES, corresponding to all states except those mentioned in 1) – 3).

The four-state model is shown in Figure 8.6.

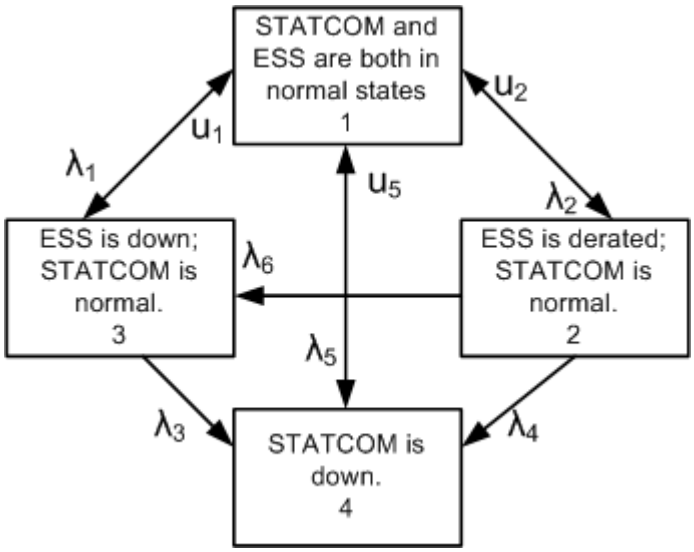

Figure 8.6: Simplified state space model of STATCOM/BES.

The state space corresponds to a Markov process. The transitional probability matrix is derived as

$$P_{Trans} = \begin{bmatrix} 1-(\lambda_1+\lambda_2+\lambda_5)\Delta t & \lambda_2\Delta t & \lambda_1\Delta t & \lambda_5\Delta t \\ \mu_2\Delta t & 1-(\mu_2+\lambda_4+\lambda_6)\Delta t & \lambda_6\Delta t & \lambda_4\Delta t \\ \mu_1\Delta t & 0 & 1-(\mu_1+\lambda_3)\Delta t & \lambda_3\Delta t \\ \mu_5\Delta t & 0 & 0 & 1-\mu_5\Delta t \end{bmatrix} \quad \textbf{(8.1)}$$

where Δt is a very small time interval.

The matrix multiplication method has been used in assessing the probabilities of residing in each of the four states [12]. The probability of existing in state i is denoted as P_i and the device is initially assumed to be in state 1. The steady-state probability vector is therefore

$$\begin{aligned} P &= [P_1 \quad P_2 \quad P_3 \quad P_4] \\ &= [1 \quad 0 \quad 0 \quad 0] P_{Trans}^{n} \end{aligned} \tag{8.2}$$

where subscript n is a sufficiently large number.

In this project, the STATCOM/BES runs as a spinning reserve that remains on standby during normal conditions; it provides real and reactive power output when a fault occurs in the system. The real and reactive power output of the STATCOM/BES at any moment is determined through the following procedures:

1) If the stored energy is depleted, the real power output is zero. However, the reactive power output from the STATCOM component is determined by an optimisation algorithm to minimise the cost of load curtailment.

2) If there is stored energy, the real and reactive power output are controlled by the central control unit. An optimisation algorithm for minimising the cost of load curtailment is then called. However, the real power output should be lower than the maximum power output level. The reactive power output is bounded by the output limit of the STATCOM.

Immediately after the system returns to normal status, the STATCOM/BES begins charging itself until it reaches full energy.

The AC optimisation model is given below

$$\min \mathrm{CCDF}(P_L^{Cur}) \tag{8.3}$$

subject to

$$P_{Gi} - P_{Li} + P_{Li}^{Cur} + P_{ESSi} = P_i^{inj}(V, \theta) \tag{8.4}$$

$$Q_{Gi} - Q_{Li} + Q_{Li}^{Cur} + Q_{\mathrm{STATCOM}i} = Q_i^{inj}(V, \theta) \tag{8.5}$$

$$S_{ij} < S_{ij}^{\max} \tag{8.6}$$

$$V_i^{\min} < V_i < V_i^{\max} \tag{8.7}$$

$$0 < P_{Li}^{Cur} < P_{Li} \tag{8.8}$$

$$\frac{P_{Li} - P_{Li}^{Cur}}{Q_{Li} - Q_{Li}^{Cur}} = \frac{P_{Li}}{Q_{Li}} \tag{8.9}$$

$$0 < P_{ESSi} < P_{ESS}^{\max} \quad \textbf{(8.10)}$$

$$Q_{\mathrm{STATCOM}i}^{\min} \le Q_{\mathrm{STATCOM}i} \le Q_{\mathrm{STATCOM}i}^{\max} \quad \textbf{(8.11)}$$

where

P_{Li}, Q_{Li} Active and reactive load at bus i;

P_{Gi}, Q_{Gi} Active and reactive generation at bus i;

$P_{Li}^{Cur}, Q_{Li}^{Cur}$ Active and reactive load curtailment at bus i;

P_i^{inj}, Q_i^{inj} Active and reactive power injection at bus i;

S_{ij} Load flows at branch ij;

V_i, θ_i Voltage magnitude and angle at bus i;

P_{ESSi}, $P_{ESS}^{\max}$ The active power output of BES and its upper limit.

$Q_{\mathrm{STATCOM}}, Q_{\mathrm{STATCOM}}^{\min}, Q_{\mathrm{STATCOM}}^{\max}$ The reactive power output, the lower limit of the reactive power output and the upper limit of the reactive power output of the STATCOM, respectively.

8.6 Case Study

Two test systems are investigated in this chapter. These are the 6-bus RBTS and 24-bus Modified Reliability Test System (MRTS).

8.6.1 RBTS

The first test system is the RBTS, whose topology is provided in [142].

The bus voltage constraint and branch transfer capacity limit are taken into account. Power line failures, STATCOM/BES failures, and central control unit failure are considered. The failure of generation units is not considered in the case study for the following reasons:

1) the focus is on network reliability; that is, the reliability of passing the electrical energy from generation units to load buses; and
2) power lines are generally more reliable than generation units. Considering the generation unit failure may mask network risk, which is the primary concern of this study.

All relevant data are given in Appendix D. The central control unit failure results in the outage of all STATCOM/BES devices. STATCOM/BES devices provide active and reactive power support under contingencies and remains on standby under normal conditions. The charging and discharging efficiencies of the BES are both 90%. The dynamic behaviours of BES are not considered.

Hourly loads over a year are discretised into 10 levels. Multiple load levels are used in this test case because these are necessary for the modelling of wind generation. The loads of all the buses are assumed to be fully correlated. The annual load growth rate is assumed to be 2.5% and the simulation covers up to 10 years from the base case at year 1.

LINWRI in this particular test case is defined as follows:

$$\mathrm{LINWRI} = 0.8\frac{\mathrm{EENS}}{\mathrm{EENS}_{\mathrm{ref}}} + 0.2\frac{\mathrm{AAOD}}{\mathrm{AAOD}_{\mathrm{ref}}} \qquad \textbf{(8.12)}$$

The location of the STATCOM/BES is decided by enumeration.

1) First, a number of candidate cases are defined by placing a STATCOM/BES at different PQ buses for different cases. For the RBTS, the number of candidate cases is 4 because this is the number of PQ buses in this system.
2) The reliability of each candidate case is assessed by state enumeration up to the first order considering only power line failures.
3) The candidate case with the highest reliability is selected.

Therefore, four scenarios are defined as follows:

1) the base scenario, i.e., the 'doing nothing at all' scenario;
2) a STATCOM/BES located at bus 6;
3) a wind farm with a STATCOM/BES located at bus 6; and,
4) the scenario with a duplicated branch connecting buses 5 and 6.

At this stage, the central control unit is assumed to be 100% reliable for scenarios 2 and 3.

The hourly wind speed profile over a year is plotted in Figure 8.7.

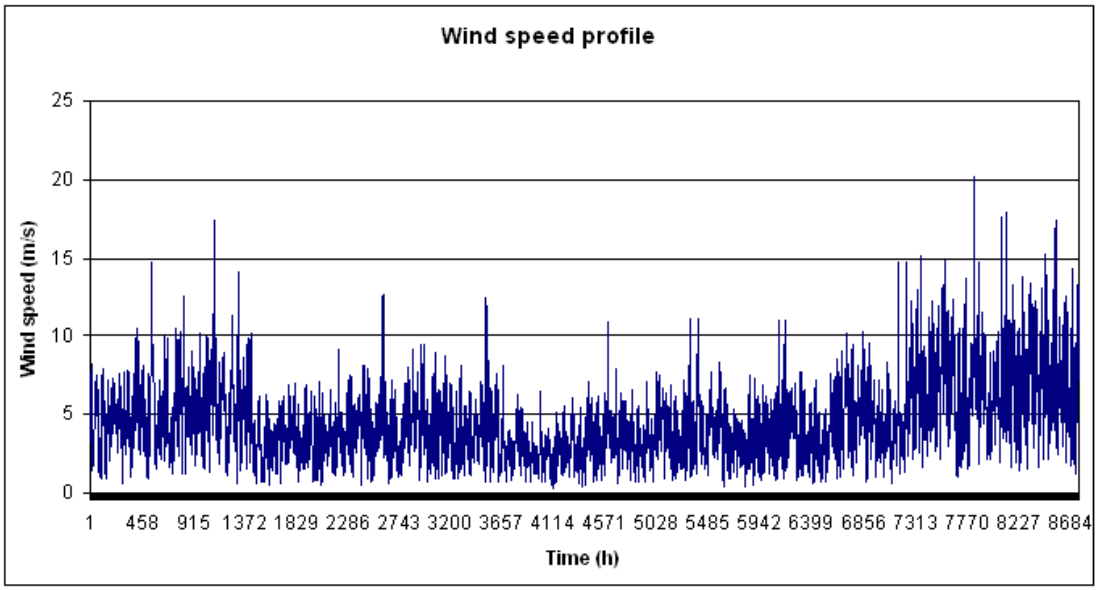

Figure 8.7: the wind speed hourly profile over a year.

The output of each wind turbine is the function of wind speed as given below:

$$p(v) = \begin{cases} 0 & v \le v_c \\ \mathrm{K}v + \mathrm{b} & v_c \le v \le v_r \\ \mathrm{P}_{\mathrm{rated}} & v_r \le v \le v_f \\ 0 & v \ge v_f \end{cases} \qquad \textbf{(8.13)}$$

where $v_c = 5$ m/s , $v_r = 15$ m/s , $v_f = 25$ m/s , $\mathrm{P}_{\mathrm{rated}} = 20$ kW ,

$\mathrm{K} = \mathrm{Prated}/(v_r - v_c)$

and $b = -K v_c$.

The number of wind turbines is $N = 64$, and the array coefficient is $\alpha = 0.6$. Therefore, the output of the wind farm is

$$P = \alpha N \bullet p(v) \qquad \textbf{(8.14)}$$

The EENS results from CMCS for the four scenarios are shown in Figure 8.8.

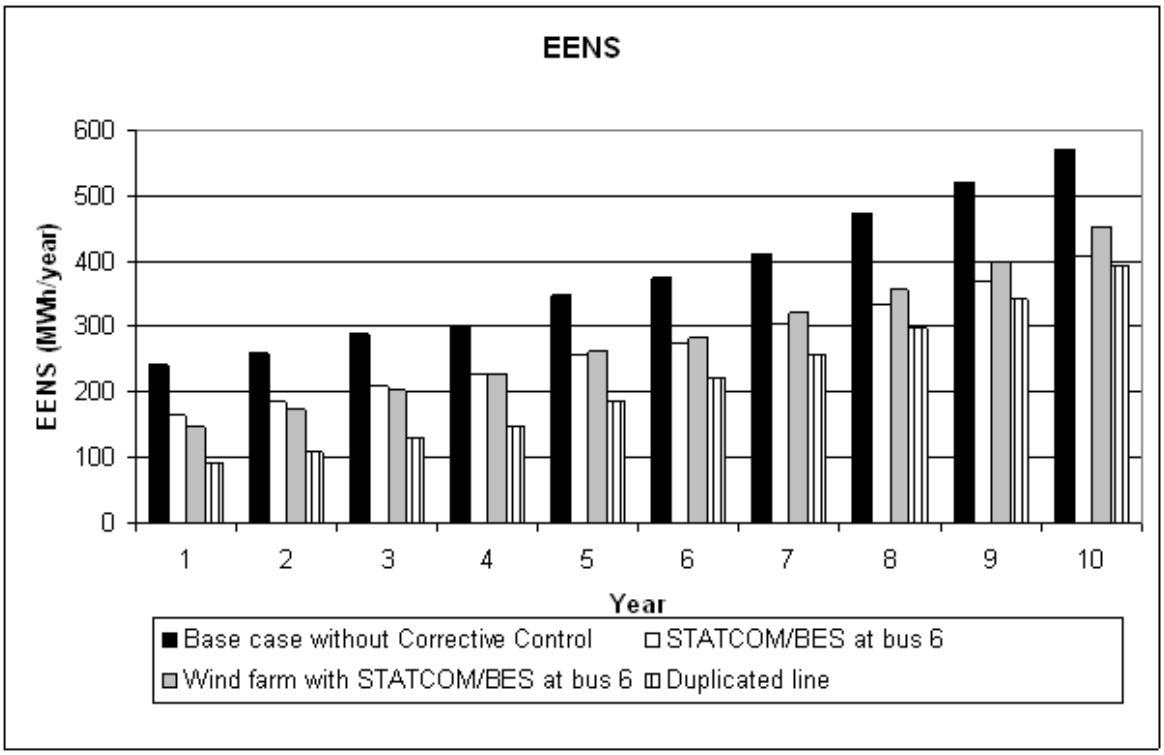

Figure 8.8: EENS results for the four scenarios.

The results for annual average outage duration (AAOD) are illustrated in Figure 8.9.

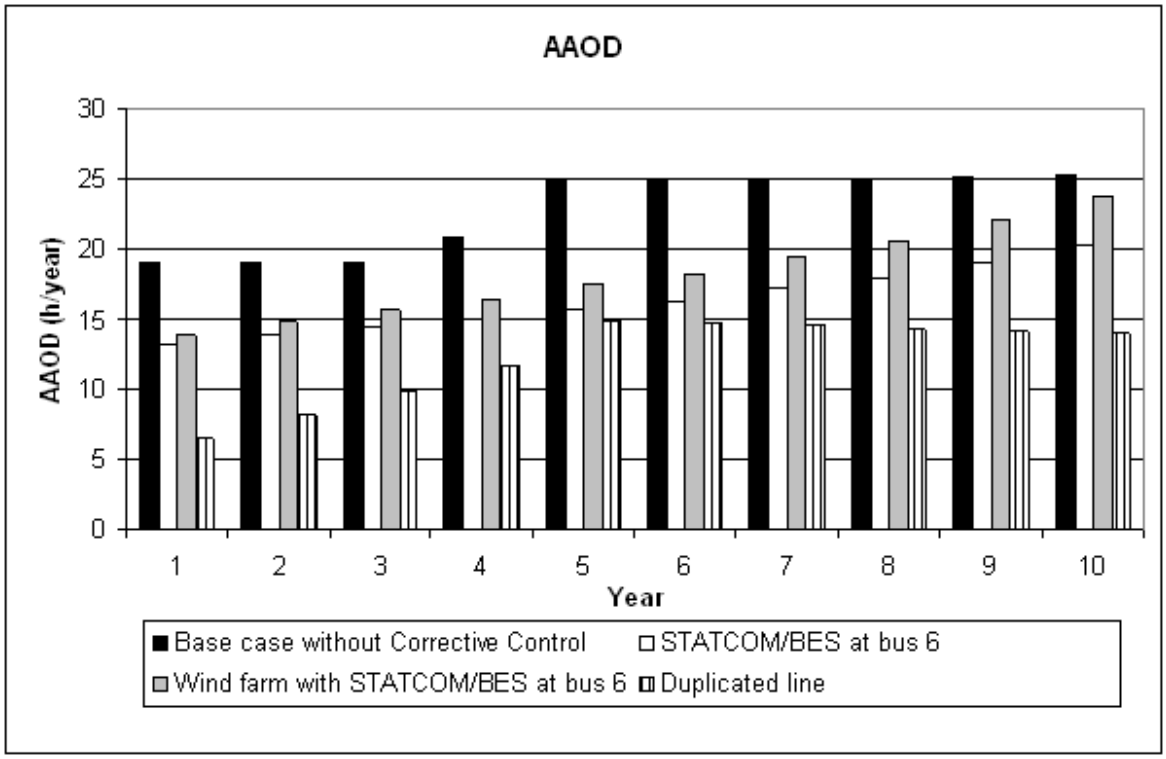

Figure 8.9: AAOD results for the four scenarios.

The LINWRI results are shown in Figure 8.10.

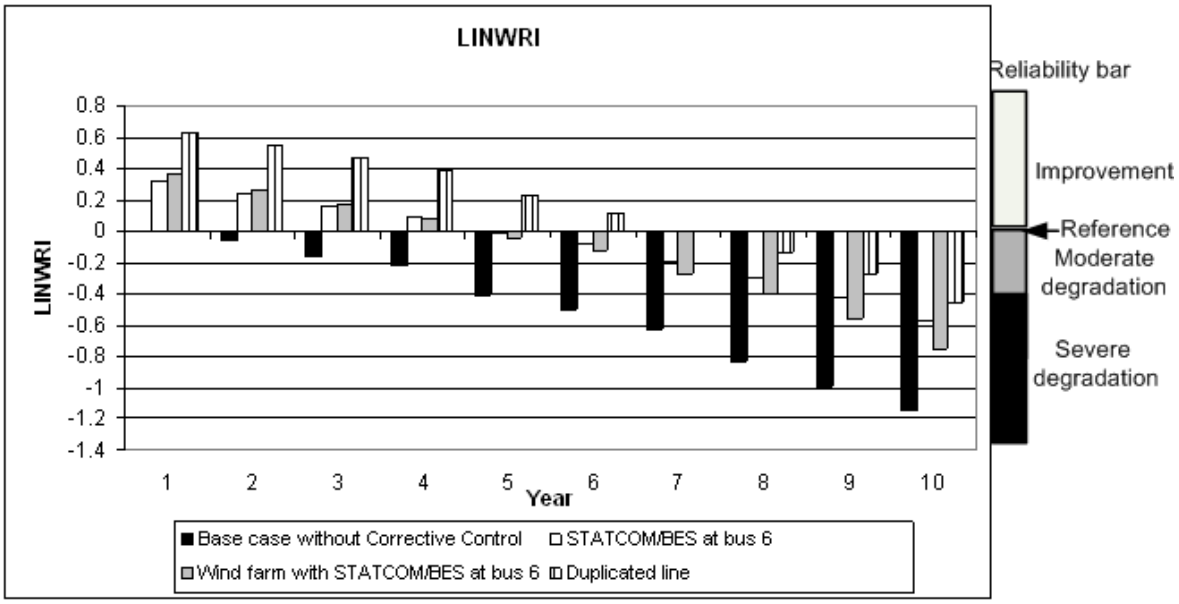

Figure 8.10: LINWRI results for the four scenarios.

Figure 8.8, Figure 8.9, and Figure 8.10 clearly show the improvement in reliability brought about by the STATCOM/BES and traditional reinforcement compared with the reference scenario. According to Figure 8.8, scenario 1 has the highest EENS (a negative contribution to overall reliability) and scenario 4 has the lowest EENS in any given year. However, no consistent ranking is observed between scenarios 2 and 3. They exhibit almost the same level of EENS before year 8 with a difference of less than 5%. In years 9 and 10, scenario 2 has a lower EENS than does scenario 3.

A similar phenomenon can be observed from the LINWRI results in Figure 8.10. Scenario 1 exhibits the lowest LINWRI value (poorest overall reliability), whereas scenario 4 has the highest at any given year. Scenarios 2 and 3 show mid-level values, which do not reflect a consistent ranking.

The AAOD results for scenarios 1 and 4 do not increase monotonically over years but are rather capped at a certain level, whereas those for scenarios 2 and 3 are lower than that of scenario 1 but higher than that of scenario 4 in any given year. The reason for this 'capped' phenomenon is that AAOD is defined as the average number of hours in a year when load is curtailed. A fault in the system does not always lead to load curtailment, whereas load curtailment always confirms the existence of a fault (at least one power line/transformer is down) in the system. Therefore, the theoretical maximum value of AAOD is the total number of hours in a year when a fault occurs in the system. However, AAOD is generally much lower than the theoretical maximum value because of the ability of the system to ride through the fault without load curtailment. The number of hours with faults in a year is determined by the failure rate of network components rather than the load level, and does not rise with load growth. Therefore, AAOD is capped at this value.

In this case, the unacceptable level of system reliability is defined as $\mathrm{LINWRI} = -0.4$, corresponding to the reliability level in year 5 under scenario 1. This is the level at which traditional network reinforcement should be immediately applied. The effect of transmission investment deferral is therefore directly obtained from Figure 8.10; the deferrals under scenarios 2 and 3 are both 3 years. In other words, scenarios 2 and 3 delay the system from dropping to the unacceptable reliability level by 3 years. This result is

based on an annual load growth rate of 2.5%. The deferral can be more significant under a more conservative estimation of the load growth rate.

An economic analysis is conducted in the same manner as that introduced in Chapter 7.

The investment cost for each scenario, except scenario 1, is assumed to be paid off in five equal yearly installments. The investment cost is converted to a present value by

$$IC = In\frac{1-(1+i)^{-n}}{i} \quad (£) \tag{8.15}$$

IC investment cost

In installment

i discount rate

n number of payments

Similarly, the present value of O&M cost is given by

$$OC = O_{annual}\frac{1-(1+i)^{-m}}{i} \quad (£) \tag{8.16}$$

OC present value of operation cost

O_{annual} annual operation cost

m economic life

The present value of the risk-associated cost is given by

$$R = R_{annual}\frac{1-(1+i)^{-m}}{i} \quad (£) \tag{8.17}$$

R present value of risk-associated cost

R_{annual} annual risk associated cost

m the maximum number of years considered in the simulation

The annual risk-associated cost is calculated from load curtailment using the customer damage function (CDF). In this test case, the CDF is defined as the function of outage duration (CDF is in £/MW; t is in hours):

$$\text{CDF} = f(t) = \begin{cases} 10,000 & t \le 1 \\ \\ 6,000 & t > 1 \end{cases} \qquad \textbf{(8.18)}$$

Therefore, the risk-associated cost in year j is $R_j = \sum_i \text{LOL}_i \bullet \text{CDF}(t_i)$, where LOL denotes load curtailment. Subscript i denotes the ith loss of load in year j.

The annual risk-associated cost is given by

$$R_{annual} = \frac{\sum_{j=1}^{N} R_j}{N} \quad \text{(£/year)} \qquad \textbf{(8.19)}$$

where N is the total number of years simulated.

The discount rate is assumed to be 5% and the economic life for each FACTS device or the extra line is 25 years.

According to [143], the investment cost of a 230kV power line ranges from $ 0.3m to $1.6m/mile. For a power line with a length of 100 miles, it is reasonable to assume an investment consisting of 10 equal instalments where each instalment is £30m.

According to [144], the investment cost for BES ranges from $0.17 to $1.50/Wh. For a BES with a maximum energy of 40MWh, the investment cost therefore falls in the range of $ 6.8m to $ 60m. This project assumes a STATCOM/BES investment consisting of 10 equal instalments with each having a value of £7m.

The investment costs are given in Table 8.4.

Table 8.4: Investment costs for RBTS

Scenario No.	Value of each instalment (£k)	Present value of investment cost (£k)
1	0	0
2	7,000	54,052.14
3	10,000	77,217.35
4	30,000	231,652.05

According to [3], the O&M cost is assumed to be a fixed percentage of investment cost. In this project, the O&M cost of a reinforcement scenario is assumed to be between 0.1% to 2% of the investment cost (present values).

The O&M costs are presented in Table 8.5.

Table 8.5: O&M costs of for RBTS

Scenario No.	Annual O&M cost (£k)	Present value of O&M cost (£k)
1	0	0
2	60	845.64
3	100	1,409.39
4	20	281.88

The risk-associated costs are presented in Table 8.6. The annual risk-associated cost is calculated from the reliability assessment algorithm.

Table 8.6: Risk-associated costs for RBTS

Scenario No.	Annual risk-associated cost (£k)	Present value of risk-associated cost (£k)
1	1,447.47	20,400.53
2	982.32	13,844.73
3	878.54	12,382.07
4	544.24	7,670.54

The cost structure is shown in Figure 8.11.

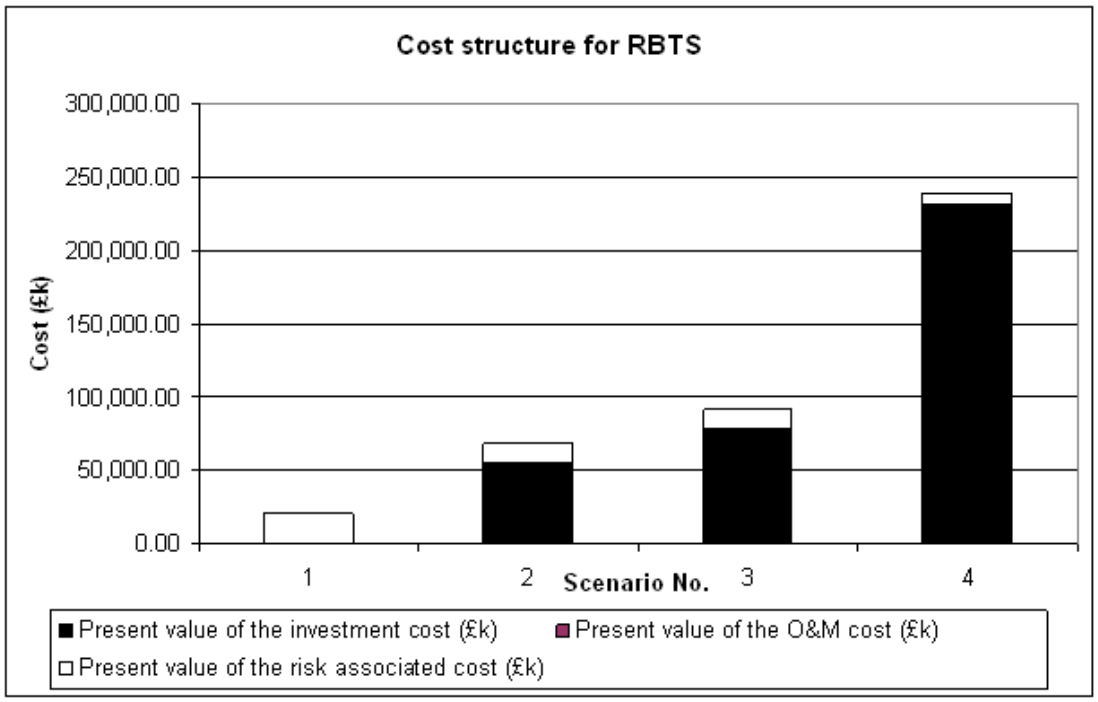

Figure 8.11: Cost structure for RBTS.

The IBSR results are plotted in Figure 8.12.

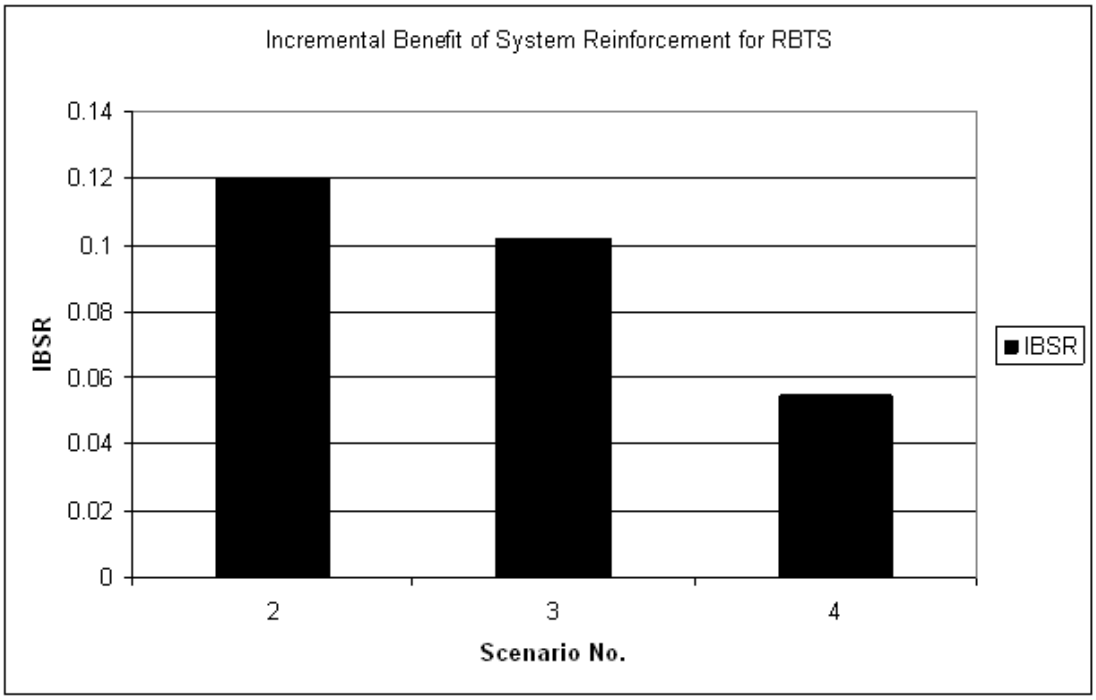

Figure 8.12: IBSR results for RBTS.

According to the cost structure, the investment cost takes up the largest proportion (>70%) of total cost, followed by risk-associated and O&M costs for scenarios 2, 3, and 4. The O&M cost for each scenario is negligible in the long term within the economic life of the reinforcement scenario.

That IBSR is lower under scenario 3 than under scenario 2 is a reasonable result. According to Figure 8.10, the reliability improvement brought about by the wind farm (i.e., that from scenarios 2 to 3) is negligible. Such reliability improvement fails to justify the extra investment (42.6% more from scenario 2) in the wind farm.

The lowest IBSR value of scenario 4 confirms that although the traditional reinforcement scenario provides the highest improvement in system reliability in this test case, the prohibitive amount of investment cost fails to provide a comparable reliability benefit.

In this case, the IBSR results for all the reinforcement scenarios indicate that investment cost outweighs the reliability benefit, i.e., the reduction in risk-associated cost. This result is consistent with the trend of total cost. The ranking of total cost in increasing order is scenario 1, 2, 3, and 4.

On the basis of the IBSR results, the conclusion can be drawn that none of the reinforcement scenarios is economically worthwhile given that the only benefit considered is reliability benefit. A discussion of this conclusion is presented.

1) The number of load levels and average load as input data have significant effects on system reliability. In the test case in Chapter 7, a single peak load level is used, and the IBSR results exceed 1 for some of the reinforcement scenarios. However, in this test case, multiple load levels are used in which the peak load occurs for no more than 5% of the total hours in a year. The lower average load level and shorter duration of peak load result in a system that is less likely to suffer from load losses. Given that the system is already highly reliable under multiple load levels, the reliability improvement brought by the system reinforcement scenarios is not as significant.

2) The only benefit considered in this research is the reliability benefit. Other types of benefits, such as the benefit of transmission investment deferral, benefit from incentive policies, and externalities, are not considered. The IBSR corresponds only to the reliability benefit.

The effect of the central control unit failure on system reliability is investigated as follows. Scenario 2 with different levels of central control unit reliability is studied. The failure rate of the central control unit is denoted as λ_C.

i) Scenario 2 with $\lambda_C = 0$ occ/year, i.e., the perfectly reliable case;

ii) Scenario 2 with $\lambda_C = 0.2$ occ/year;

iii) Scenario 2 with $\lambda_C = 0.6$ occ/year;

iv) Scenario 2 with $\lambda_C = 5$ occ/year.

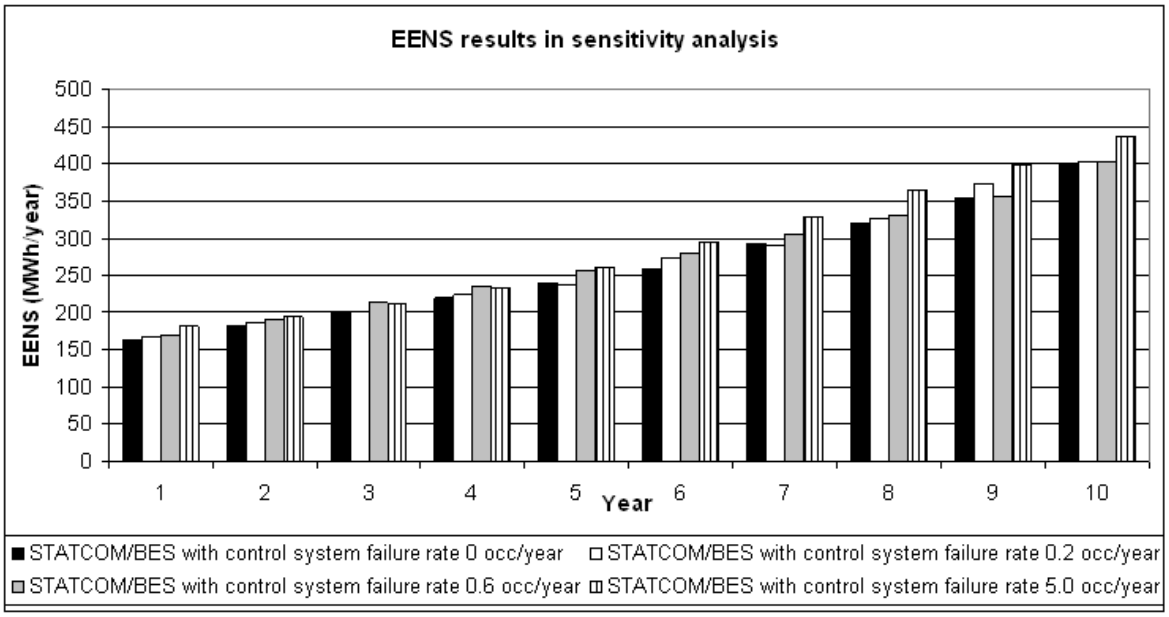

Figure 8.13: EENS for RBTS with STATCOM/BES.

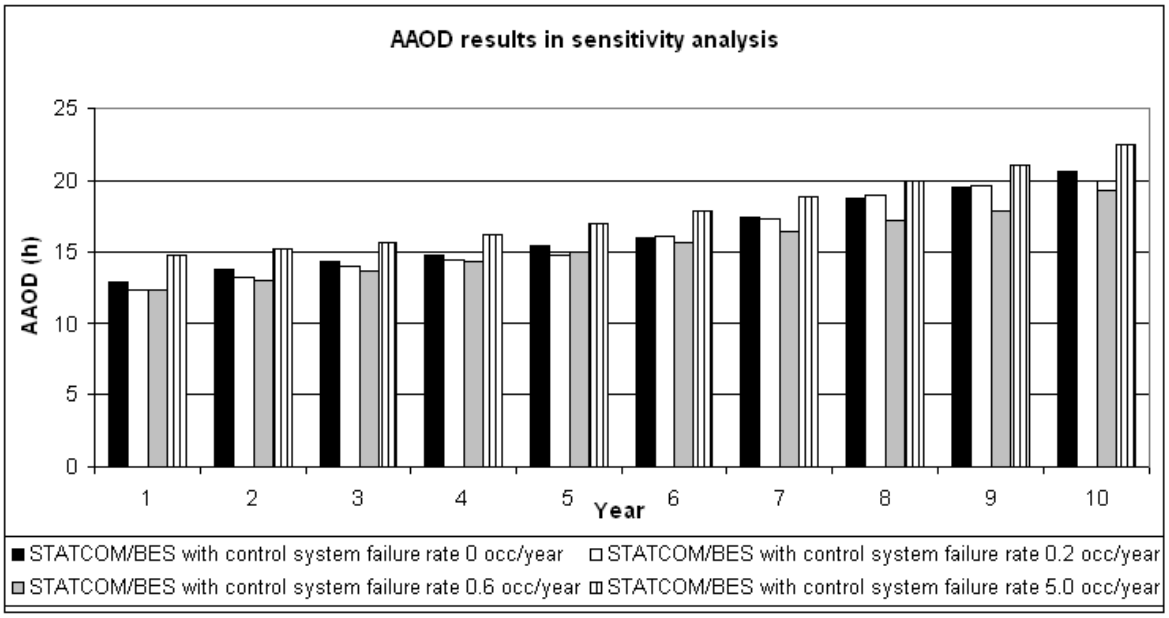

Figure 8.14: AAOD for RBTS with STATCOM/BES.

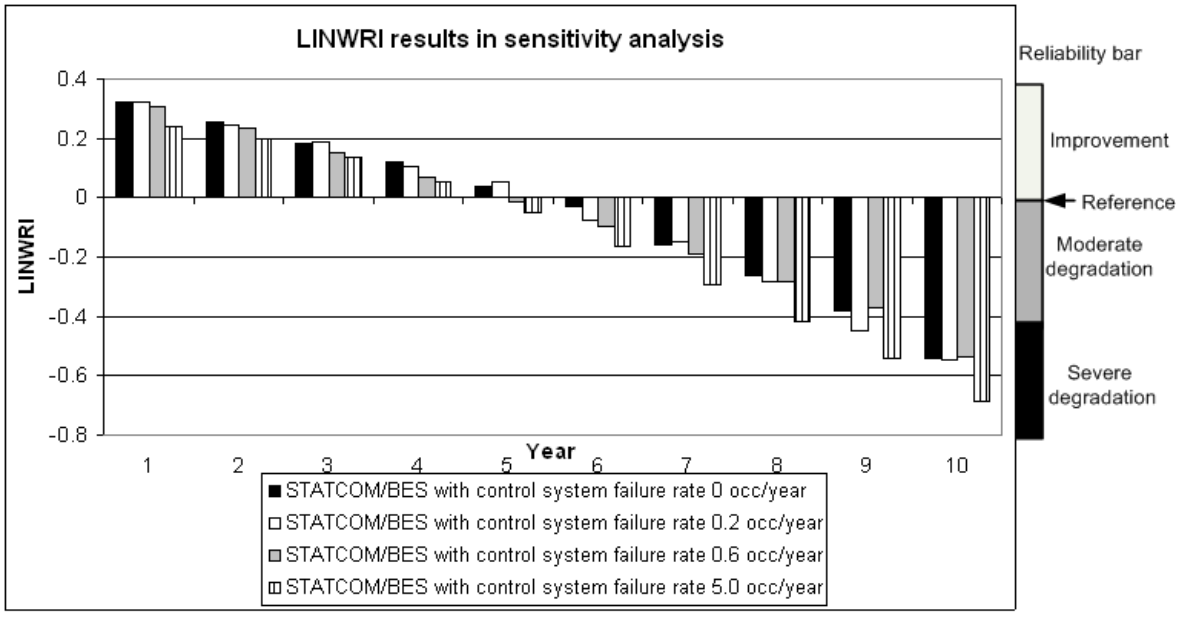

Figure 8.15: LINWRI results for RBTS with STATCOM/BES and control system of different reliability levels.

According to Figure 8.14, scenario 2 with a fully reliable control system shows a trend of greater AAOD than that with failure rate of 0.2 occ/year. However, it does not prove a systematic feature of the control system. A detailed explanation is given below:

1) Due to the stochastic nature of Monte Carlo, it is impossible for results from different times of simulations to be exactly the same. From the practice of simulations, the author has found that results are tolerable if they fall within a band of ± 5%. This band of ± 5% means that the maximum difference of two results of the same scenario of the same year could be up to 10%.

2) Reliability assessment based on Monte Carlo consists of two steps: the first is sequential sampling; the second is state analysis. Once a sequence of system behaviours is sampled in the first step, it is used for all years. Therefore, this may result in the same 'trend' for all years which should not be interpreted as a systematic feature of the control system. Rather, it results from the calculation procedure.

3) In the simulation, some variables exhibit a higher level of convergence whereas others do not. For example, EENS results from different times of simulations fall

into a slightly narrower band than AAOD results, showing a higher level of convergence than the latter. As a composite index, LINWRI results show a medium level of convergence among EENS and AAOD.

4) Conducting the simulation for multiple times and calculating the average result are likely to enhance accuracy but at the cost of increased computational burden, if all given parameters were accurate, which is hardly the case in reality. The author concludes that the bottleneck to accuracy is the error in prediction of future load level, rather than the stochastic nature of MCS. Therefore, in practice, it is rather meaningless to improve the accuracy of non-bottleneck while leaving the bottleneck unrelieved.

The effect of control system failure on system reliability is negligible when the failure rate of the central control unit is no greater than 0.6 occ/year. The slight variation in system reliability caused by different λ_C values is shadowed by the stochastic nature of CMCS.

To demonstrate the effect, a theoretical (unrealistic) high failure rate (i.e., 5 occ/year) is proposed, under which the change in EENS from the 'perfectly reliable case' is between 3% (occurring in year 5) to 11% (occurring in year 1), and the change in AAOD from the 'perfectly reliable case' is between 8% (occurring in year 4) to 12% (occurring in year 1).

A significantly unreliable central control unit compromises the effect of transmission investment deferral, i.e., reduces the years of transmission investment deferral. For the 'perfectly reliable case', system reliability diminishes to the unacceptable level in year 9, corresponding to a deferral of more than 3 years (Figure 8.10). For case iv where $\lambda_C = 5$ occ/year, system reliability diminishes to the unacceptable level in year 8, indicating that the transmission investment deferral is reduced to 3 years.

From this case study, the control system failure does not have a significant effect on system reliability if its reliability is comparable to that of the power line.

8.6.2 Modified Reliability Test System (MRTS)

The Modified IEEE 24 bus Reliability Test System (MRTS-24) is used as another test case [145]. Relevant data are provided in Appendix E.

The bus voltage constraint and branch transfer capacity limit are taken into account. The power line failures, STATCOM/BES failure, and central control unit failure are considered. The central control unit failure causes the outage of all the STATCOM/BES devices. The STATCOM/BES provides active and reactive power support under contingencies, but remains on standby under normal conditions. The charging and discharging efficiencies of the BES are both 90%. The dynamic behaviours of BES are not considered.

The load profile is the same as that in the RBTS. The loads of all the buses are assumed to be fully correlated. The annual load growth rate is assumed to be 2.5% and the simulation covers up to 10 years from the base case at year 1.

Four scenarios are defined for this test case:

1) no corrective control;
2) a STATCOM/BES at bus 3;
3) a STATCOM/BES at buses 3 and 9; and
4) a duplicated element between bus 3 and bus 24.

LINWRI is defined in the same manner as in the RBTS case.

The EENS results are shown in Figure 8.16.

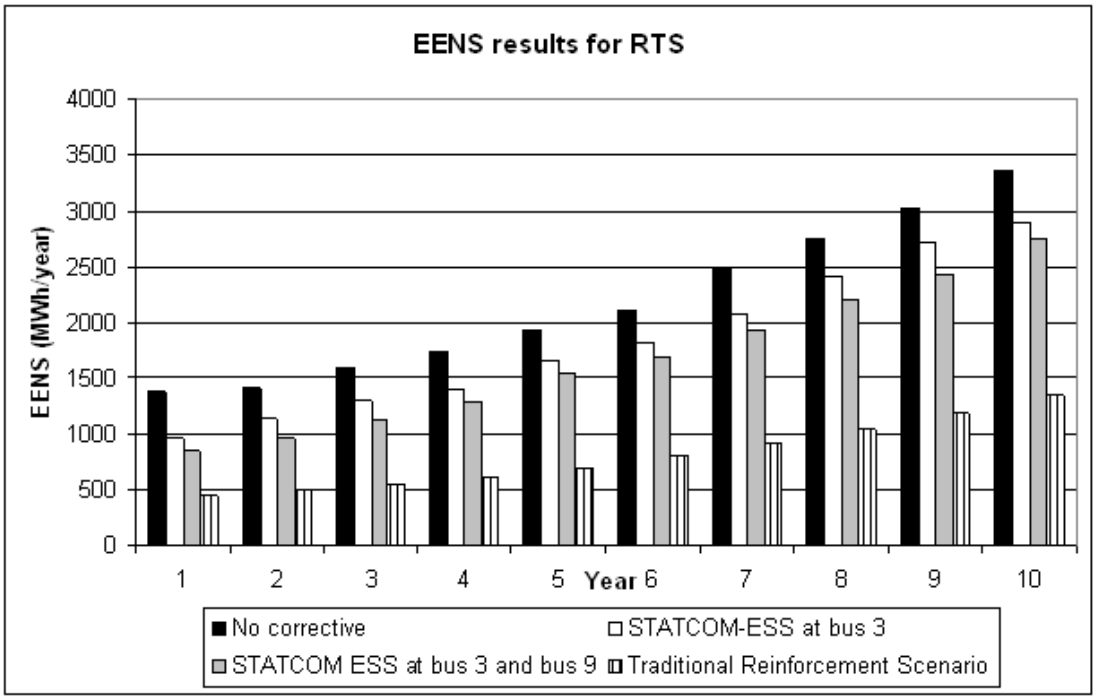

Figure 8.16: EENS results for MRTS.

The AAOD results are illustrated in Figure 8.17.

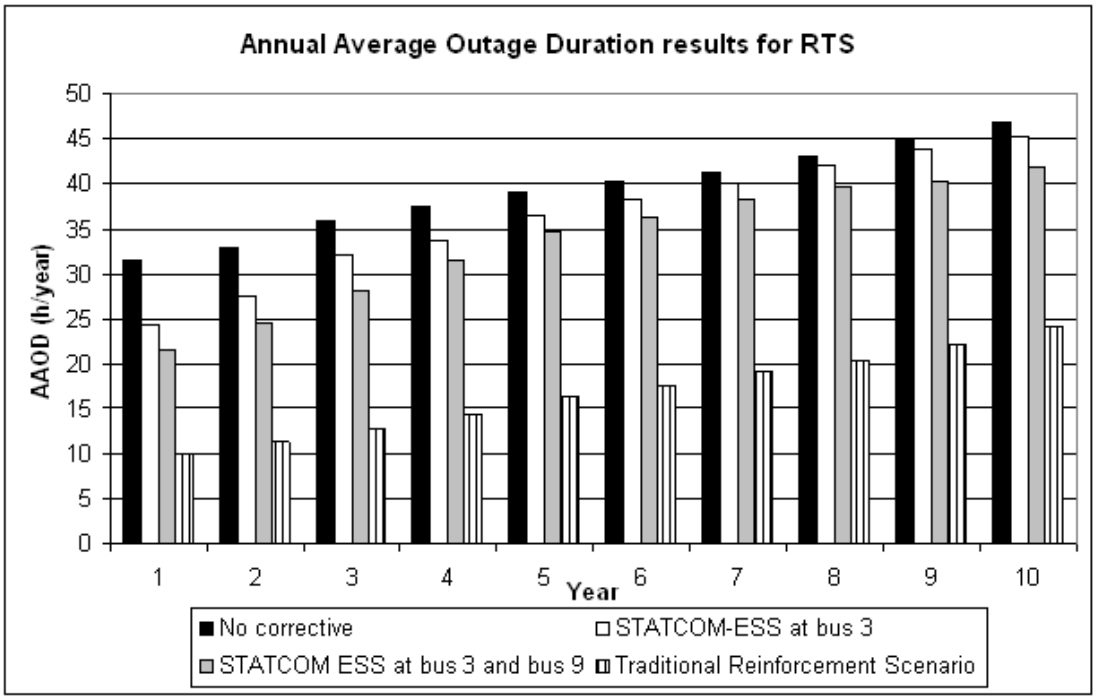

Figure 8.17: AAOD results for MRTS.

The LINWRI results are shown in Figure 8.18.

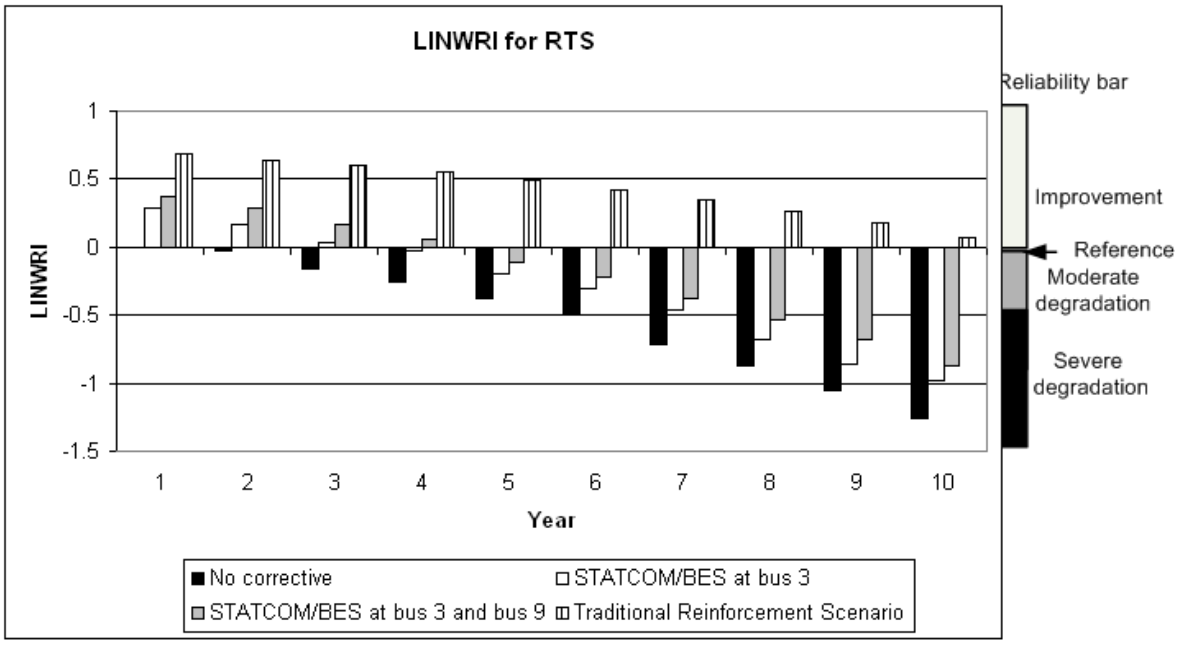

Figure 8.18: LINWRI results for MRTS.

The reliability improvement brought forth by scenarios 2 and 3 is clearly observable, although not as significant as that by scenario 4 (i.e., the traditional reinforcement scenario). By relieving the stress in the bottleneck, the duplicated element between buses 3 and 24 can significantly improve system reliability.

At any given year, the ranking of all the scenarios with respect to system reliability in decreasing order is scenario 4, 3, 2, and 1.

The unacceptable level of system reliability is defined at $\text{LINWRI} = -0.5$. Given this level, the effect of transmission investment deferral is imperceptible under scenarios 2 and 3, which reflect deferrals by 1 and 2 years, respectively. This confirms that a 2.5% annual load growth is sufficiently large to cause rapid degradation in system reliability over years (Figure 8.18). The reinforcement scenarios that implement the STATCOM/BES in this test case enable limited capability in counterbalancing the effect of continued load growth.

The discount rate is assumed to be 5% and the economic life for each STATCOM/BES device or the extra line is 25 years.

The investment costs are given in Table 8.7.

Table 8.7: Investment costs for MRTS

Scenario No.	Value of each instalment (£k)	Present value of investment cost (£)
1	0	0
2	7,000	54,052.14
3	14,000	108,104.29
4	30,000	231,652.05

The O&M costs are presented in Table 8.8.

Table 8.8: O&M costs for MRTS

Scenario No.	Annual O&M cost (£k)	Present value of O&M cost (£k)
1	0	0
2	60	845.64
3	120	1,691.27
4	20	281.88

The risk-associated costs are presented in Table 8.9.

Table 8.9: Risk-associated costs for MRTS

Scenario No.	Annual risk-associated cost (£k)	Present value of risk-associated cost (£k)
1	8,242.94	116,175.52
2	5,792.63	81,641.07
3	5,080.63	71,606.18
4	2,640.57	37,215.98

The cost structure is given in Figure 8.19.

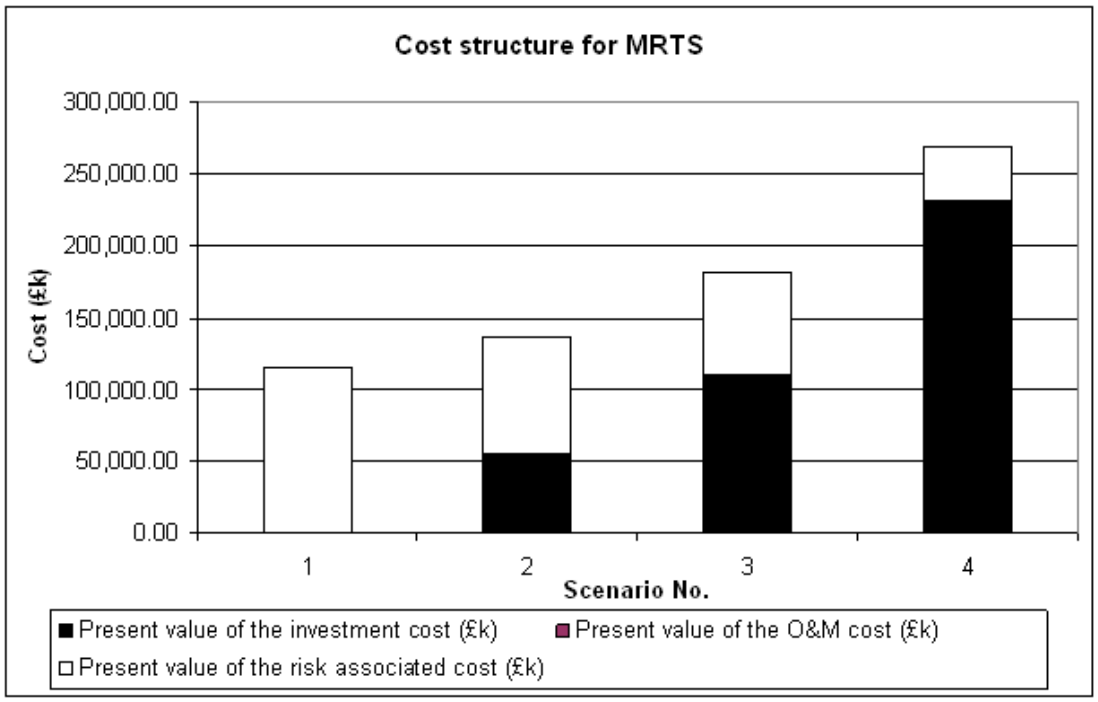

Figure 8.19: Cost structure for MRTS.

The IBSR results are presented in Figure 8.20.

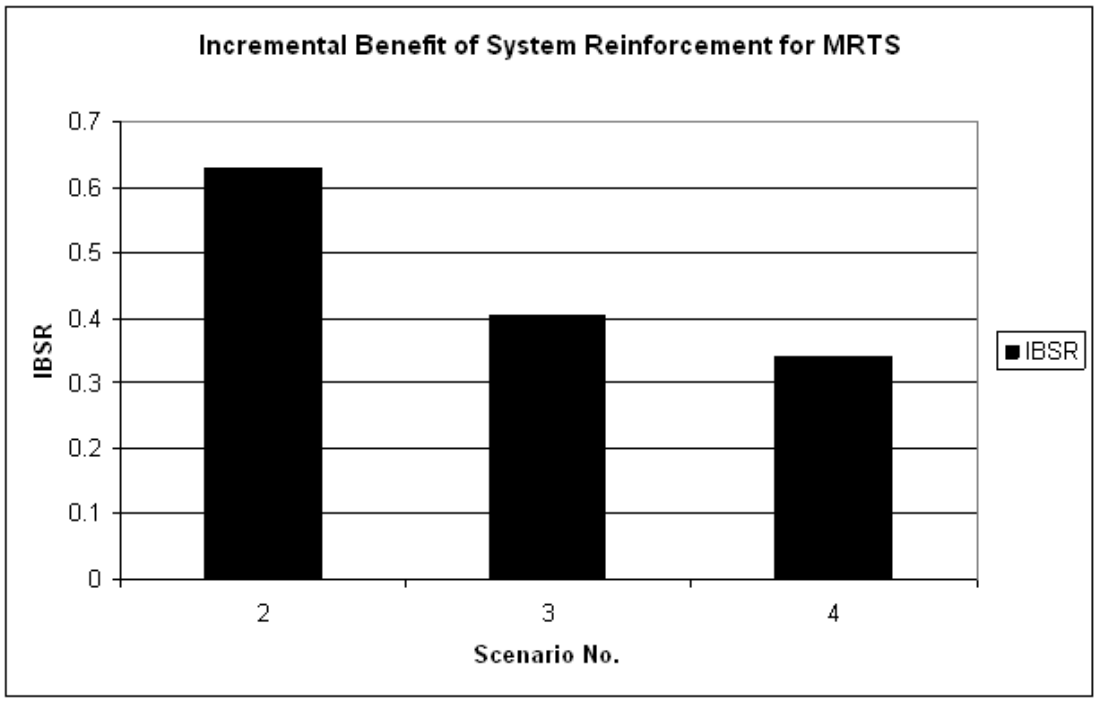

Figure 8.20: IBSR results for MRTS.

The O&M cost is negligible throughout the economic life of the reinforcement scenario. In scenario 2, the risk-associated cost is greater than the investment cost, whereas the opposite holds true for scenarios 3 and 4.

The IBSR results show a similar trend to that observed in the RBTS case. The extra investment in scenario 3 over scenario 2 outweighs the reliability benefits. Compared with scenario 2, scenario 3 incurs an extra investment cost of £54.05 M, which brings a reduction in risk-associated cost of £10.04 M. This results in scenario 3 having a higher total cost and a lower IBSR value than scenario 2. Despite providing the highest reliability improvement, scenario 4 has the lowest IBSR value because of its prohibitive investment cost. The IBSR results indicate that none of the reinforcement scenarios provide a reliability benefit that outweighs the investment cost.

The effect of the central control unit failure on system reliability is investigated as follows. Scenario 3 with different levels of central control unit reliability is considered. The failure rate of the central control unit is denoted as λ_C.

i) Scenario 3 with $\lambda_C = 0.2$ occ/year

ii) Scenario 3 with $\lambda_C = 0.6$ occ/year

iii) Scenario 3 with $\lambda_C = 1$ occ/year

The EENS, AAOD, and LINWRI results are shown in Figure 8.21, Figure 8.22 and Figure 8.23, respectively.

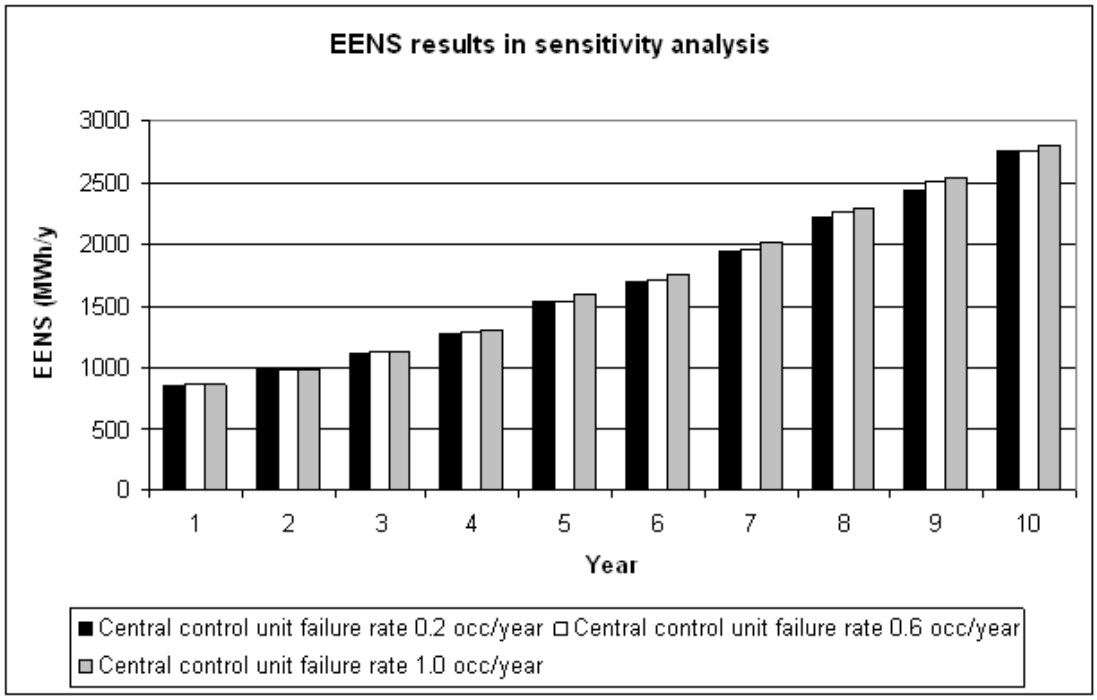

Figure 8.21. EENS results for sensitivity analysis of MRTS.

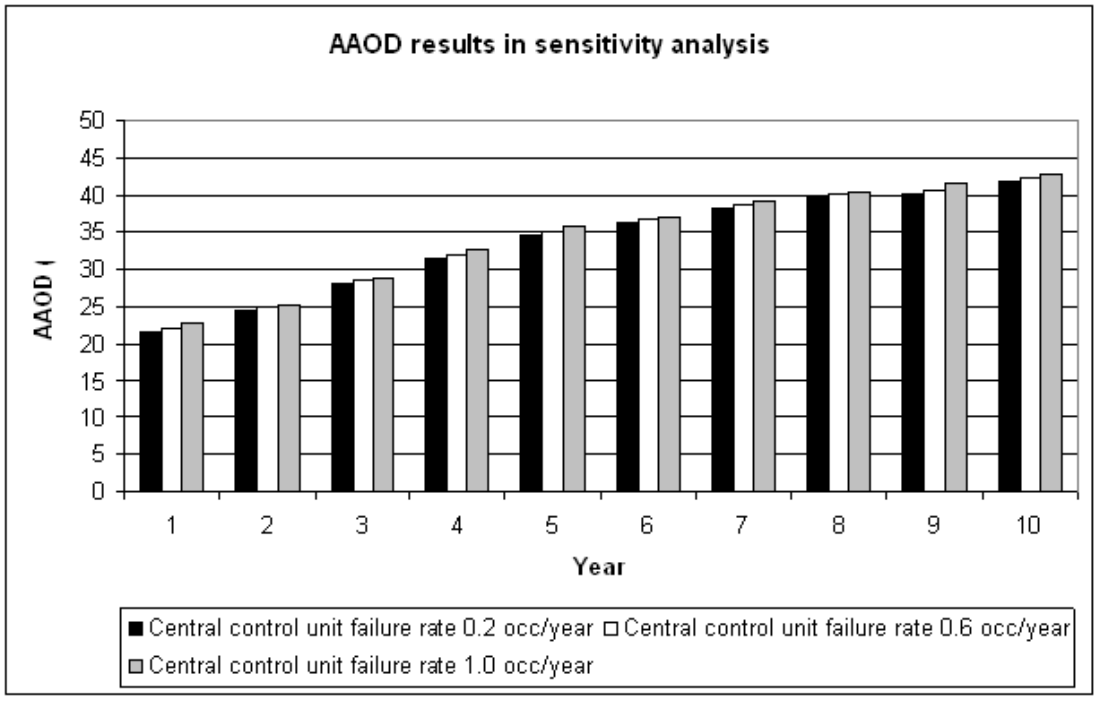

Figure 8.22: AAOD results for sensitivity analysis of MRTS.

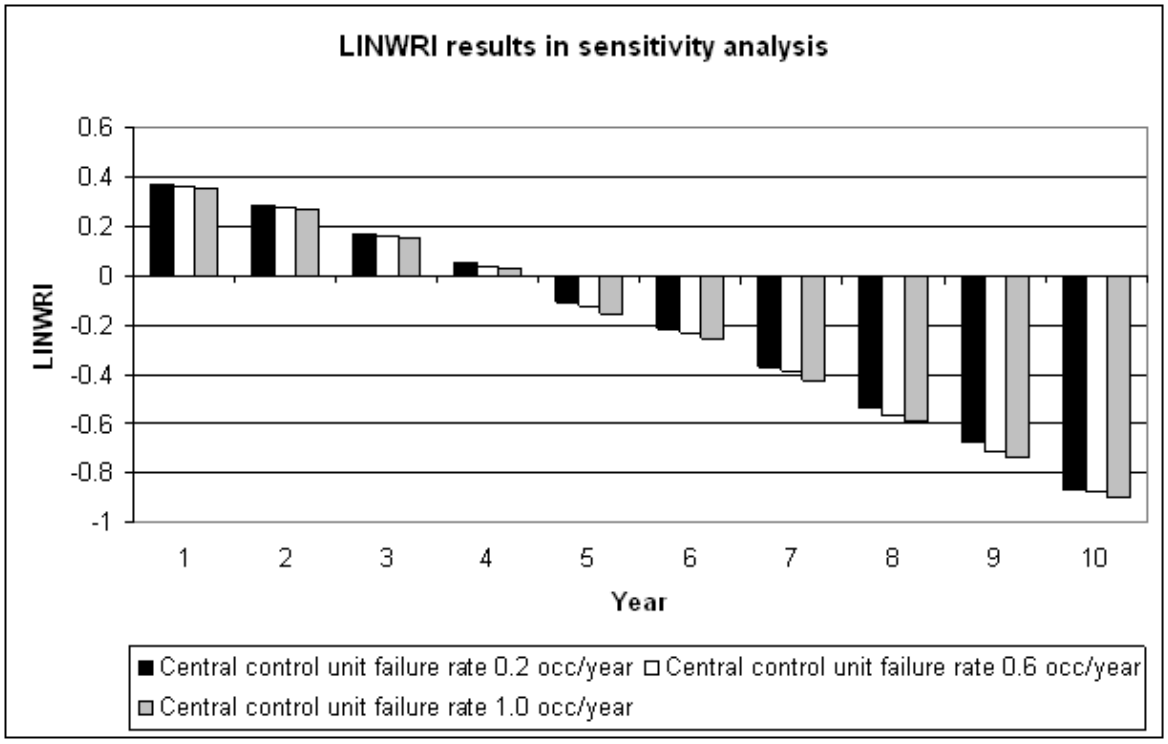

Figure 8.23: LINWRI results for sensitivity analysis of MRTS.

The effect of the central control unit failure on system reliability is imperceptible. In any given year, the difference in EENS ranges from 1% to 4%. The difference in AAOD ranges from 1.7% to 4.7%. Such differences fail to verify a credible ranking because of the stochastic nature of CMCS. The reason for this negligible effect is that the short annual average duration (less than 16 hours per year) of the central control unit failure makes coincidence with the failure of a branch highly unlikely.

8.7 Conclusion

Both test cases have shown the effect of load growth on power system reliability. A compounded load growth at a rate of 2.5% causes considerable degradation of system reliability over a decade. The quantitative results of system reliability over years are highly dependent on the estimated rate of load growth because of the compounding effect in the

long term. To obtain a more accurate and realistic load growth rate, tremendous effort is required in surveying, data filtering, and modelling.

The improvement in power system reliability brought about by the STATCOM/BES and traditional reinforcement has been demonstrated in both cases. In each case, STATCOM/BES implementation causes a transmission investment deferral of no more than five years, which is not significant given the load growth rate of 2.5%. The effect of duplicating a network element at a critical (often stressed) corridor on system reliability is also demonstrated. In both test cases, the traditional reinforcement scenario provides the highest improvement to system reliability among all the candidate reinforcement scenarios.

Compared with the study in Chapter 7, the number of load levels used in the simulation has a significant effect on system reliability and IBSR. Using multiple load levels rather than a single peak load level may result in a considerably higher system reliability level and a lower reliability improvement by the reinforcement scenarios.

An economic assessment has been carried out on both test systems in which three types of costs are considered, i.e., the investment, O&M, and risk-associated costs. These costs are converted to present values. The IBSR index indicates whether a reinforcement scenario brings reliability benefit that outweighs the investment and O&M costs and the extent of such outweighing. In both test systems, all the reinforcement scenarios have an IBSR value below 1. The investment and O&M costs of these scenarios outweigh the reliability benefit. Although the traditional reinforcement scenarios provide the highest improvement in system reliability over the study period in the two test systems, they correspond to the lowest IBSR results. When no benefits other than the reliability benefit are considered, they are the least favourable scenarios in terms of cost benefit. However, the IBSR quantifies reliability benefit only. Other benefits, such as transmission investment deferral, incentive policies, externalities, etc., may have to be assessed depending on assumption.

The effect of the central control unit failure on system reliability is generally negligible when its failure rate is comparable to that of the line. Its negative effect on power system reliability is revealed given an incredibly large failure rate.

9 Conclusion

Summary

This chapter gives an overview of the project followed by a summary of contributions and achievements of this research. Then future work is suggested.

9.1 Key Conclusions

This research has studied the impact of corrective control on power system reliability and whether corrective control is economically favourable over preventive control considering risk-associated cost. The three means of corrective control considered in this research are FACTS, DR and ES. AM on the distribution level is a joint application of SVC and ES. The following conclusions have been drawn from the research:

- ***AM increases the maximum capacity of wind generation that can be connected to the network***. The extent of this increase depends on the configuration of AM: a key function is the wind generation output control (WGOC), without which the ability to accommodate wind generation is largely compromised. The reliability of AM also affects this ability: poor AM reliability compromises this ability.
- ***System reliability can be improved by implementing AM, especially when AM is configured with WGOC***. This impact is affected by wind generation capacity as well: the reliability improvement is greater when the wind generation capacity connected to the system is higher. Poorer AM reliability corresponds to less reliability improvement for the power system. When there is a large penetration of

intermittent generation, power system reliability becomes highly sensitive to the reliability of AM system, and ensuring the reliability of AM is critical.

- ***A 'win-win' situation can be expected for DNO and the owner of the wind generation under AM scenario, given that the wind generation capacity is within an appropriate range determined by the individual test case.*** DNO charges wind generation owners for initial connection and for providing AM services, whereas the owner of wind generation earns a revenue from selling electricity. When the wind generation capacity falls below the 'win-win' range, it is not possible for DNO to recover the investment of AM. On the other hand, the maximum capacity of wind generation is limited by either the system reliability constraint or the cost barrier the wind generation owner faces, whichever is lower. In this test case, the system reliability constraint is the bottleneck.

- ***Traditional reinforcement scenario may not be a cost-effective option for DNO since it incurs a prohibitive investment cost***. The case study in this project has proved some of the AM scenarios to be more cost-effective than traditional reinforcement scenario. Two factors that affect the cost-effectiveness of AM scenarios are the configuration of AM and the reliability of AM control system. AM is unlikely to generate a profit for DNO, if it is configured without WGOC. The poorer reliability of AM control system also reduces the net benefit for DNO. This effect is more significant when the wind generation capacity is higher. In general, a relatively reliable AM system configured with WGOC function, controlling an adequate capacity of wind generation, is likely to generate a profit for DNO.

- ***DR slows down the degradation of system reliability in the context of continued load growth.*** For the test case presented in chapter 5, such improvement is greater when the load level is higher. A greater implementation level of DR brings a greater improvement in system reliability. However, the marginal reliability benefit finally decreases.

- ***Not every reliability index deteriorates with growing load level, e.g., MAIFI. MAIFI is insensitive to load growth, but is determined by the network topology***.

- ***Emergency Interruptible Load Programme (EILP) reduces the Expected Interruption Cost.*** However, it does not have a noticeable impact on SAIFI, SAIDI and LINWRI, because, rather than completely avoid load shedding, EILP only reduces the amount the load shedding under emergencies.

- ***Corrective control scenarios utilising FACTS or ES devices and traditional reinforcement scenarios exhibit their effect in slowing down the deterioration of reliability over years of load growth***. The reliability improvement fails to justify the prohibitive investment cost for traditional reinforcement scenarios. Some corrective control scenarios are more cost-effective than traditional reinforcement scenarios. The impact of load growth on system reliability should not be underestimated. A compounded load growth rate of 2.5% leads to a significant degradation in system reliability over five years. In other words, system reliability is highly sensitive to the load growth rate in the long term, because of the compounding effect. Therefore, improving the accuracy of the load growth estimation is critical for a realistic long-term reliability and economic assessment.

- ***The number of load levels considered in the test case has a significant impact on system reliability and IBSR***. Given the same test case or two test cases with comparable size, a single peak load level is likely to result in a considerably lower system reliability level, a greater impact of reinforcement scenarios on system reliability and a higher IBSR value than multiple load levels.

- ***IBSR quantifies a key aspect of benefit namely, the benefit in reliability brought by incremental investment in system reinforcement***. It is defined as the incremental benefit in reliability over incremental investment and O&M cost. IBSR value depends on the 'departure status', i.e., the pre-reinforced status. A system reinforcement process can be either a lump project (one-off construction) or an accumulative process consisting of several small projects. The IBSR results for each small projects and the lump project have been calculated separately. Given that a lump project consists of project A and project B in chronological order, and that project A has a higher IBSR value than the lump project, this means project B has the lowest IBSR value, or is the least cost-effective among the three.

- ***The impact of control system failure on system reliability is generally negligible when its failure rate is comparable to that of the power line***, i.e., normally no more than 1 occ/year. Its negative impact on system reliability is revealed given an incredibly large failure rate.

9.2 Achievement and Contributions

In the context of the research objectives set out Chapter 1 and reiterated in section 9.1, this work has made significant methodological and conceptual contributions to reliability assessment of power systems under post contingency corrective control. The main achievements and contributions are summarised below.

9.2.1 An in-depth and wide ranging literature review of reliability assessment of power systems

A comprehensive critical review has been undertaken as summarised below:

- Chapter 2 reviewed the basic concept of power system reliability, the underlying assumptions, the division of power systems, classic methodologies for reliability assessment, and nonlinear optimisation methodologies;
- The benefits and challenges associated with DG, the need for a fundamentally new solution to address the challenge of increasing penetration of DG, i.e., AM, and the features of AM were reviewed in Chapter 5;
- The benefits and cost of DR, two categories of DR programmes and three basic load models of DR were summarised in Chapter 6;
- Chapter 7 summarised the development of power electronics technology and its impact on FACTS devices, real examples of FACTS applications, and wide area control of FACTS devices;
- The benefits and applications of ES devices, a comparison of different types of ES technologies, and a general ES configuration were reviewed in Chapter 8.

9.2.2 Development of New Reliability Indices

Existing reliability indices have the drawback of being 'partial-sighted' and 'non-representative', i.e., each of the existing indices quantifies only one aspect of system reliability and may not represent overall system reliability. Furthermore, indices that quantify the benefit of corrective control in system reliability were lacking. There was also a need for an index that identifies voluntary energy curtailment from total energy curtailment under emergencies. In response to the gaps mentioned above, a couple of new reliability indices have been proposed in this thesis. They are Linear Weighed Reliability Index (LINWRI), Demand Response Incremental Cost Benefit (DRICB), Incremental Benefit of Corrective Control (IBCC), Incremental Benefit of System Reinforcement (IBSR), and Voluntary Energy Curtailment Level (VECL).

By assigning weighting factors to indices of different aspects, LINWRI represents the overall system reliability. The ways in which LINWRI can be interpreted are:

1) Given a future year and the same current status, the comparison of different scenarios with regard to their LINWRI values shows the reliability ranking of these scenarios and the reliability zone to which each scenario belongs.

2) Given a certain LINWRI level in the future, LINWRI results show the number of years it takes for the system reliability under each scenario to degrade to that level. A larger number of years correspond to a higher reliability improvement the scenario brings to the system.

A reliability bar has also been proposed as a visualisation of LINWRI. Each candidate scenario under each year was projected on the reliability bar consisting of three reliability zones, i.e., the reliability improvement zone, moderate degradation zone, and significant degradation zone. The two boundaries that separate the three zones are the reference point and the unacceptable point. The reference point is normally defined as the reliability level under the 'doing nothing at all' scenario in the current year. The unacceptable point is defined as where network investments in branches and other relative facilities should be immediately put into practice. Arbitrariness often exists when defining the unacceptable point.

DRICB has been proposed in the context of DR. DRICB represents the incremental monetary benefit in system reliability when one more unit of DR (expressed in MWh/year) is implemented. It is an indispensable index when determining the economic viability of DR.

IBCC and IBSR are defined in a similar way as DRICB: they all quantify incremental benefits in reliability, although in different contexts. IBCC focuses on the incremental benefit in reliability from incremental implementation of corrective control, whereas IBSR focuses on incremental benefit in reliability from incremental implementation of system reinforcement. IBCC can be regarded as a subset of IBSR. In this project, the benefit in reliability is converted to a monetary value. The incremental implementation of system reinforcement is also on a monetary basis: it is defined as the incremental investment and O&M costs arising from the reinforcement scenario. IBSR is crucial in determining the economic viability of the system reinforcement scenario.

Load curtailments on a voluntary basis and those by force incur different costs to the network operator as well as to the society as a whole. Ideally, all load curtailments should be conducted according to prearranged contracts on a voluntary basis. However, this is not true in reality. Therefore, there was a need for an index that tells one from the other. Voluntary Energy Curtailment Level (VECL) quantifies annual voluntary energy curtailment as a percentage of annual total energy curtailment under emergencies. The voluntary energy curtailed in this project is the energy curtailed through EILP in which the participation is on a voluntary basis. Therefore, VECL represents the implementation level of EILP. A greater VECL value indicates a higher implementation level of EILP.

9.2.3 Modelling of Control System Reliability

Although widely applied in previous publications, the assumption that components are independent of each other requires justification. Improper application of this assumption may lead to an overly-optimistic reliability result. Previous work did not consider the possibility of control system failure in power system reliability study.

In this project, the assumption of independence does not apply to FACTS and ES devices. The model of the control system has been proposed. FACTS devices are subject to common cause failure (CCF), i.e., the failure of the control system. Given that the communication is conducted via radio, the control system is modelled as a simplified 'party-line' model where the communication system failure is integrated into the failure of the central control unit. The beta factor method has been applied in separating the CCF portion from that of the independent failure.

9.2.4 Development of State Space Models of BES and STATCOM/BES

Creating the state space models of BES and STATCOM/BES is necessary before implementing these devices into the reliability assessment methodology. This is where previous work left a gap. Therefore, the state space models of BES and STATCOM/BES have been derived in this project.

The state space model of BES is based on a double-bank battery with a power interface (PI) and a Charge-Discharge Control System (CDCS). It is valid based on the following assumptions:

- All repair jobs restores full functionality of the BES. In other words, there is no 'partial repair' that leaves any component still inoperative.
- When both banks are out of service, BES is disconnected, and no further outage will develop.
- When the PI or the CDCS is down, BES is disconnected, and no further outage will develop.

The state space model of STATCOM/BES considers the failure of the following component: the two banks of the battery, the STATCOM, the CDCS, and the PI between the battery and the STATCOM. Both the full state space models and the simplified ones are derived based on the same list of assumptions:

- All repair jobs restore full functionality of the STATCOM/BES.

- The outage of both banks, the PI or the CDCS causes the BES being disconnected. Under this circumstance, the whole device runs as a pure STATCOM.
- When the STATCOM is down, the STATCOM/BES becomes inoperative, and no further component outage will occur.

9.2.5 Incorporating Risk-Associated Cost into the Economic Assessment of AM

The original formula that calculates the net benefit for the DNO fails to recognise the risk-associated cost, which is a key element in the economic analysis [56]. In this project, the formula has been updated and applied to a distribution network with wind generation under AM. The original version considers wind generation connection charge, O&M charges for providing AM services, and investment cost of AM [56]. In this project, the risk-associated cost, as an output of the reliability assessment algorithm, is incorporated into the formula. In this way, a comprehensive picture of the benefits and costs of AM can be obtained.

9.2.6 Incorporating Corrective Control into Reliability Assessment Methodology

Three means of corrective control, i.e., FACTS, DR and ES have been incorporated into reliability assessment methodology.

The reliability behaviour of SVC was modelled by a four-state model. The m-out-of-n: G model has been adopted as the reliability model of STATCOM. TCSC was simply modelled by the two-state model where the interaction with power lines is ignored due to the lack of practical information. These state space models along with the control system failure have been incorporated into CMCS.

Three DR models were summarised in Chapter 6: the load shifting model, the load reduction model and the Emergency Interruptible Load Programme (EILP) model. The load

shifting model curtails electricity demand during peak hours and replaces it at off-peak hours, whereas the load reduction model reduces electricity demand at peak hours without making it up later. The EILP model considers the type of DR programmes where large industrial customers cut their demand upon request from the DNO under emergency circumstances. These DR models have been incorporated into the reliability assessment algorithm.

The BES and STATCOM/BES models proposed in Chapter 8 have also been implemented in CMCS when performing reliability assessment of the power system.

9.3 Suggestions for Future Work

Although this project has made innovations and bridged a number of gaps in the field of power system reliability in a corrective control paradigm, it is by no means an exhaustive exploration of this continuously changing field but a step into it. There is still a vast space for future work including possible improvements based on this research and parallel projects. Some of them are suggested below:

1) ***A more rigorous system planning process prior to reliability assessment is suggested.***

   One of the limitations of this research is that it is on system reliability only, rather than on combined system planning and reliability study. Determining the locations of FACTS devices, ES devices and new branches for a candidate scenario is a system planning task which is beyond the scope of this project. System planning itself is a vast topic where numerous techniques have been applied, e.g., the multi-objective Genetic Algorithm. This project does not guarantee that the candidate scenarios are optimally planned. Instead, only preliminary planning by enumeration is conducted. The value of this project will be further improved if it is conducted on a system that has undergone a more rigorous planning process.

2) ***A nonlinear optimisation toolbox with higher efficiency, a higher chance of finding the global optimum and the ability to model nonlinear constraints is yet to be developed.***

One of the limitations of this project stems from the non-perfect nonlinear optimisation tool box. As is mentioned in chapter 2, the nonlinear optimisation toolbox, i.e., 'fmincon' does not guarantee a global optimum for all circumstances. This may affect the system analysis results. Justifications for 'fmincon' have been made in Chapter 2 regarding its overall performance considering efficiency, accuracy and the ability of processing nonlinear constraints: it is not perfect but is suitable for this project. However, the project can be further improved if a superior nonlinear optimisation toolbox is developed. Compared with 'fmincon', a superior toolbox is expected to exhibit higher efficiency, a higher chance of finding the global optimum as well as the ability to take nonlinear constraints into account. However, the development of a superior nonlinear optimisation toolbox is a challenging and time-consuming mathematical task.

3) ***DR models can be upgraded.***

The DR models can be upgraded in order to take into account a more complex market condition. The signal that triggers DR programmes, whether a price signal or a signal dictated by the contract, can be modelled in a more practical way if real data are provided. It is expected that the upgraded DR models can be readily implemented into existing reliability assessment methodology and system analysis algorithm.

4) ***The control system model can be upgraded.***

This project has recognised the correlation among the failures of FACTS devices as a single CCF, i.e., the failure of central control unit. In reality, the correlation between different FACTS devices may be more complicated: there may be multiple CCF events determined by the structure of the control system, e.g., a multilevel control system. The model of the control system can be upgraded if there were knowledge of the real structure of the control system.

5) ***A practical test case will enhance the value of this project.***

The practical value of this project will be further demonstrated if the methodology is applied to the UK transmission network model, apart from being tested on RTS and RBTS.

6) ***Transient analysis can serve as a supplement to the reliability assessment process.***

Steady-state inadequacy (either a shortage in generation capacity caused by the outage of generation units or a shortage in network capacity caused by branch outage) is only one type of problems that may lead to load curtailment. Transient instability is another type of the same importance. Despite a couple of existing papers [9, 146], reliability considering transient stability issues is a field that still requires much research effort. Further exploration can add value to this project: transient stability evaluations can be performed. The model of the control system and the new indices proposed in this project can be applied in transient stability assessments.

7) ***The state space models of ES devices need to be validated against actual operation data.***

A detailed knowledge of the operation strategy and the characteristics of ES devices is required for the development of sufficiently accurate state space models of ES devices.

APPENDIX A: Input Data for the 16-Bus Test Network for AM study

Table A1: Input data for the 16 bus network [65].

Branch (bus to bus)	Section Resistance (p.u)	Section Reactance (p.u)	End bus real load (MW)	End bus reactive load (MVar)
1-2	0.01	0.01	N/A	N/A
1-3	0.01	0.01	N/A	N/A
1-4	0.2	0.3	2.0	1.6
4-5	0.2	0.3	3.0	1.5
4-6	0.2	0.3	2.0	0.8
6-7	0.2	0.3	1.5	0.2
2-8	0.2	0.3	4.0	2.7
8-9	0.2	0.3	5.0	3.0
8-10	0.2	0.3	1.0	0.9
9-11	0.2	0.3	0.6	0.1
9-12	0.2	0.3	4.5	2.0
3-13	0.2	0.3	1.0	0.9
13-14	0.2	0.3	1.0	0.7
13-15	0.2	0.3	1.0	0.9
15-16	0.2	0.3	2.1	1.0

* The load data are for the base case.

Table A2: The load profile for a typical winter day and a typical summer day

Hour	Load in a typical winter day (per unit)	Load in a typical summer day (per unit)
1	0.6	0.2
2	0.3	0.2
3	0.3	0.2
4	0.3	0.2
5	0.3	0.3
6	0.3	0.3
7	0.3	0.2
8	0.3	0.3
9	0.4	0.5
10	0.5	0.6
11	0.6	0.5
12	0.5	0.6
13	0.5	0.7
14	0.6	0.5
15	0.6	0.5
16	0.6	0.7
17	0.8	0.9
18	1	0.9
19	1	1
20	0.9	0.9

21	0.9	0.7
22	0.9	0.5
23	0.9	0.3
24	0.8	0.2

The load for the base case is scaled down to 1.

All loads are assumed to be fully correlated.

The typical summer day repeats itself from hour 2161 to 6552 (inclusive) in a year.

The typical winter day repeats itself from hour 1 to 2160 and from hour 6553 to 8760.

Table A3: BES characteristics

Bus No.	Maximum Energy (MWh)	Maximum power output (MW)	Charge rate (MW)
12	0.5	0.2	0.1

Table A4: SVC characteristics

Bus No.	Maximum Var injection into the bus (Var)	Maximum Var absorption from the bus (Var)
7	1.0	1.0

The hourly wind profile over a year is included in the CD attached to this thesis.

Table A5: the reliability data of SVC, BES and the central control unit

Device or system	Failure rate (occ/year)	Mean Time To Repair (MTTR: occ/year)
SVC	2	20
BES	2	20
Central control unit	2	20

Based on above parameters and formulae, the numerical results are given in Table A6.

Risk associated cost needs to be corrected.

Table A6: results for economic analysis of the test case

Scenario No.	1	1	1	2	2
Wind capacity (MW)	2.0	4.0	6.0	2.0	4.0
Connection charge (£k)	100.00	200.00	300.00	100.00	200.00
AM service charge (£k)	NA	NA	NA	482.952	965.905
Risk associated cost (£k)	1,513.252	1,513.252	1,513.252	1,417.496	1,417.496
AM investment (£k)	NA	NA	NA	2000.00	2000.00
Net benefit for DNO (£k)	-1,413.252	-1,313.252	-1,213.252	-2,834.543	-2,251.591
Scenario No.	2	3	3	3	3
Wind capacity (MW)	6.0	2.0	4.0	6.0	8.0
Connection charge (£k)	300.00	100.00	200.00	300.00	400.00
AM service charge (£k)	1,448.857	482.952	965.905	1,448.857	1,931.00
Risk associated	1,417.496	1,417.496	1,417.496	1,417.496	1,417.496

cost (£k)					
AM investment (£k)	2000.00	2000.00	2000.00	2000.00	2000.00
Net benefit for DNO (£k)	-1,668.638	-2,834.543	-2,251.591	-1,668.638	-1,086.495
Scenario No.	3	3	3	3	3
Wind capacity (MW)	10.0	12.0	14.0	16.0	18.0
Connection charge (£k)	500.00	600.00	700.00	800.00	900.00
AM service charge (£k)	2,403.482	2,848.293	3,268.921	3,666.427	4,046.634
Risk associated cost (£k)	1,417.496	1,417.496	1,417.496	1,417.496	1,417.496
AM investment (£k)	2000.00	2000.00	2000.00	2000.00	2000.00
Net benefit for DNO (£k)	-514.013	30.798	551.426	1,048.931	1,529.138
Scenario No.	3	4	4	4	4
Wind capacity (MW)	20.0	2.0	4.0	6.0	8.0
Connection charge (£k)	1,000.00	100.00	200.00	300.00	400.00
AM service charge (£k)	4,400.204	482.952	965.905	1,448.857	1,930.746
Risk associated	1,417.496	1,430.228	1,430.583	1,432.246	1,434.033

cost (£k)					
AM investment (£k)	2000.00	2000.00	2000.00	2000.00	2000.00
Net benefit for DNO (£k)	1,982.708	-2,847.276	-2,264.678	-1,683.389	-1,103.287
Scenario No.	4	4	4	4	4
Wind capacity (MW)	10.0	12.0	14.0	16.0	18.0
Connection charge (£k)	500.00	600.00	700.00	800.00	900.00
AM service charge (£k)	2,403.262	2,848.107	3,268.671	3,666.195	4,046.402
Risk associated cost (£k)	1,478.875	1,503.130	1,584.399	1,613.898	1,773.325
AM investment (£k)	2000.00	2000.00	2000.00	2000.00	2000.00
Net benefit for DNO (£k)	-575.612	-55.012	384.272	852.298	1,173.077

Note: All charges/costs are in present value.

NA: not applicable.

Results of benefits for the wind generation owner are in the CD attached to this thesis.

Table A7: reliability results and economic analysis results under TRS

Wind capacity (MW)	EENS (MWh/year)	EENS reduction compared to the base case	Net benefit for DNO (£)
2	45.93	14.45%	-464,728

4	45.93	14.45%	-364,728
6	45.93	14.45%	-264,728
8*	80.37	8.8%	-213,267

*This case has unacceptable reliability.

APPENDIX B: Input Data for the 16-Bus Test Network for DR Study

The branch data and the base load data for year 1 are the same as in Appendix A.

The load profile is included in the CD attached to this thesis.

The Composite Customer Damage Function (CCDF) is given in Table B1 [145]:

Table B1: the CCDF for the test case used in Chapter 6

Bus No.	Composite customer damage cost (£/MW)				
	OD = 1 min	OD = 20 min	OD = 1h	OD = 4h	OD=8h
4	1,625	3,868	9,085	25,160	55,810
5	381	2,969	8,552	31,320	83,010
6	1	93	482	4,914	15,690
7	1	93	482	4,914	15,690
8	1,625	3,868	9,085	25,160	55,810
9	381	2,969	8,552	31,320	83,010
10	1	93	482	4,914	15,690
11	1	93	482	4,914	15,690
12	1	93	482	4,914	15,690
13	1,625	3,868	9,085	25,160	55,810
14	381	2,969	8,552	31,320	83,010
15	1	93	482	4,914	15,690
16	1	93	482	4,914	15,690

*OD stands for outage duration.

CCDF for each bus is expressed by a piecewise function connecting the data points given in Table B1.

APPENDIX C: Input Data for the IEEE 24-Bus Reliability Test System

Data for IEEE 24-bus Reliability Test System (RTS) [7]:

Table C1: bus data for RTS

Bus No.	Bus type	PL (MW)	QL (MVar)	PGmax (MW)	Qmin (MVar)	Qmax (MVar)
1	PV	119.21	24.28	211.93	-110.38	132.46
2	PV	107.07	22.08	211.93	-110.38	132.46
3	PQ	198.69	40.84	0	0	0
4	PQ	81.68	16.56	0	0	0
5	PQ	78.37	15.45	0	0	0
6	PQ	150.11	28.70	0	0	0
7	PV	137.98	27.60	264.92	0	198.69
8	PQ	188.75	38.63	0	0	0
9	PQ	193.17	39.74	0	0	0
10	PQ	215.24	44.15	0	0	0
11	PQ	0	0	0	0	0
12	PQ	0	0	0	0	0
13	Slack	292.51	59.61	2207.63	-551.91	551.91
14	PV	214.14	43.05	2.21	-220.76	331.14
15	PV	349.91	70.64	237.32	-220.76	331.14
16	PV	110.38	22.08	171.09	-220.76	331.14

17	PQ	0	0	0	0	0
18	PV	367.57	75.06	442.15	-220.76	331.14
19	PQ	199.79	40.84	0	0	0
20	PQ	141.29	28.70	0	0	0
21	PV	0	0	441.53	-110.38	220.76
22	PV	0	0	331.14	-110.38	220.76
23	PV	0	0	728.52	-110.38	220.76
24	PQ	0	0	0	0	0

Table C2: line data for RTS

Bus-bus	R (p.u)	X (p.u)	B (p.u)	Transfer limit (MVA)	Failure rate (occ/year)	Repair time (h)
1-2	0.003	0.014	0.461	193	0.24	16
1-3	0.055	0.211	0.057	208	0.51	10
1-5	0.022	0.085	0.023	208	0.33	10
2-4	0.033	0.127	0.034	208	0.39	10
2-6	0.05	0.192	0.052	208	0.48	10
3-9	0.031	0.119	0.032	208	0.38	10
3-24	0.002	0.084	0	400	0.02	768
4-9	0.027	0.104	0.028	208	0.36	10
5-10	0.023	0.088	0.024	208	0.34	10
6-10	0.014	0.061	0.459	175	0.33	35
7-8	0.016	0.061	0.017	208	0.3	10

8-9	0.043	0.165	0.045	208	0.44	10
8-10	0.043	0.165	0.045	208	0.44	10
9-11	0.002	0.084	0	510	0.02	768
9-12	0.002	0.084	0	400	0.02	768
10-11	0.002	0.084	0	400	0.02	768
10-12	0.002	0.084	0	400	0.02	768
11-13	0.006	0.048	0.1	600	0.4	11
11-14	0.005	0.042	0.088	600	0.39	11
12-13	0.006	0.048	0.1	600	0.4	11
12-23	0.012	0.097	0.203	600	0.52	11
13-23	0.011	0.087	0.182	600	0.49	11
14-16	0.005	0.059	0.082	600	0.38	11
15-16	0.002	0.017	0.036	600	0.33	11
15-21	0.006	0.049	0.103	600	0.41	11
15-21	0.006	0.049	0.103	600	0.41	11
15-24	0.007	0.052	0.109	600	0.41	11
16-17	0.003	0.026	0.055	600	0.35	11
16-19	0.003	0.023	0.049	600	0.34	11
17-18	0.002	0.014	0.03	600	0.32	11
17-22	0.014	0.105	0.221	600	0.54	11
18-21	0.003	0.026	0.055	600	0.35	11
18-21	0.003	0.026	0.055	600	0.35	11
19-20	0.005	0.04	0.083	600	0.38	11

19-20	0.005	0.04	0.083	600	0.38	11
20-23	0.003	0.022	0.046	600	0.34	11
20-23	0.003	0.022	0.046	600	0.34	11
21-22	0.009	0.068	0.142	600	0.45	11

Table C3: STATCOM data for RTS

Bus	Inductance Q (MVar)	Capacitance Q (MVar)
3	-100	100

The STATCOM has three phases with each phase consisting of 10 VSIs. For any phase if more than 2 VSIs fail at the same time, the phase is down and the STATCOM is down.

The failure rate and the repair time of VSI independent failure is 5 occ/year and 20 hours, respectively.

Table C4: TCSC data for RTS

Line sending bus	Line receiving bus	X min (Ω)	X max (Ω)	Failure rate (occ/year)*	Repair time (h) **
3	24	-13.27	13.27	0.2	20

*Failure rate corresponds to self-originated (independent) failure.

** Repair time corresponds to the duration for repairing an independent failure.

Table C5: SVC data for RTS

Bus	Inductance Q (MVar)	Capacitance Q (MVar)

3	-112.5	112.5

The reliability data for SVC is shown in the state space model below where all data correspond to independent failure of the SVC:

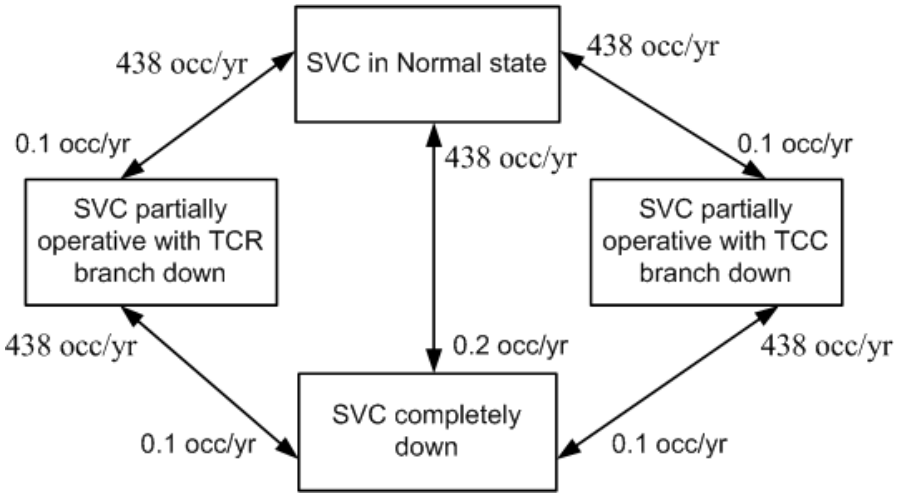

Figure C1: reliability data of SVC.

Table C6: the reliability data for the central control unit in RTS

Failure rate (occ/year)	Repair rate (occ/year)
0.2	438

Economic assessment data:

The discount rate is 5%. The economic life for all reinforcement scenarios is 25 years.

The input data for economic assessment is given in Table C7 where the risk-associated cost is the output of reliability assessment.

Table C7: the input data for economic assessment

Scenario No.	Risk associated cost (£/yr)	Investment mortgage per payment (£/yr)	Mortgage duration (yr)	O&M cost of the reinforcement scenario (£/yr)
1	7,450,862.50	0.00	0	0.00
2	2,057,961.72	400,000.00	5	50,000.00
3	6,877,945.31	500,000.00	5	50,000.00
4	1,892,526.00	600,000.00	5	50,000.00
5	1,928,533.10	800,000.00	5	75,000.00
6	2,361,502.80	2,000,000.00	5	50,000.00

APPENDIX D: Input Data for RBTS

Data for RBTS [142]:

Table D1: bus data for RBTS

Bus No.	Bus type	PL (MW)	QL (MVar)	PGmax (MW)	Qmin (MVar)	Qmax (MVar)
1	Slack	0	0	124.45	-41.86	59.96
2	PV	22.62	4.52	101.82	-48.65	84.85
3	PQ	96.16	19.23	0	0	0
4	PQ	45.25	9.05	0	0	0
5	PQ	22.62	4.52	0	0	0
6	PQ	22.62	4.52	0	0	0

Table D2: line data for RBTS

Bus-bus	R (p.u)	X (p.u)	B (p.u)	Transfer limit (MVA)	Failure rate (occ/year)	Repair time (h)
1-3	0.0342	0.180	0.0212	85	0.24	16
2-4	0.1140	0.600	0.0704	71	0.24	16
1-2	0.0912	0.480	0.0564	71	0.24	16
3-4	0.0228	0.120	0.0142	71	0.24	16
3-5	0.0028	0.120	0.0142	71	0.24	16
1-3	0.0342	0.180	0.0212	85	0.24	16

2-4	0.1140	0.600	0.0704	71	0.24	16
4-5	0.0228	0.120	0.0142	71	0.24	16
5-6	0.0028	0.120	0.0142	71	0.24	16

Table D3: STATCOM/BES data for RBTS

Bus	Inductance Q (MVar)	Capacitance Q (MVar)	Max Energy in BES (MWh)	Max active power output (MW)
6	-10	10	40	20

The reliability data for STATCOM/BES is given in the figure below:

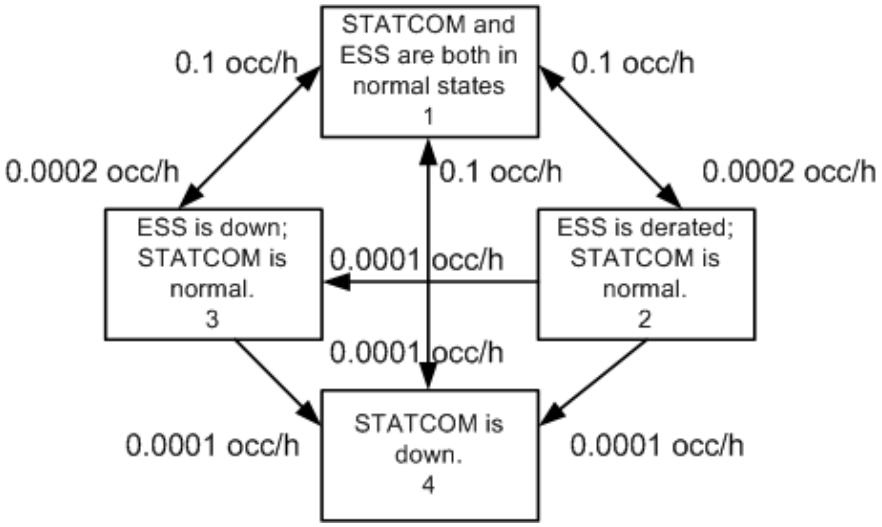

Figure D1: reliability data of STATCOM/BES.

Table D4: the reliability data for the central control unit in RBTS

Failure rate (occ/year)	Repair rate (occ/year)
0.2	547.5

All loads are assumed to be fully correlated. The hourly load profile over a year is given in [7]. The hourly load levels are discretised into 10 steps as follows:

Table D5: discretisation of the load profile

Original load level (per unit)	Discretised load level
<0.1	0.05
[0.1,0.2)	0.15
[0.2,0.3)	0.25
[0.3,0.4)	0.35
[0.4,0.5)	0.45
[0.5,0.6)	0.55
[0.6,0.7)	0.65
[0.7,0.8)	0.75
[0.8,0.9)	0.85
[0.9,1)	0.95

The hourly wind profile over a year is stored in the CD attached to this thesis.

Table D6: data for economic analysis in RBTS

Sccenario No.	Mortgage per year (£k)	Mortgage duration (yrs)	Economic Life	O&M cost per year (£k)
2	7,000	10	25	60
3	10,000	10	25	100
4	30,000	10	25	20

APPENDIX E: Input Data for MRTS

The data for MRTS [145] :

Table E1: Bus Data for MRTS

Bus No.	Bus type	PL (MW)	QL (MVar)	PGmax (MW)	Qmin (MVar)	Qmax (MVar)
1	PV	108	22	192	-100	120
2	PV	97	20	192	-100	120
3	PQ	180	37	0	0	0
4	PQ	74	15	0	0	0
5	PQ	71	14	0	0	0
6	PQ	136	26	0	0	0
7	PV	125	25	240	0	180
8	PQ	171	35	0	0	0
9	PQ	175	36	0	0	0
10	PQ	195	40	0	0	0
11	PQ	0	0	0	0	0
12	PQ	0	0	0	0	0
13	Slack	265	54	2000	-500	500
14	PV	194	39	2	-200	300
15	PV	317	64	215	-200	300
16	PV	100	20	155	-200	300

17	PQ	0	0	0	0	0
18	PV	333	68	400.57	-200	300
19	PQ	181	37	0	0	0
20	PQ	128	26	0	0	0
21	PV	0	0	400	-100	200
22	PV	0	0	300	-100	200
23	PV	0	0	660	-100	200
24	PQ	0	0	0	0	0

Table E2: line data for MRTS

Bus-bus	R (p.u)	X (p.u)	B (p.u)	Transfer limit (MVA)	Failure rate (occ/year)	Repair time (h)
1-2	0.003	0.014	0.461	193	0.24	16
1-5	0.022	0.085	0.023	208	0.33	10
2-4	0.033	0.127	0.034	208	0.39	10
2-6	0.05	0.192	0.052	208	0.48	10
3-9	0.031	0.119	0.032	208	0.38	10
3-24	0.002	0.084	0	400	0.02	768
4-9	0.027	0.104	0.028	208	0.36	10
5-10	0.023	0.088	0.024	208	0.34	10
6-10	0.014	0.061	0.459	175	0.33	35
7-8	0.016	0.061	0.017	208	0.3	10
8-9	0.043	0.165	0.045	208	0.44	10

8-10	0.043	0.165	0.045	208	0.44	10
9-12	0.002	0.084	0	400	0.02	768
10-11	0.002	0.084	0	400	0.02	768
10-12	0.002	0.084	0	400	0.02	768
11-14	0.005	0.042	0.088	600	0.39	11
12-13	0.006	0.048	0.1	600	0.4	11
12-23	0.012	0.097	0.203	600	0.52	11
13-23	0.011	0.087	0.182	600	0.49	11
14-16	0.005	0.059	0.082	600	0.38	11
15-16	0.002	0.017	0.036	600	0.33	11
15-21	0.006	0.049	0.103	600	0.41	11
15-21	0.006	0.049	0.103	600	0.41	11
15-24	0.007	0.052	0.109	600	0.41	11
16-17	0.003	0.026	0.055	600	0.35	11
16-19	0.003	0.023	0.049	600	0.34	11
17-18	0.002	0.014	0.03	600	0.32	11
17-22	0.014	0.105	0.221	600	0.54	11
18-21	0.003	0.026	0.055	600	0.35	11
19-20	0.005	0.04	0.083	600	0.38	11
20-23	0.003	0.022	0.046	600	0.34	11
21-22	0.009	0.068	0.142	600	0.45	11

All loads are assumed to be fully correlated. The hourly load profile over a year is given in [7]. The loads are discretised in the same way as introduced in Appendix D.

The hourly wind profile over a year is stored in the CD attached to this thesis.

Table E3: STATCOM/BES data for MRTS

Bus	Inductance Q (MVar)	Capacitance Q (MVar)	Max Energy in BES (MWh)	Max active power output (MW)
6	-10	10	40	20

The reliability data for STATCOM/BES in MRTS is the same as introduced in Appendix D.

Table E4: the reliability data for the central control unit in MRTS

Failure rate (occ/year)	Repair rate (occ/year)
0.2	547.5

Table E5: input data for economic analysis in MRTS

Sccenario No.	Mortgage per year (£k)	Mortgage duration (yrs)	Economic Life	O&M cost per year (£k)
2	7,000	10	25	60
3	14,000	10	25	120
4	30,000	10	25	20

References

1. Wietze, L.a.L., Vincent. *Electricity Market Liberalization in Europe - Who's Got the Power?* 2004 [cited; Available from: http://ssrn.com/abstract=869543.
2. Le-Cao, Q., T. Tran-Quoc, and A. Nguyen-Hong. *Study of FACTS device applications for the 500kV Vietnam's power system*. in *Transmission and Distribution Conference and Exposition, 2010 IEEE PES*. 2010.
3. Sumranwanich, T., *Analysis of EGAT's Transmission System Development Project By Using Economic and Financial Justification Methods*. 2010, Electricity Generating Authority of Thailand (EGAT).
4. Sergel, R., *Executive Remarks: Demand Response & Reliability*. 2008, North American Electric Reliability Corporation.
5. Torriti, J., M.G. Hassan, and M. Leach, *Demand response experience in Europe: Policies, programmes and implementation.* Energy. **35**(4): p. 1575-1583.
6. Butler, S., *The nature of UK electricity transmission and distribution networks in an intermittent renewable and embedded electricity generation future*. 2001, Imperial College of Science, Technology and Medicine.
7. Anna Driver, E.O.G. *Analysis: Scrutiny on global nuclear industry intensifies*. 2011 [cited; Available from: http://uk.reuters.com/article/2011/03/16/us-japan-quake-industry-idUKTRE72FA0D20110316.
8. *Investing in a Low Carbon Britain*. 2009, Department for Business, Enterprise and Regulatory Reform, Department of Energy and Climate Change, and Department for Innovation, Universities and Skills.
9. Amjady, N., *A framework of reliability assessment with consideration effect of transient and voltage stabilities.* Power Systems, IEEE Transactions on, 2004. **19**(2): p. 1005-1014.
10. Samaan, N., *Reliability Assessment of Electric Power Systems Using Genetic Algorithms*, in *Electrical & Computer Engineering*. 2004, Texas A&M University.
11. Roy Billinton, R.N.A., *Reliability Evaluation of Power Systems*. 1996: Plenum Press.
12. Billinton, R., Ronald, N.A., *Reliability Evaluation of Engineering Systems: Concepts and Techniques*. 1985: Pitman Publishing Ltd.
13. Ault, G.W., I.M. Elders, and R.J. Green, *Transmission Use of System Charges Under Future GB Power System Scenarios.* Power Systems, IEEE Transactions on, 2007. **22**(4): p. 1523-1531.
14. Krippendorff, K. *Web Dictionary of Cybernetics and Systems: Combinatorial Explosion*. [cited 29 November 2010]; Available from: http://pespmc1.vub.ac.be/ASC/Combin_explo.html.
15. Fang, Y., et al. *Security-Constrained Adequacy Evaluation of Bulk Power System Reliability*. in *Probabilistic Methods Applied to Power Systems, 2006. PMAPS 2006. International Conference on*. 2006.

16. Fang, Y., et al. *A Comprehensive Approach for Bulk Power System Reliability Assessment*. in *Power Tech, 2007 IEEE Lausanne*. 2007.
17. Sakis Meliopoulos, D.T., Chanan Singh, Fang Yang, Sun Wook Kang, George Stefopoulos, *Comprehensive Power System Reliability Assessment*. 2005, Power Systems Engineering Research Center.
18. Samaan, N. and C. Singh. *Genetic algorithms approach for the assessment of composite power system reliability considering multistate components*. in *Probabilistic Methods Applied to Power Systems, 2004 International Conference on*. 2004.
19. Gao, Z.Y., W. Peng, and W. Jianhui. *Impacts of energy storage on reliability of power systems with WTGs*. in *Probabilistic Methods Applied to Power Systems (PMAPS), 2010 IEEE 11th International Conference on*.
20. Brad, L.M. and E.G. David, *Genetic algorithms, selection schemes, and the varying effects of noise.* Evol. Comput., 1996. **4**(2): p. 113-131.
21. Li, W., *Risk Assessment of Power Systems: Models, Methods, and Applications*. 2005: Wiley Interscience-IEEE Press.
22. Qiyuan Jiang, J.X., *Mathematical Experiment for College*. Vol. 2. 2005, Beijing: Tsinghua University Press.
23. Clausen, J., *Branch and Bound Algorithms - Principles and Examples*. 1999, Department of Computer Science, University of Copenhagen.
24. Mathworks. *Linear Programming - Optimization Toolbox for MATLAB & Simulink*. [cited 23 Nov 2010]; Available from: http://www.mathworks.com/products/optimization/description3.html.
25. Katta G. Murty, V.F.Y. *Linear Complementarity, Linear and Nonlinear Programming -- Internet Edition*. 2010 [cited 23 Nov 2010]; Available from: http://ioe.engin.umich.edu/people/fac/books/murty/linear_complementarity_webbook/.
26. Himmelblau, D.M., *Applied Nonlinear Programming*, New York: McGraw-Hill
27. Mathworks. *Optimization Toolbox: Q&A*. [cited 23 Nov 2010]; Available from: http://www.mathworks.com/support/solutions/en/data/1-19HX9/index.html?solution=1-19HX9.
28. Mathworks. *Genetic Algorithm Examples*. [cited 23 Nov 2010]; Available from: http://www.mathworks.com/help/toolbox/gads/f6691.html.
29. Billinton, R., M. Fotuhi-Firuzabad, and L. Bertling, *Bibliography on the Application of Probability Methods in Power System Reliability Evaluation 1996-1999.* Power Engineering Review, IEEE, 2001. **21**(8): p. 56-56.
30. Schilling, M.T., et al., *An integrated approach to power system reliability assessment.* International Journal of Electrical Power & Energy Systems, 1995. **17**(6): p. 381-390.
31. Billinton, R. and W. Wangdee, *Delivery point reliability indices of a bulk electric system using sequential Monte Carlo simulation.* Power Delivery, IEEE Transactions on, 2006. **21**(1): p. 345-352.
32. Wen, J., Y. Zheng, and F. Donghan, *A review on reliability assessment for wind power.* Renewable and Sustainable Energy Reviews, 2009. **13**(9): p. 2485-2494.

33. Dobakhshari, A.S. and M. Fotuhi-Firuzabad, *A Reliability Model of Large Wind Farms for Power System Adequacy Studies.* Energy Conversion, IEEE Transactions on, 2009. **24**(3): p. 792-801.
34. Karki, R., P. Hu, and R. Billinton. *Reliability Evaluation of a Wind Power Delivery System Using an Approximate Wind Model*. in *Universities Power Engineering Conference, 2006. UPEC '06. Proceedings of the 41st International*. 2006.
35. Bhuiyan, F.A. and A. Yazdani, *Reliability assessment of a wind-power system with integrated energy storage.* Renewable Power Generation, IET. **4**(3): p. 211-220.
36. Hu, P., R. Karki, and R. Billinton, *Reliability evaluation of generating systems containing wind power and energy storage.* Generation, Transmission & Distribution, IET, 2009. **3**(8): p. 783-791.
37. Peng, W. and R. Billinton, *Reliability benefit analysis of adding WTG to a distribution system.* Energy Conversion, IEEE Transactions on, 2001. **16**(2): p. 134-139.
38. Wangdee, W. and R. Billinton, *Reliability assessment of bulk electric systems containing large wind farms.* International Journal of Electrical Power & Energy Systems, 2007. **29**(10): p. 759-766.
39. Billinton, R. and Y. Cui, *Adequacy Assessment of Composite Power Systems with FACTS Devices Using a DC Load Flow Method.* Electric Power Components and Systems, 2004. **32**(11): p. 1137 - 1149.
40. Nilsson, S.L., *Security aspects of flexible AC transmission system controller applications.* International Journal of Electrical Power & Energy Systems, 1995. **17**(3): p. 173-179.
41. Murray, R.M., *An Introduction to Networked Control Systems*. 2006: Control and Dynamical Systems

California Institute of Technology.

42. A.S. Siddiqui1, A.A., *Use of SCADA Systems in Power System Automation.* International Journal of Engineering Studies, 2010. **2**: p. 10.
43. Motorola. *SCADA Systems*. [cited; Available from: http://www.motorola.com/web/Business/Products/SCADA%20Products/_Documents/Static%20Files/SCADA_Sys_Wht_Ppr-2a_New.pdf.
44. Borcsok, J. and P. Holub. *Different approaches for probability of common cause failure on demand calculations for safety integrity systems*. in *Computer Systems and Applications, 2008. AICCSA 2008. IEEE/ACS International Conference on*. 2008.
45. Borcsok, J., S. Schaefer, and E. Ugljesa. *Estimation and Evaluation of Common Cause Failures*. in *Systems, 2007. ICONS '07. Second International Conference on*. 2007.
46. Guey, C.N. and C.D. Heising, *Development of a common cause failure analysis method: The inverse stress--strength interference (ISSI) technique.* Structural Safety, 1986. **4**(1): p. 63-77.
47. Oka, A.A. *Demand not supplied, loss of load probability, and the joint loss of load probability reliability indices for industrial customers*. in *Harmonics and Quality of Power, 2000. Proceedings. Ninth International Conference on*. 2000.

48. Goran Strbac, N.J., Martin Hird, Predrag Djapic, Guy Nicholson, *Integration of operation of embedded generation and distribution networks*. 2002.
49. Association, B.W.E., *Actions for 33GW*. 2008.
50. Zerriffi, H., *Power market reforms, Climate Change and Distributed Power Generation*. 2005, Program on Energy and Sustainable Development, Stanford University.
51. CONSULTING, I.E., *The tradable value of Distributed Generation*. 2005, Department of Trade and Industry.
52. Rodriguez, G.A.R. and E. O'Neill-Carrillo. *Economic assessment of distributed generation using life cycle costs and environmental externalities*. in *Power Symposium, 2005. Proceedings of the 37th Annual North American*. 2005.
53. Gordijn, J. and H. Akkermans, *Business models for distributed generation in a liberalized market environment.* Electric Power Systems Research, 2007. **77**(9): p. 1178-1188.
54. Rawson, M., *DISTRIBUTED GENERATION COSTS AND BENEFITS ISSUE PAPER*. 2004, Public Interest Energy Research, California Energy Commission.
55. Shafiu, A., et al. *Active management and protection of distribution networks with distributed generation*. in *Power Engineering Society General Meeting, 2004. IEEE*. 2004.
56. Zhang, J., H. Cheng, and C. Wang, *Technical and economic impacts of active management on distribution network.* International Journal of Electrical Power & Energy Systems. **31**(2-3): p. 130-138.
57. Currie, R.A.F., et al. *Fundamental research challenges for active management of distribution networks with high levels of renewable generation*. in *Universities Power Engineering Conference, 2004. UPEC 2004. 39th International*. 2004.
58. MacDonald, R., G. Ault, and R. Currie. *Deployment of Active Network Management technologies in the UK and their impact on the planning and design of distribution networks*. in *SmartGrids for Distribution, 2008. IET-CIRED. CIRED Seminar*. 2008.
59. McDonald, J., *Adaptive intelligent power systems: Active distribution networks.* Energy Policy, 2008. **36**(12): p. 4346-4351.
60. Mutale, J. *Benefits of Active Management of Distribution Networks with Distributed Generation*. in *Power Systems Conference and Exposition, 2006. PSCE '06. 2006 IEEE PES*. 2006.
61. Masters, G.M., *Renewable and Efficient Electric Power Systems*. 2004: Wiley Interscience.
62. M. Fotuhi-Firuzabad, A.S.D., *Reliability-based Selection of Wind Turbines for Large-Scale Wind Farms.* World Academy of Science, Engineering and Technology, 2009(49).
63. Jietan, Z., et al. *Quantitive assessment of active management of distribution network with distributed generation*. in *Electric Utility Deregulation and Restructuring and Power Technologies, 2008. DRPT 2008. Third International Conference on*. 2008.

64. *Wind energy and the facts -- Investment costs*. 2006 [cited 2010 26 December]; Available from: http://www.wind-energy-the-facts.org/en/part-3-economics-of-wind-power/chapter-1-cost-of-on-land-wind-power/cost-and-investment-structures/.
65. R. Srinivasa Rao, S.V.L.N., M. Ramalingaraju, *Optimization of Distribution Network Configuration for Loss Reduction Using Artificial Bee Colony Algorithm.* World Academy of Science, Engineering and Technology, 2008(45).
66. Knight, E., *Proposals for a DG connection charging Framework in the EU*. 2006, Rolls-Royce plc: Berlin.
67. Eco, B. *Return on Investments -- Wind Turbines*. [cited 2010 26 December]; Available from: http://www.britisheco.com/Return-on-Investment-_-Wind-Turbines.aspx.
68. Albadi, M.H. and E.F. El-Saadany, *A summary of demand response in electricity markets.* Electric Power Systems Research, 2008. **78**(11): p. 1989-1996.
69. Energy, U.S.D.o., *Benefits of Demand Response in Electricity Markets and Recommendations for Achieving Them*. 2006.
70. Vernon Smith, L.K., Rasmuson Chair, *A Market-Based Model for ISO-Sponsered Demand Response Programs*. 2005, Center for the Advancement of Energy Markets (CAEM) and Distributed Energy Financial Group, LLC (DEFG).
71. Peter Cappers, C.G., David Kathan, *Demand Response in U.S. Electricity Markets: Empirical Evidence*. 2009, Energy Analysis Department, Ernest Orlando Lawrence Berkeley National Laboratory.
72. Roscoe, A., *Demand Response and Embedded Storage to Facilitate Diverse and Renewable Power Generation Portfolios in the UK*, in *Energy Systems Research Unit*. 2003, University of Strathclyde: Glasgow.
73. Hamidi, V., F. Li, and F. Robinson, *Demand response in the UK's domestic sector.* Electric Power Systems Research, 2009. **79**(12): p. 1722-1726.
74. Aalami, H.A., M.P. Moghaddam, and G.R. Yousefi, *Demand response modeling considering Interruptible/Curtailable loads and capacity market programs.* Applied Energy. **87**(1): p. 243-250.
75. Nguni, A. and T. Le Le. *Interruptible Load and Demand Response: Worldwide Picture and the Situation in Sweden*. in *Power Symposium, 2006. NAPS 2006. 38th North American*. 2006.
76. Azbe, V. and R. Mihalic, *Energy functions for FACTS devices with an energy-storage system.* European Transactions on Electrical Power, 2007. **17**(5): p. 471-485.
77. Yousefi, A., et al. *Risk based spinning reserve allocation considering emergency Demand Response Program*. in *Universities Power Engineering Conference, 2008. UPEC 2008. 43rd International*. 2008.
78. Hirst, E., *PRICE-RESPONSIVE DEMAND AS RELIABILITY RESOURCES*. 2002, Consulting in Electric-Industry Restructuring.
79. Joseph H. Eto, J.N.-H., *Demand Response Spinning Reserve Demonstration – Phase 2 Findings from the Summer of 2008*. 2009, Lawrence Berkeley National Laboratory.

80. Lauby, M. *Demand Response and Reliability*. 2008 [cited; Available from: http://tdworld.com/customer_service/demand_response_reliability/.
81. Couper, C. *Optimizing Demand Response to Improve Economic Dispatch and Reliability*. [cited; Available from: http://www.generatinginsights.com/whitepaper/optimizing-demand-response-to-improve-economic-dispatch-and-reliability.html.
82. SURENDER KUMAR YELLAGOUD, K.S., VEERANJANEYULU PUPPALA, *COST-WORTH ASSESSMENT OF AUTOMATED RADIAL DISTRIBUTION SYSTEM.* International Journal of Engineering Science and Technology, 2010. **2**(11).
83. Heydt, G.T. and T.J. Graf, *Distribution System Reliability Evaluation Using Enhanced Samples in a Monte Carlo Approach.* Power Systems, IEEE Transactions on. **25**(4): p. 2006-2008.
84. da Silva, A.M.L., et al. *Chronological Monte Carlo-Based Assessment of Distribution System Reliability*. in *Probabilistic Methods Applied to Power Systems, 2006. PMAPS 2006. International Conference on*. 2006.
85. Das, D., *Reconfiguration of distribution system using fuzzy multi-objective approach.* International Journal of Electrical Power & Energy Systems, 2006. **28**(5): p. 331-338.
86. Newsham, G.R., *The role of dimmable lighting in demand-responsive buildings*. 2009, National Research Council Canada.
87. Paula Rochay, A.S., *Risk Analysis of Interruptible Load Contracts*. 2008, Department of Statistical Science, University College London.
88. Huang, G.M. and Y. Ping. *The impacts of TCSC and SVC on power system load curtailments*. in *Power Engineering Society Summer Meeting, 2001. IEEE*. 2001.
89. Le Anh, T. and K. Bhattacharya, *Competitive framework for procurement of interruptible load services.* Power Systems, IEEE Transactions on, 2003. **18**(2): p. 889-897.
90. Vikal, R. and G. Goyal. *TCSC Controller Design Using Global Optimization for Stability Analysis of Single Machine Infinite-Bus Power System*. in *Intelligent System Applications to Power Systems, 2009. ISAP '09. 15th International Conference on*. 2009.
91. Pranith, G.P.S. and T. Gowri. *Novel program for selecting FACTS devices for power flow studies*. in *Computational Technologies in Electrical and Electronics Engineering (SIBIRCON), 2010 IEEE Region 8 International Conference on*.
92. Xiao-Ping Zhang, C.R., Bikash Pal, *Flexible AC transmission systems: modelling and control*. 2006: Springer.
93. Enrique Acha, C.R.F.-E., Hugo Ambriz-Perez, Cesar Angeles-Camacho, *FACTS: Modelling and Simulation in Power Networks*. 2004: John Wiley & Sons, LTD.
94. Joerissen, L., et al., *Possible use of vanadium redox-flow batteries for energy storage in small grids and stand-alone photovoltaic systems.* Journal of Power Sources, 2004. **127**(1-2): p. 98-104.

95. Rydh, C.J., *Environmental assessment of vanadium redox and lead-acid batteries for stationary energy storage.* Journal of Power Sources, 1999. **80**(1-2): p. 21-29.
96. Brook, B. *Pumped-hydro energy storage – cost estimates for a feasible system*. 2010 [cited 23 Nov 2010]; Available from: http://bravenewclimate.com/2010/04/05/pumped-hydro-system-cost/.
97. Oskoui, A., et al. *Holly STATCOM - FACTS to Replace Critical Generation, Operational Experience*. in *Transmission and Distribution Conference and Exhibition, 2005/2006 IEEE PES*. 2006.
98. Arthit Sode-Yome, N.M., *Comparison of shunt capacitor, SVC and STATCOM in static voltage stability margin enhancement.* International Journal of Electrical Engineering Education, 2004. **41**.
99. *SVCs for voltage control and power oscillation damping in weak 115 kV system in Alaska*. 2005 [cited; Available from: http://www05.abb.com/global/scot/scot221.nsf/veritydisplay/47de00a4bc627056c12577450023a48b/$File/Alaska%20A02-0145%20E.pdf.
100. *Supercapacitors*. [cited 23 Nov 2010]; Available from: http://www.illinoiscapacitor.com/pdf/Papers/supercapacitors.pdf.
101. *Supercapacitors and Ultracapacitors -- New Energy Storage*. [cited 23 Nov 2010]; Available from: http://www.supercapacitors.org/.
102. Castaneda, J., et al. *Application of STATCOM with energy storage for wind farm integration*. in *Transmission and Distribution Conference and Exposition, 2010 IEEE PES*.
103. Nitus Voraphonpiput, T.B., Somchai Chatratana, *Power Flow Control with Static Synchronous Series Compensator (SSSC).* International Energy Journal, 2008. **9**(2).
104. P.V.Chopade, B.E.K., M. T. Hiwase, Dr. D.G.Bharadwaj, *FACTS :UNIFIED POWER FLOW CONTROLLER (UPFC) - MATHEMATICAL MODELLING AND PERFORMANCE EVALUATION*.
105. Saraf, N., et al. *A model of the static synchronous series compensator for the real time digital simulator*. in *Future Power Systems, 2005 International Conference on*. 2005.
106. Pourbeik, P., et al. *Operational Experiences with SVCs for Local and Remote Disturbances*. in *Power Systems Conference and Exposition, 2006. PSCE '06. 2006 IEEE PES*. 2006.
107. Kowalski, J., et al. *Application of Static VAR Compensation on the Southern California Edison System to Improve Transmission System Capacity and Address Voltage Stability Issues - Part 1. Planning, Design and Performance Criteria Considerations*. in *Power Systems Conference and Exposition, 2006. PSCE '06. 2006 IEEE PES*. 2006.
108. Gudmundsson, Ã., G. Nielsen, and N. Reddy. *Dynamic VAR Compensator (DVC) Application in Landsnet Grid, Iceland*. in *Power Systems Conference and Exposition, 2006. PSCE '06. 2006 IEEE PES*. 2006.
109. Ray, B. *Recent Experience at PG&E with FACTS Technology Application*. in *Transmission and Distribution Conference and Exhibition, 2005/2006 IEEE PES*. 2006.

110. Alhasawi, F.B., J.V. Milanovic, and A.A. Alabduljabbar. *Economic viability of application of FACTS devices for reducing generating costs*. in *Power and Energy Society General Meeting, 2010 IEEE*. 2010.
111. Rogers, K.M. and T.J. Overbye. *Some applications of Distributed Flexible AC Transmission System (D-FACTS) devices in power systems*. in *Power Symposium, 2008. NAPS '08. 40th North American*. 2008.
112. Rahimzadeh, S., M. Tavakoli Bina, and A.H. Viki, *Simultaneous application of multi-type FACTS devices to the restructured environment: achieving both optimal number and location.* Generation, Transmission & Distribution, IET, 2010. **4**(3): p. 349-362.
113. Shakib, A.D. and G. Balzer. *Optimal location and control of shunt FACTS for transmission of renewable energy in large power systems*. in *MELECON 2010 - 2010 15th IEEE Mediterranean Electrotechnical Conference*. 2010.
114. Glanzmann, G. and G. Andersson. *Coordinated control of FACTS devices based on optimal power flow*. in *Power Symposium, 2005. Proceedings of the 37th Annual North American*. 2005.
115. Hug-Glanzmann, G. and G. Andersson. *Coordinated control of FACTS devices in power systems for security enhancement*. in *Bulk Power System Dynamics and Control - VII. Revitalizing Operational Reliability, 2007 iREP Symposium*. 2007.
116. Hager, U., et al. *Multi-Agent System for Coordinated Control of Facts Devices*. in *Intelligent System Applications to Power Systems, 2009. ISAP '09. 15th International Conference on*. 2009.
117. Rehtanz, C. and U. Hager. *Coordinated wide area control of FACTS for congestion management*. in *Electric Utility Deregulation and Restructuring and Power Technologies, 2008. DRPT 2008. Third International Conference on*. 2008.
118. Huang, G.M. and Y. Li. *Impact of thyristor controlled series capacitor on bulk power system reliability*. in *Power Engineering Society Summer Meeting, 2002 IEEE*. 2002.
119. Zongxiang, L. and L. Wenhua. *Reliability Evaluation of STATCOM Based on the k-out-of-n: G Model*. in *Power System Technology, 2006. PowerCon 2006. International Conference on*. 2006.
120. Sahoo, A.K., S.S. Dash, and T. Thyagarajan. *Modeling of STATCOM and UPFC for power system steady state operation and control*. in *Information and Communication Technology in Electrical Sciences (ICTES 2007), 2007. ICTES. IET-UK International Conference on*. 2007.
121. Zhiping, Y., et al. *The steady state characteristics of a StatCom with energy storage*. in *Power Engineering Society Summer Meeting, 2000. IEEE*. 2000.
122. *STATCOM (Static Synchronous Compensator)*. 2007 [cited; Available from: http://www.donsion.org/calidad/cc8/c8-11.pdf.
123. Ambriz-Pérez, H., E. Acha, and C.R. Fuerte-Esquivel, *TCSC-firing angle model for optimal power flow solutions using Newton's method.* International Journal of Electrical Power & Energy Systems, 2006. **28**(2): p. 77-85.
124. Grigg, C., et al., *The IEEE Reliability Test System-1996. A report prepared by the Reliability Test System Task Force of the Application of Probability*

Methods Subcommittee. Power Systems, IEEE Transactions on, 1999. **14**(3): p. 1010-1020.
125. Ter-Gazarian, *Energy storage for power systems*. 1994: Institution of Engineering and Technology
126. Yeleti, S. and F. Yong. *Impacts of energy storage on the future power system*. in *North American Power Symposium (NAPS), 2010*.
127. Rodriguez, G.D. *A utility perspective of the role of energy storage in the smart grid*. in *Power and Energy Society General Meeting, 2010 IEEE*.
128. Jonah Levine, G.M., Richard Moutoux, *Large Scale Electrical Energy Storage in Colorado*. 2007, University of Colorado.
129. Billinton, R. and Bagen. *Reliability Considerations in the Utilization of Wind Energy, Solar Energy and Energy Storage in Electric Power Systems*. in *Probabilistic Methods Applied to Power Systems, 2006. PMAPS 2006. International Conference on*. 2006.
130. Muyeen, S.M., J. Tamura, and T. Murata, *Integration of an Energy Storage System into Wind Farm*, in *Stability Augmentation of a Grid-connected Wind Farm*. 2009, Springer London. p. 137-162.
131. Shuang, Y., T.J. Mays, and R.W. Dunn. *A new methodology for designing hydrogen energy storage in wind power systems to balance generation and demand*. in *Sustainable Power Generation and Supply, 2009. SUPERGEN '09. International Conference on*. 2009.
132. Bo, Y., et al. *On the use of energy storage technologies for regulation services in electric power systems with significant penetration of wind energy*. in *Electricity Market, 2008. EEM 2008. 5th International Conference on European*. 2008.
133. Wei, L. and G. Joos. *Comparison of Energy Storage System Technologies and Configurations in a Wind Farm*. in *Power Electronics Specialists Conference, 2007. PESC 2007. IEEE*. 2007.
134. Onar, O.C., M. Uzunoglu, and M.S. Alam, *Dynamic modeling, design and simulation of a wind/fuel cell/ultra-capacitor-based hybrid power generation system.* Journal of Power Sources, 2006. **161**(1): p. 707-722.
135. H. Bludszuweit, J.M.F., J.A. Domínguez, A. Llombart, J. Sanz, *Simulation of a hybrid system Wind Turbine – Battery – Ultracapacitor*, in *International Conference on Renewable Energies and Power Quality (ICREPQ'11)*. 2005: Zaragoza, Spain.
136. Yang, Z., et al., *Integration of a StatCom and Battery Energy Storage.* Power Engineering Review, IEEE, 2001. **21**(5): p. 63-63.
137. Xue, X.D. and et al., *A study of the status and future of superconducting magnetic energy storage in power systems.* Superconductor Science and Technology, 2006. **19**(6): p. R31.
138. Chong, H., et al. *Modeling and design of a transmission ultracapacitor (TUCAP) integrating modular voltage source converter with ultracapacitor energy storage*. in *Applied Power Electronics Conference and Exposition, 2006. APEC '06. Twenty-First Annual IEEE*. 2006.
139. Kuldeep Sahay, B.D., *Energy Storage Technology for Performance Enhancement of Power Systems*, in *Electrical Power Quality & Utilization Magazine* 2009.

140. Ibrahim, H., A. Ilinca, and J. Perron. *Comparison and Analysis of Different Energy Storage Techniques Based on their Performance Index*. in *Electrical Power Conference, 2007. EPC 2007. IEEE Canada*. 2007.
141. D. Hackworth, J.W., M. Sarkozi, R. Nelson, *FACTS With Energy Storage: Conceptual Design Study*. 1999, Siemens FACTS & Power Quality Division.
142. Billinton, R., et al., *A reliability test system for educational purposes-basic data.* Power Systems, IEEE Transactions on, 1989. **4**(3): p. 1238-1244.
143. Andrew Mills, R.W., Kevin Porter, *The Cost of Transmission for Wind Energy: A Review of Transmission Planning Studies*. 2009, Environmental Energy Technologies Division, U.S. Department of Energy.
144. *Battery energy -- What battery provides more?* [cited; Available from: http://www.allaboutbatteries.com/Battery-Energy.html.
145. Roy Billington, W.L., *Reliability Assessment of Electric Power Systems Using Monte Carlo Methods* Vol. 2. 1994: Wiley Interscience
146. Huang, G.M. and L. Yishan. *Power system reliability indices to measure impacts caused by transient stability crises*. in *Power Engineering Society Winter Meeting, 2002. IEEE*. 2002.